

**THE ROLE OF BCL-2 FAMILY PROTEINS  
AND CALMODULIN IN CALCIUM SIGNALLING  
IN PANCREATIC ACINAR CELLS**

Thesis submitted in accordance with the requirements of Cardiff University  
for the degree of Doctor of Philosophy

**Paweł Ferdek**

**November, 2011**

---

**To my Parents**

*for their endless support and encouragement*

---

### **Declaration**

This work has not previously been accepted in substance for any degree and is not concurrently submitted in candidature for any degree. Parts of this thesis have been published in peer-reviewed journals or scientific conference abstracts and presented in lectures and posters.

### **Statement 1**

This thesis is being submitted in partial fulfillment of the requirements for the degree of PhD.

### **Statement 2**

This thesis is the result of my own independent work / investigation, except where indicated by specific reference.

### **Statement 3**

I hereby give consent for my thesis, if accepted, to be available for photocopying and for inter-library loan, and for the title and summary to be made available to outside organisations.

### **Statement 4: Previously approved bar on access**

I hereby give consent for my thesis, if accepted, to be available for photocopying and for inter-library loans **after expiry of a bar on access previously approved by the Graduate Development Committee.**

---

## ABSTRACT

Bcl-2 proteins are very well known regulators of the programmed cell death. Accumulating evidence suggests that they are also involved in regulation of calcium signalling events. Bcl-2 has been reported to affect calcium release from the intracellular calcium stores through regulation of inositol trisphosphate receptors and endoplasmic reticulum calcium pumps. Physiological and pathological processes in pancreatic acinar cells are controlled by calcium. Intracellular  $Ca^{2+}$  signals regulate not only gene expression and trigger enzyme secretion but also might contribute to premature trypsinogen activation and development of pancreatitis, which is characterised by extensive necrosis of the pancreatic tissue. Detailed investigation of Bcl-2 family-dependent mechanisms of intracellular  $Ca^{2+}$  regulation and its association with cell death induction is required for understanding of the basic physiological signalling pathways as well as pathophysiological processes leading to development of severe diseases of pancreas. This study investigates the effects of Bcl-2 family proteins on intracellular calcium homeostasis, with particular focus on their involvement in  $Ca^{2+}$  fluxes and CICR phenomenon. Also, the  $Ca^{2+}$ -related actions of different doses of ethanol in pancreatic acinar cells and their contribution to pancreatitis are presented and assessed.

The results indicate that pharmacological inhibition of anti-apoptotic Bcl-2 and Bcl-xL proteins with BH3 mimetics BH3I'-2' or HA14-1 sensitizes pancreatic acinar cells to CICR; and overexpression of Bcl-2 has the opposite effect significantly decreasing rising phase of CICR-types of responses in pancreatic cell line AR42J. Responses to BH3 mimetics are at least partially dependent on both  $IP_3$ Rs and RyRs,

---

since inhibition of either of them results in a substantial decrease in  $\text{Ca}^{2+}$  release from the intracellular stores. However, simultaneous blockade of  $\text{IP}_3\text{Rs}$  and  $\text{RyRs}$  did not completely abolish BH3 mimetic-elicited  $\text{Ca}^{2+}$  release, which indicates engagement of other factors in the development of the response. Importantly, the effects of BH3 mimetics on intracellular  $\text{Ca}^{2+}$  were effectively inhibited by loss of Bax protein, suggesting Bax involvement in the regulation of  $\text{Ca}^{2+}$  release from the ER.

Further, the results presented here demonstrate that moderate concentrations of ethanol (10 - 100 mM), although having only a minor effect on intact cells, induce substantial  $\text{Ca}^{2+}$  release from both the ER and the acidic store in permeabilized cells, and trigger intracellular trypsinogen activation - the hallmark of acute pancreatitis. The data suggest that calmodulin, which is present in intact cells but is lost in permeabilized cells, constitutes a part of natural defence mechanism responsible for the differences in the severity of the responses to ethanol. What is more, the evidence indicates that specific pre-activation of calmodulin by  $\text{Ca}^{2+}$ -like peptides boosts this defence and reduces the pathological calcium responses to ethanol as well as to BH3 mimetics in pancreatic acinar cells decreasing necrosis. Finally, the effects of Bcl-2 protein on calcium fluxes in pancreatic acinar cells were investigated. Cells lacking functional Bcl-2 showed substantially more rapid clearance of thapsigargin / high  $\text{Ca}^{2+}$ -induced cytosolic calcium plateau as compared to wild type cells. This effect has been explained by increased activity of the PMCA that results in a marked increase of apoptosis / necrosis ratio in oxidative stress induced cell death. Overexpression of Bcl-2 in AR42J cells reduces ER calcium content, while silencing of Bcl-2 expression by siRNA results in substantially increased releasable calcium

---

pool in the ER. The data indicate that at least a fraction of Bcl-2 in both AR42J cells and pancreatic acinar cells locates in the ER and is present in close proximity to the plasma membrane, making possible the direct regulation of the PMCA.

In conclusion, this study provides new insights into roles of Bcl-2 family proteins and calmodulin in intracellular calcium homeostasis. This thesis presents evidence for involvement of anti-apoptotic Bcl-2 members in  $\text{Ca}^{2+}$ -induced  $\text{Ca}^{2+}$  release; demonstrates previously unknown regulation of the PMCA by Bcl-2; and suggests involvement of Bax protein in regulation of  $\text{Ca}^{2+}$  release from the intracellular stores. The study also proposes that  $\text{Ca}^{2+}$ -like peptides can boost natural protective mechanisms and suggests their potential applications as therapeutic agents.

---

## ACKNOWLEDGEMENTS

First and foremost I would like to thank my supervisors Dr Oleg Gerasimenko and Dr Julia Gerasimenko for their continued support and invaluable guidance throughout my PhD research. Their vast knowledge and inspiring ideas had a major influence on my personal scientific progress.

Further, I am very grateful to Professor Ole Petersen for his brilliant advices and regular feedback that helped to shape this project.

I would also like to thank Professor Alexei Tepikin, Professor Paul Kemp, Professor Vincenzo Crunelli and Swapna Khandavalli, who took care for the formal side of my transfer from Liverpool to Cardiff making it easy and trouble-free.

Thanks to Professor Mark Pritchard for sharing his colonies of knockout mice.

Many thanks to Victoria Walker and Emma Lewis from the animal house at Cardiff University and Lynn McLaughlin from the animal unit in Liverpool for being my allies in the battle against never-ending problems with our transgenic mice!

Special thanks to all my past and present colleagues from both Cardiff and Liverpool labs. You made my life more fun and interesting! Thank you all!

Finally, I shall thank the Wellcome Trust for funding this project. Without this generous support my postgraduate studies in the UK would not be possible.

---

## TABLE OF CONTENT

<b>Abstract</b> .....	<b>4</b>
<b>Acknowledgements</b> .....	<b>7</b>
<b>Table of Content</b> .....	<b>8</b>
<b>Table of Figures</b> .....	<b>13</b>
<b>Abbreviations</b> .....	<b>16</b>
<b>Chapter 1: Introduction</b> .....	<b>20</b>
1.1. Pancreas.....	21
1.2. Pancreatic acinar cell.....	24
1.2.1. Structure and functions of pancreatic acinar cell.....	24
1.2.2. Synthesis and sorting of secretory proteins .....	26
1.2.3. Membrane fusion and secretion.....	27
1.3. Calcium signalling in pancreatic acinar cells .....	30
1.3.1. Calcium as an intracellular messenger.....	30
1.3.2. Store operated calcium entry (SOCE) .....	31
1.3.3. The role of Ca <sup>2+</sup> in physiology and pathology of pancreatic acinar cells.....	33
1.3.4. CCK signalling .....	37
1.3.5. ACh signalling.....	38
1.3.6. Distribution of IP <sub>3</sub> Rs and RyRs in pancreatic acinar cells .....	39
1.4. Calcium Imaging .....	41
1.4.1. Basis of fluorescence .....	41
1.4.2. Calcium-sensitive fluorescent probes .....	44
1.5. Diseases of pancreas.....	48
1.5.1. Pancreatic cancer .....	48
1.5.2. Acute pancreatitis .....	49
1.6. Cell death.....	52
1.7. Bcl-2 family proteins.....	55
1.7.1. Bcl-2 family members .....	57
1.7.2. Apoptosis induction .....	61
1.7.3. Subcellular localization of the Bcl-2 family members .....	62
1.8. BH3 mimetics.....	64

---

1.9. Aims of the study .....	68
<b>Chapter 2: Materials and Methods .....</b>	<b>70</b>
2.1. Reagents and materials .....	71
2.2. Animals .....	73
2.3. Tissue culture .....	75
2.4. Bcl-2-GFP plasmid amplification .....	75
2.5. pcDNA-Bcl-2 plasmid amplification .....	76
2.6. Plasmid isolation .....	76
2.7. Preparation of NaHEPES solution .....	77
2.8. Preparation of KHEPES solution .....	79
2.9. Preparation of NMDG-HEPES solution.....	79
2.10. Preparation of collagenase.....	79
2.11. Preparation of BH3 mimetics .....	79
2.12. Isolation of pancreatic acinar cells .....	79
2.13. Calcium measurements in intact cells. ....	80
2.14. Calcium measurements in permeabilized cells. ....	82
2.15. Two-photon permeabilization. ....	82
2.16. Measurements of trypsinogen activation in permeabilized cells.....	83
2.17. Calculation of cytosolic calcium extrusion rates.....	83
2.18. Transient transfection of AR42J cells with plasmids .....	84
2.19. Stable transfection of AR42J cells with pcDNA-Bcl-2 plasmid.....	86
2.20. Silencing Bcl-2 expression in AR42J cells .....	86
2.21. Transduction of AR42J cells with CellLight BacMam 2.0 Plasma Membrane-RFP .....	87
2.22. Transient transfection of pancreatic acinar cells with Bcl-2-GFP plasmid by electroporation .....	87
2.23. Genotyping .....	88
2.24. Protein isolation – total protein .....	89
2.25. Determination of protein concentration.....	89
2.26. Subcellular fractionation by differential centrifugation .....	91
2.27. Immunoprecipitation .....	91

---

2.28. Immunoblotting .....	92
2.29. Immunofluorescence .....	92
2.30. Apoptosis assay .....	93
2.31. Cell death assay .....	94
2.32. Equipment .....	94
2.33. Software.....	95

**Chapter 3: Effects of Bcl-2 inhibition by BH3 mimetics on calcium-induced calcium release (CICR) process in pancreatic acinar cells..... 96**

3.1. Overview of CICR in pancreatic acinar cells .....	97
3.2. Localization of anti-apoptotic Bcl-2 proteins in pancreatic acinar cells .....	100
3.3. BH3 mimetics BH3I-2' and HA14-1 disrupt the interaction between anti- and pro-apoptotic Bcl-2 family members.....	103
3.4. BH3 mimetics induce increase in cytosolic Ca <sup>2+</sup> followed by sustained Ca <sup>2+</sup> plateau formation.....	103
3.5. Inhibitors of anti-apoptotic Bcl-2 proteins release calcium from the intracellular stores.....	105
3.6. BH3 mimetic-induced Ca <sup>2+</sup> release from the intracellular stores is only partially dependent on IP <sub>3</sub> Rs and RyRs.....	110
3.7. CICR type of response and cytosolic calcium plateau induced by BH3I-2' are substantially reduced in AR42J cells overexpressing Bcl-2.....	116
3.8. Bcl-2 family protein-dependent CICR is crucial for apoptosis induction in pancreatic acinar cells.....	119
3.9. Discussion .....	119

**Chapter 4: Calmodulin dependent mechanism of calcium responses induced by BH3 mimetics..... 125**

4.1. Overview of calmodulin.....	126
4.2. Effects of Calcium-Like Peptides on BH3I-2'-releted Ca <sup>2+</sup> responses.....	131
4.3. Effects of CALPs on BH3I-2'-induced cell death in pancreatic acinar cells.	137
4.4. The effects of gossypol on calcium homeostasis in pancreatic acinar cells..	139
4.5. Effects of CALPs on gossypol-induced Ca <sup>2+</sup> responses.....	140
4.6. Effects of CALPs on gossypol-induced cell death in pancreatic acinar cells	146
4.7. CALPs do not affect physiological calcium responses to ACh in pancreatic acinar cells .....	148

---

4.8. CALPs have only a minor effect on CCK-induced calcium responses in pancreatic acinar cells.....	149
4.9. Discussion .....	157
<b>Chapter 5: Protective role of calmodulin against ethanol in pancreatic acinar cells .....</b>	<b>161</b>
5.1. Overview of ethanol actions on pancreas.....	162
5.2. Responses induced by ethanol in intact pancreatic acinar cells .....	165
5.3. Responses induced by ethanol in permeabilized pancreatic acinar cells .....	168
5.4. Ethanol-induced responses are dependent on calmodulin.....	172
5.5. Activation of calmodulin in intact cells protects against ethanol-induced responses.....	175
5.6. Involvement of the acidic stores in ethanol-induced Ca <sup>2+</sup> release .....	179
5.7. Ethanol induces activation of trypsinogen .....	183
5.8. Trypsinogen activation by ethanol is inhibited by calmodulin .....	186
5.9. Discussion .....	189
<b>Chapter 6: Bcl-2 family proteins and passive calcium leak from the endoplasmic reticulum .....</b>	<b>192</b>
6.1. Overview of passive calcium leak form the ER .....	193
6.2. Loss of Bax protein inhibits BH3 mimetic-induced calcium release .....	197
6.3. BH3 mimetic-induced Ca <sup>2+</sup> release in only partially mediated by IP <sub>3</sub> Rs or RyRs .....	201
6.4. Discussion .....	206
<b>Chapter 7: The role of Bcl-2 protein in regulation of calcium fluxes across the plasma membrane .....</b>	<b>210</b>
7.1. Overview of calcium extrusion mechanisms through the plasma membrane.....	211
7.2. Loss of Bcl-2 affects calcium release from the intracellular stores and calcium extrusion from the cytosol .....	218
7.3. Bcl-2 regulates calcium extrusion across the plasma membrane in pancreatic acinar cells.....	221
7.4. Cytosolic calcium extrusion in pancreatic acinar cells is mainly dependent on the plasma membrane calcium-activated ATPase .....	225
7.5. Bcl-2 regulates calcium extrusion independently on its roles in mitochondria .....	229

---

7.6. Bcl-2 regulates resting calcium levels in the cytosol and in the ER .....	233
7.7. Bcl-2 is present in close proximity to the plasma membrane.....	240
7.8. Bcl-2 is localized in close proximity to the PMCA at the plasma membrane in AR42J cells.....	245
7.9. Loss of Bcl-2 promotes apoptosis and protects against necrosis .....	250
7.10. Discussion .....	257
<b>Chapter 8: Concluding Remarks.....</b>	<b>262</b>
8.1. Summary .....	263
8.2. The effects of BH3 mimetics on calcium homeostasis in pancreatic acinar cells and their consequences .....	264
8.3. The effects of ethanol on calcium homeostasis in pancreatic acinar cells ....	267
8.4. Calcium-like peptides as a potential tool against toxic effects of calcium....	269
8.5. Novel roles of Bcl-2 family protein in cellular Ca <sup>2+</sup> homeostasis.....	273
<b>References .....</b>	<b>277</b>

---

## TABLE OF FIGURES

Fig. 1.1. Schematic illustration of human pancreas .....	22
Fig. 1.2. Structure of a pancreatic acinar cell.....	25
Fig. 1.3. Physiological and pathological calcium responses in pancreatic acinar cells .....	34
Fig. 1.4. Local calcium uncaging experiments .....	40
Fig. 1.5. Schematic illustration of Jablonski Energy Diagram .....	43
Fig. 1.6. Schematic illustration of intrinsic and extrinsic apoptotic pathways .....	54
Fig. 1.7. Schematic domain structure of Bcl-2 family proteins .....	56
Fig. 1.8. Chemical structures of BH3 mimetics .....	67
Fig. 2.1. Photographs of transgenic mice used in the study.....	74
Fig. 2.2. Digestion patterns of pcDNA3-Bcl-2 and Bcl-2-GFP plasmids.....	78
Fig. 2.3. Calcium calibration experiments .....	85
Fig. 2.4. Genotyping of Bax KO and Bcl-2 KO mice.....	90
Fig. 3.1. Comparison of the subcellular localization of RyR2 and IP <sub>3</sub> R3 in pancreatic tissue.....	99
Fig. 3.2. Intracellular localization of Bcl-2 and Bcl-xL.....	102
Fig. 3.3. BH3 mimetics disrupt the interaction between anti- and pro-apoptotic Bcl-2 members .....	104
Fig. 3.4. Calcium responses to BH3 mimetics in pancreatic acinar cells .....	106
Fig. 3.5. BH3 mimetics release calcium from the intracellular stores .....	111
Fig. 3.6. Involvement of IP <sub>3</sub> Rs and RyRs in BH3 mimetic-induced Ca <sup>2+</sup> release...	114
Fig. 3.7. Overexpression of Bcl-2 affects CICR .....	117
Fig. 3.8. Inhibition of IP <sub>3</sub> Rs and RyRs decreases BH3I-2'-induced apoptosis .....	120

---

Fig. 4.1. Calmodulin and CALPs .....	129
Fig. 4.2. Effects of CALPs on BH3I-2'-induced calcium responses .....	133
Fig. 4.3. Effects of CALPs on BH3I-2'-induced cell death in acinar cells .....	138
Fig. 4.4. Calcium responses to gossypol in pancreatic acinar cells .....	141
Fig. 4.5. Effects of CALPs on gossypol-induced responses in acinar cells .....	144
Fig. 4.6. Effects of CALPs on gossypol-induced cell death in acinar cells .....	147
Fig. 4.7. Effects of CALPs on ACh-induced calcium responses .....	150
Fig. 4.8. Effects of CALPs on CCK-induced calcium responses .....	153
Fig. 5.1. Calcium responses induced by POAEE .....	164
Fig. 5.2. Calcium responses to ethanol in pancreatic acinar cells .....	166
Fig. 5.3. Responses of the intracellular stores in permeabilized pancreatic acinar cells to ethanol .....	169
Fig. 5.4. Effects of calmodulin on ethanol-induced responses in permeabilized pancreatic acinar cells .....	173
Fig. 5.5. Activation of CaM by CALP-3 reduces 200 mM EtOH-induced responses in intact pancreatic acinar cells .....	176
Fig. 5.6. Ethanol releases Ca <sup>2+</sup> from thapsigargin-insensitive acidic store in permeabilized pancreatic acinar cells .....	181
Fig. 5.7. Ethanol induces trypsinogen activation .....	184
Fig. 5.8. Calmodulin inhibits ethanol-mediated activation of trypsinogen .....	187
Fig. 6.1. Passive calcium leak from the intracellular stores .....	194
Fig. 6.2. Loss of Bax inhibits calcium release caused by BH3I-2' and HA14-1 .....	199
Fig. 6.3. BH3 mimetic-induced Ca <sup>2+</sup> release is mediated by IP <sub>3</sub> Rs and RyRs .....	203
Fig. 6.4. Schematic illustration of possible interactions between Bcl-2 family members and calcium channels / pumps .....	209

---

Fig. 7.1. Loss of Bcl-2 affects Tg-induced Ca <sup>2+</sup> responses.....	216
Fig. 7.2. Loss of Bcl-2 increases Ca <sup>2+</sup> clearance from the cytosol .....	220
Fig. 7.3. Bcl-2 regulates Ca <sup>2+</sup> extrusion across the plasma membrane.....	223
Fig. 7.4. Involvement of the PMCA and the NCX in Ca <sup>2+</sup> extrusion in pancreatic acinar cells.....	227
Fig. 7.5. Condition of mitochondria does not markedly affect Ca <sup>2+</sup> extrusion.....	231
Fig. 7.6. Bcl-2 regulates resting Ca <sup>2+</sup> levels in the cytosol and in the ER.....	237
Fig. 7.7. Bcl-2 is present in close proximity to the plasma membrane.....	242
Fig. 7.8. Bcl-2 is present in close proximity to the PMCA in AR42J cells.....	247
Fig. 7.9. Loss of Bcl-2 promotes apoptosis and protects against necrosis.....	254

---

## ABBREVIATIONS

[Ca <sup>2+</sup> ]	calcium concentration
2-APB	2-aminoethoxydiphenyl borate
A1	Bcl-2-related protein A1
acetyl-CoA	Acetyl coenzyme A
ACh	acetylcholine
ADH	alcohol dehydronegase
ADP	adenosine 5'-diphosphate
AM	acetoxymethyl
Amp	ampicillin
Apaf-1	Apoptotic protease activating factor 1
apoCaM	apocalmodulin
ATP	adenosine 5'-triphosphate
Bad	Bcl-2-associated death promoter
Bak	Bcl-2 antagonist / killer
BAPTA	1,2-bis(o-aminophenoxy)ethane-N,N,N',N'-tetraacetic acid
Bax	Bcl-2-associated X protein
Bcl-2	B-cell leukaemia / lymphoma 2
bcl-2 <sup>-/-</sup>	bcl-2 gene knockout
Bcl-w	Bcl-2-like protein 2
Bcl-xL	B-cell lymphoma - extra large
BFP	blue fluorescent protein
BH	Bcl-2 Homology
BH3I-2'	3-iodo-5-chloro-N-[2-chloro-5-((4-chlorophenyl)sulphonyl)phenyl]-2-hydroxybenzamide
Bid	BH3 interacting domain death agonist
Bik	Bcl-2-interacting killer
Bim	Bcl-2-interacting mediator of cell death
BRET	bioluminescence energy transfer
BSA	bovine serum albumin
BZiPAR	rhodamine 110, bis-(N-CBZ-L-isoleucyl-L-prolyl-L-arginine amide
cADPR	cyclic adenosine diphosphate ribose
CALP	Ca <sup>2+</sup> -like peptides
CaM	calmodulin
CaMK	Ca <sup>2+</sup> /calmodulin-dependent protein kinases
cAMP	cyclic adenosine monophosphate

---

CCD	charge-coupled device
CCE	capacitative Ca <sup>2+</sup> entry
CCK	cholecystokinin
CCK-A	CCK receptor A
CCK-B	CCK receptor B
CFP	cyan fluorescent protein
CICR	calcium induced calcium release
COX IV	mitochondrial cytochrome c oxidase
CPA	cyclopiazonic acid
CRAC	calcium release activated current
DAG	diacylglycerol
DMSO	Dimethyl sulfoxide
DNA	deoxyribonucleic acid
EDTA	ethylene diamine tetraacetic acid
EF-hand	calcium binding helix-loop-helix structural domain
EGFP	enhanced green fluorescent protein
EGTA	ethylene glycol tetraacetic acid
ER	endoplasmic reticulum
ER-CaM	ER-targeted cameleon
EtOH	ethanol
FAEE	fatty acid ethyl esters
Fas receptor	apoptosis antigen 1
FBS	foetal bovine serum
FITC	fluorescein isothiocyanate
FM 4-64	N-(3-triethylammoniumpropyl)-4-(6-(4-(diethylamino)phenyl) hexatrienyl) pyridinium dibromide
FRET	fluorescence resonance energy transfer
G418	geneticin
GDP	guanosine 5'-diphosphate
GFP	green fluorescent protein
Gly	glycine
GTP	Guanosine-5'-triphosphate
HA14-1	2-Amino-6-bromo- $\alpha$ -cyano-3-(ethoxycarbonyl)-4H-1-benzopyran-4-acetic acid ethyl ester
HeLa	human cervical cancer cell line
HEPES	4-(2-hydroxyethyl)-1-piperazineethanesulfonic acid
HRP	horse radish peroxidase
IgG	immunoglobulin G
IP <sub>3</sub>	inositol 1,4,5-triphosphate
IP <sub>3</sub> R	inositol 1,4,5-triphosphate receptor

---

IRE1	inositol-requiring enzyme 1
Kan	kanamycin
KO	knockout
LB	Luria / Lysogeny Broth
Men	menadione
Mcl-1	Induced myeloid leukemia cell differentiation protein
mRNA	messenger RNA
Munc-18	mammalian uncoordinated-18
NAADP	nicotinic acid adenine dinucleotide phosphate
NAD <sup>+</sup>	nicotinamide adenine dinucleotide
NADP <sup>+</sup>	Nicotinamide adenine dinucleotide phosphate
NCKX	Na <sup>+</sup> /Ca <sup>2+</sup> -K <sup>+</sup> exchanger
NCX	Na <sup>+</sup> -Ca <sup>2+</sup> exchanger
NFκB	nuclear factor kappa-light-chain-enhancer of activated B cells
NMDG <sup>+</sup>	N-methyl D-glucamine
NMR	nuclear magnetic resonance
NSF	soluble N-ethylmaleimide-sensitive adapter protein
ORAI1	calcium release-activated calcium channel protein 1
p53	tumour protein 53
PBS	phosphate buffered saline
PCR	polymerase chain reaction
PDI	protein disulfide isomerase
PIP2	phosphatidylinositol 4,5-bisphosphate
PKA	protein kinase A
PKC	protein kinase C
PKD1	polycystin 1
PKD2	polycystin 2
PLC	phospholipase C
PMCA	plasma membrane calcium ATP-ase
POAEE	palmitoleic acid ethyl ester
PS1	presenilin 1
PS2	presenilin 2
PTP	permeability transition pore
PUMA	p53 upregulated modulator of apoptosis
Q	glutamine
R	arginine
RFP	red fluorescent protein
RIPA	radio-immunoprecipitation assay
RNA	ribonucleic acid

---

ROC	receptor operated Ca <sup>2+</sup> channels
ROS	reactive oxygen species
RPM	Revolutions per minute
RPMI	Roswell Park Memorial Institute medium
Ru360	( $\mu$ -oxo) bis (trans-formatotetramine ruthenium)
RyR	ryanodine receptor
SAM	sterile $\alpha$ -motif
SDS	sodium dodecyl sulphate
SDS-PAGE	sodium dodecyl sulfate polyacrylamide gel electrophoresis
SE	standard error
Ser	serine
SERCA	sarcoplasmic/endoplasmic reticulum calcium ATP-ase
siRNA	small interfering RNA
SM	Sec1 / Munc18 family
SMOC	second messenger operated channels
SNAP25	Synaptosomal-associated protein 25
SNARE	soluble N-ethylmaleimide-sensitive factor attachment protein
SOCE	store operated calcium entry
SRP	signal recognition particle
STIM	stromal interaction molecule
t-Bid	truncated Bid
TBS	Tris buffered saline
TBST	Tris-buffered saline with Tween 20
Tg	thapsigargin
TM	transmembrane
TNF-R	tumour necrosis factor receptor
TRAIL	(TNF)-related apoptosis-inducing ligand
TRP	transient receptor potential
TRPC1	transient receptor potential channel 1
t-SNARE	target SNARE
Tyr	tyrosine
UV	ultraviolet
VAMP2	vesicle-associated membrane protein 2
VOC	voltage operated Ca <sup>2+</sup> channels
v-SNARE	vesicle SNARE
WT	wild type
YFP	yellow fluorescent protein

---

**CHAPTER 1:**  
**INTRODUCTION**

---

## Chapter 1: Introduction

### 1.1. Pancreas

The pancreas is a crucial organ in the digestive as well as endocrine system in all vertebrates. However its structure substantially varies between different species. In humans, and also in rodents such as rats and mice, the pancreas is a separate organ closely located to the duodenum. In contrast, in certain other species, for instance rabbits, pancreatic tissue does not form a discrete organ but is distributed at the small intestine wall, liver and spleen.

The name of the organ originates from two Greek words: "*pan*" meaning "all" and "*kreas*" - "flesh", which probably reflects its macroscopic homogeneous structure. Human pancreas (as depicted in *Fig. 1.1*) is an elongated organ, slightly irregular in shape, where three different parts can be easily distinguished: broad end at the duodenum is called the head (*caput pancreatis*); the main portion of the organ is called the body (*corpus pancreatis*); and thin end of the pancreas forms the tail (*cauda pancreatis*). Usually the length of human pancreas does not exceed 15 cm with its weight ranging from 70 to 100 g.

The pancreas is engaged in production and secretion of both endocrine hormones and digestive enzymes. Endocrine functions are performed by islets of Langerhans, which are cell clusters that contain  $\alpha$ ,  $\beta$ ,  $\delta$  and PP cells. They secrete two types of hormones: (1) those involved in blood glucose homeostasis such as glucagon ( $\alpha$  cells) and insulin ( $\beta$  cells); (2) and hormones involved in regulation of pancreatic

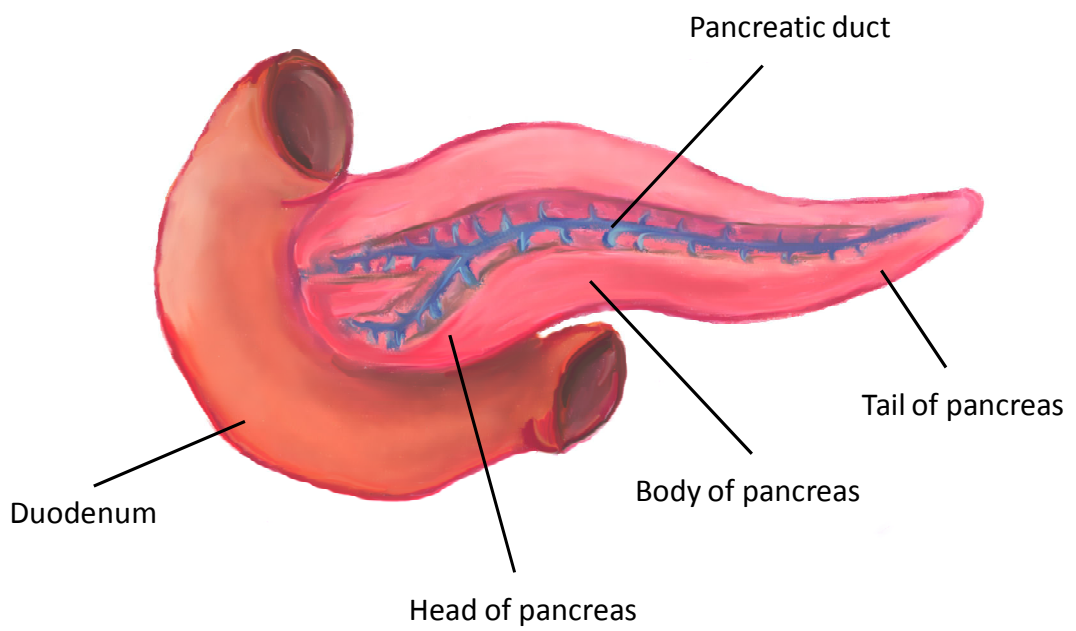


**Fig. 1.1. Schematic illustration of human pancreas**  
See full description in text.

---

secretion: somatostatin ( $\delta$  cells) and pancreatic polypeptide (PP cells). In contrast, exocrine functions are performed by pancreatic acinar cells. These cells produce digestive enzymes (such as trypsin, chymotrypsin, pancreatic amylase and lipase) and secrete them to the small intestine in response to small intestine hormones: cholecystikinin (CCK) and secretin; or in response to acetylcholine (ACh) released from parasympathetic nerve synapses in pancreatic tissue.

The structure of exocrine pancreas is reflected by its functions. Morphologically it bears high resemblance to salivary glands, being more diffuse and softer in texture. The exocrine part forms more than 90 % of the organ and mainly consists of acinar and ductal cells. Clusters of pancreatic acinar cells are organized in grape-like lobular forms called acini, which are attached to intralobular ducts. Intralobular ducts merge into slightly bigger extralobular ducts, which in turn are connected to the main collecting duct that empties into the duodenum<sup>1</sup>.

Pancreas originates from endoderm, which is one of the three germ layers that develop after gastrulation in all vertebrates. The first apparent event of its development in embryogenesis is a condensation of mesenchyme that surrounds the dorsal side of the endodermal primitive gut tube. Then shortly after (in the 9th or 26th day of gestation in mice and humans, respectively<sup>2</sup>) the gut thickens and endoderm evaginates into the mesenchyme forming a dorsal bud. Simultaneously, in the 10th day of mouse and 32nd day of human embryogenesis ventral bud arises laterally from the gut, close to hepatic and bile duct endoderm<sup>3</sup>. The buds thicken and develop further, which, after gut rotation, eventually leads to their fusion and subsequent branching into the surrounding mesenchyme. Importantly, both exocrine and endocrine portions of pancreas have a common origin<sup>4</sup>. Glucagon-positive

---

endocrine cells are present as early as 10th day in mouse and in the third month of human embryonic development<sup>5</sup>. Subsequently, endocrine cells amplify; also acinar cells differentiate and rapidly increase in number. Interestingly, pancreatic acinar cells can perform their secretive functions already in prenatal life.

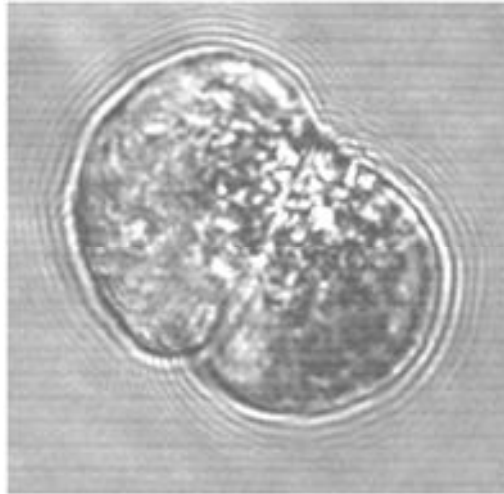
Although pancreatic tissue is highly specialized, its differentiation is not a completely irreversible process. Pancreatic acinar cells have the potential to re-differentiate into ductal cells. However, this seems to be rather a pathological process that occurs during pancreatitis or carcinogenesis. What is more, pancreatic acinar cells in some conditions can undergo transdifferentiation into hepatic cells<sup>6</sup>. Pancreas and liver share a common developmental lineage.

## **1.2. Pancreatic acinar cell**

### **1.2.1. Structure and functions of pancreatic acinar cell**

Functions of pancreatic acinar cells correspond with their highly specialized structure. Each pyramid-shaped pancreatic acinar cell is polarized with two visible areas: basolateral and apical (*Fig. 1.2*). The basolateral pole is larger (even up to 90 % of the cell volume) and contains most of the endoplasmic reticulum; the apical pole faces the acinar lumen and contains secretory granules, where digestive enzymes are stored. Generally, receptors at the basolateral plasma membrane receive stimuli for secretion (such as acetylcholine and cholecystinin) leading to generation of a second messenger response, which in turn releases calcium from the intracellular stores. This signal triggers fusion of secretory granules with the apical membrane and release of digestive enzymes into the tiny intercalated duct.

A.



B.

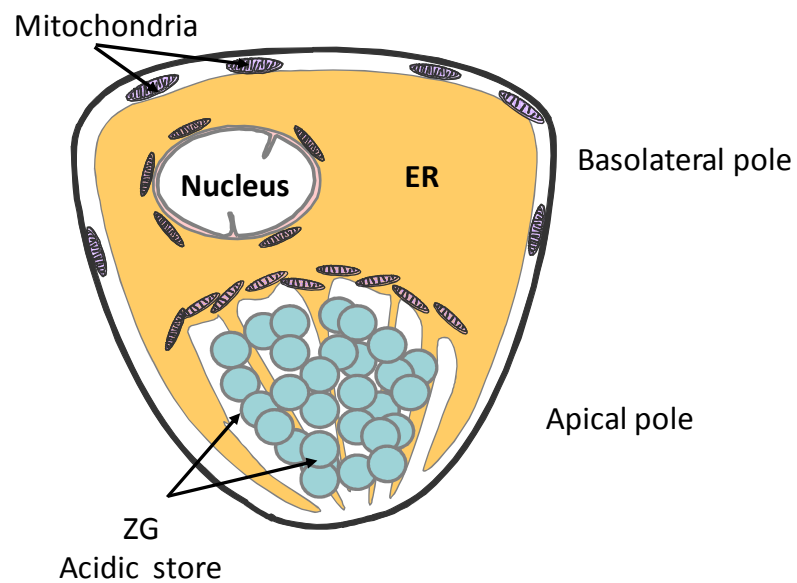


**Fig. 1.2. Structure of a pancreatic acinar cell**

(A) Transmitted light image from the confocal microscope showing a typical pancreatic acinar cell doublet isolated from mouse pancreas. (B) Schematic illustration of pyramid-shaped structure of a pancreatic acinar cell. The basolateral pole contains most of the ER; zymogen granules are stored in the apical pole.

---

As was previously mentioned, pancreatic acinar cells produce, store and release three classes of digestive enzymes:  $\alpha$ -amylase, pancreatic lipase and proteases, which perform hydrolysis of carbohydrates, lipids and proteins, respectively. The enzymes are stored and secreted as inactive zymogens and under physiological conditions are only activated by low pH in the duodenum. Since pancreatic acinar cells store and perform controlled release of digestive enzymes, any damage to the organ or impaired regulation of digestive enzyme secretion is potentially very dangerous. Premature enzyme activation inside the cells might lead to autodigestion of the pancreas and injury of other organs and tissues.

### **1.2.2. Synthesis and sorting of secretory proteins**

The actual synthesis of pancreatic digestive enzymes is performed by ribosomes. The process is initiated by formation of a translation complex in the cytosol. Soon after the ER sorting sequence of the growing polypeptide is recognized by a cytosolic protein called SRP (signal recognition particle) and the translation is temporarily inhibited. This allows docking of the ribosome at the ER and interaction between SRP and SRP receptor localized at the ER membrane. This interaction opens a translocon (translation channel) in the ER, which leads to translocation of the growing polypeptide across the membrane to the ER lumen. After their synthesis and folding secretory proteins are targeted into the Golgi network, where they undergo maturation and where they are sorted from the constitutively secreted proteins and packed into the granules. Two models have been proposed to explain this process<sup>7</sup>. The "sorting for entry" model states that there is a specific, pH-dependent recognition of secretory proteins by receptors in the trans-Golgi network, which separates them from other proteins and directs into secretory granules. On the other

---

hand, the "sorting by retention" model assumes that secretory proteins spontaneously aggregate at acidic pH in trans-Golgi compartment, which itself is a signal for their packaging into granules.

Once the dense aggregates of zymogens are formed within the trans-Golgi compartment, they interact with the Golgi membranes. This process eventually leads to their separation as immature granules. However, the factors mediating that interaction have not yet been identified.

### **1.2.3. Membrane fusion and secretion.**

At the plasma membrane, vesicle fusion may occur constitutively or it might be subjected to strict control, as in regulated exocytosis performed by pancreatic acinar cells. In general, exocytosis consists of the same series of events: recruitment of the vesicle to the membrane; tethering at the membrane; priming and fusion<sup>8</sup>.

Among all proteins engaged in exocytosis, SNAREs (soluble N-ethylmaleimide-sensitive factor attachment protein receptors) were shown to be completely indispensable for fusion in all investigated species from yeast to mammals<sup>9</sup>. SNAREs form a superfamily of proteins defined by the presence of characteristic 60 - 70 amino acid sequence, called the SNARE motif, which has high potential to form coiled-coil complexes<sup>10</sup>. There have been 25 SNARE members identified in *Saccharomyces cerevisiae* and 36 members are currently known to be present in humans<sup>11</sup>. Most of them possess a single transmembrane domain located close to the C-terminal end. Some SNAREs have additional domains positioned between N-terminus and SNARE motif. Traditionally, SNAREs have been classified as v- and t-SNAREs, because fusion requires v-SNARE proteins (e.g. VAMP2/synaptobrevin-2)

---

on the vesicle membrane and t-SNAREs (e.g. syntaxin-1, SNAP25) on the target membrane. Another classification of these proteins is based on their structure – mainly, on the central amino acid residue present in the SNARE motif. Since this amino acid can be glutamine (Q) or arginine (R), SNAREs are divided into Q-SNAREs (syntaxin, SNAP25) and R-SNAREs (synaptobrevin)<sup>12</sup>.

Assembly of SNAREs generates the force for membrane fusion – ‘zippering’ of the SNARE proteins from donor and acceptor membranes releases enough energy to overcome hydrophilic barrier that keeps membranes separate<sup>13</sup>. After fusion, both v- and t-SNAREs are present on the target membrane in so called cis-complexes, which are extremely stable. To recover the functional SNAREs that can enter another fusion cycle, the activity of NSF (soluble N-ethylmaleimide-sensitive adapter protein) is required. NSF is an ATPase that binds to SNARE complexes and mediates ATP-dependent conformational change of the complexes leading to their dissociation<sup>14</sup>.

Although SNAREs have been shown to be sufficient to drive fusion *in vitro*<sup>15</sup>, in physiological conditions other proteins interact with SNAREs and enhance the speed of the process. Out of those fusion regulators Sec1/Munc18 (SM) family of proteins is probably the most important. The SM proteins usually contain about 600 amino acid residues and are characterised by high sequence homology, but without any specific motifs. They are soluble cytoplasmic proteins, which bind to SNAREs, becoming an established component of the fusion machinery. Members of SM proteins are present in all investigated species – for example three different Munc18s can be found in mammals, among which Munc18-1 plays the major role in regulated exocytosis. The importance of Sec1/Munc18 proteins is very well demonstrated by the

---

fact that a null mutation of the gene encoding Munc18-1 results in strong fusion defects<sup>16</sup>.

Indeed it has been confirmed that the v-SNARE synaptobrevin-2 is present on the membranes of zymogen granules in pancreatic acinar cells<sup>17</sup>. The cells also contain three isoforms of t-SNARE syntaxin, each of which has a strictly defined distribution. Syntaxin-2 is present on the apical plasma membrane, whereas syntaxin-4 is on the basolateral membrane; and syntaxin-3 is localized only to the zymogen granules<sup>18</sup>. Therefore it is believed that regulated exocytosis in pancreatic acinar cells is dependent on syntaxin-2 and -3. Syntaxin-2 is responsible for the actual release of digestive enzymes mediating fusion between the zymogen granules and the apical plasma membrane. On the other hand, syntaxin-3 is most likely involved in homotypic fusion between granules. An equivalent of neuronal SNAP25, SNAP23 is expressed in many cell types including pancreatic acinar cells. Interestingly, SNAP23 was found on the basolateral membrane and seems to be absent on the apical membrane. Therefore it is unlikely to play a role in enzyme secretion under physiological conditions<sup>19</sup>. This function is probably performed by a still unidentified homologue of SNAP23. Out of three known mammalian isoforms of Munc-18 two of them, Munc-18-2 and -3, have been found in acini<sup>20</sup>. Their exact functions have not yet been studied in detail.

Interestingly, exocrine tissues including pancreas appear to possess a unique protein called syncollin, which is not related to any other protein engaged in membrane fusion. Syncollin was found inside the zymogen granules attached to the inner leaflets of their membranes<sup>21</sup> and it seems to form pH-sensitive oligomers. Syncollin

---

was postulated to regulate exocytosis through binding to syntaxin in calcium-dependent manner<sup>22</sup>.

### **1.3. Calcium signalling in pancreatic acinar cells**

#### **1.3.1. Calcium as an intracellular messenger**

In eukaryotic cells resting cytosolic calcium concentration is maintained around 100 nM, whereas extracellular calcium is as high as 1 mM. This very tight control is possible due to the coordinated functions of various proteins: membrane calcium pumps, channels and exchangers; and proteins that regulate their activity. Sudden changes in cytosolic calcium concentration encode stimulus-induced messages and trigger specific cell responses. There are two major sources of calcium influx to the cytosol that cause  $[Ca^{2+}]$  increase: 1) the endoplasmic reticulum and 2) extracellular environment.

The endoplasmic reticulum is the main intracellular calcium store and the most important regulator of intracellular calcium fluxes. Storage of ER calcium depends on its binding to  $Ca^{2+}$ -binding proteins such as calreticulin or calsequestrin. Movement of calcium across ER membranes is tightly regulated: transport into the ER is dependent on the action of the sarco- / endoplasmic reticulum calcium-ATPase (SERCA), which pumps  $Ca^{2+}$  ions from the cytosol to the ER lumen; whereas efflux is mediated by ligand-activated channels, which transiently release calcium to the cytosol.

Calcium influx from the extracellular space is dependent on the calcium channels located on the plasma membrane. These channels can be divided into three classes

---

based on the mechanism gating: 1) the voltage operated  $\text{Ca}^{2+}$  channels (VOCs), which are found in excitable cells and thus are not present in pancreatic acinar cells; opening of these channels is triggered by a decrease in the plasma membrane potential; 2) the receptor operated  $\text{Ca}^{2+}$  channels (ROCs), which open after binding a specific external ligand; 3) and the second messenger operated channels (SMOCs), which conduct  $\text{Ca}^{2+}$  ions only upon binding a specific second messenger at their cytosolic site<sup>23</sup>.

### **1.3.2. Store operated calcium entry (SOCE)**

The increase in cytosolic calcium above resting values is cleared by the combined activities of extrusion mechanisms, which include components located both at the plasma membrane and the ER. The sarcoplasmic / endoplasmic reticulum calcium-ATPase (SERCA) refills the intracellular stores, whereas the plasma membrane calcium ATPase (PMCA) and the  $\text{Na}^+$ - $\text{Ca}^{2+}$  exchanger (NCX) transport  $\text{Ca}^{2+}$  against its electrochemical potential from the cytosol to the external space. Thus not all  $\text{Ca}^{2+}$  released from the ER is taken back to the store. A substantial portion of that released  $\text{Ca}^{2+}$  is transported out of the cell through the plasma membrane and is inevitably lost. Therefore a specific pathway must exist by which cells can replenish their intracellular calcium stores using extracellular  $\text{Ca}^{2+}$ . In 1986 J. Putney defined the mechanism, where depletion of the intracellular stores triggers  $\text{Ca}^{2+}$  flux from the extracellular space<sup>24</sup>. Initially, the process was named the capacitative  $\text{Ca}^{2+}$  entry (CCE); currently it is referred in the literature as the store operated calcium entry (SOCE). Pharmacological inhibition of the SERCA by reagents such as thapsigargin (Tg) or cyclopiazonic acid (CPA) blocks replenishment of the ER and leads to store depletion due to passive leak of  $\text{Ca}^{2+}$  from the ER<sup>25</sup>. That in turn activates inward

---

calcium flux from the extracellular space identified as  $\text{Ca}^{2+}$  release - activated  $\text{Ca}^{2+}$  current (CRAC). It was clear that the SOCE machinery requires three main components: (1) a regulated channel that mediates  $\text{Ca}^{2+}$  influx, (2) a calcium sensor in the intracellular stores, (3) and an efficient mechanism that allows communication between them. Until recently these components remained a mystery unsolved for almost two decades.

In 2006 S. Feske identified and named ORAI1 ( $\text{Ca}^{2+}$  release-activated  $\text{Ca}^{2+}$  channel protein 1) as the crucial component of SOCE mediating  $\text{Ca}^{2+}$  influx upon store depletion<sup>26</sup>. ORAI1 and other members of the family: ORAI2 and ORAI3 are transmembrane proteins of 28 - 33 kDa<sup>27</sup>. They are highly glycosylated, contain four transmembrane domains, whose C- and N-terminus are located at the cytoplasmic site<sup>28</sup>. Most likely four ORAIs build a functional tetrameric calcium channel<sup>29</sup>.

STIM1 (stromal interaction molecule 1), the ER calcium store sensor, turned out to be GOK protein initially described in 1996<sup>30</sup> and was eventually linked to calcium homeostasis in 2005<sup>31,32</sup>. There are two known mammalian orthologs: STIM1 and STIM2, which both are single pass transmembrane proteins containing two EF hand motifs directed toward the ER lumen<sup>31</sup>. STIM1 is believed to be the actual sensor and responder to ER calcium depletion. Significant decrease in  $[\text{Ca}^{2+}]_{\text{ER}}$  leads to dissociation of  $\text{Ca}^{2+}$  bound to the EF hand motif at the N-terminus of STIM1. This triggers STIM1 association into multimers via SAM (sterile  $\alpha$ -motif) domain and subsequent translocation of STIM1 oligomers within the ER membranes to areas located close to the plasma membrane, which initiates CRAC channel activation<sup>33</sup>. In the literature there is some evidence that STIM1 can also regulate members of TRP channels such as TRPC1<sup>34-36</sup>. STIM1 has also been found inserted into the plasma

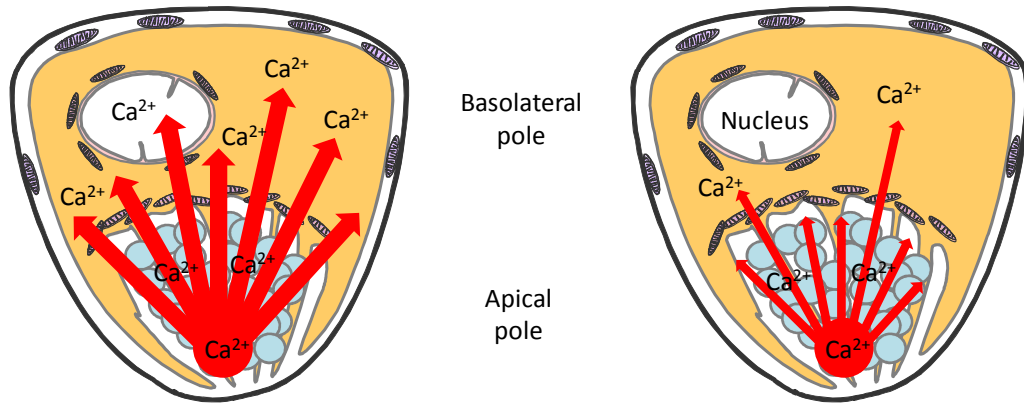
---

membrane; however, it is still not entirely clear what the functional reason of this insertion might be, especially because it does not seem to be required for ORAI regulation<sup>28,33</sup>. The role of STIM2 is less clear. The protein exclusively located to the ER membranes and when expressed at physiological levels it appears to increase SOCE<sup>37</sup>. On the other hand its overexpression leads to decrease in calcium influx<sup>38</sup>. Since STIM2 becomes fully activated earlier during store depletion than STIM1, it was postulated that STIM2 might have regulatory functions sensing basal ER Ca<sup>2+</sup> levels and regulating Ca<sup>2+</sup> influx in response to low intensity stimulation<sup>37,39</sup>.

### **1.3.3. The role of Ca<sup>2+</sup> in physiology and pathology of pancreatic acinar cells**

Physiological functions of pancreatic acinar cells are predominantly controlled by calcium. Calcium also plays an important role in development of pancreatitis<sup>40,41</sup>. Therefore different patterns of cytosolic calcium responses, dependent on calcium release from the intracellular stores, differentiate between physiology and pathology of pancreatic acinar cells. Acetylcholine (ACh) and cholecystinin (CCK) are two secretagogues that control physiological functions of pancreatic acinar cells. They induce various types of intracellular calcium responses depending on the intensity of stimulation. Physiological doses of ACh and CCK evoke small cytosolic [Ca<sup>2+</sup>] oscillations, which are often confined only to the apical area of the cell; or global calcium waves that originate in the apical area and spread toward the basolateral area<sup>42,43</sup>. On the other hand excessive doses of ACh and CCK or treatment with menadione (induction of oxidative stress)<sup>44,45</sup> cause large sustained increases in cytosolic [Ca<sup>2+</sup>], which are toxic and might lead to cell death<sup>40,46</sup> (*Fig. 1.3.A-C*). A specific cell response is strongly dependent on the type of the calcium signal. For

A.



B.

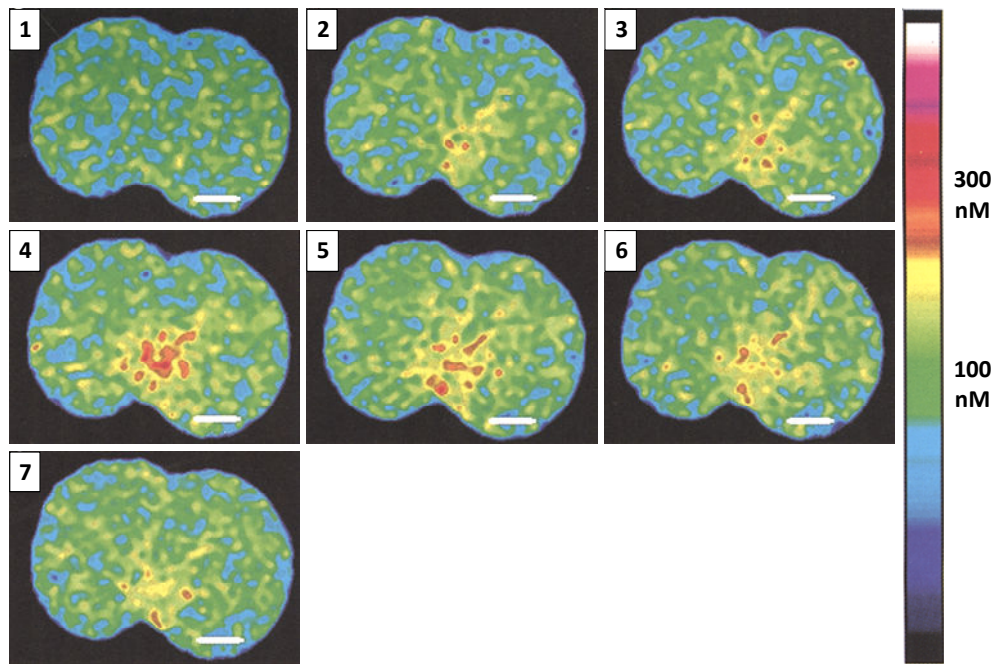
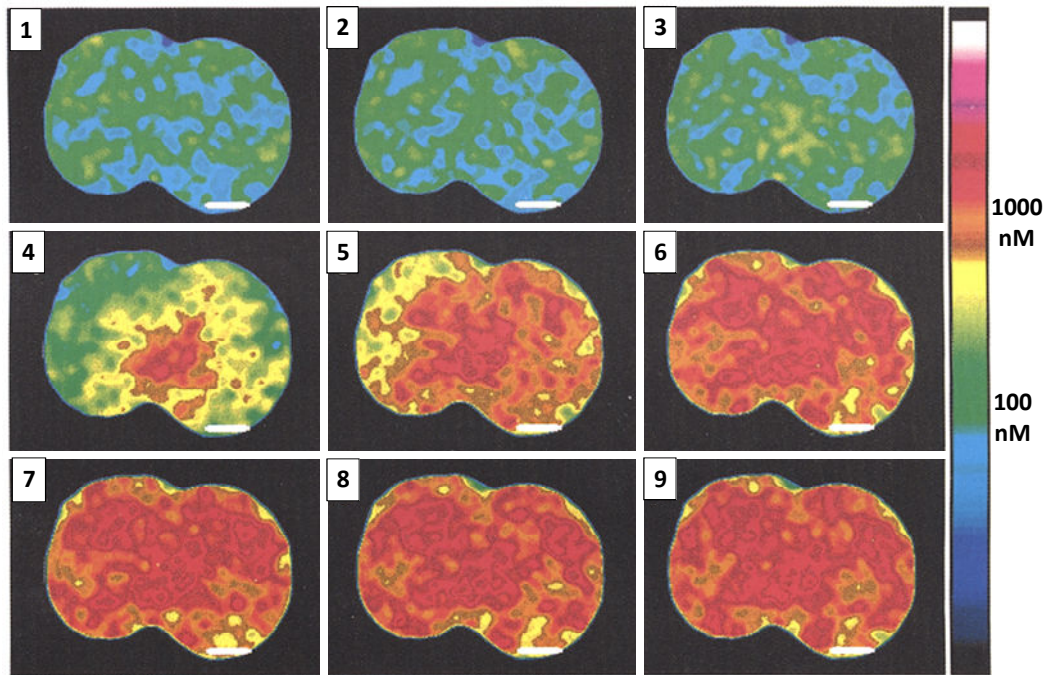


**Fig. 1.3. Physiological and pathological calcium responses in pancreatic acinar cells**

(A) Schematic illustration of differences in pathological (left) and physiological (right)  $\text{Ca}^{2+}$  signals in the cytosol of pancreatic acinar cells. (B) Physiological calcium responses to small doses of ACh in pancreatic acinar cells are restricted to granular area [Adapted from *Gerasimenko OV, 1996*]<sup>47</sup>.

C.



D.

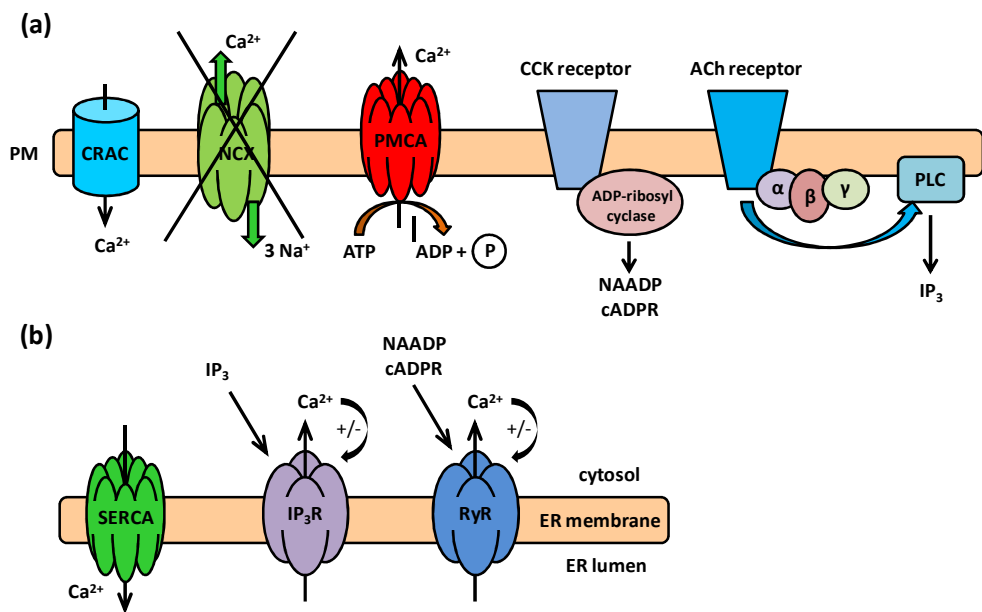


**Fig. 1.3.** (continues)

(C) Excessive doses of ACh induce sustained global  $\text{Ca}^{2+}$  rise in the cytosol of pancreatic acinar cells [Adapted from *Gerasimenko OV, 1996*]<sup>47</sup>. (D) Schematic illustration of calcium signalling events occurring at (a) the plasma membrane, (b) and the ER membrane [Based on *Petersen OH 2006*]<sup>48</sup>. See full description in text.

---

example, local calcium oscillations are associated with enzyme secretion; whereas global calcium waves control gene expression<sup>49</sup>. The receptors for pancreatic secretagogues belong to the family of G-protein coupled metabotropic receptors, which are characterised by seven transmembrane domains (*Fig. 1.3.D*). Many different G proteins are present in pancreatic acinar cells, each of which is composed of three subunits:  $\alpha$ ,  $\beta$  and  $\gamma$ . From that variety of G proteins,  $G_q$  family members mediate responses associated with pancreatic secretion<sup>50</sup>. Upon ligand binding, the intracellular part of the receptor changes conformation and activates the specific G protein by facilitating exchange of GDP to GTP. Activated G protein (usually its  $\alpha$  subunit) triggers production of a specific intracellular second messenger. Upon activation of phospholipase C (PLC) by the  $\alpha$  subunit, phosphatidylinositol 4,5-bisphosphate ( $PIP_2$ ) is cleaved and as a result inositol 1,4,5-trisphosphate ( $IP_3$ ) and diacylglycerol (DAG) are formed. G proteins can also activate ADP-ribosyl cyclase, which catalyses synthesis of cyclic ADP ribose (cADPR) from nicotinamide adenine dinucleotide ( $NAD^+$ ). Both  $IP_3$  and cADPR bind to their intracellular receptors, which effectively are calcium sensitive ligand - gated calcium channels (*Fig. 1.3.D*). That initiates calcium release from the intracellular stores. There are two major types of channels responsible for calcium release from the ER: inositol 1,4,5-trisphosphate receptors ( $IP_3Rs$ ) and ryanodine receptors (RyRs).  $IP_3$  binds to  $IP_3$  receptors and cADPR is an endogenous regulator of ryanodine receptors. Out of three isoforms of RyRs, type 2 and 3 are sensitive to cADPR, whereas type 1 is not<sup>51</sup>. What is more, calcium release induced by cADPR seems dependent on calmodulin<sup>51</sup>. Once generated,  $IP_3$  and cADPR act on  $IP_3Rs$  or RyRs, respectively, which leads to release of calcium from the intracellular stores. This small increase in cytosolic calcium

---

activates even more IP<sub>3</sub>Rs and RyRs leading to further release of calcium from the intracellular stores in a process called calcium-induced calcium release (CICR).

NAADP is another important messenger, synthesized from NADP<sup>+</sup> by the ADP ribosyl cyclase, that has been shown to have calcium releasing potential<sup>51,52</sup>. It is believed that NAADP might mediate its actions through a still unidentified receptor. The existence of this receptor is indicated by the facts that: (1) NAADP can release calcium from a thapsigargin-insensitive store in sea urchin eggs<sup>53</sup>; (2) NAADP-induced calcium release can be blocked by dihydropyridines, gallopamil or diltiazem, which do not affect IP<sub>3</sub>Rs or RyRs<sup>54,55</sup>; (3) it has very specific binding kinetics; (4) and it has capability to undergo self-desensitization<sup>49</sup>. In contrast to IP<sub>3</sub>Rs and RyRs, NAADP receptor does not seem to be sensitive to activation by calcium<sup>56</sup>. However, since effects of NAADP can be blocked by inhibition of RyRs in pancreatic acinar cells it is possible that NAADP also affects RyRs opening<sup>55</sup>.

#### **1.3.4. CCK signalling**

CCK can be considered as a hormone and a neuropeptide at the same time, since it is secreted not only by small intestine endocrine cells after food ingestion<sup>57</sup>, but also by neurons from gastrointestinal tract and central nervous system<sup>58</sup>. There are two types of CCK receptors named as CCK-A and CCK-B (the latter is also called gastrin receptor). In most mammals, including mouse and human, only CCK-A receptor is present in pancreatic acinar cells. CCK-B receptor, whose expression is usually restricted to the brain, can be found in pancreatic acinar cells of only certain species, such as guinea pig and dog<sup>49</sup>.

---

CCK-A receptors are slightly more sensitive to sulfated than unsulfated CCK and are characterised by only very low sensitivity to gastrin. They have two CCK binding sites, one of which binds CCK with high affinity and the other one is a low affinity binding site. The high affinity site stimulates physiological responses of pancreatic acinar cells, including enzyme synthesis and secretion; whereas the low affinity binding site most likely has inhibitory functions<sup>49</sup>. CCK receptors are coupled through G proteins to various enzymes, such as adenylate cyclase and phospholipases C, D and A<sub>2</sub><sup>50,57,59</sup>. Physiological concentrations of CCK (1 - 10 pM), that lead to activation of the high affinity binding site of the receptor, induce calcium oscillations within the pancreatic acinar cell without generating detectable amounts of IP<sub>3</sub>; even though DAG is present (possibly due to breakdown of choline metabolites such as phosphorylcholine)<sup>60</sup>. Only strong stimulation, which activates low affinity site of CCK receptor, leads to intracellular IP<sub>3</sub> production<sup>60</sup>. cADPR is an important and specific calcium releasing messenger of CCK<sup>61</sup>. What is more, NAADP has been proposed to be a second messenger of CCK-mediated actions. Effects of stimulation with physiological doses of CCK can be easily blocked with a cADPR agonist - 8-amino-cADPR<sup>62</sup>.

### **1.3.5. ACh signalling**

Acetylcholine (ACh) is a neurotransmitter present in both the central and peripheral nervous system. Its synthesis is performed in certain neurons by choline acetyltransferase from choline and acetyl-CoA. There are two main types of ACh receptors: (1) nicotinic, which are ionotropic receptors permeable to Na<sup>+</sup>, K<sup>+</sup> and to a lesser extent to Ca<sup>2+</sup>; (2) muscarinic - typical metabotropic receptors, stimulated by both ACh and muscarine and inhibited by atropine. In pancreatic acinar cells ACh

---

binds to M3 type muscarinic receptors at the cell membrane and induces mainly IP<sub>3</sub> production, which releases calcium from the ER through IP<sub>3</sub>Rs<sup>63,64</sup>.

### **1.3.6. Distribution of IP<sub>3</sub>Rs and RyRs in pancreatic acinar cells**

Localization of IP<sub>3</sub>Rs and RyRs in the ER of pancreatic acinar cells is not identical. IP<sub>3</sub>Rs are mainly present in the apical pole of the cell<sup>65,66</sup>, whereas RyRs are evenly distributed at the ER membranes in the apical as well as basolateral area<sup>67,68</sup>. As was previously mentioned, despite the stimulus acting on the basolateral membrane, the calcium response originates in the apical region of the cell. Therefore the observed pattern of calcium responses is due to (1) distribution of calcium release channels in pancreatic acinar cell; (2) Ca<sup>2+</sup> buffering role of mitochondrial belt surrounding the apical area; and (3) phenomenon of calcium-induced calcium release (CICR), where small increase in cytosolic [Ca<sup>2+</sup>] induces further release of calcium from the intracellular stores via activation of additional calcium channels. Accumulation of both IP<sub>3</sub>Rs and RyRs in the granular area is associated with increased sensitivity of this region for CICR as compared to the basolateral pole. This differential sensitivity has been previously demonstrated by local calcium uncaging experiments: calcium uncaged in the basolateral region did not induce CICR; whereas calcium uncaging in the apical area led to a long-lasting CICR type of response<sup>69</sup> (*Fig. 1.4*). IP<sub>3</sub>Rs and RyRs are both necessary for CICR because inhibitors of each of the receptors effectively prevented CICR triggered by local release of caged calcium<sup>69</sup>.

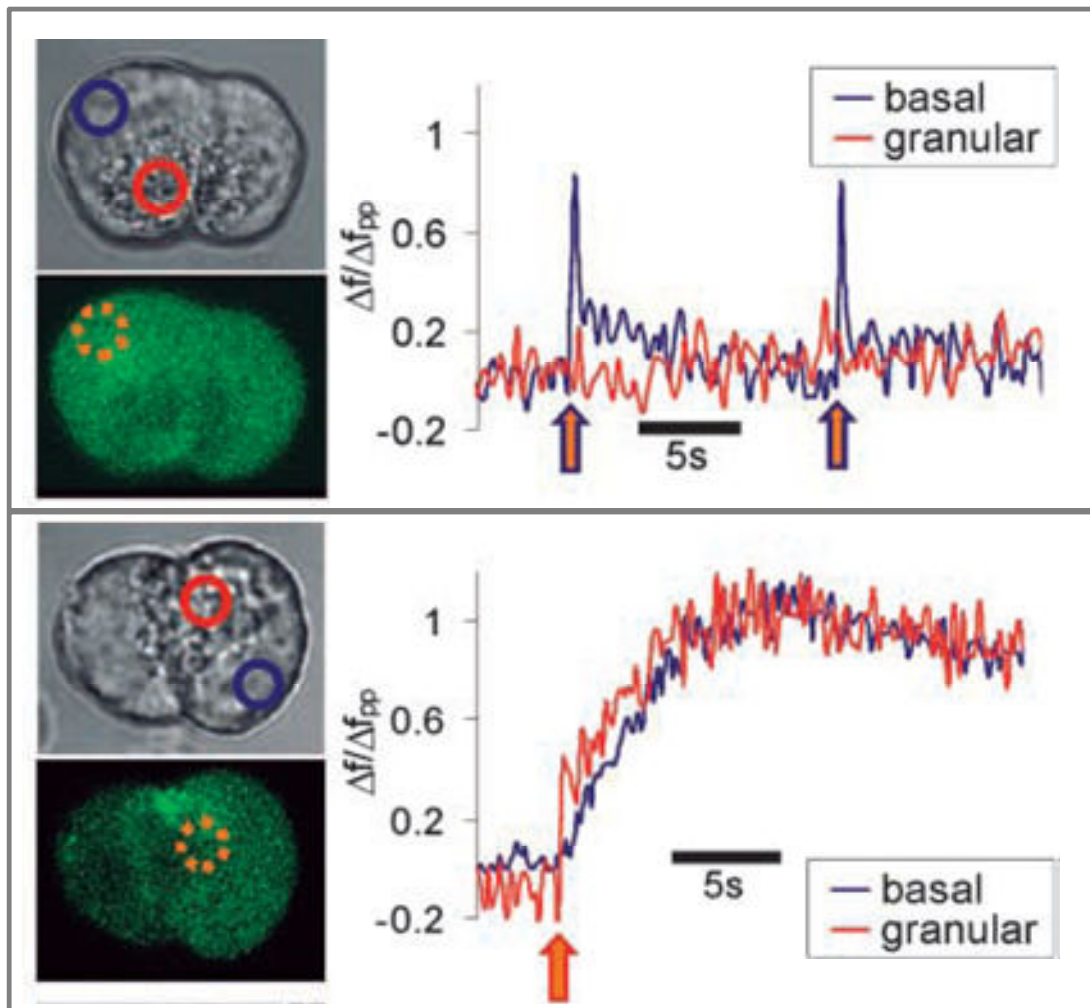


**Fig. 1.4. Local calcium uncaging experiments**

Experiments of  $\text{Ca}^{2+}$  uncaging in different parts of pancreatic acinar cells demonstrate that different sensitivity of granular and basolateral areas to CICR. Blue traces represent  $\text{Ca}^{2+}$  responses recorded in basolateral region and red traces - in granular area [Adapted from *Ashby M, 2002*]<sup>69</sup>. See description in text.

---

## 1.4. Calcium Imaging

Application of calcium-sensitive fluorescent probes made possible the real-time detection of  $[Ca^{2+}]$  changes inside the cell, in cytosol as well as in various cell compartments. A simple detection system can be composed of a fluorescence microscope, a relatively sensitive CCD camera and a computing hardware able to store and process recorded images. Application of confocal microscopes gives an advantage of significantly better spatial resolution over conventional fluorescence microscopes; and is suitable for more advanced tasks, when for example imaging of small organelles is required<sup>70</sup>. Having a confocal pinhole makes the microscope reject out of focus fluorescent light from the specimen, which effectively leads to acquisition of light from only a thin section of the sample.

### 1.4.1. Basis of fluorescence

Fluorescence is a type of luminescence, the term which is used to describe the property of certain molecules, called fluorophores, to emit light upon excitation as a result of absorption of electromagnetic radiation<sup>71</sup>. The process of fluorescence takes place only when emission of the photon by a fluorophore is associated with its return to the ground state from an excited singlet state. Such transitions are permitted and happen relatively quickly; therefore fluorescence is a rapid process that takes place on a timescale of nanoseconds.

The photons of electromagnetic radiation absorbed by fluorophores are always of certain energy range (which corresponds to the certain wavelength), that is equal to the energy needed for promotion of an electron in the ground state of the fluorophore

---

to one of the vibrational levels of an excited state, usually the first excited state  $S_1$ . Immediately after absorption of a photon several processes may occur, but the most common is transition to the lowest vibrational energy levels of the state  $S_1$ . This phenomenon is defined as vibrational relaxation or internal conversion and describes loss of energy in a form of kinetic energy (in the absence of light emission) due to collisions with other molecules. Internal conversion usually occurs within picoseconds. Transition of the molecule from the lowest vibrational levels of excited singlet state to one of the vibrational energy levels of the ground singlet state  $S_0$ , accompanied by emission of a photon constitutes the principle of fluorescence. Energy of the emitted photon will be equal to the difference in energy of the levels between which the transition took place. Since the distance between the vibrational levels of the excited state resembles that of the ground state, the emission spectrum of a fluorophore is a mirror image of absorption spectrum, but it is moved to the higher wavelengths (Stokes shift).

Other relaxation transitions may occur and they compete with the process of fluorescence. The energy of the excited state can be lost either as heat or as kinetic energy upon collisions with other molecules. What is more, an interesting phenomenon called intersystem crossing can take place with a low probability. Intersystem crossing defines the transition between the lowest excited singlet state and the lowest excited triplet state. This process may result in emission of a photon through phosphorescence upon transition from the  $T_1$  (excited triplet state) to the  $S_0$  (ground singlet state). Since such transitions are effectively forbidden, phosphorescence is much slower than fluorescence ranging from milliseconds to seconds. Alternatively, a transition from the excited triplet state back to the excited

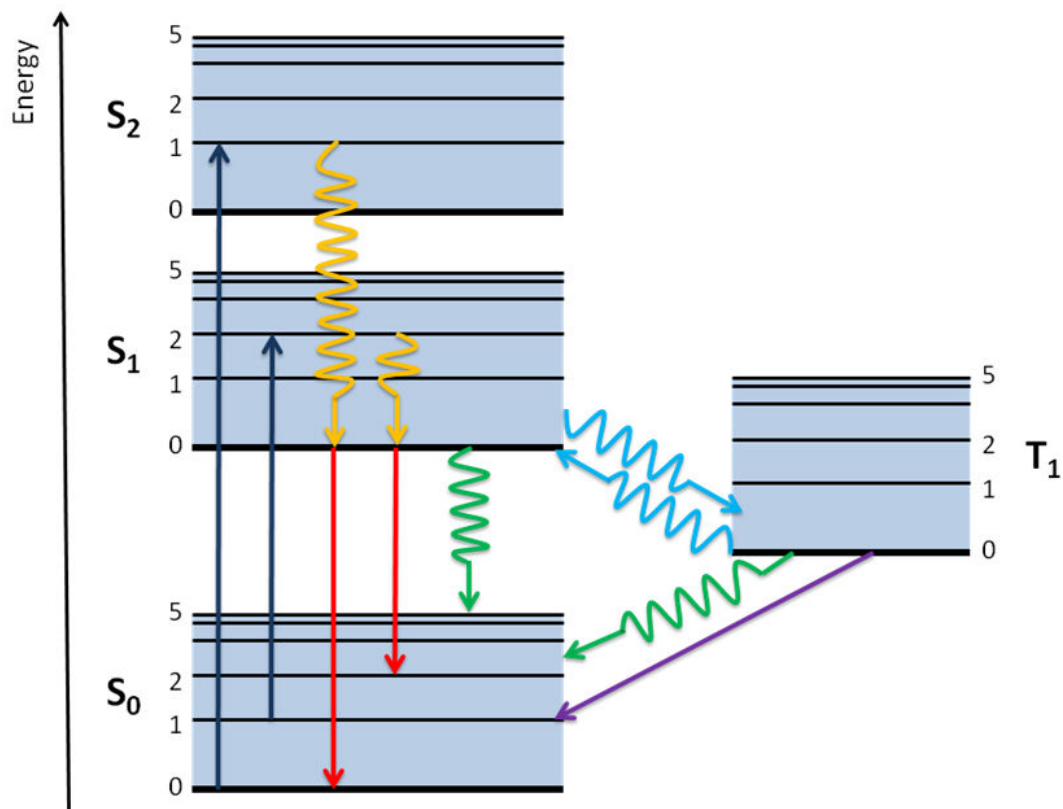


**Fig. 1.5. Schematic illustration of Jablonski Energy Diagram**

Dark blue arrows represent absorption / excitation ( $10^{-15}$  s); orange arrows - vibrational relaxation ( $10^{-14}$  -  $10^{-11}$  s); red arrows - fluorescence ( $10^{-9}$  -  $10^{-7}$  s); light blue arrows - intersystem crossing; green arrows - non-radiative relaxation and violet arrow - phosphorescence ( $10^{-3}$  -  $10^2$  s).

---

singlet state can occur, which causes delayed fluorescence. All described transitions are presented on Jablonski Energy Diagram (*Fig. 1.5*).

Most fluorophores can be excited multiple times repeating the excitation - emission cycles till they are eventually photobleached, which results in destruction of fluorophore and thus loss of fluorescent response upon excitation.

#### **1.4.2. Calcium-sensitive fluorescent probes**

Three types of calcium sensitive fluorescent probes can be distinguished: (1) fluorescent dyes, (2) recombinant aequorins, (3) probes based on green fluorescent protein (GFP) and its engineered analogues<sup>70</sup>.

Currently used fluorescent dyes for  $\text{Ca}^{2+}$  imaging were derived from popular ion chelators such as bis-(2-aminophenoxy)-ethane tetraacetic acid (BAPTA) or bis-(2-aminoethyl ether) tetraacetic acid (EGTA)<sup>72</sup>. The chelator backbone is responsible for  $\text{Ca}^{2+}$  binding and is conjugated to a fluorescent residue. Calcium-sensitive fluorescent dyes can be divided into different groups depending on their physical and chemical properties such as absorption / emission spectrum (UV light- vs. visible light- excited indicators; ratiometric vs. non-ratiometric dyes) and  $K_d$  value (high affinity vs. low affinity for  $\text{Ca}^{2+}$ ).

For efficient delivery of fluorescent indicators into the living cells, the probes need to be able to penetrate the plasma membrane, and / or the intracellular membranes when loading to organelles is required. For that purpose carboxylic acid moieties are chemically modified with acetoxymethyl (AM) groups resulting in uncharged molecules that more efficiently cross cell membranes. Inside cells, AM groups are removed by nonspecific esterases, which again apply charge to the molecule of

---

indicator preventing its leak from the cell. However, use of AM esters forms of calcium indicators is associated with a problem: hydrophobic AM esters are poorly soluble in aqueous solution. Therefore to support efficient cell loading often dispersing agents are used, such as Pluronic F-127.

Ratiometric calcium indicators are characterised by a shift in either excitation or emission spectral peak upon  $\text{Ca}^{2+}$  binding. This property is very useful as it allows recording of ratio of fluorescence measured at two different wavelengths. Depending on the type of the dye either fluorescence is measured at one emission peak upon two sequential excitations at different wavelengths, or one excitation results in two emission peaks - for high and low calcium conditions. Ratiometric measurements compensate for various artefacts such as photobleaching, differences in loading or cell thickness. The most widely used ratiometric dyes include fura-2 and indo-1. Fura-2 is relatively photostable, easy to load and, with  $K_d = 224$  nM, is useful for detecting  $\text{Ca}^{2+}$  changes in physiological range<sup>73</sup>. For ratiometric measurement with fura-2, sequential excitation at 340 nm and 380 nm is often used and fluorescence is recorded at about 510 nm. Upon calcium binding the excitation maximum is shifted to 340 nm. In contrast to fura-2, indo-1 has a single excitation peak at 338 nm but dual emission peak, which shows a shift from 485 nm to 405 nm upon calcium binding<sup>73</sup>.

Alternatives to UV-excited ratiometric calcium indicators are long-wavelength dyes, which lack  $\text{Ca}^{2+}$ -dependent spectral shifts, but show changes in fluorescence intensity. Although such calcium indicators do not allow ratiometric measurements they offer an advantage of lower autofluorescence. Fluo-4 is frequently used as a non-ratiometric calcium indicator, whose excitation peak is at 488 nm and emission

---

peak is at 515 nm<sup>74</sup>. It is characterised by lower affinity for calcium than fura-2 ( $K_d = 345$  nM) and very low fluorescence in unbound state<sup>74</sup>. For ratiometric measurements it is possible to combine fluo-4 with another dye such as fura red, which exhibits opposite shifts in fluorescence intensity upon  $Ca^{2+}$  binding. Alternatively use of  $Ca^{2+}$ -insensitive dye together with fluo-4 provides a reference line for semi-ratiometric measurements.

The second group of calcium indicators is based on luminescent recombinant aequorins originally obtained from jellyfish *Aequorea victoria*<sup>75</sup>. In this organism aequorin is a protein working together with GFP to produce bioluminescent green light. Aequorin consists of: non-luminescent apoaequorin of a size of 21 kDa; and coelenterazine - a tightly bound prosthetic group (0.4 kDa).  $Ca^{2+}$  binding to aequorin induces peroxidation of coelenterazine that breaks the link between apoaequorin and coelenterazine, which is associated with emission of a single photon of blue light (emission peak at 470 nm). This blue light normally in the jellyfish excites acceptor GFP utilizing the biophysical process called bioluminescence energy transfer (BRET), which eventually leads to emission of green fluorescence by *Aequorea victoria*. The rate of aequorin peroxidation exhibits dependence on  $Ca^{2+}$  concentration within certain  $Ca^{2+}$  range (less than 100  $\mu$ M)<sup>75</sup>. Recombinant apoaequorin can be expressed in various cell types or even specifically targeted to organelles; addition of exogenous coelenterazine leads to reconstitution of fully working holoprotein. However, a serious limitation of aequorin applications is the irreversible nature of the peroxidation reaction. Therefore during a single experiment only one photon of blue light can be collected from one photoprotein molecule. For

---

that reason during recent years fluorescent calcium dyes have gained more appreciation and popularity than aequorin-based probes.

The third type of calcium indicators is based on another protein of *Aquorea victoria*: green fluorescent protein (GFP). GFP absorbs short wavelength light (blue) and emits light of a longer wavelength (green)<sup>76</sup>. It has a structure of a beta barrel constructed from a single  $\beta$ -sheet surrounding  $\alpha$ -helix that contains chromophore formed by the tripeptide Ser65-Tyr66-Gly67<sup>77</sup>. Spontaneous formation of the chromophore means that no other non-peptide cofactors are required for fully functional protein, and that all elements needed for fluorescent properties are encoded by a single gene. Therefore engineered versions of GFP can be easily expressed in various cell types and cell compartments. Targeted mutagenesis helped to improve GFP expression in mammalian cells by replacing rare codons in gene sequence with those that are more common. Further, "enhanced" versions of GFP were created, which exhibit increased light emission upon excitation. Eventually, substitution of certain amino acids in chromophore group or in its neighbourhood led to development of the whole family of fluorescent proteins, which includes blue BFP (Y66H), cyan CFP (Y66W) and yellow YFP (T203Y).

Currently GFP-derived fluorescent proteins have multiple applications. They can be used as fluorescent tags for visualisation and tracking various proteins inside living cells<sup>78,79</sup>. They might also serve as a tool for assessment of transfection efficiency both in prokaryotic and eukaryotic cells<sup>80</sup>. Applications of fluorescent proteins are even extended by the process of fluorescence resonance energy transfer (FRET), which can take place between two different fluorescent proteins when emission spectrum of the donor protein overlaps with the excitation spectrum of the acceptor

---

protein. Additionally, another requirement for FRET to occur is close location of the donor and acceptor proteins, usually in the range of a few nanometres. Among other uses, FRET found an application in intracellular  $\text{Ca}^{2+}$  concentration monitoring. For this purpose reporters, called cameleons, were developed in the laboratory of Roger Y. Tsien and subsequently improved<sup>81-83</sup>. Cameleons usually consist of two fluorescent proteins capable of FRET, connected with a linker composed of N-terminal fragment of calmodulin and M13 peptide, which associated with calmodulin in a  $\text{Ca}^{2+}$ -dependent manner<sup>84,85</sup>. Calcium binding by cameleon changes the orientation of fluorescent proteins and increases FRET between them, which can be observed as increased signal from the acceptor and decreased signal from the donor. cameleon can be expressed inside the cytosol of living cells or specifically targeted into cell compartments and thus it can be used as ratiometric calcium indicator.

## **1.5. Diseases of pancreas**

The most common pancreatic acinar cell dysfunctions include pancreatitis (chronic and acute) and pancreatic cancer. Among them acute pancreatitis is the most frequent disease of pancreas and pancreatic cancer is the most fatal.

### **1.5.1. Pancreatic cancer**

Pancreatic cancer is a malignant neoplasm of pancreatic tissue. Up to 99 % of the cases of pancreatic cancer are associated with the exocrine pancreas, with ductal adenocarcinoma being the most common<sup>86</sup>. Pancreatic cancer has a very poor prognosis, with survival rate lower than 5 % in five years post diagnosis. One of the main problems is detection of pancreatic cancer. Since it gives no obvious symptoms

---

in early stages of development and in late stages the symptoms are nonspecific (such as abdominal pain, loss of appetite, vomiting or jaundice) pancreatic cancer is often called a "silent killer".

Causes of pancreatic cancer are still not clear. Several risk factors have been identified, including smoking, obesity, diabetes or *Helicobacter pylori* infection<sup>87</sup>. Also the incidence of pancreatic cancer increases with age, affects more males than females, and is substantially potentiated by chronic pancreatitis.

Up to now there is no effective cure against pancreatic cancer. Treatment approach depends of the stage of development and localization of the cancer. Malignancies of the tail of pancreas can be surgically removed. When the cancer is localized to the head of pancreas, the surgery aims to remove both pancreatic head and a fragment of duodenum attached to it. Surgery is often followed by chemotherapy with gemcitabine. Gemcitabine is also used for palliative treatment in patients who do not qualify for surgical intervention.

### **1.5.2. Acute pancreatitis**

Acute pancreatitis affects annually on average 1 individual out of 2000<sup>88</sup> and continues to increase showing a strong correlation with chronic heavy alcohol intake and gallstones<sup>89</sup>. Initial symptoms usually include severe upper abdominal pain, nausea and vomiting<sup>90</sup>. Approximately one out of four patients suffering from pancreatitis develops even more severe stage of the disease, characterised by extensive pancreatic necrosis or even a systemic inflammatory response, which often leads to injury of multiple organs and eventually to death<sup>90</sup>. Currently there is still no effective pharmacological treatment available, which could specifically and

---

effectively target and cure pancreatitis. Developed stages of the disease with infected pancreatic necrosis are an indication for surgical intervention<sup>91</sup>.

Acinar cell injury has been found to be very often associated with migrating gallstones. According to the hypothesis gallstones might obstruct the common channel (which binds common bile duct and the pancreatic duct) and therefore they can potentially induce biliary reflux into the pancreas<sup>92,93</sup>. Some findings indicate that bile salts can be toxic for pancreatic acinar cells and induce pancreatic cell death<sup>94</sup>. In contrast, other findings do not support a role of biliary reflux in the pathogenesis of gallstone-induced acute pancreatitis, indicating that high pressure of bile would be crucial for pancreatic injury to occur<sup>93</sup>. What is more, the size of the common channel seems to be too short for efficient bile reflux<sup>95</sup>. Therefore although association of acute pancreatitis and gallstones is very strong, the exact pathogenesis of gallstone-induced pancreatitis remains unclear.

Alcohol abuse is known to be associated with acute as well as chronic pancreatitis. Risks of developing pancreatitis show a linear increase with the amount of alcohol intake<sup>96</sup>. However, since only a small fraction of alcoholics suffers from pancreatitis, additional factors are required for the effective development of the disease<sup>97</sup>. Effects of ethanol on pancreatic cells have been studied in several animal models, mainly in rodents. It was demonstrated that ethanol both infused in vivo to rats or given simultaneously with high fat diet causes vacuolisation, inflammation and oedema of the pancreas<sup>98,99</sup>. However, now it is believed that the main source of acinar injury lies not in ethanol itself but in its non-oxidative metabolites - fatty acid ethyl esters (FAEEs)<sup>100</sup>.

---

Pancreas can metabolise ethanol through two pathways: oxidative and non-oxidative. In the oxidative pathway, ethanol is converted to acetaldehyde by an enzyme called alcohol dehydrogenase (ADH). Oxidation of ethanol is associated with the formation of reactive oxygen species (ROS), which are short-lived, extremely reactive and thus potentially harmful. Under normal conditions cells efficiently remove ROS via reactions catalysed by catalase, peroxidases or superoxide dismutase. However, oxidative stress caused by an imbalance between ROS and protective mechanisms of the cell can result in induction of pancreatic cell death.

FAEEs are products of non-oxidative pathway of ethanol metabolism. They are formed by pancreatic ester synthases from ethanol and fatty acids. It has actually been shown that FAEEs are produced in pancreatic acinar cells upon ethanol treatment<sup>101,102</sup>. They have been found to promote trypsinogen activation in rat pancreatic acinar cells and extracellular matrix deposition in pancreas<sup>103-105</sup>. Potentially, FAEEs can utilize a different mechanism of toxicity<sup>93</sup>. For example, having a hydrophobic component, FAEEs may physically interact with cellular or lysosomal membranes destabilizing them<sup>106</sup>. FAEEs might also support inflammation in pancreas by promoting induction of NF- $\kappa$ B and AP-1, which are transcription factors regulating pro-inflammatory cytokine production<sup>101</sup>. Further, FAEEs might be hydrolysed to fatty acids (FAs), which are involved in induction of mitochondrial dysfunction<sup>107</sup>. And, importantly, FAEEs and FAs significantly affect calcium homeostasis in pancreatic acinar cells.

Both FAEEs and FAs have been demonstrated do induce slow but substantial increase in cytosolic calcium concentration in pancreatic acinar cells<sup>100</sup>. FAEEs release calcium from the ER,<sup>108</sup> most likely via activation of IP<sub>3</sub>Rs<sup>109</sup>. On the other

---

hand, FAs might block ATP production in mitochondria, which would inhibit ATP-dependent  $\text{Ca}^{2+}$  pumps in the plasma membrane and the ER, and as a result - calcium extrusion from the cytosol<sup>109</sup>.

It is agreed, that acinar cell death represents a key event in pathology of acute pancreatitis. Importantly, severe acute pancreatitis involves extensive acinar cell necrosis, but only very little apoptosis<sup>110</sup>. On the other hand, cases of mild acute pancreatitis were found to be associated with apoptotic acinar cell death rather than necrotic<sup>110</sup>. Therefore it is now believed that the balance between apoptosis and necrosis can influence the severity of the disease<sup>111</sup>. It has been even observed that pancreatic acinar cells might be protected against cerulein-elicited pancreatitis by induction of apoptosis<sup>112</sup>.

## **1.6. Cell death**

Cell death can be a physiological process as well as a pathological event. Therefore, it can be divided into two main categories: apoptosis and necrosis. Necrosis is a form of uncontrolled premature cell death induced by severe external stimuli, such as an injury, inflammation or chemical agents. In contrast, apoptosis is a mechanism of programmed cell death, which is tightly regulated, dependent on different stimuli and cellular insults and, as a physiological process, it is essential for successful development and tissue homeostasis. Apoptosis serves in removal of damaged or excessive cells during embryogenesis and is crucial for fighting infections. The importance of strict control of cell death can be demonstrated by the facts, that failure to eliminate undesired cells leads to cancer or various autoimmune diseases; on the other hand, excessive cell death is characteristic for degenerative disorders<sup>113</sup>.

---

Generally, apoptosis can occur via two pathways: intrinsic (classical, mitochondrial) and extrinsic (receptor-mediated). They both consist of cascades of events that lead to membrane blebbing, DNA fragmentation, cell shrinkage and removal of the dead cells from the tissue. These events are not present in necrosis, during which the intracellular content is released from the cell usually triggering inflammation and tissue damage<sup>114</sup>. The crucial mediators of apoptosis are caspases (cysteiny-l-aspartic acid proteases), which can function as initiators of the cascade (caspase 8 and 9) that eventually leads to activation of executioner caspases (caspase 3, 6 and 7) responsible for proteolytic cleavage of target proteins.

From the two above described apoptotic cell death pathways, only the intrinsic pathway is tightly regulated by Bcl-2 family proteins. It is triggered by various cytotoxic insults including viral infections, DNA damage and deprivation of growth factors. Activation of intrinsic pathway is a result of alteration of mitochondrial function and structure – pro-apoptotic Bcl-2 proteins, Bax and Bak, are believed to initiate the outer mitochondrial membrane permeabilization, which leads to the formation of PTP (permeability transition pore). As a result, apoptogenic factors, such as cytochrome c, are released from the mitochondria<sup>115</sup>. Cytochrome c is then involved in the formation of Apaf-1 complex that promotes activation of caspase 9<sup>116</sup>, which in turn activates the downstream executioner caspases 3, 6 and 7. The second apoptotic pathway, the extrinsic pathway, does not involve Bcl-2 proteins. It is dependent on the activation of death-receptors, such as TNF-R, Fas and other related receptors<sup>117</sup>. This leads to activation of the initiator caspase 8, which subsequently activates the downstream effector caspases. Importantly, caspase 8 can not only cleave the downstream caspases, but also Bid, a proapoptotic protein.

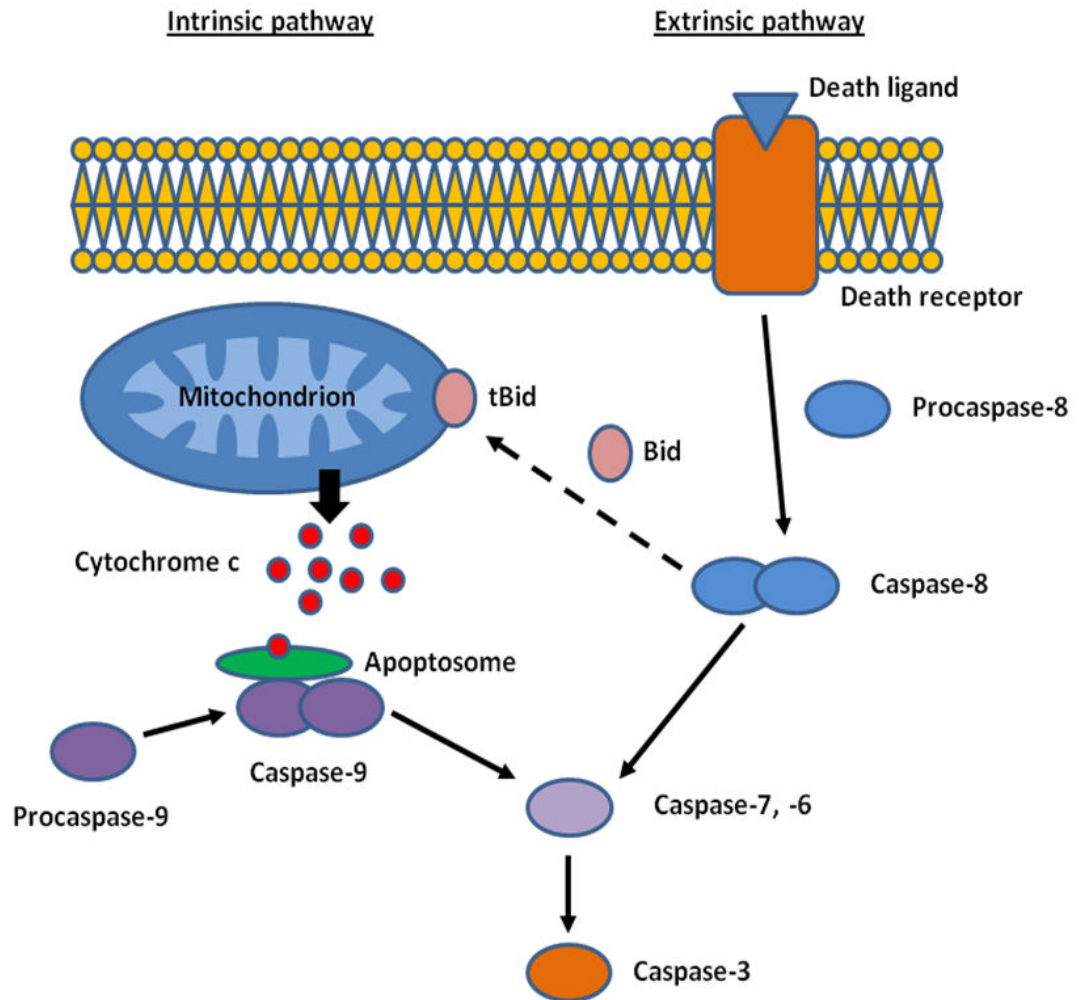


**Fig. 1.6. Schematic illustration of intrinsic and extrinsic apoptotic pathways** (full description in text).

---

C-terminal truncated Bid (t-Bid) translocates to mitochondria and causes cytochrome c release, which promotes further caspase activation (caspase 9 and then 6, 7 and 3)<sup>118</sup>. This mechanism constitutes an important crosstalk between intrinsic and extrinsic pathways (see *Fig. 1.6*).

### **1.7. Bcl-2 family proteins**

The Bcl-2 (B cell lymphoma-2) family proteins are the most important regulators of intrinsic apoptotic pathway. Based on their structure and functions they are grouped into three classes: (1) Inhibitors of apoptosis (Bcl-2, Bcl-xl, Bcl-w, Mcl-1, A1); (2) pro-apoptotic proteins (Bax, Bak); (3) and divergent class of BH3-only proteins (such as Bad, Bid, Bik, Bim, PUMA and other members) (*Fig. 1.7*). Almost all anti-apoptotic Bcl-2 proteins contain four BH (Bcl-2 Homology) domains along with a single transmembrane domain. Pro-apoptotic proteins have three BH domains (BH1-3); and BH3-only members, as the name suggests, are characterised by the presence of only one conserved BH3 domain.

Current general understanding of the process of apoptosis induction states that various cytotoxic insults result in transcriptional or post-transcriptional activation of one or more BH3-only proteins, which in turn interact with other Bcl-2 family members leading to activation of proapoptotic Bax and Bak. The latter pro-apoptotic Bcl-2 family members are crucial for induction of outer mitochondrial membrane permeabilization, which is a key event in intrinsic apoptotic pathway. Pro-apoptotic Bax and Bak undergo conformational changes followed by oligomer formation and their insertion into the outer mitochondrial membrane.

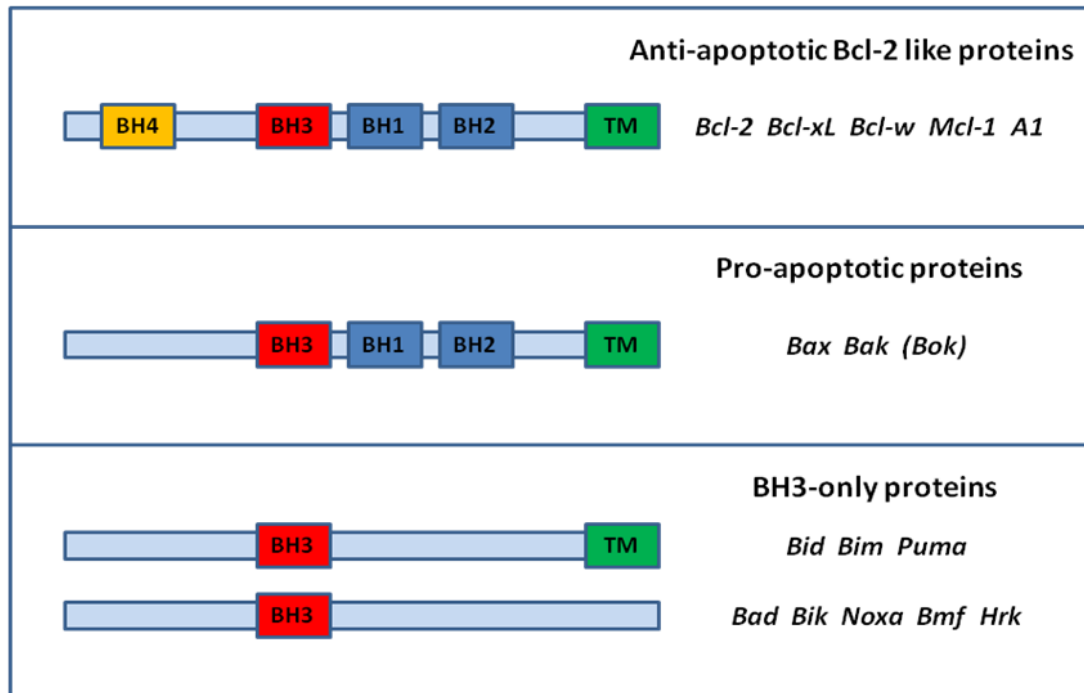


**Fig. 1.7. Schematic domain structure of Bcl-2 family proteins**

Anti-apoptotic proteins possess BH1 - BH4 domains; pro-apoptotic proteins have three BH domains: BH1 - BH3; and BH3-only proteins are characterised by only one BH3 domain.

---

### 1.7.1. Bcl-2 family members

In all mammals there are five pro-survival Bcl-2 family members that antagonise the pro-apoptotic functions of Bax and Bak. These are: Bcl-2, Bcl-xL, Bcl-w, Mcl-1 and A1. They exhibit different tissue distribution and are involved in control of specific processes. For example Bcl-2 is crucial for survival of lymphocytes<sup>119</sup>; Bcl-xL regulates embryogenesis of neuronal cells and erythroid progenitors<sup>120</sup>; whereas Bcl-w controls spermatogenesis<sup>121</sup>.

Bcl-2 protein, the first member of the whole family, was identified in 1980s during analysis of a frequent chromosomal translocation in B cell lymphoma<sup>122</sup>. In those cells a portion of chromosome 18 with the actual *bcl-2* locus translocates onto 14th chromosome in the way that places the *bcl-2* gene under the control of antibody heavy chain gene enhancer. Another pro-survival protein Bcl-xL was the first family member, whose three dimensional structure was determined by NMR and X-ray crystallography<sup>123</sup>.

Pro-survival Bcl-2 proteins contain N-terminal BH4 domain followed by so called "Bcl-2 core"<sup>124</sup>, which is common for anti-apoptotic and multi domain pro-apoptotic proteins. The only exception is Mcl-1, which has N-terminal unstructured domain in a place of BH4 motif. Bcl-2 core is a 20 kDa structure consisting of 7 to 8  $\alpha$ -helices, which in turn compose three BH domains: BH1, BH2 and BH3. Together these domains build up a hydrophobic groove, into which the BH3 domain of pro-apoptotic proteins binds. This interaction is believed to be the hallmark of the mechanism by which pro-survival Bcl-2 members neutralize the apoptotic functions of Bax and Bak.

---

It has been observed that anti-apoptotic proteins bind pro-apoptotic Bax and Bak with different affinities. Bcl-xL and Mcl-1 were found to interact preferentially with Bak<sup>125,126</sup>. In the absence of Bcl-xL and Mcl-1 Bak-mediated apoptosis can proceed<sup>125</sup>. In contrast, Bax interacts with all pro-survival Bcl-2 members; therefore Bax-mediated apoptosis requires neutralization of each anti-apoptotic protein present in a cell<sup>115</sup>.

BH3-only proteins are the initial stress signal responders, which serve as a connection between various stress or cytotoxic stimuli and apoptosis. Every BH3-only member responds to a different set of apoptotic stimuli in its specific manner (described later in the text). What is more, existence of many members of BH3-only proteins provides high degree of redundancy in terms of the response to the signal they recognize.

As was previously stated, BH3-only members have only one BH motif: BH3 domain. Apart from that, at the level of primary protein structure they do not share much similarity with each other or with other Bcl-2 members. BH3 domain usually consists of 9 to 16 amino acids and forms an amphipathic  $\alpha$ -helix<sup>127</sup>. The hydrophobic side of that helix is responsible for the interaction with the hydrophobic pocket formed by BH1-BH3 domains of anti-apoptotic Bcl-2 members. Peptides derived from BH3 domains of certain BH3-only proteins were shown to interact with anti-apoptotic Bcl-2 members. For instance, Bad and Bim peptides have been found to bind to Bcl-xL<sup>128,129</sup>; and Bid peptide have been demonstrated in complex with Bcl-w<sup>130</sup>. What is more, molecular modelling approach revealed possibilities for other partners between anti-apoptotic and BH3-only members<sup>131,132</sup>. Amino acids forming BH3 domains are not strictly conserved. This diversity of BH3 domains seems to be responsible for

---

some binding selectivity of pro-apoptotic and BH3-only proteins to anti-apoptotic Bcl-2 members<sup>133,134</sup>. Consistently, it has been demonstrated that for example Bad and Bmf more specifically bind to Bcl-2, Bcl-w and Bcl-xL; on the other hand Noxa interacts only with A1 and Mcl-1<sup>135</sup>. Further, Puma, Bid and Bim appear to be stronger inducers of cell death over other BH3-only proteins<sup>136</sup>. However, for complete apoptosis induction all BH3-only proteins require Bax or Bak, which underlines the fact that multi-domain pro-apoptotic Bcl-2 members act downstream to BH3-only proteins<sup>137</sup>.

Since pro-apoptotic proteins Bax and Bak have three BH domains they could potentially bind BH3 domain of BH3-only proteins. However, in contrast to very well documented interaction between BH3-only proteins and anti-apoptotic proteins, there is only little data demonstrating BH3-only and pro-apoptotic protein binding. Some of the examples include Bid/Bax and Bid/Bak<sup>138</sup>, or Bim/Bax<sup>139</sup>. What is more, it is not entirely clear whether the whole BH1-BH3 hydrophobic pocket of pro-apoptotic proteins is absolutely required for this interaction<sup>140</sup>.

Since BH3-only proteins are responsible for triggering the process of programmed cell death, their functions and activity require very strict regulation. These proteins are present in cells under normal physiological conditions; however they do not induce apoptosis, because (1) their expression is kept at a very low level which is insufficient for overcoming inhibitory functions of anti-apoptotic Bcl-2; (2) they are inactive and require further post-translational modifications in order to exert their effects; (3) or they are physically separated from mitochondria. Therefore triggering apoptosis usually requires either induction of expression of certain BH3-only proteins (e.g. PUMA, Noxa); or their post-transcriptional alteration such as

---

dephosphorylation (e.g. Bad); release from sequestering proteins (interaction of Bim and Bmf with dynein)<sup>141,142</sup> or proteolytic cleavage that promotes translocation (truncation of Bid by caspase-8 and subsequent translocation of tBid from cytosol to outer mitochondrial membrane)<sup>143</sup>.

Bax (Bcl-2 associated x protein) and Bak (Bcl-2 antagonist killer) belong to pro-apoptotic Bcl-2 members that contain three BH domains: BH1, BH2 and BH3. They both are the main effectors of apoptosis and they are believed to be actively involved in the permeabilization of the outer mitochondrial membrane and the release of cytochrome c. Although their functions appear to be similar, localization of Bax and Bak in healthy cells is different. Bax exists predominantly as an inactive cytosolic monomer<sup>144,145</sup>, whose BH3 domain is hidden inside, and thus is unavailable for interactions with other Bcl-2 protein members. Activation of Bax involves conformational change that exposes the BH3 domain; translocation to the intracellular membranes, predominantly (but not only) to the outer mitochondrial membrane; and subsequent oligomerization<sup>146</sup>. In contrast to Bax, Bak is localized to the mitochondrial membrane even in healthy cells<sup>147,148</sup> and a fraction of it is bound to anti-apoptotic Bcl-2 members (predominantly Bcl-xL and Mcl-1)<sup>125</sup>. Indeed, application of 16-amino acid peptide derived from BH3 domain of Bak protein demonstrated that BH3  $\alpha$ -helix of Bak binds into the hydrophobic pocket of Bcl-xL, formed by its three BH1-3 domains<sup>126</sup>. In contrast, some recent data indicate that in one of the conformations of Bak BH3 domain can also be hidden inside the protein and thus Bak might not be binding anti-apoptotic proteins in healthy cells<sup>149</sup>.

---

### 1.7.2. Apoptosis induction

Early stages of Bcl-2 protein family dependent apoptotic pathway are still intensively debated. Currently there are two models describing how BH3-only proteins transfer apoptotic signal to the mediators of apoptosis. The first one assumes that BH3-only proteins by binding to anti-apoptotic BH1-4 members can 'neutralize' them and displace pro-apoptotic proteins, which leads to activation of the latter. Indeed, Bak fits well into this model. Most of the time Bak is bound to anti-apoptotic proteins, mainly Bcl-xL; and its release is associated with oligomerization. However, activation of Bax cannot be simply explained by 'neutralization' of anti-apoptotic Bcl-2 proteins. Bax has been found in complex with Bcl-2<sup>150</sup>. Nevertheless, as was previously mentioned, a substantial fraction of Bax exists as inactive monomers in the cytosol. Therefore displacement from anti-apoptotic partners cannot be the only requirement for Bax activation.

The second model of apoptosis supports the opposite idea, which explains that activation of Bax and Bak is dependent on direct binding to BH3-only proteins. A BH3-only protein Bid would be a perfect example of such mechanism, since Bid does not interact with anti-apoptotic Bcl-2 members, but maintains interaction with Bax and has strong pro-apoptotic properties. However, there is no strong structural evidence for actual complex formation between pro-apoptotic members and native BH3-only proteins. What is more, such interaction appears to be restricted only to a small fraction of BH3-only members: isoforms of Bim can interact with Bax<sup>139</sup>; and above mentioned Bid, which can bind to Bax and Bak in its processed active form of tBid<sup>138</sup>. Additionally, so far BH3-only proteins have not been detected in oligomers formed by Bax and Bak.

---

Taken the two models together, BH3-only proteins were divided into two subgroups: activators (e.g. Bim and Bid) and sensitizers (eg. Bad, Noxa). Activators activate anti-apoptotic proteins through direct interaction; whereas sensitizers compete for binding site and therefore displace BH3-only activators from pro-survival Bcl-2 members. Since both of these models have limitations and neither of them cannot alone be applied to all BH3-only members, it is possible that neutralization of anti-apoptotic Bcl-2 and direct activation of pro-apoptotic Bax and Bak happen simultaneously and thus can be used to explain induction of intrinsic apoptotic pathway.

### **1.7.3. Subcellular localization of the Bcl-2 family members**

Although their main apoptotic function is associated with mitochondria, Bcl-2 family proteins are present in various intracellular compartments. As was previously mentioned, pro-apoptotic Bax and BH3-only proteins are primarily localized to the cytosol. In contrast, Bak as well as anti-apoptotic Bcl-2 members have a C-terminal hydrophobic transmembrane domain, which anchors them to the intracellular membranes. Bax also contains such transmembrane domain, which most of the time is internalized into hydrophobic core of the protein and becomes exposed only after Bax activation. Accumulating evidence indicate that Bak is present not only on the surface of mitochondria but also at the endoplasmic reticulum<sup>151</sup>. What is more, Bcl-2 and Bcl-xL were found on the mitochondrial membrane, the ER and the nuclear envelope<sup>152,153</sup>.

In the ER Bcl-2 family proteins perform additional functions related to apoptosis. For example they play a role in unfolded protein response, which is an adaptive ER stress

---

response induced by protein misfolding. Pro-apoptotic proteins Bax and Bak were demonstrated to directly interact with one of the ER stress sensor protein - IRE1<sup>154</sup>. This interaction stabilizes IRE1 in its active form and thus enhances unfolded protein response. When the apoptotic stress reaches certain threshold apoptosis is induced.

Anti-apoptotic proteins Bcl-2 and Bcl-xL are involved in regulation of ER stress-dependent autophagy. They were shown to bind beclin-1, which is an essential autophagy inducer<sup>155</sup>. Interaction between anti-apoptotic Bcl-2 / Bcl-xL and beclin-1 inhibits starvation-induced autophagy<sup>156</sup>.

Since the ER is the major intracellular calcium store, Bcl-2 proteins have been proposed to be engaged in the regulation of cellular calcium homeostasis. For example it has been observed that Bcl-2 overexpression decreases Ca<sup>2+</sup> concentration in the ER and diminishes Ca<sup>2+</sup> entry to this cell compartment<sup>157,158</sup>. However, other studies support the opposite effects of Bcl-2 on ER calcium: preservation of ER calcium by upregulation of the SERCA<sup>159</sup>. What is more, the interaction between Bcl-2 and IP<sub>3</sub>Rs is well established and is believed to inhibit calcium release from the ER<sup>160</sup>. On the other hand, overexpression of Bax and Bak (that localize both to mitochondria and ER) leads to mobilization of Ca<sup>2+</sup> from the ER to mitochondria during apoptosis<sup>161</sup>. And cells deficient in these two pro-apoptotic proteins have dramatically reduced calcium concentration in the ER and decreased Ca<sup>2+</sup> uptake by mitochondria. In general, Bax and Bak seem to be involved in regulation of calcium release from the ER, which might contribute to the initiation of apoptosis<sup>162</sup>.

---

## 1.8. BH3 mimetics

Pathways controlling apoptosis are usually altered in cancer cells. Human cancers commonly have different mutations in *p53* tumour suppressor gene, all of which disturb the ability of p53 protein to induce apoptotic cell death<sup>163</sup>. What is more, increased levels of anti-apoptotic Bcl-2 members are found in wide variety of tumours<sup>164,165</sup>. Defective regulation of apoptosis promotes acquisition of further tumorigenic characteristics, such as extensive genetic mutations, extended lifespan, angiogenic and metastatic properties.

Anti-cancer agents induce apoptosis mainly through the mitochondrial pathway regulated by the Bcl-2 protein family<sup>166</sup>. Therefore overexpression of these proteins in cancer is associated with resistance to chemotherapy. Importantly, apoptosis in tumours is almost always affected only upstream of Bax / Bak, whereas downstream apoptotic machinery remains functional<sup>166</sup>. Based on this fact, manipulating the equilibrium between pro- and anti-apoptotic Bcl-2 family members is a promising therapeutic approach. The strategy aiming to inhibit anti-apoptotic functions of Bcl-2 proteins should potentially restore normal apoptotic processes in the tumour cells and make them sensitive to cytotoxic drugs<sup>167</sup>.

Initial attempts to inhibit anti-apoptotic Bcl-2 members involved antisense technology applied in order to block protein translation, unfortunately with little success. Another approach was the application of BH3 inhibitors in order to disrupt the interaction between anti- and pro-apoptotic Bcl-2 members. Initially several short peptides derived from BH3 domains of BH-only proteins were designed. However, due to their limited length the peptides did not have correct helical structure

---

characteristic to native BH3 domains<sup>168</sup>. Longer peptides, on the other hand, usually have unfavourable pharmacological properties (permeability, solubility, bioavailability), which makes their use as therapeutic agents very limited. Replacement of less essential amino acids from the sequence by synthetic amino acids having carbon chain with double bounds and connecting them in metathesis reaction gives the peptides more rigid structure, enhances their helicity, membrane permeability and resistance to serum proteases<sup>169</sup>.

BH3 mimetics are small molecule synthetic inhibitors of Bcl-2 and Bcl-xL. They are terphenyl-based compounds that reproduce spatial arrangement of key amino acids in BH3 domain. They were initially developed as potential anti-cancer agents that would inhibit heterodimerization of anti- and pro-apoptotic Bcl-2 family members, and therefore sensitize cells to apoptosis. In contrast to BH3 peptides, BH3 mimetics seem to have greater therapeutic potential for controlled inhibition of anti-apoptotic Bcl-2 members.

The first BH3 mimetic obtained with aid of molecular modelling and computer screening was HA14-1<sup>167</sup>. It was confirmed that HA14-1 was able to displace Bax protein from Bcl-2 and induce apoptosis in cultured cells, which was characterised by loss of mitochondrial potential and activation of caspases<sup>167</sup>. A family of BH3 mimetics called BH3 inhibitors (BH3Is) was discovered in a fluorescence polarization-based screening<sup>170</sup>. BH3Is contain seven members that belong to two structurally unrelated groups: one group is derived from BH3I-1 and the other one from BH3I-2. All the members of BH3I family were found to displace Bak peptide from Bcl-xL and induce apoptosis with cytochrome c release and caspase

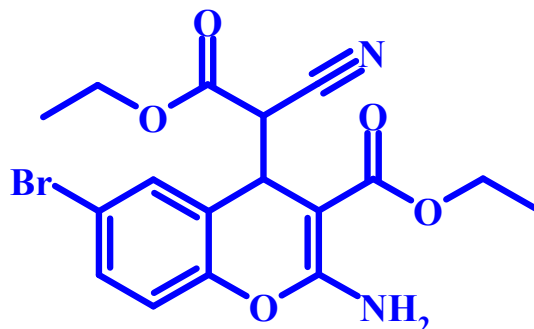
---

activation<sup>170</sup>. *Fig. 1.8* shows molecular structure of two BH3 mimetics described above: HA14-1 and BH3I-2'.

The main application of BH3 mimetics is associated with anti-cancer approach. Overexpression of Bcl-2 protein has been reported in multiple cancer types and it correlates with chemotherapy resistance and poor prognosis<sup>171</sup>. Simultaneous application of a BH3 mimetic and a chemotherapeutic agent could potentially overcome drug resistance in these cancer types increasing the success rate of the treatment. In fact, BH3I-2' and HA14-1 compounds have been demonstrated to act as sensitizers for TRAIL-induced apoptosis in leukemic cells<sup>172</sup>. BH3 mimetic-based therapy might preferentially target cancer cells, since they often exhibit increased sensitivity to inhibition of pro-survival proteins than the normal cells and tissues<sup>173</sup>. What is more, it might be possible to develop BH3 mimetics of the structure that specifically interacts only with the anti-apoptotic proteins overexpressed in target cancer cells<sup>166</sup>.

From perspective of pancreas, BH3 mimetics are a particularly exciting approach, because by their pro-apoptotic properties they can target two serious conditions of the organ: acute pancreatitis and pancreatic cancer. What is more, controlled inhibition of anti-apoptotic Bcl-2 members is a useful tool for investigation of Bcl-2 family protein functions in cellular calcium homeostasis.

**A.**



**B.**

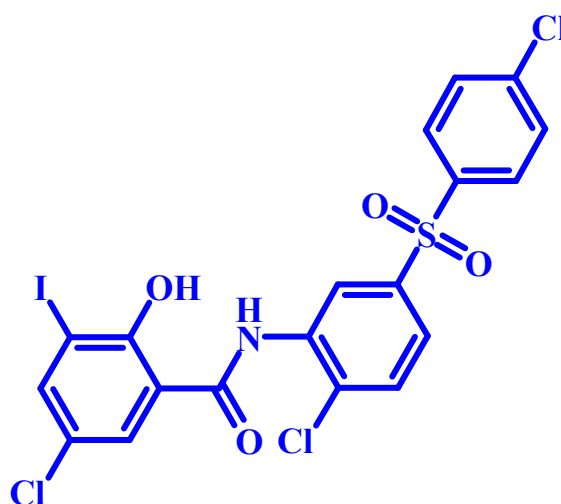


**Fig. 1.8. Chemical structures of BH3 mimetics**

**(A)** HA14-1 = ethyl 2-amino-6-cyclopentyl-4-(1-cyano-2-ethoxy-2-oxoethyl)-4H-chromene-3-carboxylate;

**(B)** BH3I-2' = (3-iodo-5-chloro-N-[2-chloro-5-((4-chlorophenyl) sulphonyl)phenyl]-2-hydroxybenzamide).

---

## 1.9. Aims of the study

The main aim of this study was to investigate the role of Bcl-2 family proteins in calcium homeostasis in pancreas, with particular focus on Bcl-2 itself and Bax. Bcl-2 proteins appear to perform multiple functions in cells. Their mitochondria-related actions are well reported; however Bcl-2 proteins are also engaged in control of ER calcium levels and calcium fluxes in the cell, which are still unclear. Therefore this study aims to determine potential roles of Bcl-2 family members in the regulation of calcium pumps and / or channels as well as their involvement in the passive calcium leak from the intracellular stores. Different strategies, such as pharmacological inhibition of pro-apoptotic Bcl-2 members, knockout mice, techniques of gene silencing and overexpression together with confocal microscopy, are expected to provide reliable experimental data. Investigation of Bcl-2-regulated calcium signalling pathways might shed more light on our understanding of both physiological and pathological processes in pancreatic acinar cells and help to develop new therapeutic approaches against pancreatic cancer and pancreatitis. Importantly, those questions are not exclusive to pancreatic acinar cells, but can be extrapolated to other cell types and different tissues as (1) ubiquitously expressed Bcl-2 proteins; (2) proper regulation of apoptosis; (3) and calcium signalling are important for all cells. Possible involvement of Bcl-2 proteins in regulation of intracellular channels and pumps is particularly exciting; therefore these issues have long been attracting substantial attention in calcium signalling area, but the answer still remains elusive<sup>174,175</sup>. Nevertheless, this thesis focuses mainly on physiology and pathology of pancreatic acinar cells. Therefore it also aims to test the effects of ethanol on the intracellular calcium homeostasis and its role in the pathogenesis of

---

pancreatitis. Alcohol abuse is known to be associated with both acute and chronic pancreatitis; however the mechanisms of ethanol-induced pancreatitis are still unclear. Understanding the actions of ethanol on the cellular functions as well as identification of native cell defence mechanisms against alcohol poisoning might substantially contribute to the development of new therapeutic approaches against pancreatitis.

---

**CHAPTER 2:**  
**MATERIALS AND METHODS**

---

## Chapter 2: Materials and Methods

### 2.1. Reagents and materials

Fluorescent dyes for calcium measurement fluo-4, AM (cat. F14201), fluo-5N, AM (cat. F14204) and fura-2, AM (cat. F1221) and rhod-2, AM (cat. R1245MP) were obtained from Molecular Probes, Invitrogen.

BH3 mimetics were purchased from different sources: HA14-1 (cat. 430-101-M005) was bought from Alexis Biochemicals, Switzerland; BH3I-2' (cat. 286891) from Calbiochem; and gossypol (cat. sc-200501) from Santa Cruz Biotechnology. Ca<sup>2+</sup>-like peptides: CALP-1 (cat. 2090) and CALP-3 (cat. 2321) were obtained from Tocris.

Other chemicals used in experiments, such as caffeine (cat. 205548), thapsigargin (cat. 586005), ionomycin (cat. 407952), 2-aminoethoxydiphenyl borate (cat. 100065) and Ru360 (cat. 557440) were supplied by Calbiochem. Ruthenium red (cat. 1439) was obtained from Tocris.

Collagenase (various batches) for tissue digestion came from Worthington.

Cover glass 32 x 32 mm, thickness No 1 (cat. 631-0129) and cover class 13 mm thickness No 1 (cat. 631-0149) were supplied by VWR International. Trypsin inhibitor TypeI-S from soybean, poli-L-lysine 0.01 % solution (cat. P4832) and acetylcholine chloride (cat. A6625-25G) all came from Sigma; and calcium chloride (cat. 2114) - from Fluka.

---

PCR reagents were supplied by Promega: 5x Green GoTaq reaction buffer (cat. M791B), GoTaq DNA Polymerase 2,500u (cat. M830C), dNTPs mix 10 mM (cat. U151B). Also, all restriction enzymes were purchased from Promega: EcoR I (cat. R4014), Bgl II (cat. R4084) and Hind III (cat. R6041). SYBR<sup>®</sup>Safe DNA gel stain was obtained from Molecular Probes, Invitrogen (cat. S33102) and GelRed nucleic acid gel stain 10,000x from Biotium (cat. 41003). Agarose tablets (cat. BIO-41028), DNA marker HyperLadder I (cat. BIO-33025) and Crystal 5x DNA Loading Buffer Blue (cat. BIO-37045) came from Biotium. Tris Acetate-EDTA buffer 10x (cat. 099K8410) was bought from Sigma. Media for bacterial culture: ImMedia<sup>™</sup> Kan Agar (cat. Q61120), ImMedia<sup>™</sup> Kan Liquid (cat. Q61020), ImMedia<sup>™</sup> Amp Agar (cat. Q60120), ImMedia<sup>™</sup> Amp Liquid (cat. 60020) and SOC Medium (cat. 15544-034) were purchased from Invitrogen.

Tissue culture media and reagents such as RPMI 1640 medium (cat. 21875), FBS (cat. 10108-157), Fungizone (cat. 15290-018), Trypsin-EDTA 0.05% (cat.25300), MEM Amino Acids (cat. 11130) were obtained from GIBCO. PBS (cat. BE17-516F) was bought from Cambrex. 1 M HEPES solution (cat. 17-737F) was purchased from Lonza, Walkersville, MD, USA. PromoFectin 2000 transfection reagent (cat. PK-CT-2000-100) came from PromoKine. Antibiotic Antimycotic Solution 100x containing 10,000 units/ml penicillin, 10 mg/ml streptomycin and 25 µg/ml amphotericin B was obtained from Sigma (cat. A5955).

pEGFP-C1 containing human Bcl-2 insert (often referred later in text as Bcl-2-GFP plasmid) was obtained through Addgene (Addgene plasmid 17999), courtesy of Clark Distelhorst<sup>176</sup>. pcDNA3 expressing human Bcl-2 protein were obtained through Addgene (Addgene plasmid 8768<sup>177</sup>). CellLight Plasma Membrane-RFP

---

BacMam 2.0 was supplied by Invitrogen (cat. C10608). Calcium sensitive ER targeted cameleon D1 probe was a kind gift from Roger Y. Tsien laboratory.

Reagents for specific gene silencing: Bcl-2 siRNA (cat. sc-29215) and control siRNA-A (cat. sc-37007) were obtained from Santa Cruz Biotechnology.

All the other chemicals were supplied by Sigma, unless otherwise stated.

## 2.2. Animals

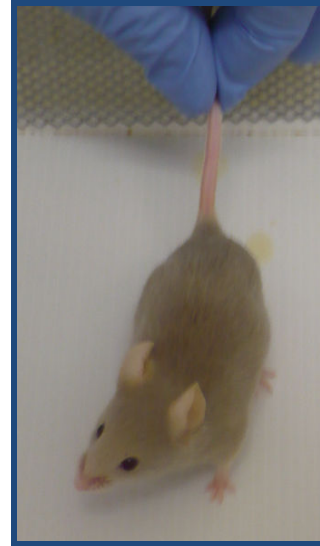
Wild type CD1 male mice and wild type C57BL6/J male mice were supplied by Charles Rivers. Transgenic animals B6.129-Bak1<sup>tm1Thsn/J</sup> (stock no: 004183), B6.129X1-Bax<sup>tm1Sjk/J</sup> (stock no: 002994), B6.129S2-BCL-2 (stock no: 002265) were obtained from Jackson Laboratories and were bred in house: null x null (Bak); or het x het (Bax, Bcl-2). *Fig. 2.1* shows photographs of a wild type C57BL6/J mouse and all three types of transgenic animals used in this study. Bax KO mice (Bax nulls), which contain two alleles of disrupted *bax* gene, do not display immediately noticeable physical features. However, loss of Bax causes cell lineage-specific aberrations in cell death pathway. As a result males are infertile due to aspermatogenesis and thus cannot be used as breeders<sup>178</sup>. Oocyte development in females is relatively normal. Interestingly, the gray coat color loci (*tyr*) and pink eyes (*p*) are both linked to the *bax* gene<sup>179</sup>. Statistically, a Bax null should be 99.6% C57BL/6-like at all loci not linked to the *bax* gene, but they might retain the *tyr* allele and the *p* allele from the 129-derived RAW-4 ES cell line originally used for targeted disruption of *bax* gene. As a result, a small percentage of Bax nulls can be gray in colour and have pink eyes. A Bax null of such phenotype is shown in *Fig. 2.1.B*.

---

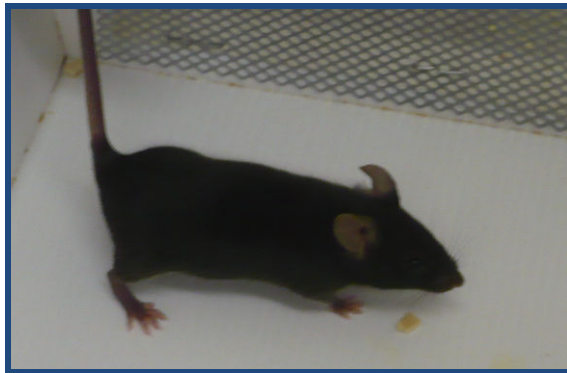
**A.**



**B.**



**C.**



**D.**

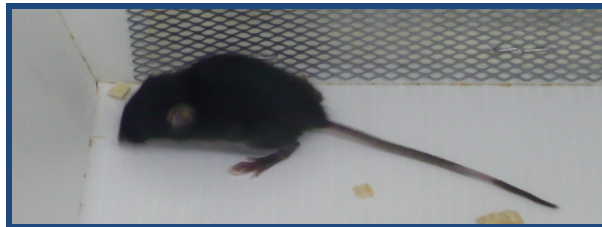


**Fig. 2.1. Photographs of transgenic mice used in the study (A) wild type, (B) Bax KO, (C) Bak KO (D) and Bcl-2 KO.**

---

Bak KO mice (Bak nulls) do not show any physical or behavioral abnormalities; they are normal in size, viable and fertile, which makes possible using nulls as breeders (*Fig. 2.1.C*). Finally, Bcl-2 KO mice (Bcl-2 nulls) exhibit severe phenotype characterised by growth retardation (30 % - 90 %), small external ears and immature front head features (*Fig. 2.1.D*)<sup>119</sup>. The smallest individuals often become ill and die around the 3rd – 4th week of age usually as a result of renal failure due to the development of polycystic kidney disease. Another typical trait of the nulls is hair pigmentation loss during the second follicle cycle, which results in their coat colour turning gray and eventually white.

### **2.3. Tissue culture**

AR42J cells (rat exocrine pancreatic tumour cells) were obtained from ECACC General Collection (cat. 93100618). AR42J cells were maintained in RPMI 1640 medium with 10 mM HEPES, 10 % FBS, 50 µg/ml gentamycin (GIBCO) and 2.5 µg/ml Fungizone; at 37°C, 5 % CO<sub>2</sub> in 25 cm<sup>3</sup> tissue culture flasks. Cells were split once a week: trypsin was used to detach the cells and 1/10 of the total cell suspension was transferred to a new flask with 10 ml fresh medium. For the purpose of microscope visualization, cells were plated onto 5 cm<sup>3</sup> glass bottom dishes, allowed to attach for 2 days, then transfected with Bcl-2-GFP plasmid, ER CaM plasmid or siRNA and incubated for another 48 h.

### **2.4. Bcl-2-GFP plasmid amplification**

Bcl-2-GFP plasmid was supplied in bacterial stabs. Bacterial culture was streak out onto LB-agar plate with Kanamycin (100 µg/ml) and incubated overnight at 37°C.

---

The following day selected colonies were transferred into 3 ml LB medium with Kanamycin (100 µg/ml) and incubated overnight at 37°C with vigorous agitation. On the next day 3 ml of overnight culture were transferred into 100 ml LB medium containing Kanamycin and again incubated in 37°C.

### **2.5. pcDNA-Bcl-2 plasmid amplification**

pcDNA-Bcl-2 plasmid was also supplied in bacterial stabs. Bacterial culture was streak out onto LB-agar plate with Ampicillin (100 µg/ml) and incubated overnight at 37°C. The following day selected colonies were transferred into 3 ml LB medium with Ampicillin (100 µg/ml) and incubated overnight at 37°C with vigorous agitation. On the next day 3 ml of overnight culture were transferred into 100 ml LB medium containing Ampicillin and again incubated in 37°C.

### **2.6. Plasmid isolation**

EndoFree Plasmid Maxi Kit (cat. 12362) was supplied by Qiagen. Isolation was performed according to manufacturer's protocol. In order to confirm the presence of Bcl-2 insert pcDNA3 plasmid and in Bcl-2-GFP plasmid DNA digestion reactions was prepared as follows:

For pcDNA3-Bcl-2 plasmid:

dH <sub>2</sub> O	32.6µl
Promega Buffer "H"	4 µl
BSA	0.4µl
Plasmid DNA	2µl

---

EcoR I	1 $\mu$ l
--------	-----------

For Bcl-2-GFP plasmid:

dH <sub>2</sub> O	31.6 $\mu$ l
Promega Buffer "D"	4 $\mu$ l
BSA	0.4 $\mu$ l
Plasmid DNA	2 $\mu$ l
EcoR I	1 $\mu$ l
Bgl II	1 $\mu$ l

The samples were incubated for 3 h at 37°C and then run on 1 % agarose gel for 70 min at 90 V. *Fig. 2.2* shows restriction pattern obtained after digestion of pcDNA3-Bcl-2 plasmid with EcoR I enzyme and Bcl-2-GFP plasmid with EcoR I and Bgl II.

### **2.7. Preparation of NaHEPES solution**

NaHEPES solution was prepared as follows: 140 mM sodium chloride (cat. S3014-500G, Sigma); 4.7 mM potassium chloride (cat. 529552, Calbiochem); 1.13 mM magnesium chloride (1 M stock, cat. M1028-10X1ML, Sigma); 10 mM HEPES, Free Acid (cat. 391338, Calbiochem); 10 mM D(+)glucose (cat. G-5400, Sigma). pH was adjusted to 7.2 with NaOH. For pancreatic acinar cell isolation and experiments with the presence of extracellular calcium NaHEPES solution was supplemented with 1 mM calcium chloride.

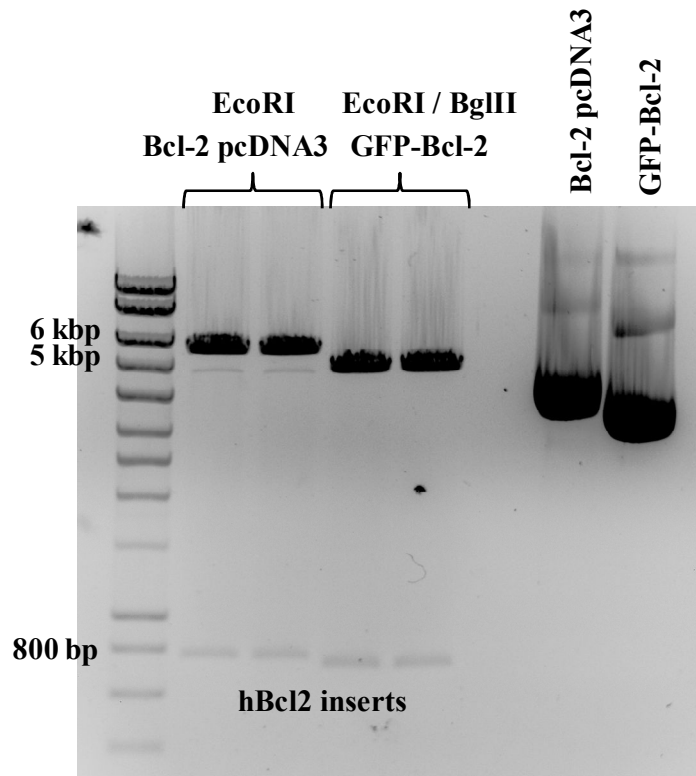


**Fig. 2.2. Digestion patterns of pcDNA3-Bcl-2 and Bcl-2-GFP plasmids**

Digestion of pcDNA3-Bcl-2 plasmid with EcoRI and digestion of Bcl-2-GFP plasmid with EcoRI and BglII restriction enzymes resulted in removal of hBcl-2 inserts. The inserts had about 750 bp and are clearly visible on the gel. Supercoiled uncut pcDNA3-Bcl-2 and GFP-Bcl-2 plasmids (on right) migrated further on the gel than their cut backbones (left).

---

## **2.8. Preparation of KHEPES solution**

KHEPES solution was prepared as follows: 130 mM KCl; 18 mM NaCl; 1.13 mM MgCl<sub>2</sub>; 10 mM HEPES, Free Acid; 3 mM ATP (Calbiochem, cat. 1191); 100 μM EGTA; and 50 μM CaCl<sub>2</sub>. pH was adjusted to 7.2 with KOH.

## **2.9. Preparation of NMDG-HEPES solution**

NMDG-HEPES solution was prepared as follows: 140 mM N-methyl-D-glucamine (cat. 66930, Fluka); 4.7 mM potassium chloride; 1.13 mM magnesium chloride; 10 mM HEPES; 10 mM D(+)glucose. pH was adjusted to 7.2 with HCl.

## **2.10. Preparation of collagenase**

20 ml of NaHEPES (supplemented with Ca<sup>2+</sup>) buffer were added to 4000 u collagenase stock resulting in 200 u/ml collagenase solution. The solution was aliquoted into 20 x 1.5 ml tubes and stored at -20°C.

## **2.11. Preparation of BH3 mimetics**

BH3I-2', HA14-1 and gossypol were all supplied as powders. Stock concentrations of BH3 mimetics were prepared by dissolving powders in DMSO, which resulted in 15 mM BH3I-2', 30 mM HA14-1 and 30 mM gossypol.

## **2.12. Isolation of pancreatic acinar cells**

CD1 or C57BL6/J mice were sacrificed by cervical dislocation in accordance with the Animal (Scientific Procedures) Act, 1986. The pancreas was isolated from a

---

mouse and washed two times with NaHEPES buffer supplemented with 1 mM  $\text{Ca}^{2+}$ . Then the tissue was injected with 1 ml 200 u/ml collagenase and incubated in 1.5 ml eppendorf type tube in collagenase solution for 15 min at 37°C (water bath). After incubation the tube was filled up with NaHEPES + 1 mM  $\text{Ca}^{2+}$  and agitated for about 20 s. The tissue suspension was pipetted up and down to release single cells and the supernatant was collected to a 15 ml tube. Fresh NaHEPES buffer (+ 1 mM  $\text{Ca}^{2+}$ ) was added to the tube and the procedure of supernatant collection was repeated several times. Then, the cells were spun for 1 min at 1000 RPM in a ‘swinging bucket’ type centrifuge. The supernatant was discarded and the cell pellet was resuspended in 10 ml of NaHEPES buffer (+ 1 mM  $\text{Ca}^{2+}$ ). The cell suspension was filtered through the filter mesh and spun again for 1 min. The final pellet was resuspended in 2 ml NaHEPES buffer (+ 1 mM  $\text{Ca}^{2+}$ ).

### **2.13. Calcium measurements in intact cells**

Freshly isolated pancreatic acinar cells were loaded with AM form of calcium sensitive dye fluo-4 dye for 30 min at room temperature; the final concentration of the dye was 5  $\mu\text{M}$  in DMSO (5  $\mu\text{l}$  of 2 mM stock into 2 ml of cell suspension)<sup>65,180</sup>. After incubation the dye was replaced by fresh NaHEPES buffer supplemented with 1 mM  $\text{Ca}^{2+}$  and cytosolic calcium changes were recorded in real time using fluorescence microscopy (excitation 488 nm; emission > 510 nm).

For ratiometric cytosolic calcium measurements, freshly isolated pancreatic acinar cells or AR42J cells were loaded with AM form of calcium sensitive dye fura-2 for 45 min at room temperature or for 1 h at 37°C, respectively. The final concentration of the dye was 10  $\mu\text{M}$ . After incubation, the dye was replaced with fresh NaHEPES

---

buffer supplemented with 1 mM  $\text{Ca}^{2+}$  and calcium changes in the cytosol were recorded in real time using Nikon Diaphot 200 imaging system (excitation 340 nm and 380 nm, green emission with a peak at 510 nm; or with LED excitation 365 nm and 385 nm, green emission at 510 nm).

For ER calcium measurements AR42J cells were transfected with ER-targeted cameleon plasmid using PromoFectin reagent. ER calcium measurements were performed on the third day after transfection using Leica confocal microscope. For accurate collection of FRET signal only CFP part of cameleon was excited with 458 nm laser and emission was collected at both 465-505 nm for CFP and 525-600 nm for YFP. Multiple images were taken in order to assess the resting ER calcium concentration and decrease of YFP / CFP ratio in time was recorded upon 20  $\mu\text{M}$  CPA treatment.

For calcium measurement in mitochondria freshly isolated pancreatic acinar cells were loaded with AM form of calcium sensitive dye rhod-2 for 45 min at room temperature. The final concentration of the dye was 5  $\mu\text{M}$ . Rhod-2 preferentially accumulated into the mitochondria; however a substantial fraction of it was also present in the cytosol. After incubation the cells were spun for 1 min at 1200 RPM and resuspended in fresh NaHEPES buffer supplemented with 1 mM  $\text{Ca}^{2+}$ . Changes of both mitochondrial and cytosolic calcium in rhod-2-loaded pancreatic acinar cells were recorded using confocal imaging system (excitation 532 nm; and emission was collected between 552 – 652 nm).

---

## **2.14. Calcium measurements in permeabilized cells**

Freshly isolated pancreatic acinar cells were loaded with AM form of calcium sensitive dye fluo-5N dye for 50 min at 37°C; the final concentration of the dye was 5 μM in DMSO (5 μl of 2 mM stock into 2 ml of cell suspension)<sup>181</sup>. In these conditions fluo-5N preferentially accumulated in the intracellular stores. After incubation the dye was replaced by fresh NaHEPES buffer supplemented with 1 mM Ca<sup>2+</sup>. Just before the experiments the cells were washed with an intracellular solution - KHEPES; and subsequently permeabilized using two-photon laser pulses. Localized membrane perforation resulted in loss of cytosolic content (including cytosolic fraction of fluo-5N); whereas the intracellular stores remained intact and loaded with the calcium-sensitive dye.

## **2.15. Two-photon permeabilization**

The technique of cell permeabilization with high intensity two-photon light was developed in our laboratory as a modification of previously described method of temporal cell perforation for foreign DNA delivery<sup>182</sup>. Before permeabilization, pancreatic acinar cells were perfused with intracellular solution KHEPES. Then two-photon light (720 – 750 nm) at high intensity was applied at a small area of the plasma membrane of pancreatic acinar cell. The area was preferentially chosen at the apical region of the acinar cell in order to preserve the ER, which is mainly localized in the basolateral region. Application of the two-photon laser pulse at the membrane area resulted in heating of that area followed by its disruption. Successful permeabilization can be confirmed by monitoring the localization of fluorescently labelled dextran (such as Texas Red dextran or Alexa Fluo 647 dextran): present in

---

the extracellular medium, dextran can penetrate inside the cell only after the membrane has been broken.

## 2.16. Measurements of trypsinogen activation in permeabilized cells

Pancreatic acinar cells were permeabilized with two-photon laser beam as described above. Then 10  $\mu$ M BZiPAR (rhodamine 110, bis-(N-CBZ-L-isoleucyl-L-prolyl-L-arginine amide), dihydrochloride) was added to the perfusion chamber. BZiPAR acts as a substrate for trypsin and becomes fluorescent when the enzyme cleaves two oligopeptide residues. BZiPAR fluorescence was monitored upon excitation by 488 nm laser light, and the signal was collected at 510 - 600 nm.

## 2.17. Calculation of cytosolic calcium extrusion rates

For calculation of calcium extrusion rates in fura-2-loaded pancreatic acinar cells, fura-2 ratio obtained upon excitation with 340/380 nm light was converted into free calcium concentration using Grynkiewicz equation<sup>183,184</sup>:

$$[Ca^{2+}] = K_d \times \beta \times \frac{R - R_{\min}}{R_{\max} - R}$$

Symbols:

$K_d$  – dissociation constant of  $Ca^{2+}$  binding site

$\beta$  – coefficient equal to the ratio of fluorescence intensity of fura-2 at the first  
and at the second wavelength

R – ratio value

$R_{\min}$  – minimal ratio value

---

$R_{\max}$  – maximal ratio value

Coefficient  $\beta$  was calculated for known  $[Ca^{2+}]$  values. Separate calibration experiments were performed in order to obtain extreme ratio values:  $R_{\max}$  was obtained by treatment of fura-2-loaded cells with 20  $\mu$ M ionomycin in the presence of  $Ca^{2+}$ ; and  $R_{\min}$  – by perfusion with 2 mM EGTA for 30 min after permeabilization with ionomycin. Examples of the traces are shown on *Fig. 2.3*.

### **2.18. Transient transfection of AR42J cells with plasmids**

In one 1.5 ml tube, 2  $\mu$ g DNA were added to 100  $\mu$ l RPMI medium (without FBS and antibiotics). In a second 1.5 ml tube, 6  $\mu$ l PromoFectin were added to 100  $\mu$ l RPMI medium. Both tubes were vigorously shaken and briefly spun, then combined together. The mixture was again vortexed and briefly centrifuged and then incubated at room temperature for 30 min. After incubation the solution was added drop-wise to AR42J cells, which had been previously plated on glass bottom petri dishes in 2 ml RPMI medium (supplemented with 10 % FBS, gentamycin and fungizone). Cells were incubated at 37°C, 5 % CO<sub>2</sub> for 6 - 8 h. Medium was then replaced with 2 ml of fresh RPMI (with FBS, gentamycin and fungizone) and incubated for another 48 h at 37°C, 5 % CO<sub>2</sub> before visualization using confocal imaging system.

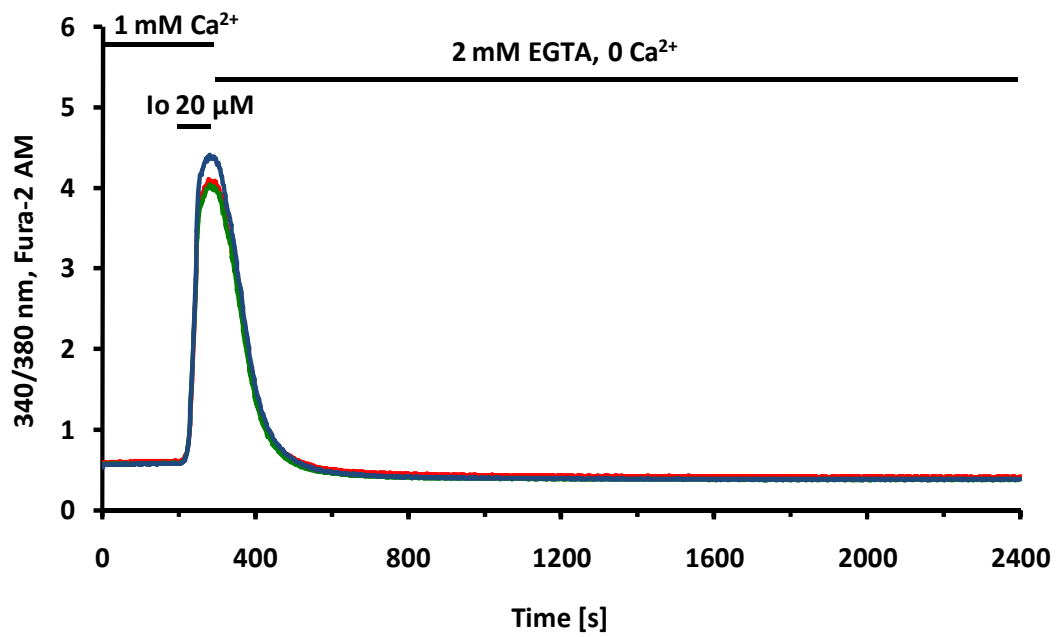


**Fig. 2.3. Calcium calibration experiments**

Three sample traces showing the results of  $\text{Ca}^{2+}$  calibration experiments in WT pancreatic acinar cells.  $R_{\text{max}}$  is the maximum ratio value obtained upon treatment with  $20 \mu\text{M}$  ionomycin, whereas  $R_{\text{min}}$  refers to the minimum ratio value obtained upon long perfusion with  $2 \text{ mM}$  EGTA.

---

### **2.19. Stable transfection of AR42J cells with pcDNA-Bcl-2 plasmid**

AR42J cells were seeded on 6-well plates and transfected in the same way as described for transient transfection. On the second day after transfection complete RPMI medium (supplemented with FBS, gentamycin and fungizone) was replaced by selection medium, which is a complete medium containing 0.8 mg/ml of antibiotic G418. Since pcDNA-Bcl-2 plasmid contains neomycin resistance gene, transfected cells survive in the presence of G418, whereas untransfected cells eventually die. After 21 days of selection, live cells from each 6-well plate were pooled together and transferred to a 25 cm<sup>3</sup> tissue culture flasks. Stably transfected AR42J cells were maintained in RPMI medium supplemented with FBS, gentamycin, fungizone and 400 µg/ml G418.

### **2.20. Silencing Bcl-2 expression in AR42J cells**

In one tube (“1”) 8 µl of 10 µM stock of Bcl-2 siRNA (80 pmols) were added to 100 µl RPMI medium (without FBS and antibiotics). In the second tube (“2”) 8 µl of 10 µM stock of control siRNA-A (80 pmols) were added to 100 µl RPMI medium. In the third (“3”) and fourth (“4”) tube 6 µl PromoFectin were added to 100 µl RPMI medium. All tubes were vigorously shaken and briefly spun, then tube “1” was combined with tube “3” and tube “2” was combined with tube “4”. The mixtures was again vigorously shaken, briefly centrifuged and then incubated at room temperature for 30 min. After incubation the mixtures were added drop-wise to separate glass-bottom petri dishes with AR42J cells, which had been previously plated in 2 ml RPMI medium (supplemented with 10 % FBS, gentamycin and fungizone). Cells

---

were incubated for 48 h at 37°C, 5 % CO<sub>2</sub> before visualization using confocal imaging system.

### **2.21. Transduction of AR42J cells with CellLight BacMam 2.0 Plasma Membrane-RFP**

CellLight BacMam solution was mixed several times by gentle pipetting. 10 µl of the original solution was added directly to the glass-bottom petri dishes containing AR42J cells in 2 ml RPMI supplemented with 10 % FBS, gentamycin and fungizone. Cells were incubated for 48 h at 37°C, 5 % CO<sub>2</sub> before visualization using confocal imaging system.

### **2.22. Transient transfection of pancreatic acinar cells with Bcl-2-GFP plasmid by electroporation**

For transfection of freshly isolated pancreatic acinar cells three different buffers were prepared as follows:

*Buffer 1* (total volume of 100 ml): NaHEPES supplemented with 1 mM CaCl<sub>2</sub>, 0.005 % trypsin inhibitor from soybean (5 mg) and, cat. 11836170001); the solution was filtered through 0.45 µm filter and pH was adjusted to 7.3 with NaOH; then 1 ml of Sigma Antibiotic Antimycotic Solution (100x) was added to the buffer.

*Buffer 2* (total volume of 10 ml): NaHEPES without Ca<sup>2+</sup>, supplemented with 0.005 % trypsin inhibitor from soybean (0.5 mg); the solution was filtered through 0.45 µm filter and pH was adjusted to 7.3 with NaOH; then 0.1 ml of Sigma Antibiotic Antimycotic Solution (100x) was added to the buffer.

---

*Buffer 3* (“medium” for short-term culture of pancreatic acinar cells, total volume of 100 ml): NaHEPES supplemented with 1 mM CaCl<sub>2</sub>, 2 ml MEM amino acids 50x (Sigma, cat. M5550), 1 mM sodium pyruvate (1 ml from 100 mM stock, Sigma, cat. S8636), 0.005 % trypsin inhibitor from soybean (5 mg) and 1 tablet of Complete mini EDTA-free protease inhibitor cocktail (Roche); the solution was filtered through 0.45 µm filter and pH was adjusted to 7.3 with NaOH; then 1 ml of Sigma Antibiotic Antimycotic Solution (100x) was added to the buffer.

Pancreatic acinar cells were isolated as described above using “*Buffer 1*”. The final centrifugation was performed in “*Buffer 2*” and then the cells were spun again at 1200 RPM for 1 min and resuspended in 400 µl of Amaxa Nucleofector Solution with supplement (from Amaxa Basic Nucleofector Kit for Primary Mammalian Epithelial Cells, Lonza, cat. VPI-1005). The cell suspension was aliquoted into 4 tubes, 100 µl per sample. 2 µg of Bcl-2-GFP plasmid were added to each tube and gently mixed. The content of each tube was transferred into an Amaxa cuvette (from Amaxa Basic Nucleofector Kit, Lonza). Each cuvette was closed, inserted into Amaxa Nucleofector II and the cells were electroporated using programme A-20. After electroporation 400 µl of “*Buffer 2*” was added to each cuvette; the cuvettes were incubated for 5 min at 30-32°C. Then the cells were transferred to glass-bottom petri dishes with 2 ml of “*Buffer 3*” and incubated overnight at 30-32°C.

### **2.23. Genotyping**

PureLink™ Genomic DNA Mini Kit (Invitrogen, cat. K1820-02) was used for genomic DNA isolation from mouse tissue (tail and ear) according to the manufacturer's protocol. For purpose of genotyping PCR reaction was performed.

---

*Fig. 2.4.A* shows sequences of the primers used in the reaction and PCR protocol is shown in *Fig. 2.4.B* Amplified DNA was resolved on 1 % agarose gel for 1.5 h at 90 V and visualized using BioRad Molecular Imager ChemiDoc XRS+. *Fig. 2.4.C* shows a typical result of Bax / Bcl-2 genotyping.

#### **2.24. Protein isolation – total protein**

Pancreatic acinar cells were isolated just as described above. Then the cells from one pancreas were resuspended in 300  $\mu$ l of RIPA buffer (Sigma, cat. R0278) containing 150 mM NaCl, 1 % IGEPAL CA-630, 0.5 % sodium deoxycholate, 0.1 % SDS, 50 mM Tris, pH 8.0. The buffer was additionally supplemented with Complete mini EDTA-free protease inhibitor cocktail (Roche). The cell suspension was vigorously vortexed for 1 min and then centrifuged for 5 min at 10,000 $\times$ g in order to remove cell debris. The supernatant was transferred into a fresh 1.5 ml tube and used for protein analysis.

#### **2.25. Determination of protein concentration**

Determination of protein concentration was performed using DC Protein Assay (BioRad, cat. 500-0116). Serial dilutions of standard (BSA) in water were prepared as follows: 5.0, 2.5, 1.25, 0.625, 0.312, 0.156 and 0.078 mg/ml. 5  $\mu$ l of standards and the same amount of samples were added to the 98-well EIA plate in duplicates. In a boat 20  $\mu$ l Reagent S (Bio-Rad) was added to every 1 ml Reagent A. 25  $\mu$ l of this mixture followed by 200  $\mu$ l of Reagent B was pipetted to every well. Absorbance was measured at 750 nm. Concentrations of the samples were determined based on the standard curve equation.

A.

	Name	Sequence
Bax primers	common	5'- GTT GAC CAG AGT GGC GTA GG -3'
	wild type forward	5'- GAG CTG ATC AGA ACC ATC ATG -3'
	mutant forward	5'- CCG CTT CCA TTG CTC AGC GG -3'
Bcl-2 primers	reverse	5'- CGT CCC GCC TCT TCA CCT TTC AGC -3'
	wild type forward	5'- GCC CAG ACT CAT TCA ACC AGA CAT -3'
	PGK	5'- GCC TAC CCG CTT CCA TTG CTC AGC -3'

B.

Step	Temp [°C]	Time	
1	94	5 min	Initial denaturation
2	94	30 s	35 cycles
3	60	1 min	
4	72	1 min	
5	72	2 min	Final extension
6	4	until stopped	

C.

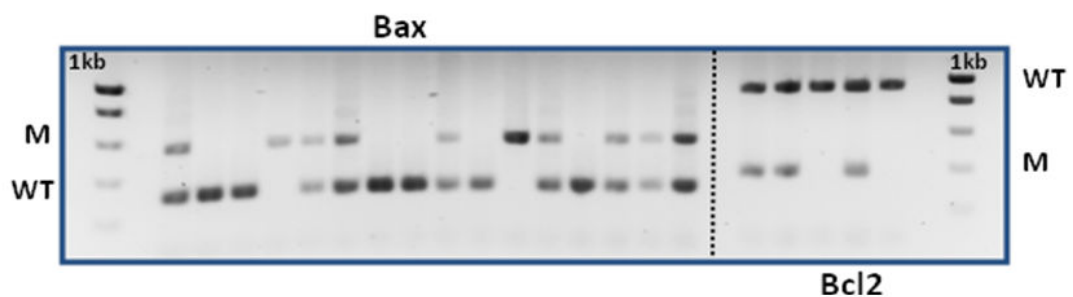


**Fig. 2.4. Genotyping of Bax KO and Bcl-2 KO mice**

(A) Sequences of primers used for genotyping of mice from Bcl-2 and Bax colonies. (B) PCR protocol used for genotyping. (C) A typical result of Bax / Bcl-2 genotyping. "WT" refers to a fragment of a wild type allele of Bax or Bcl-2 gene, and "M" stands for a mutated allele.

---

## **2.26. Subcellular fractionation by differential centrifugation**

The protocol of subcellular fractionation of pancreas was a modification of previously published method<sup>185,186</sup>. The pancreatic tissue isolated from CD1 mice was homogenised in 8 ml of homogenization buffer (0.3 M sucrose, 10 mM HEPES pH 7.6, 0.1 M EGTA, 10 mM KCl, 1 mM dithiothreitol, 0.5 mM PMSF, 0.74 mM spermidine, 15 mM spermine, 2 mg/ml aprotinin, 2 mg/ml leupeptin and 2 mg/ml bestatin) by 5 full strokes in glass-Teflon homogenizer. Low speed centrifugation at 150×g for 15 min, 4°C was performed to sediment nuclei, cell debris and unbroken cells. In this way obtained post-nuclear supernatant was then spun at 1300×g for 15 min, 4°C in order to pellet zymogen granules. The pellet was removed and the supernatant was centrifuged again, this time at 12,000×g for 12 min, 4°C and both the pellet containing lysosomes / mitochondria and the supernatant containing microsomes were collected.

## **2.27. Immunoprecipitation**

Pancreatic tissue was isolated from CD1 mice and lysed in lysis buffer, which contained 10 mM HEPES, 140 mM KCl, 5 mM MgCl<sub>2</sub>, 0.5 mM EGTA, 2% CHAPS (containing 1 mM dithiothreitol, 10 µg/ml leupeptin, 10 µg/ml aprotinin and 1 mM PMSF); pH of the buffer was adjusted to 7.4. The lysates were spun at 15,000×g for 20 min, 4°C and the volume of the supernatant containing 500 µg of protein was immunoprecipitated overnight with either Bcl-2 or Bcl-xL using Catch and Release Reversible Immunoprecipitation System (Millipore, cat. 17-500) and following the manufacturer's protocol.

---

## 2.28. Immunoblotting

The volume containing 50 µg of protein lysate was brought to 16 µl by addition of dH<sub>2</sub>O. Then 6 µl 4 x SDS-PAGE loading buffer was added to each sample. Samples were vortexed and spun (5 min 8,000 g) following by heating at 95°C for 5 min. Proteins were then separated by SDS-PAGE (5 % stacking gel, 10 % resolving gel, for 50 min at 200 V), then transferred to nitrocellulose (25 V, 2 h) and blocked for 1 h with 5 % milk. For detection of PDI or COX IV<sup>187</sup> nitrocellulose membranes were incubated for 2 h at room temperature or overnight at 4°C in Tris-buffered saline with 0.05 % Tween-20 (TBST), 1 % milk and a 1:1000 dilution of primary antibody. Membranes were then washed three times for 10 min with TBS-Tween (0.05 %) and then incubated for 1 h with 1:5000 dilution of HRP conjugated IgG secondary antibody. The membranes were washed four times for 10 min with TBS-Tween (0.05 %). The blots were developed using Enhanced Chemiluminescence (ECL) Detection Kit (Pierce, cat. 32209) according to the manufacturer's protocol.

## 2.29. Immunofluorescence

Immunofluorescence was applied in order to investigate endogenous protein distribution in fixed pancreatic acinar cells or AR42J cells. Freshly isolated acinar cells or were plated on 13 mm poly-L-lysine coated glass cover slips and allowed to adhere for 5 min at room temperature. AR42J cells were plated on 13 mm poly-L-lysine coated glass cover slips, transfected with Bcl-2-GFP plasmid using PromoFectin 2000 and incubated for 48 h in the tissue culture incubator (37°C, 5 % CO<sub>2</sub>). The cells were fixed by incubation in 100 % ice-cold methanol for 10 min at -20°C. After fixation cover slips were washed in 0.1 M phosphate buffered saline

---

(PBS) three times, for 5 minutes each. The first wash was performed in ice-cold PBS, and two subsequent washes - in PBS at room temperature. Potential nonspecific binding sites were then blocked by incubation in 10 % goat serum in PBS for 30 - 60 min at room temperature. Then the cells were incubated with 1:100 primary antibody solution containing 5 % goat serum in PBS for 1 h at room temperature. Primary antibodies used in the study were rabbit anti-Bcl-2 (Abcam) and mouse anti-PMCA (Abcam). The cells were washed 3 times with PBS for 5 min each. Subsequently the fixed cells were incubated for 1 h at room temperature with 1:500 dilution of appropriate secondary antibody prepared in PBS containing 5 % goat serum. Secondary antibodies were: goat anti-rabbit conjugated to AlexaFluor 488 (Invitrogen, Paisley, UK), and goat anti-mouse conjugated to AlexaFluor 635 (Invitrogen, Paisley, UK). Unbound antibody was removed by four washes, 5 min each in PBS. Finally cover slips were mounted on glass microscope slides with a droplet of ProlongGold anti-fade mounting medium (Invitrogen, Paisley, UK) and left to dry at 4 °C in darkness for 24 hours before viewing.

### **2.30. Apoptosis assay**

Freshly isolated pancreatic acinar cells were centrifuged at 1200×g for 1 min and resuspended in calcium-free NaHEPES solution: 10 mM HEPES, 140 mM NaCl, 1 mM MgCl<sub>2</sub>, 4.7 mM KCl, 10 mM glucose, 1.5 mM EGTA, pH 7.2. The cells were loaded with 10 μM general caspase substrate (rhodamine 110, bis-(L-aspartic acid amide), Invitrogen, cat. R22122) for 20 min at room temperature. After loading the cells were spun again (1200×g for 1 min) and resuspended in standard NaHEPES solution supplemented with 1 mM Ca<sup>2+</sup>. Then the cells were treated with apoptosis

---

inducer alone, in this case 15  $\mu$ M BH3I-2'; or 15  $\mu$ M BH3I-2' in the presence or of 100  $\mu$ M 2-APB and 10  $\mu$ M ruthenium red in order to inhibit IP<sub>3</sub>Rs and RyR, respectively. The cells were visualized using confocal imaging system (excitation: 488 nm, emission: 505 - 543 nm).

### **2.31. Cell death assay**

Cell death assay was performed on freshly isolated pancreatic acinar cells using Sigma Annexin V-FITC Apoptosis Detection Kit (cat. APOAF-20TST). After treatment cells were incubated for 15 min at room temperature with appropriate concentration of Annexin V-FITC and propidium iodide (according to the manufacturer's protocol). Annexin V-FITC staining of apoptotic cells was visualized upon excitation with 488 nm laser light and emission was collected between 510 – 570 nm; propidium iodide staining of necrotic cells was detected by using 535 nm laser and collecting emission between 585 – 705 nm. Multiple pictures (20 - 35) per treatment group were taken; live, apoptotic and necrotic cells were counted in each treatment group. Unless otherwise stated in the result section, three independent experiments of each assay were performed; average values and standard errors were calculated and presented as bar charts.

### **2.32. Equipment**

Cell visualization and cytosolic / ER calcium measurements with fluo-4 and fluo-5N dyes were performed using (1) Leica Confocal Two-Photon Microscope SP2 with Leica Confocal Software v.2.61, Leica Microsystems, Heidelberg GmbH, (2) Leica Confocal SP5 II Multi-Photon with Leica Confocal Software, Leica Microsystems,

---

Heidelberg GmbH and (3) Leica Confocal TCS SPE Workstation, Leica Microsystems. Fura-2 recordings were performed on (1) Nikon Diaphot 200 imaging system using software Image-Pro Plus, MediaCybernetics; (2) and Photometrics – Cairn imaging system using software Image-Pro Plus, MediaCybernetics.

### **2.33. Software**

Microsoft Word 2007 served as a main tool for writing and editing this thesis. Calculations, graphs and charts were made in Microsoft Excel 2003 and 2007. Origin v8.5 was used for fitting exponential functions and calculation of derivatives. Cell images were taken using Leica confocal software. Diagrams were prepared in Microsoft PowerPoint and Adobe Photoshop Version 9.0. ISIS™/Draw 2.4 was used to create schematic representation of chemical structures of compounds used in the experiments. The reference list was generated using Reference Manager Professional Edition Version 10.

---

**CHAPTER 3:**

**EFFECTS OF BCL-2 INHIBITION BY BH3 MIMETICS ON  
CALCIUM-INDUCED CALCIUM RELEASE (CICR) PROCESS IN  
PANCREATIC ACINAR CELLS**

---

## **Chapter 3: Effects of Bcl-2 inhibition by BH3 mimetics on calcium-induced calcium release (CICR) process in pancreatic acinar cells**

### **3.1. Overview of CICR in pancreatic acinar cells**

Calcium-induced calcium release (CICR) is a positive feedback mechanism by which a small rise in cytosolic  $\text{Ca}^{2+}$  triggers further calcium release from the intracellular stores. As was described in the introduction,  $\text{IP}_3\text{Rs}$  and  $\text{RyRs}$  are the main players in CICR process. Opening of both receptors is regulated by  $\text{Ca}^{2+}$  in a biphasic mode: modest increases in cytosolic  $\text{Ca}^{2+}$  sensitize the receptors, whereas higher  $\text{Ca}^{2+}$  concentration has an inhibitory effect<sup>188-191</sup>. It is generally agreed that  $\text{Ca}^{2+}$ -dependent regulation is predominantly based on direct binding of  $\text{Ca}^{2+}$  ions to the receptors. Experiments with purified  $\text{IP}_3\text{Rs}$  reconstituted into lipid bilayers demonstrated clear sensitivity of  $\text{IP}_3\text{Rs}$  to  $\text{Ca}^{2+}$ , which supports the direct interaction model<sup>192</sup>. Indeed  $\text{Ca}^{2+}$  binding sites on the cytosolic part of  $\text{IP}_3\text{Rs}$  have been identified<sup>193</sup>. Interestingly these sites do not exhibit any similarities to other known  $\text{Ca}^{2+}$ -binding motifs such as EF-hands. They contain negatively charged residues that potentially might coordinate  $\text{Ca}^{2+}$  ions<sup>194</sup>.  $\text{RyRs}$  possess two types of  $\text{Ca}^{2+}$ -binding sites: high-affinity sites bind  $\text{Ca}^{2+}$  at nanomolar to low micromolar concentrations and activate the receptors, whereas low-affinity sites bind  $\text{Ca}^{2+}$  at micromolar to millimolar concentrations and have an inhibitory effect<sup>195</sup>. The full mechanism for  $\text{Ca}^{2+}$  regulation of  $\text{IP}_3\text{Rs}$  and  $\text{RyRs}$  is not entirely clear. Direct interaction of  $\text{Ca}^{2+}$  ions with the receptors cannot completely explain all observed effects and therefore

---

some accessory factors / proteins seem to be involved in the CICR process, with calmodulin being one of the candidates<sup>196-198</sup>.

Pancreatic acinar cells have highly polarized structure, with two distinct regions: apical and basolateral. Although most of the ER is localized in the basolateral area<sup>199,200</sup>, its thin extensions penetrate into the secretory region<sup>201</sup>. As was described in the introductory chapter, these thin extensions of the ER are characterised by high concentration of IP<sub>3</sub>Rs<sup>43,65,66</sup>, whereas RyRs are evenly distributed throughout the basolateral and apical area<sup>67,68</sup> (*Fig. 3.1*). Consequently, Ca<sup>2+</sup> responses to physiological stimuli always originate in the apical region and propagate to the basolateral region. Previously, CICR sensitivity was compared in different regions of the pancreatic acinar cells<sup>69</sup>. Local Ca<sup>2+</sup> uncaging in the basolateral and apical areas revealed polarized distribution of Ca<sup>2+</sup>-sensitive Ca<sup>2+</sup> release sites in pancreatic acinar cells. Ca<sup>2+</sup> uncaging in the basolateral region results in short lasting elevation in cytosolic Ca<sup>2+</sup> (the uncaging spike), but does not trigger CICR. On the other hand, Ca<sup>2+</sup> liberation in the apical region induces a long lasting CICR transient that propagates toward the basolateral region<sup>69</sup>. Both IP<sub>3</sub>Rs and RyRs are crucial for CICR, because specific inhibition of these receptors prevents Ca<sup>2+</sup> release triggered by uncaged calcium<sup>69</sup>. Apart from the ER, pancreatic acinar cells contain another Ca<sup>2+</sup> store, which has been attributed mainly to zymogen granules and named as the acidic store<sup>181,202,203</sup>. The acidic store is exclusively located in the apical region of pancreatic acinar cell and it can be distinguished pharmacologically from the ER, since the two stores utilize different refilling mechanisms: the ER accumulates Ca<sup>2+</sup> via SERCA activity, whereas the replenishment of the acidic store is dependent on vacuolar H<sup>+</sup> pumps and thus is sensitive to bafilomycin<sup>202</sup>. Uneven distribution

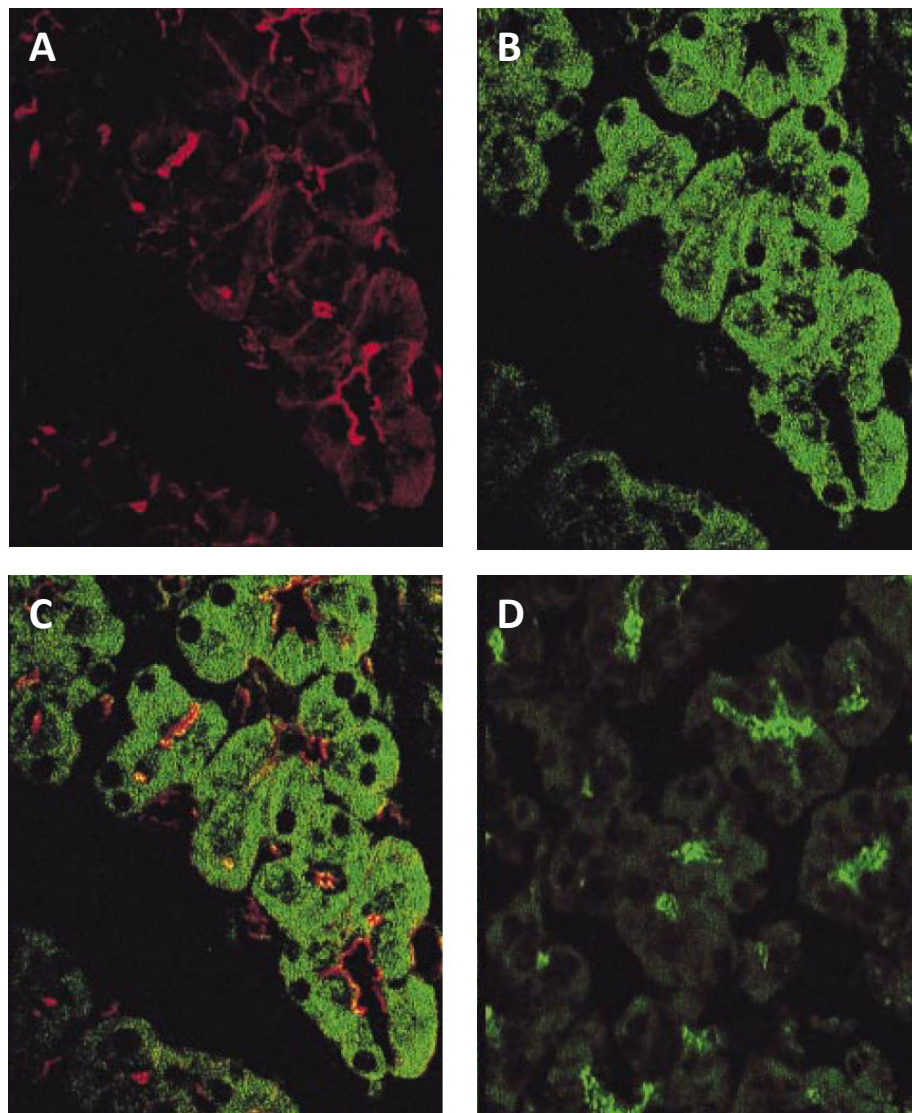


**Fig. 3.1. Comparison of the subcellular localization of RyR2 and IP<sub>3</sub>R3 in pancreatic tissue**

(A) The plasma membrane of pancreatic acinar cell is labeled with Texas Red-phalloidin. (B) Distribution of type 2 RyR (immunostaining). (C) Overlay of images (A) and (B), demonstrating that RyRs are distributed relatively evenly across the cell. (D) Distribution of the type 3 IP<sub>3</sub>R in pancreatic acinar cells (immunostaining). In contrast to RyR2, IP<sub>3</sub>R3 is concentrated in the apical region. [Adapted from *Leite MF, 1999*]<sup>67</sup>.

---

of IP<sub>3</sub>Rs and two distinct Ca<sup>2+</sup> stores still cannot fully explain the underlying factors responsible for different sensitivity of the basolateral and apical areas in pancreatic acinar cells. This chapter attempts to address this issue. There is accumulating evidence for the role of Bcl-2 family proteins in cellular calcium homeostasis, especially in regulation of ER Ca<sup>2+</sup> content and Ca<sup>2+</sup> release<sup>158,160,204</sup>. However, the direct roles of Bcl-2 proteins in the regulation of CICR have not yet been fully investigated. Considering the facts that Bcl-2 proteins regulate calcium stores and interact with receptors involved in CICR, it is reasonable to suspect that they also might influence sensitivity to CICR in pancreatic acinar cells. In order to test this hypothesis, specific inhibition of anti-apoptotic Bcl-2 proteins by BH3 mimetics has been applied.

### **3.2. Localization of anti-apoptotic Bcl-2 proteins in pancreatic acinar cells**

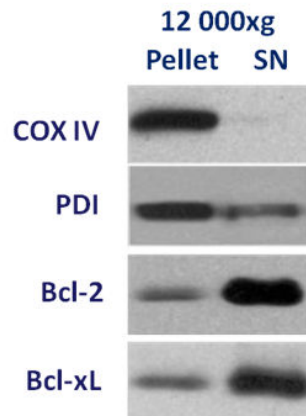
As strict regulators of intrinsic pathway of apoptotic cell death, Bcl-2 family proteins are known to localize to mitochondria. However, evidence accumulated during recent years suggest localization of some Bcl-2 family members in other cell compartments, mainly the endoplasmic reticulum<sup>176,204,205</sup>, where they are involved in the regulation of cellular calcium homeostasis<sup>158,206</sup>. Since there is no specific data demonstrating localization of Bcl-2 family members in pancreatic acinar cells, this study aimed to provide independent evidence for the presence of two anti-apoptotic proteins Bcl-2 and Bcl-xL in the ER. Both proteins are direct high-affinity targets for BH3 mimetics used in this study: BH3I-2' and HA14-1<sup>167,170</sup>. For detection of Bcl-2 and Bcl-xL Western blot analyses were performed<sup>207</sup>. Pancreas isolated from CD-1 male mice was homogenized and centrifuged at 1300×g in order to pellet and remove

---

zymogen granules. The supernatant was further spun at 12000×g. This procedure aimed to separate mitochondria (pellet) from supernatant enriched in ER microsomes. Both the pellet and the supernatant were tested for the presence of Bcl-2 and Bcl-xL as well as compartment specific markers: mitochondrial cytochrome c oxidase (COX IV) and protein disulfide isomerase (PDI), which is a chaperon protein characteristic for the endoplasmic reticulum. Western blot results (*Fig. 3.2.A*) show that 12000×g pellet contains both mitochondria and endoplasmic reticulum microsomes marked by the presence of PDI and COX IV, respectively. As predicted, this fraction also contains Bcl-2 and Bcl-xL. On the other hand, 12000×g supernatant contains PDI, but COX IV was not detected, which indicates the presence of the endoplasmic reticulum and the absence of mitochondria. Importantly, the supernatant has high amounts of Bcl-2 and Bcl-xL, which constitutes an indirect evidence for extramitochondrial localization of these proteins. Bcl-2 and Bcl-xL are associated with ER membranes, although cytosolic localization cannot be excluded.

Another piece of evidence for extramitochondrial localization of Bcl-2 protein was obtained from experiments on rat pancreatic cancer cell line AR42J. Bcl-2-GFP fusion protein was transiently overexpressed in AR42J cells using pEGFP plasmid containing *bcl-2* insert. On the third day after transfection cell medium was replaced with fresh NaHEPES (+ 1 mM Ca<sup>2+</sup>) solution and the cells were stained with ER-tracker Red (Invitrogen) in order to visualize the endoplasmic reticulum. *Fig. 3.2.B* shows three fluorescent images of AR42J cells. Green fluorescence represents cellular localization of Bcl-2-GFP protein, whereas red fluorescence comes from ER-tracker Red and marks the ER. Overlays of green and red fluorescence result in yellow colour showing that substantial fraction of Bcl-2 co-localizes with the ER.

A.



B.

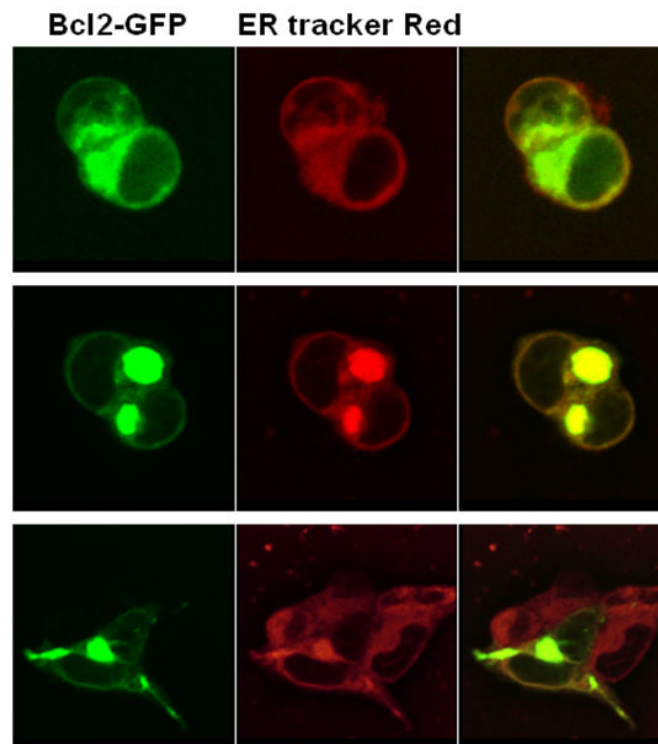


**Fig. 3.2. Intracellular localization of Bcl-2 and Bcl-xL**

(A) Western blot analysis illustrates localization of Bcl-2 and Bcl-xL in two post-nuclear fractions of pancreatic tissue. After centrifugation at 12000xg the pellet fraction contains mitochondria (marker: COX IV) and the ER (marker: PDI); whereas supernatant fraction contains the ER but no mitochondria. Bcl-2 and Bcl-xL are present in both fractions [Data obtained in collaboration; adapted from *Gerasimenko JV, Ferdek PE, 2010*]<sup>207</sup>. (B) AR42J cells overexpressing Bcl-2-GFP (green) stained with ER tracker Red (red colour); yellow overlay shows that a fraction of Bcl-2 protein can be present in the ER.

---

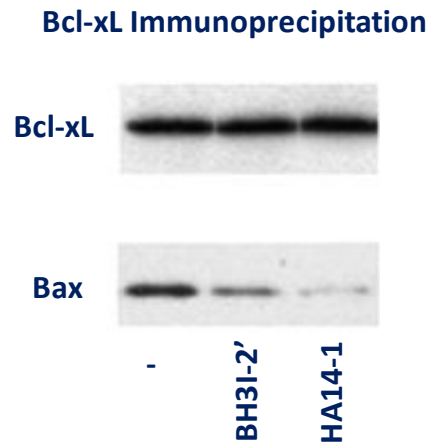
### **3.3. BH3 mimetics BH3I-2' and HA14-1 disrupt the interaction between anti- and pro-apoptotic Bcl-2 family members**

Due to their similarity to BH3 domains, BH3 mimetics bind to the hydrophobic pocket of anti-apoptotic Bcl-2 proteins and inhibit their interaction with one of the pro-apoptotic Bcl-2 members or a BH3 only protein, which eventually leads to liberation and activation of Bax and Bak. Since this study applies BH3 mimetics for investigation of cellular calcium homeostasis in pancreatic acinar cells, first it was necessary to confirm the effects of two BH3 mimetic: BH3I-2' and HA14-1 on interactions between anti-apoptotic Bcl-2 or Bcl-xL and pro-apoptotic Bax<sup>207</sup>. Pancreatic acinar cells were incubated for 1h in the presence of 5  $\mu$ M BH3I-2' or 30  $\mu$ M HA14-1; control cells were incubated for the same time but without any inhibitor. After incubation the cells were digested in RIPA lysis buffer and immunoprecipitation was performed with antibodies specific for Bcl-xL or Bcl-2. Immunoprecipitates were then probed with antibodies against Bcl-xL, Bcl-2 and Bax. The results (*Fig. 3.3*) demonstrate that the treatment with either BH3I-2' or HA14-1 markedly decreased the amount of co-precipitated Bax with anti-apoptotic Bcl-2 members. Therefore it can be concluded that both BH3I-2' and HA14-1 effectively displace Bax protein from Bcl-2 and Bcl-xL, which confirms their inhibitory activity in pancreatic tissue.

### **3.4. BH3 mimetics induce increase in cytosolic Ca<sup>2+</sup> followed by sustained Ca<sup>2+</sup> plateau formation**

In order to investigate the effects of BH3 mimetics on intracellular calcium homeostasis, freshly isolated pancreatic acinar cells were loaded with AM form of

**A.**



**B.**

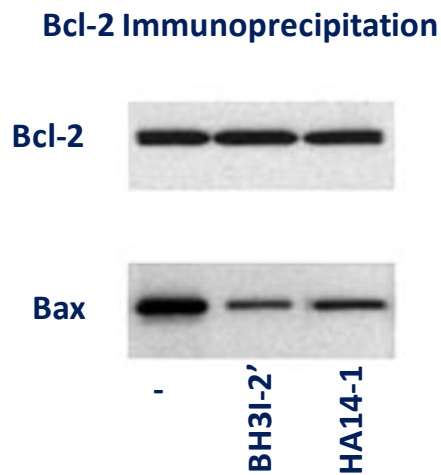


**Fig. 3.3. BH3 mimetics disrupt the interaction between anti- and pro-apoptotic Bcl-2 members**

Immunoprecipitation assays demonstrating inhibitory potential of BH3I-2' and HA14-1. These BH3 mimetics disrupt the interaction of Bcl-xL (**A**) or Bcl-2 (**B**) with Bax. [Data obtained in collaboration; adapted from *Gerasimenko JV, Ferdek PE, 2010*]<sup>207</sup>.

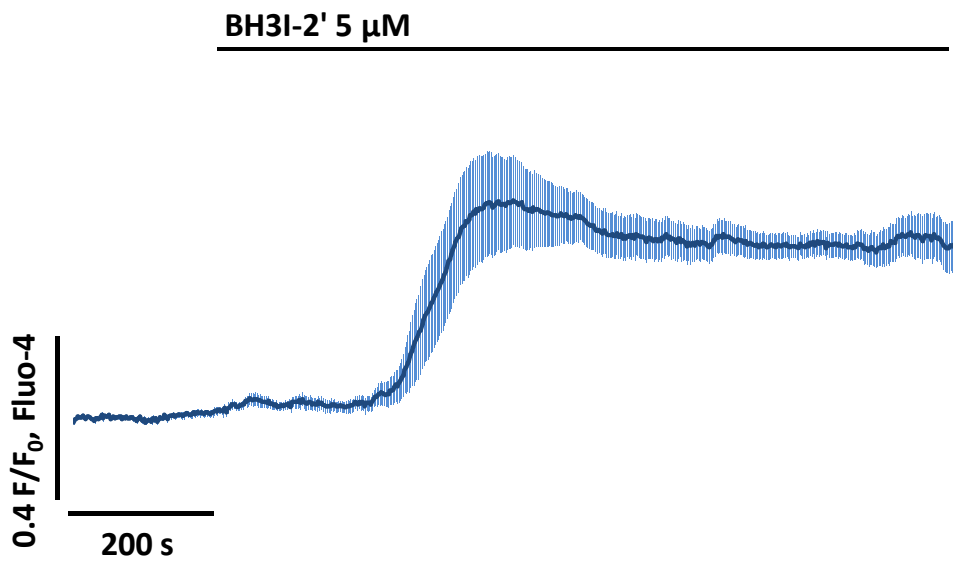
---

calcium sensitive dye fluo-4 and subsequently treated with 5  $\mu$ M BH3I-2' or 30  $\mu$ M HA14-1. Changes in cytosolic  $Ca^{2+}$  concentration were measured using confocal Leica system. The results revealed that both BH3I-2' and HA14-1 caused substantial increase in green fluorescence of the calcium sensitive dye fluo-4, which indicates an increase in cytosolic  $Ca^{2+}$  concentration (*Fig. 3.4.A-D*). Many responses were initiated by steep CICR (43 % to BH3I-2' and 45 % to HA14-1); the rest of the tested cells also developed cytosolic  $Ca^{2+}$  elevation, but without obvious CICR phase. In all cases, however, the initial increase was followed by sustained cytosolic calcium plateau (*Fig. 3.4.A-D*). Addition of 5 nM CCK (supramaximal dose) on the top of the cytosolic calcium plateau did not induce further release of calcium (*Fig. 3.4.E-F*), which suggests that treatment with BH3I-2' and HA14-1 substantially reduced the content of the intracellular calcium stores. In contrast, after treatment of pancreatic acinar cells with 5 nM CCK, which led to calcium release from the ER and global calcium increase in the cytosol, 5 and 30  $\mu$ M BH3I-2' and 30  $\mu$ M HA14-1 were still able to release even more calcium from the intracellular stores (*Fig. 3.4.G-H*).

### **3.5. Inhibitors of anti-apoptotic Bcl-2 proteins release calcium from the intracellular stores**

Simultaneously with the intact cell experiments, investigations on two photon-permeabilized pancreatic acinar cells were performed in order to determine BH3 mimetic-dependent calcium changes in the intracellular stores. The cells were loaded with calcium sensitive indicator fluo-5N, permeabilized with two photon laser and perfused with KHEPES buffer that mimics the intracellular environment. Treatment with 5  $\mu$ M BH3I-2' caused reduction in green fluorescence ( $18.5 \% \pm 2.2$  SE,  $n = 12$ )

A.



B.

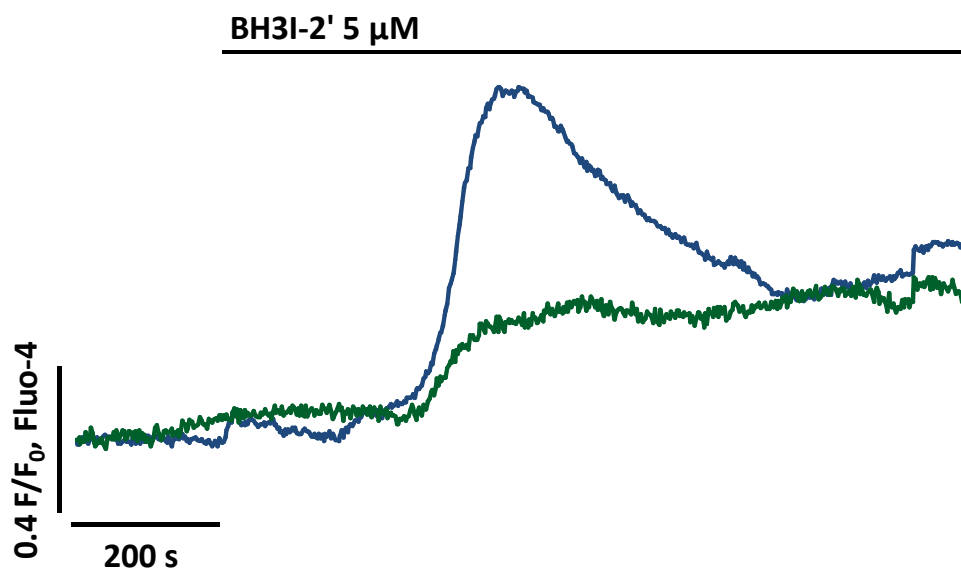
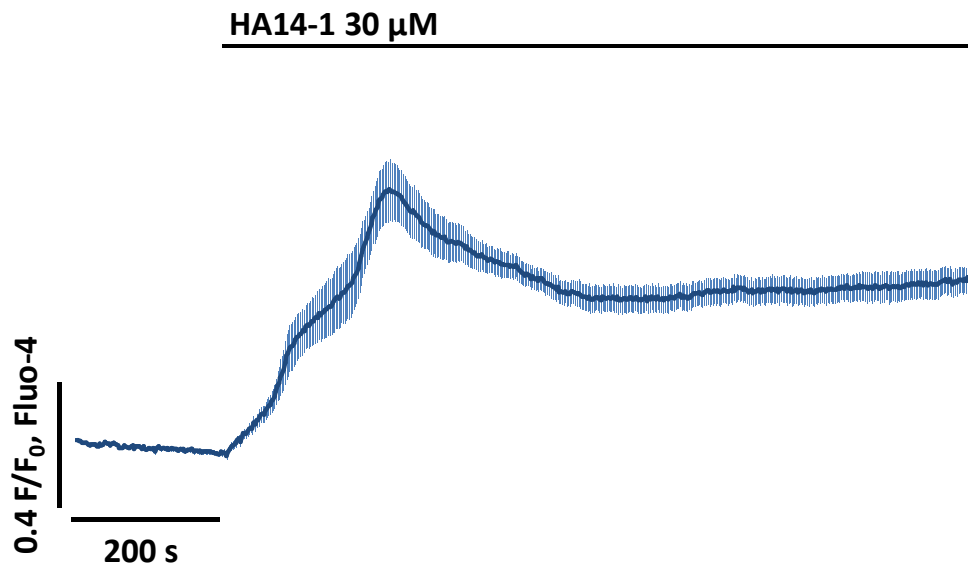


**Fig. 3.4. Calcium responses to BH3 mimetics in pancreatic acinar cells**

(A) Average calcium response to 5  $\mu$ M BH3I-2' in C57BL6/J wild type pancreatic acinar cells (n = 14, mean values  $\pm$  SE) in the absence of extracellular Ca<sup>2+</sup>. (B) Examples of the traces showing responses to 5  $\mu$ M BH3I-2' in form of CICR (blue) or gradual increase (green), both concluded with sustained calcium plateau.

C.



D.

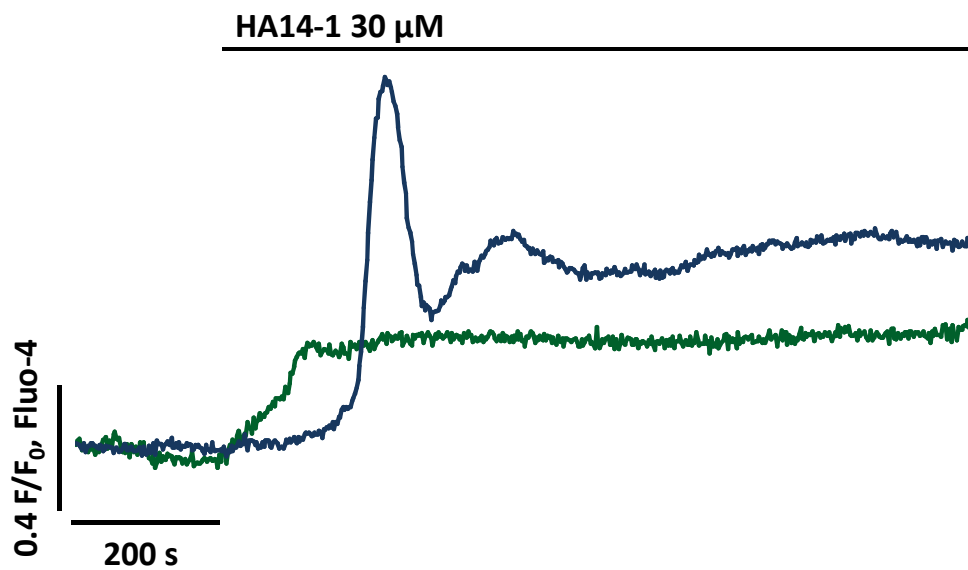


**Fig. 3.4.** (*continues*)

(C) Average calcium response to 30  $\mu$ M HA14-1 in C57BL6/J wild type pancreatic acinar cells (n = 11, mean values  $\pm$  SE) in the absence of extracellular Ca<sup>2+</sup>. (D) Examples of the traces showing responses to 30  $\mu$ M HA14-1 in form of CICR (blue) or gradual increase (green), both concluded with sustained calcium plateau.

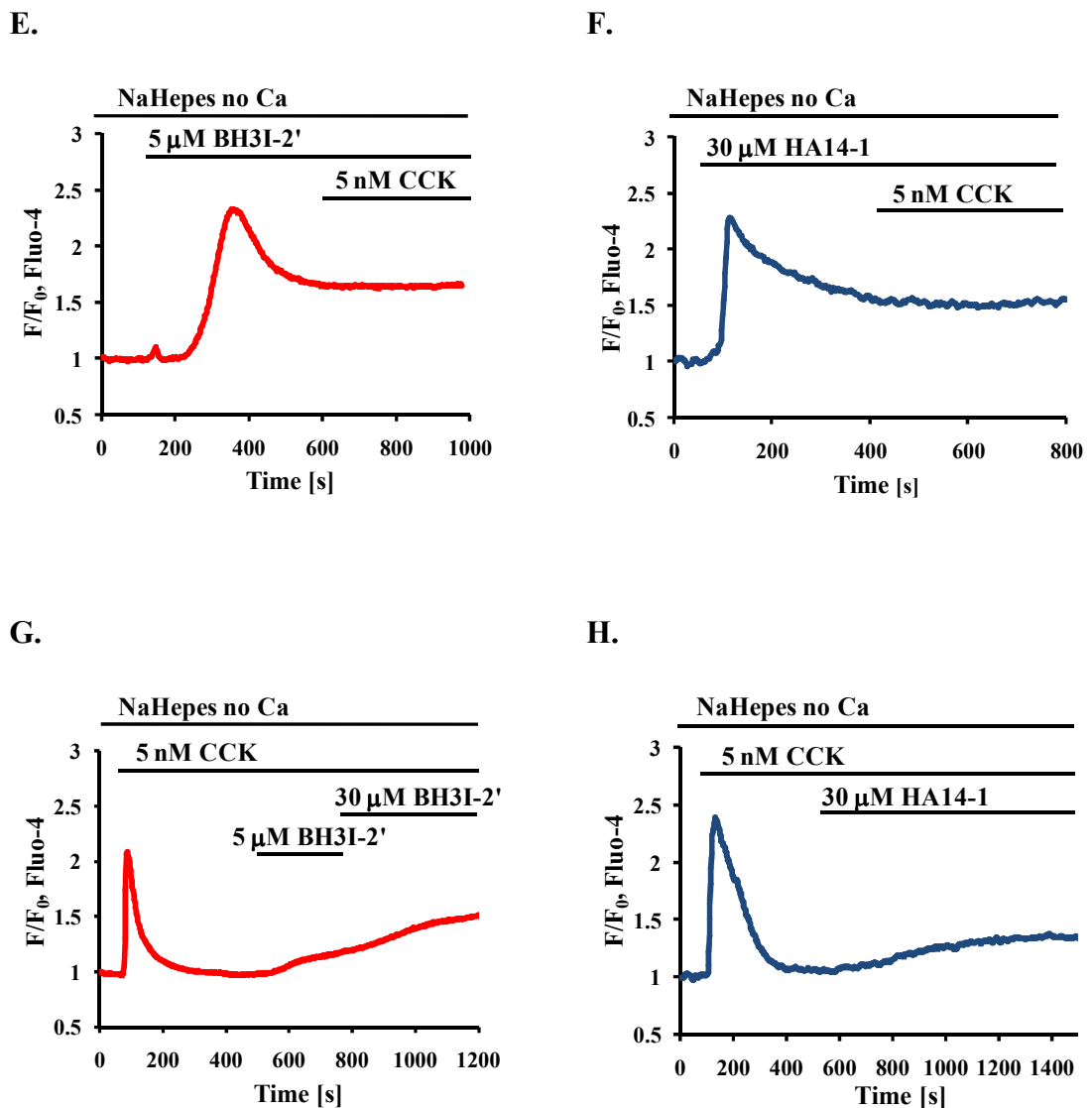


**Fig. 3.4.** (continues)

Traces show typical cytosolic calcium responses to treatments with **(E)** 5  $\mu\text{M}$  BH3I-2' and **(F)** 30  $\mu\text{M}$  HA14-1 in pancreatic acinar cells. Subsequent application of 5 nM CCK did not induce any additional response. **(G)** Treatment with 5 nM CCK resulted in global calcium response in the cytosol. Subsequent additions of 5  $\mu\text{M}$  and 30  $\mu\text{M}$  BH3I-2' induced slow elevation of cytosolic calcium and plateau formation. **(H)** 5 nM CCK elicited global cytosolic calcium response. Addition of 30  $\mu\text{M}$  HA14-1 induced slow elevation of cytosolic calcium and plateau formation. [Adapted from *Gerasimenko JV, Ferdek PE, 2010*]<sup>207</sup>.

---

of the calcium sensitive dye indicating a decrease of calcium content in the intracellular stores (*Fig. 3.5.A*). Similarly, 30  $\mu\text{M}$  HA14-1 induced a decrease ( $21\% \pm 1.5 \text{ SE}$ ,  $n = 10$ ) in calcium concentration in the intracellular stores (*Fig. 3.5.B*). This decrease was sustained and corresponded to the previously measured cytosolic calcium plateau. Since all responses were recorded in the basolateral area, they are attributed mainly to the ER.

In order to investigate whether  $\text{Ca}^{2+}$  release caused by BH3 mimetics is dependent on the effects of these inhibitors on conditions of mitochondria, ATP production in pancreatic acinar cells was blocked using two chemicals: 1) rotenone, which inhibits electron transport chain in mitochondria; and 2) oligomycin – a potent blocker of  $\text{F}_0$  subunit of ATP synthase<sup>207</sup>. For the experiments, freshly isolated pancreatic acinar cells were loaded with fluo-5N and permeabilized with 2-photon laser. Pretreatment of the cells with a mixture of 10  $\mu\text{M}$  rotenone and 10  $\mu\text{M}$  oligomycin in KHEPES solution did not prevent BH3 mimetic-induced calcium release from the intracellular stores (*Fig. 3.5.C-D*), which indicates that the effects of BH3I-2' and HA14-1 are not dependent on ATP or mitochondrial functions.

In pancreatic acinar cells thapsigargin-insensitive acidic store contains substantial amount of  $\text{Ca}^{2+}$  and has been demonstrated to be involved in pathophysiological responses<sup>181,202,203</sup>. In order to test whether  $\text{Ca}^{2+}$  release from the acidic store contributes to BH3-mimetic responses, the ER of intact pancreatic acinar cells was depleted of  $\text{Ca}^{2+}$  by treatment with 2  $\mu\text{M}$  thapsigargin. Subsequent application of 10  $\mu\text{M}$  BH3I-2' failed to induce  $\text{Ca}^{2+}$  release from thapsigargin-insensitive store (*Fig. 3.5.G*). Therefore it has been concluded that BH3 mimetics release calcium mainly from the endoplasmic reticulum.

---

Further, calcium was clamped with 10 mM BAPTA and 2 mM CaCl<sub>2</sub> in KHEPES buffer in order to eliminate CICR from the intracellular stores. Under these conditions the responses to BH3I-2' (6.8 % ± 0.3 SE, n = 6) and HA14-1 (6.1 % ± 0.3 SE, n = 6) were significantly reduced in permeabilized pancreatic acinar cells (*Fig. 3.5.E-F*). This experiment demonstrates that CICR component is crucial for proper development of BH3 mimetic-elicited responses.

Since BH3 mimetics mobilize Ca<sup>2+</sup> from the endoplasmic reticulum leading to its emptying, sustained character of cytosolic Ca<sup>2+</sup> plateau is not entirely clear. In principle, when there is no Ca<sup>2+</sup> in the extracellular solution cytosolic Ca<sup>2+</sup> should be cleared from the cytosol, thus quickly returning to its basal levels. However, the results consistently show that the elevation in cytosolic Ca<sup>2+</sup> persists for more than 1000 s after treatment with BH3 mimetics. In order to exclude the possibility that sustained Ca<sup>2+</sup> signal is in fact an artefact introduced by BH3 mimetics, fluo-4-loaded pancreatic acinar cells were treated with 5 μM BH3I-2' in NaHEPES 0 Ca<sup>2+</sup> solution that contained 100 μM of the calcium chelator EGTA. Under these conditions the responses to BH3I-2' returned to the baseline within few hundred seconds after application of the BH3 mimetic (*Fig. 3.5.H*). The experiment confirms that recorded plateau is a result of increased cytosolic Ca<sup>2+</sup> and it can be removed by calcium chelators.

### **3.6. BH3 mimetic-induced Ca<sup>2+</sup> release from the intracellular stores is only partially dependent on IP<sub>3</sub>Rs and RyRs**

Since calcium responses to BH3 mimetics are dependent on CICR process, engagement of IP<sub>3</sub>Rs and RyRs has been assessed. Pancreatic acinar cells isolated

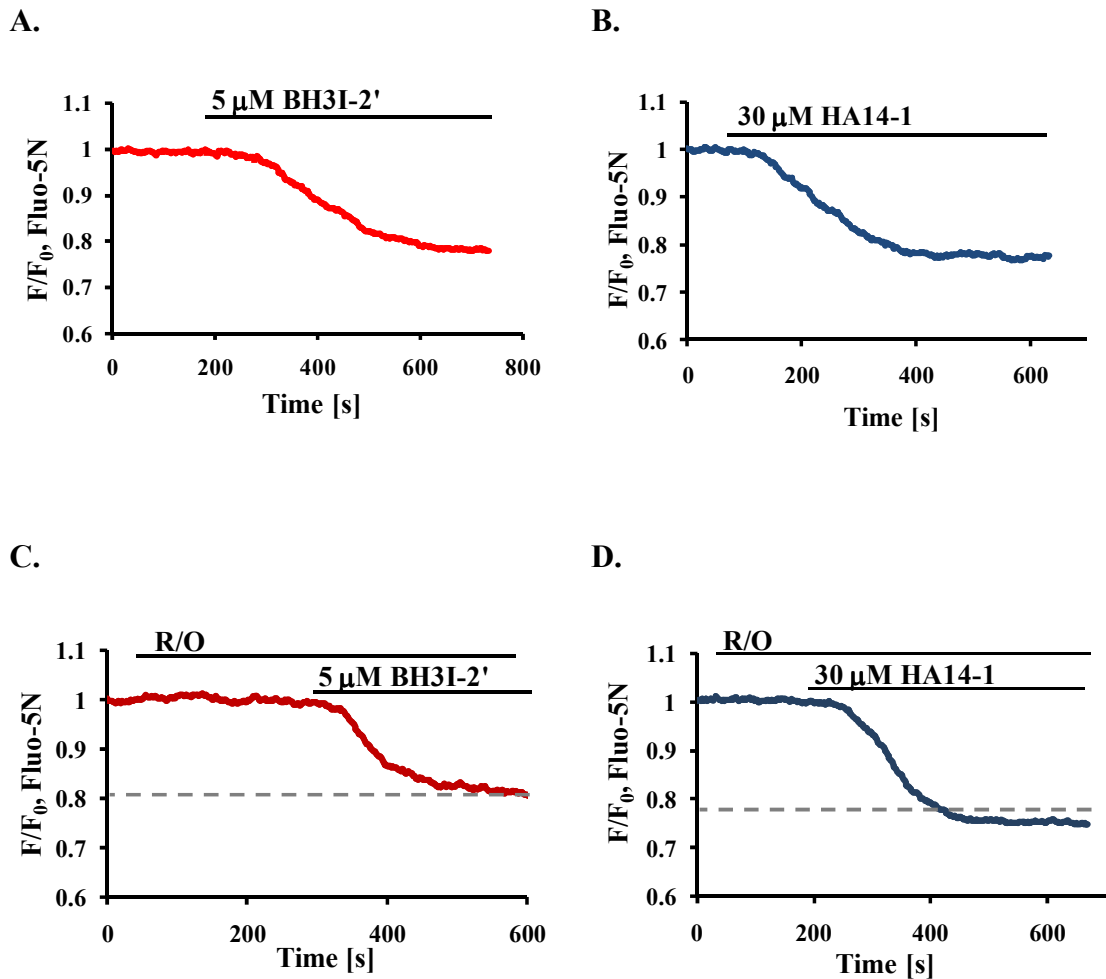


**Fig. 3.5. BH3 mimetics release calcium from the intracellular stores**

Typical traces of calcium release from the intracellular stores in response to BH3 mimetics: **(A)** 5  $\mu\text{M}$  BH3I-2' and **(B)** 30  $\mu\text{M}$  HA14-1 in permeabilized pancreatic acinar cells. Pretreatment of permeabilized cells with mixture of 10 $\mu\text{M}$  rotenone and 10  $\mu\text{M}$  oligomycin did not prevent calcium release induced by **(C)** BH3I-2' and **(D)** HA14-1. Grey dashed lines show amplitudes of the responses to BH3 mimetics alone. [Adapted from *Gerasimenko JV, Ferdek PE, 2010*]<sup>207</sup>.

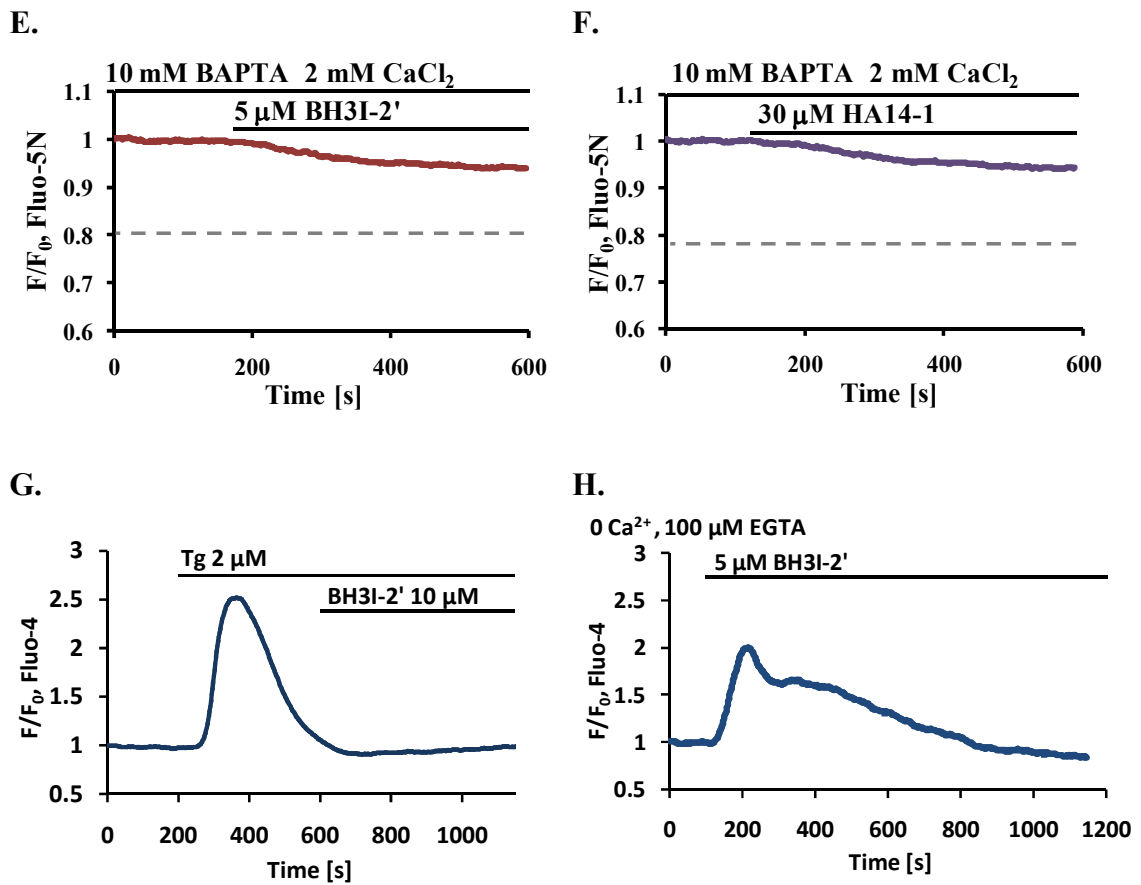


**Fig. 3.5.** (continues)

In the conditions of clamped calcium (10 mM BAPTA / 2 mM CaCl<sub>2</sub>) responses of internal stores to **(E)** BH3I-2' or **(F)** HA14-1 were markedly reduced but resolvable. Grey dashed lines show amplitudes of the responses to BH3 mimetics alone. **(G)** A typical trace obtained upon treatment with 10 μM BH3I-3' after depletion of calcium from the ER by thapsigargin in intact pancreatic acinar cells. **(H)** A typical cytosolic calcium response recorded upon treatment with 5 μM BH3I-2' in the presence of 100 μM EGTA with no extracellular Ca<sup>2+</sup> in intact pancreatic acinar cells. [Adapted from *Gerasimenko JV, Ferdek PE, 2010*]<sup>207</sup>.

---

from male CD1 mice were loaded with calcium sensitive dye fluo-5N AM under conditions that promote endoplasmic localization of the dye. The cells were then permeabilized with two photon laser light (as described in Chapter 2) and perfused with KHEPES solution containing 100  $\mu$ M 2-aminoethoxydiphenyl borate (2-APB) or 10  $\mu$ M ruthenium red, or both inhibitors. Application of 2-APB and ruthenium red aimed to block IP<sub>3</sub>Rs and RyRs, respectively<sup>208</sup>. The results were presented as reduction in green fluorescence of fluo-5N at the plateau normalized to the baseline values. The presence of 2-APB resulted in decreased amplitude of Ca<sup>2+</sup> release as compared to BH3I-2' alone (from 18.5 % to 13 %  $\pm$  1.9 SE, n = 8) as well as HA14-1 alone (from 20 % to 11.7 %  $\pm$  0.9 SE, n = 5), but did not inhibit the responses completely (*Fig. 3.6.A-B*). 10  $\mu$ M ruthenium red also caused a slight reduction in BH3I-2'- (12.5 %  $\pm$  1.2 SE, n = 5) and HA14-1-evoked (12 %  $\pm$  1.4 SE, n = 5) calcium release (*Fig. 3.6.C-D*). Simultaneous application of 100  $\mu$ M 2-APB and 10  $\mu$ M ruthenium red resulted in even stronger inhibitory effect – the responses were reduced to 8.8 %  $\pm$  0.5 SE, n = 5 for BH3I-2'; and 7.3 %  $\pm$  0.9 SE n = 5 for HA14-1 (*Fig. 3.6.E-F*). The results indicate that both IP<sub>3</sub>Rs and RyRs are partially involved in BH3 mimetic-induced calcium release from the intracellular stores. Their role in BH3 mimetic-elicited response is most likely restricted to amplification of the calcium signal through CICR process. The primary calcium release might be associated with potentiated calcium leak from the ER. This notion is developed in Chapter 6. All data obtained from the experiments on permeabilized pancreatic acinar cells (*Fig. 3.5* and *Fig. 3.6*) are summarized in a bar chart (*Fig. 3.6.G*).

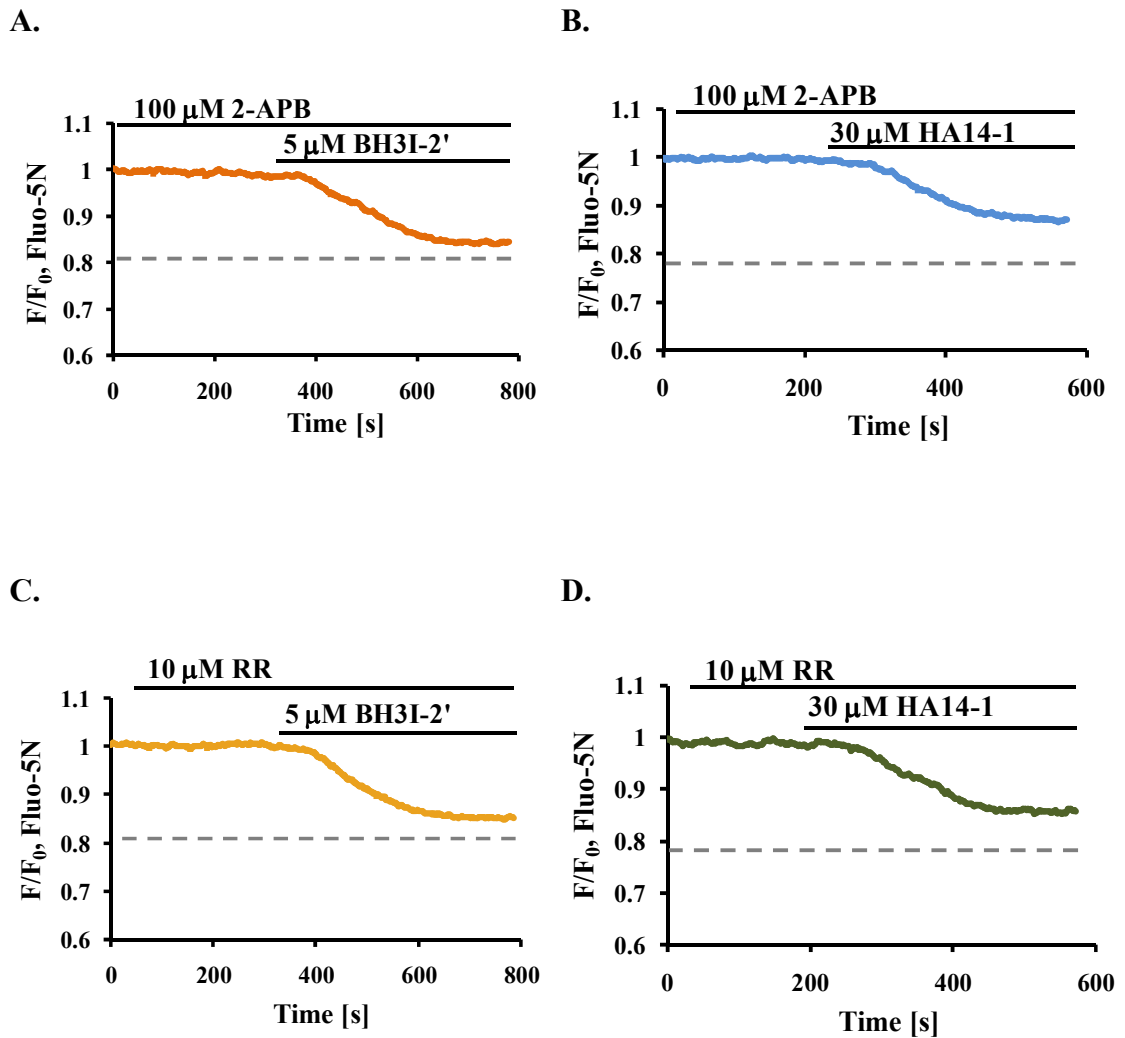


**Fig. 3.6. Involvement of IP<sub>3</sub>Rs and RyRs in BH3 mimetic-induced Ca<sup>2+</sup> release**  
 Pre-incubation of permeabilized pancreatic acinar cells with 100  $\mu\text{M}$  2-APB partially reduced responses to (A) 5  $\mu\text{M}$  BH3I-2' and (B) 30  $\mu\text{M}$  HA14-1. Pre-incubation of permeabilized cells with 10  $\mu\text{M}$  ruthenium red (RR) partially reduced responses to (C) 5  $\mu\text{M}$  BH3I-2' and (D) 30  $\mu\text{M}$  HA14-1. Grey dashed lines show amplitudes of the responses to BH3 mimetics alone. [Adapted from *Gerasimenko JV, Ferdek PE, 2010*]<sup>207</sup>.

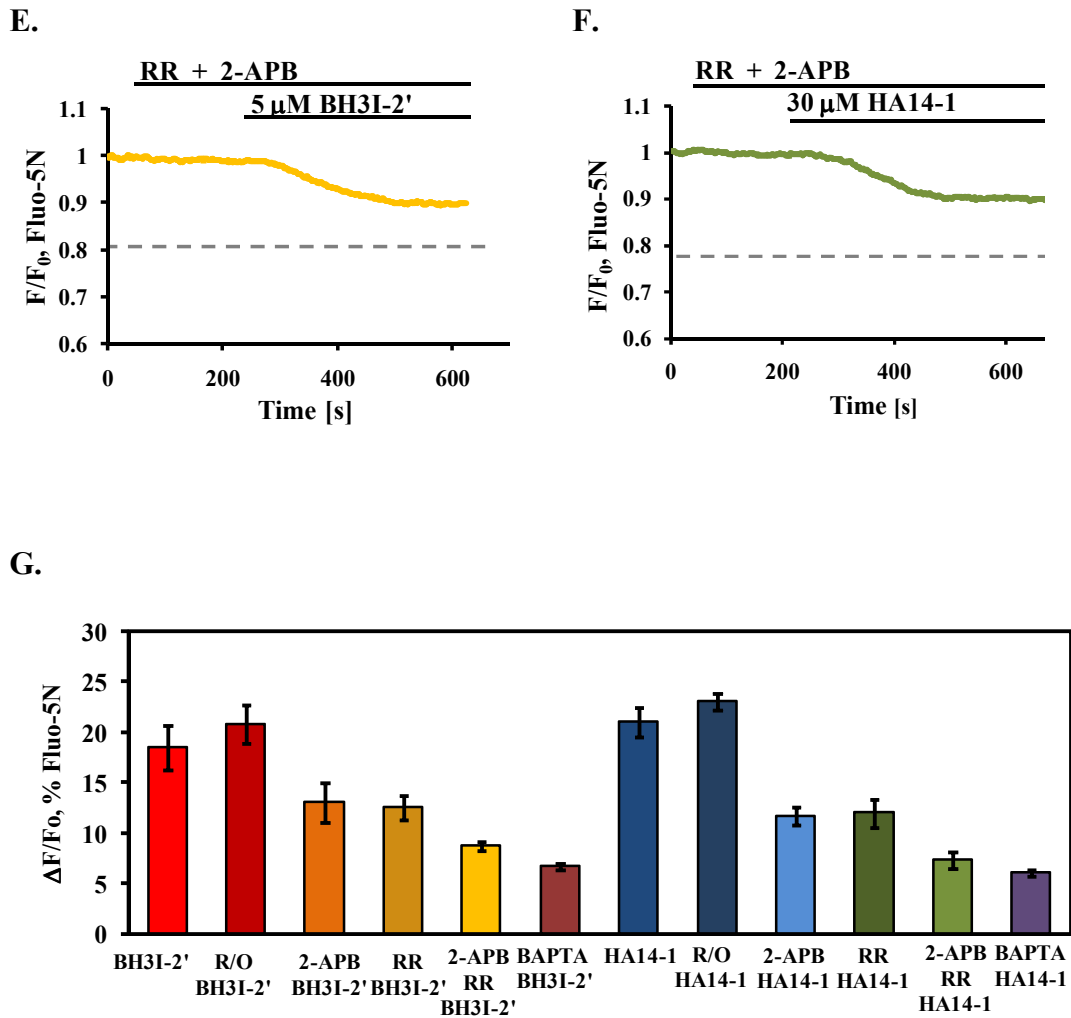


**Fig. 3.6.** (continues)

Pre-incubation of permeabilized cells with mixture of 100  $\mu\text{M}$  2-APB and 10  $\mu\text{M}$  ruthenium red substantially reduced responses to **(E)** 5  $\mu\text{M}$  BH3I-2' (n = 5) and **(F)** 30  $\mu\text{M}$  HA14-1 (n = 5). Grey dashed lines show amplitudes of the responses to BH3 mimetics alone. **(G)** Summary of data obtained on permeabilized cells (presented as traces on Fig. 3.5 and Fig. 3.6). [Adapted from Gerasimenko JV, Ferdek PE, 2010]<sup>207</sup>.

---

### **3.7. CICR type of response and cytosolic calcium plateau induced by BH3I-2' are substantially reduced in AR42J cells overexpressing Bcl-2**

In order to test whether BH3 mimetic-induced CICR could be reduced by the excess of Bcl-2, GFP-tagged human Bcl-2 protein was transiently overexpressed in pancreatic cancer cell line AR42J. GFP fluorescence was used to distinguish between transfected and untransfected cells. The latter served as controls. The cells were loaded with AM ester form of ratiometric calcium sensitive dye fura-2 and treated with different concentrations of BH3I-2' (1, 2, 5 and 15  $\mu\text{M}$ ) in NaHEPES solution, without the presence of external  $\text{Ca}^{2+}$ . The results show that BH3I-2' induces calcium release in both transfected and untransfected cells. 1  $\mu\text{M}$  BH3I-2' has only a modest effect on both control and Bcl-2-overexpressing cells. However, the effect of higher doses of BH3I-2' (2, 5 and 15  $\mu\text{M}$ ) on CICR in AR42J cells shows dependence on the level of intracellular Bcl-2. In cells overexpressing Bcl-2-GFP the initial phases of the responses were substantially reduced (*Fig. 3.7.A-E*). This result suggests that Bcl-2 can be at least partially involved in the regulation of the CICR component of BH3 mimetic-induced responses.

What is more, it was observed that in AR42J cells overexpressing Bcl-2-GFP cytosolic calcium plateau induced by higher concentrations of BH3I-2' (5 and 15  $\mu\text{M}$ ) was diminished as compared to control cells (*Fig. 3.7.F*). However, the decrease in cytosolic plateau (*Fig. 3.7.F*) was slightly more substantial with 5  $\mu\text{M}$  BH3I-2' treatment (33.9 % reduction  $\pm$  5.4 SE) and less pronounced with 15  $\mu\text{M}$  BH3I-2' (26.5 % reduction  $\pm$  7.0 SE). Since Bcl-2 is a target for BH3 mimetics higher dose of BH3I-2' is required to overcome effects of Bcl-2 overexpression. This

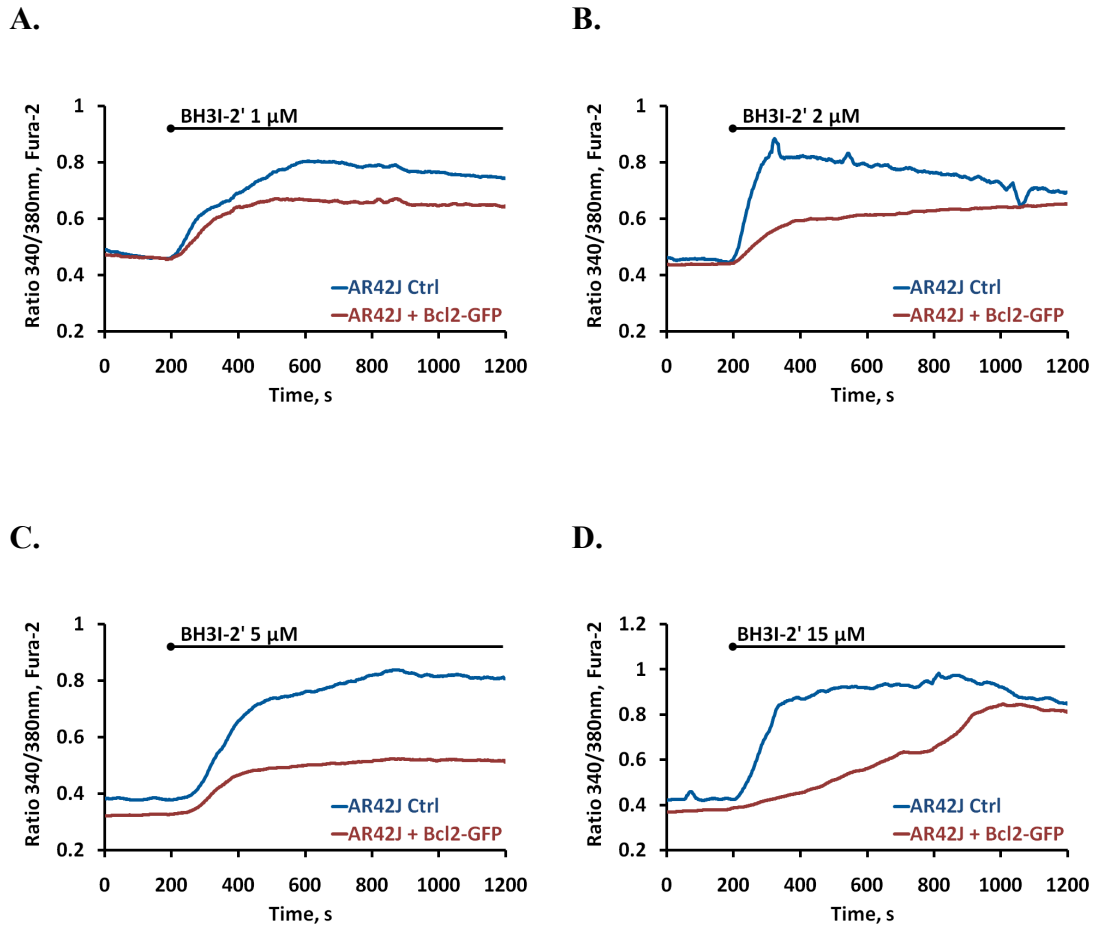
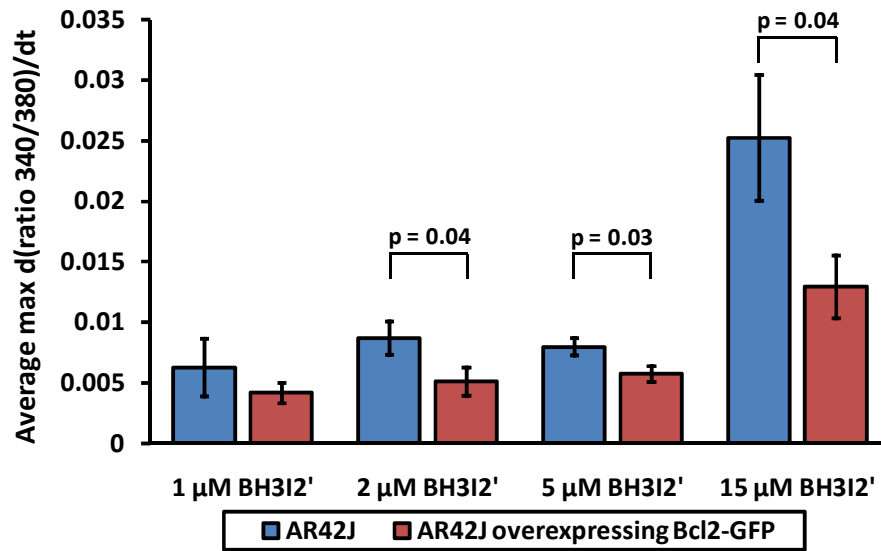


### Fig. 3.7. Overexpression of Bcl-2 affects CICR

Representative traces of responses to (A) 1  $\mu$ M BH3I-2', (B) 2  $\mu$ M BH3I-2', (C) 5  $\mu$ M BH3I-2' and (D) 15  $\mu$ M BH3I-2' in control (blue traces) and in Bcl-2 overexpressing AR42J cells (red traces). [Adapted from *Gerasimenko JV, Ferdek PE, 2010*]<sup>207</sup>.

E



F

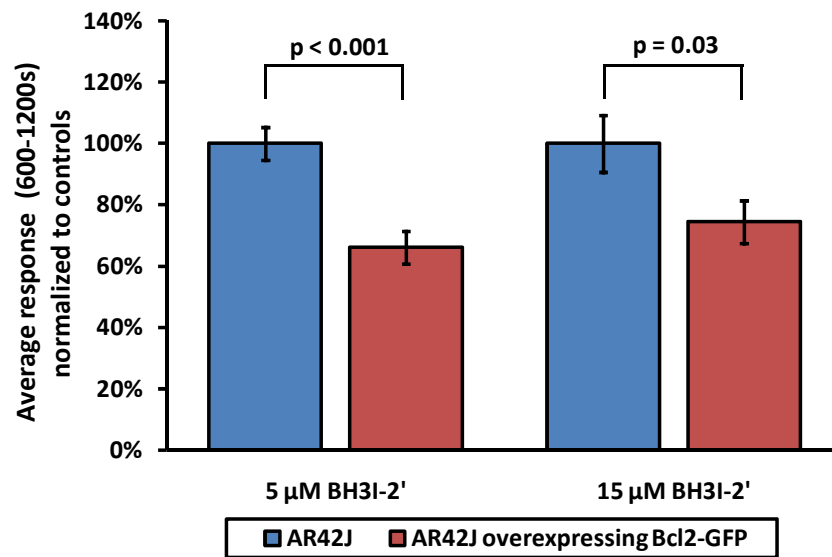


**Fig. 3.7. (continues)**

(E) Comparison of CICR type of response in control and Bcl-2 overexpressing AR42J cells to different doses of BH3I-2' presented as average rates of the increasing phase of responses (1 μM BH3I-2':  $n_{\text{Ctrl}} = 19$ ,  $n_{\text{Bcl2}} = 16$ ; 2 μM BH3I-2':  $n_{\text{Ctrl}} = 21$ ,  $n_{\text{Bcl2}} = 19$ ; 5 μM BH3I-2':  $n_{\text{Ctrl}} = 21$ ,  $n_{\text{Bcl2}} = 17$ ; 15 μM BH3I-2':  $n_{\text{Ctrl}} = 19$ ,  $n_{\text{Bcl2}} = 19$ ). (F) Comparison of calcium plateau induced by 5 μM ( $n_{\text{Ctrl}} = 21$ ,  $n_{\text{Bcl2}} = 17$ ) and 15 μM BH3I-2' ( $n_{\text{Ctrl}} = 19$ ,  $n_{\text{Bcl2}} = 19$ ) in control AR42J cells and cells overexpressing Bcl2-GFP. [Adapted from *Gerasimenko JV, Ferdek PE, 2010*]<sup>207</sup>.

---

suggests that even though CICR is substantially reduced in Bcl-2 overexpressing cells in dose-dependent manner, treatment with high doses of BH3 mimetics can still lead to development of delayed cytosolic Ca<sup>2+</sup> plateau.

### **3.8. Bcl-2 family protein-dependent CICR is crucial for apoptosis induction in pancreatic acinar cells**

Since the main function of Bcl-2 proteins is apoptosis regulation, a natural question to ask is whether attenuated CICR affects apoptosis induced by BH3I-2'. Freshly isolated pancreatic acinar cells were seeded on glass bottom petri dishes and loaded with general caspase substrate. Then the cells were treated for an hour with 15 μM BH3I-2' alone or BH3I-2' in the presence of inhibitors of IP<sub>3</sub>Rs and RyRs - 100 μM 2-APB and 10 μM ruthenium red, respectively. Apoptosis was determined based on fluorescence of cleaved general caspase substrate in three series of independent experiments with 20 to 80 cells each. BH3I-2' alone caused substantial apoptosis (58.4 % ± 2.5 SE) among plated pancreatic acinar cells (*Fig. 3.8*). However, the presence of 2-APB and ruthenium red significantly reduced the level of apoptosis to 15.8 % ± 0.7 SE, which was only slightly higher than control values (7.3 % ± 3.7 SE). The results suggest that CICR process and calcium release from the intracellular stores promotes BH3I-2'-dependent apoptosis induction.

### **3.9. Discussion**

The results presented in this chapter demonstrate functions of Bcl-2 proteins in the process of Ca<sup>2+</sup> release from the intracellular stores. The investigation is mainly based on inhibition of Bcl-2 by BH3 mimetics BH3I-2' and HA14-1. Two different

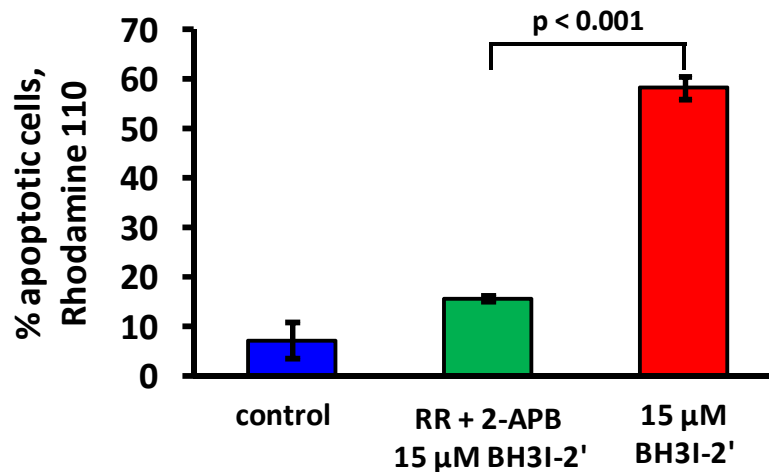


**Fig. 3.8. Inhibition of IP<sub>3</sub>Rs and RyRs decreases BH3I-2'-induced apoptosis**

The graph shows apoptosis detection via measurement of general caspase substrate cleavage by activated caspases upon treatment with 15 μM BH3I-2' in the presence / absence of the mixture of 100 μM 2-APB and 10 μM ruthenium red. 15 μM BH3I-2' caused substantial apoptosis (red bar, 58.4 % ± 2.5 SE). In the presence of the RR + 2-APB percentage of apoptotic cells was reduced to 17.8 % ± 0.7 SE (green bar), which was only slightly higher than control values (blue bar, 7.3 % ± 3.7 SE). [Adapted from *Gerasimenko JV, Ferdek PE, 2010*]<sup>207</sup>.

---

approaches (cell fractionation and staining of live cultured cells) independently confirm that anti-apoptotic members of Bcl-2 family are present not only in mitochondria but also in other cell compartments of mouse pancreatic acinar cells and rat pancreatic cancer cell line AR42J.

Also, the results of immunoprecipitation independently show that BH3 mimetics BH3I-2' and HA14-1 indeed cause dissociation of pro-apoptotic protein Bax from anti-apoptotic Bcl-2 or Bcl-xL. Interestingly, treatment of pancreatic acinar cells with BH3 mimetics and therefore disruption of the interaction between anti- and pro-apoptotic Bcl-2 proteins was associated with  $\text{Ca}^{2+}$  release from the intracellular stores, mainly the ER, which was demonstrated by the experiments on both intact and permeabilized pancreatic acinar cells.

In the literature there is very well established that Bcl-2 family proteins play a major role in regulation of apoptosis and mitochondrial homeostasis. Indeed treatment with BH3 mimetics eventually leads to mitochondrial depolarization and cytochrome c release, as was previously demonstrated<sup>209</sup>. However, the described effects of BH3 mimetics on calcium release from the intracellular stores appear to be independent on mitochondrial functions, because inhibition of ATP synthesis by combined application of rotenone and oligomycin neither affected BH3 mimetic-induced  $\text{Ca}^{2+}$  release nor released  $\text{Ca}^{2+}$  on its own.

Single and simultaneous inhibition of  $\text{IP}_3\text{Rs}$  and  $\text{RyRs}$  by 2-APB and ruthenium red revealed that these receptors play a role in  $\text{Ca}^{2+}$  response to BH3 mimetics. Pharmacological inhibition of one of the receptors substantially reduced  $\text{Ca}^{2+}$  release from the intracellular stores in permeabilized cells; and simultaneous block of both

---

receptors had additive effect confirming that both receptors are involved in the response. However, BH3 mimetic-induced  $\text{Ca}^{2+}$  release was never completely eliminated suggesting that the role of  $\text{IP}_3\text{Rs}$  and  $\text{RyRs}$  is only restricted to the amplification of already existing  $\text{Ca}^{2+}$  signal. What is more, overexpression of Bcl-2 in cell line AR42J clearly attenuated CICR induced by treatment with BH3I-2'. Therefore immediate interpretation of the data presented in this chapter could be that BH3 mimetics, which cause dissociation of pro-apoptotic proteins from anti-apoptotic Bcl-2 and Bcl-xL, increase the sensitivity of  $\text{IP}_3\text{Rs}$  and  $\text{RyRs}$  to activation by  $\text{Ca}^{2+}$ . In other words, anti-apoptotic Bcl-2 proteins seem to be involved in regulation of CICR process, because their pharmacological inhibition by BH3 mimetics significantly potentiates CICR leading to  $\text{Ca}^{2+}$  release from the stores. Importance of  $\text{IP}_3\text{Rs}$  and  $\text{RyRs}$  in BH3 mimetic responses is underlined by the fact that their inhibition dramatically influences cell viability. Application of 2-APB and ruthenium red together dramatically increased survival of the cells challenged with BH3I-2' by reducing CICR type of response.

In intact cells BH3 mimetics induce sudden  $\text{Ca}^{2+}$  release, which is followed by sustained cytosolic  $\text{Ca}^{2+}$  plateau, even in the absence of extracellular  $\text{Ca}^{2+}$ . Explanation of this sustained cytosolic  $\text{Ca}^{2+}$  is not straightforward. Pancreatic acinar cells are indeed capable of maintaining responses for a long time in calcium-free medium<sup>210</sup>. However, cytosolic calcium plateau in such conditions suggests inhibition of  $\text{Ca}^{2+}$  extrusion from the cytosol in pancreatic acinar cells<sup>211</sup>. Bcl-2 family members might indeed be involved in the regulation of  $\text{Ca}^{2+}$  transport across the membranes. The exact role of Bcl-2 protein in calcium fluxes across the plasma membrane is a subject of investigation described in Chapter 7. It has not yet been

---

investigated whether other ions, such as  $Zn^{2+}$ , could be released from the intracellular compartments upon treatment with BH3 mimetics. With no efficient extrusion pathways, such ions might accumulate in the cytosol and can be bound by  $Ca^{2+}$ -sensitive probes (although with much lower affinity) producing a signal that can be taken for  $Ca^{2+}$  increase. In this study it was demonstrated that a modest dose of EGTA (100  $\mu$ M) effectively removes the plateau, which suggests that the effect is predominantly caused by  $Ca^{2+}$  released from the intracellular stores.

This chapter constitutes a coherent demonstration that Bcl-2 family proteins are involved in the regulation of CICR. Although the role of Bcl-2 proteins in different aspects of intracellular calcium homeostasis is already relatively well established<sup>204,212</sup>, some issues still remain unclear. It is agreed that Bcl-2 family proteins regulate resting ER calcium levels. However the exact effect is a subject of disagreement. It was reported that Bcl-2 overexpression decreased  $Ca^{2+}$  concentration in the ER and diminished  $Ca^{2+}$  entry to this cell compartment<sup>157,158</sup>. However, other studies support the opposite effects of Bcl-2 on ER calcium: preservation of ER calcium by upregulation of SERCA<sup>159</sup>. Bcl-2 most likely controls multiple events in calcium signalling; therefore different conditions and experimental systems could explain that apparent controversy. Previous studies provided invaluable evidence that Bcl-2 and Bcl-xL can physically interact with the IP<sub>3</sub>R and affect its ability to release  $Ca^{2+}$  from the intracellular stores<sup>213-215</sup>. In the recent study BH4 domain of Bcl-2 was demonstrated to bind to the regulatory domain of the IP<sub>3</sub>R, which was associated with decreased  $Ca^{2+}$  release from the ER and attenuated apoptosis<sup>215</sup>. Those findings are in agreement with the data obtained in this study demonstrating that overexpression of Bcl-2 in AR42J cells decreases CICR, and with

---

the fact that application of pharmacological inhibition of anti-apoptotic Bcl-2 family members has the opposite effect leading to  $\text{Ca}^{2+}$  release from the stores. Taken together, accumulating evidence supports a model whereby anti-apoptotic Bcl-2 members such as Bcl-2 itself and Bcl-xL regulate  $\text{Ca}^{2+}$  releasing channels as a function of their interaction with pro-apoptotic Bcl-2 members such as Bax and Bak, or perhaps also with certain BH3-only proteins. When associated with its pro-apoptotic partner anti-apoptotic Bcl-2 protein might inhibit  $\text{Ca}^{2+}$  channels, whereas dissociation of pro- and anti-apoptotic proteins increases sensitivity of the receptors promoting  $\text{Ca}^{2+}$  release<sup>207</sup>. It could also be speculated that different sensitivity of distinct regions in pancreatic acinar cells might be associated with specific intracellular distribution of certain Bcl-2 family members. Alternatively, differential regulation of inhibitory functions of Bcl-2 proteins located in the basolateral area in contrast to those from the apical area could be suggested<sup>207</sup>. However, up to now there is no direct evidence for such distribution or regulation of Bcl-2 family members in pancreatic acinar cells and thus this subject constitutes an exciting opportunity for further development of the present study.

In summary this chapter provides new insights into anti-apoptotic Bcl-2 protein-dependent regulation of intracellular calcium homeostasis. Pharmacological inhibition of Bcl-2 and Bcl-xL by BH3 mimetics disrupts their interaction with anti-apoptotic Bcl-2 proteins Bax and Bak, which is associated with increased sensitivity of  $\text{IP}_3\text{Rs}$  and  $\text{RyRs}$  to activation by  $\text{Ca}^{2+}$  leading to actual  $\text{Ca}^{2+}$  release from the intracellular stores.

---

**CHAPTER 4:**  
**CALMODULIN DEPENDENT MECHANISM OF CALCIUM**  
**RESPONSES INDUCED BY BH3 MIMETICS**

---

## Chapter 4: Calmodulin dependent mechanism of calcium responses induced by BH3 mimetics

### 4.1. Overview of calmodulin

Calmodulin (CaM) is a regulatory protein present in all eukaryotic cells. It is a relatively small protein of about 17 kDa, composed of 148 conserved amino acid residues. Importantly calmodulin has four EF hand motifs of helix-loop-helix structure, each of which is capable of binding a single  $\text{Ca}^{2+}$  ion. Two of the motifs (EF1 and EF2) are located at the N-terminal domain and bind  $\text{Ca}^{2+}$  with high affinity; two other (EF3 and EF4) are present on the other site of the polypeptide chain, at the C-terminal domain, and bind  $\text{Ca}^{2+}$  with markedly lower affinity. The two domains are separated by a flexible  $\alpha$ -helical linker region (structure of calmodulin from *Paramecium tetraurelia* is shown in Fig. 4.1.A). Despite different affinity of EF motifs for  $\text{Ca}^{2+}$ , the ions are bound in cooperative manner, meaning that the presence of a  $\text{Ca}^{2+}$  ion in one EF motif increases the affinity of other  $\text{Ca}^{2+}$  binding sites<sup>216</sup>. Therefore even slight elevation of cytosolic  $\text{Ca}^{2+}$  can activate calmodulin in vivo and affect its physiological functions. The protein is believed to be fully activated at the  $\text{Ca}^{2+}$  concentration as low as 500 nM<sup>217</sup>. The process of  $\text{Ca}^{2+}$  binding to calmodulin is associated with a significant conformational change of the protein, especially in its linker region. It is possible to distinguish at least two extreme conformational configurations<sup>218</sup>. Configuration without bound  $\text{Ca}^{2+}$  is called apocalmodulin (apoCaM) and is characterised by 'closed' conformation, in which EF hand motifs in

---

both domains are tightly packed<sup>219</sup>. In contrast, Ca<sup>2+</sup>-CaM has a Ca<sup>2+</sup> ion interacting with every EF motif, resulting in four Ca<sup>2+</sup> ions bound per molecule of calmodulin. In this configuration calmodulin adopts more open conformation: EF hand motifs are located further away than in apoCaM, which leads to the exposure of hydrophobic amino acid residues in both domains and rearrangements in the flexible linker between them<sup>219</sup>. Some neuronal proteins such as unconventional myosins or ion channels can interact with apoCaM. They possess an amphipathic CaM binding motif called IQ-motif enriched with hydrophobic amino acids such as Leu, Ile, Val, Trp or Phe. Prebound calmodulin can modify target protein activity within milliseconds. Alternatively, calmodulin can interact with target proteins after binding calcium and changing conformation to Ca<sup>2+</sup>-CaM. There is no conserved consensus sequence for Ca<sup>2+</sup>-CaM binding domains, but they usually consists of 15 to 30 amino acid residues and are both hydrophobic and basic in nature (calmodulin itself is more acidic and in its open conformation hydrophobic amino acid residues are exposed).

Calmodulin is engaged in regulation of multiple intracellular processes including signalling and transcription pathways. As a multifunctional signal transducer it binds and activates various proteins, mainly phosphatases (such as calcineurin) and Ca<sup>2+</sup> / calmodulin-dependent protein kinases (CaMKs)<sup>220</sup>. Calmodulin is also involved in regulation of intracellular calcium homeostasis by modulating Ca<sup>2+</sup> responses and affecting Ca<sup>2+</sup> fluxes. For example it interacts with TRP channels, or regulates activity of the PMCA pump. Further, calmodulin interacts with RyRs and its functions depend on the receptor type. In type 1 RyRs apoCaM conformation is a partial agonist, whereas Ca<sup>2+</sup>-CaM acts as an inhibitor of the receptors<sup>221</sup>. In contrast, type 2 RyRs are inhibited by calmodulin in all its conformations<sup>195</sup>. What is more,

---

calmodulin plays a regulatory role in exocytosis mainly through modulation of membrane trafficking proteins. It was found to interact with synaptotagmin and synaptobrevin<sup>222,223</sup>.

Calcium-like peptides (CALPs) are complementary peptides to EF-hand  $\text{Ca}^{2+}$ -binding sites. They were shown to interact with calmodulin and certain calcium channels inhibiting  $\text{Ca}^{2+}$ -dependent cytotoxicity and cell death. CALPs were designed by inversion of the hydrophobic pattern of the EF-hands and thus they have a complementary surface contour to the original sequences. It has been demonstrated in the past that complementary peptides specifically interact with one another<sup>224,225</sup>; therefore the technique of hydrophobic pattern inversion can be used for generating specific ligands to the sequence of interest.

So far four different CALPs have been designed and tested<sup>226</sup>. They all interact with calmodulin with moderate affinities but exert different effects. CALP-1 and CALP-3 are calmodulin activators, whereas CALP-2 and CALP-4 act as antagonists. Since the octamer structure of the first peptide CALP-1 was based on the  $\text{Ca}^{2+}$ -binding site of the troponin C, its hydrophobic profile is not perfectly complementary to EF-hands motifs of calmodulin. Therefore, CALP-2 and CALP-3 were designed as optimized peptides complementary to the EF-4 motif of human calmodulin. CALP-2 consists of 12 amino acid residues, and CALP-3 is effectively its shorter version having only the first 8 amino acids. Finally, CALP-4 is another 12-mer peptide, which is composed of the sequence of CALP-1 with the last four amino acids of CALP-2. All four sequences are shown in *Fig. 4.1.B*.

A.



B.

Peptide	Sequence
CALP-1	VAITVLVK
CALP-2	VKFGVGFKVMVF
CALP-3	VKFGVGFK
CALP-4	VAITVLVKVMVF

**Fig. 4.1. Calmodulin and CALPs**

(A) Molecular structure of calmodulin from *Paramecium tetraurelia* in complex with 4  $\text{Ca}^{2+}$  ions (cartoon display, Jmol, Protein Data Bank). Pink spirals represent  $\alpha$ -helical structures, yellow arrows are  $\beta$ -sheets, and  $\text{Ca}^{2+}$  ions are shown in green. (B) The table shows sequences of  $\text{Ca}^{2+}$ -like peptides<sup>226</sup> (full description in text).

---

Optimized inverted hydrophobic pattern of CALP-3 is reflected by its higher affinity for calmodulin as compared to CALP-1 ( $K_d = 33 \mu\text{M}$  and  $K_d = 52 \mu\text{M}$ , respectively). Also, CALP-2 has been demonstrated to have a 14-fold higher affinity to calmodulin than CALP-1. Importantly, CALPs interact only with low affinity  $\text{Ca}^{2+}$ -binding sites in the carboxyl domain of calmodulin but not with the EF-hands in the N-terminal domain. Binding of CALPs to calmodulin is associated with conformational change, which, however, is not identical to that observed for  $\text{Ca}^{2+}$ -CaM. Nevertheless, in case of CALP-1 and CALP-3, this conformational change of calmodulin is active and sufficient for phosphodiesterase activation. Interaction of CALP-2 or CALP-4 with calmodulin does not result in active conformation, which explains the fact why these peptides antagonise  $\text{Ca}^{2+}$  / CaM-dependent activation of phosphodiesterase.

Application of CALPs requires their efficient delivery to the cytosol, where they can exert their functions. It has been demonstrated that fluorescently tagged CALP-1 can rapidly enter cultured rat neocortical neurones<sup>227</sup>. Interestingly, the intracellular effects of CALPs are not only restricted to modulation of calmodulin activity. These peptides can also interfere with calcium sensing mechanisms of certain  $\text{Ca}^{2+}$  channels and thus have inhibitory role on  $\text{Ca}^{2+}$  fluxes. This inhibition can be based on direct interaction of a peptide with the  $\text{Ca}^{2+}$ -binding site of a channel; or it can be mediated through calmodulin, a primary target of CALPs<sup>227</sup>.

This study applies CALPs to reduce toxic effects of elevated cytosolic  $\text{Ca}^{2+}$  induced by treatment with BH3 mimetics. It is known that BH3 mimetics inhibit the interaction between anti-apoptotic Bcl-2 members and pro-apoptotic Bax / Bak, which triggers induction of apoptosis. As was demonstrated in Chapter 3, treatment with BH3 mimetics such as BH3I-2' and HA14-1 is also associated with sudden  $\text{Ca}^{2+}$

---

release from the intracellular stores in pancreatic acinar cells followed by sustained  $\text{Ca}^{2+}$  plateau formation. Sustained cytosolic  $\text{Ca}^{2+}$  elevation leads to induction of necrosis, which is an undesirable cell death mode, since it is uncontrolled and characterised by release of the intracellular content, which in turn might trigger inflammatory response and further tissue damage. Therefore application of BH3 mimetics as potential anti-cancer agents will inevitably be associated with toxic effects on pancreas and perhaps on other organs as well. The aim of the work presented in this chapter is to reduce the toxic effects of BH3 mimetics in order to diminish the levels of necrosis without affecting their pro-apoptotic functions. For that purpose Calcium-Like Peptides (CALPs) were applied to exert specific pre-activation of calmodulin.

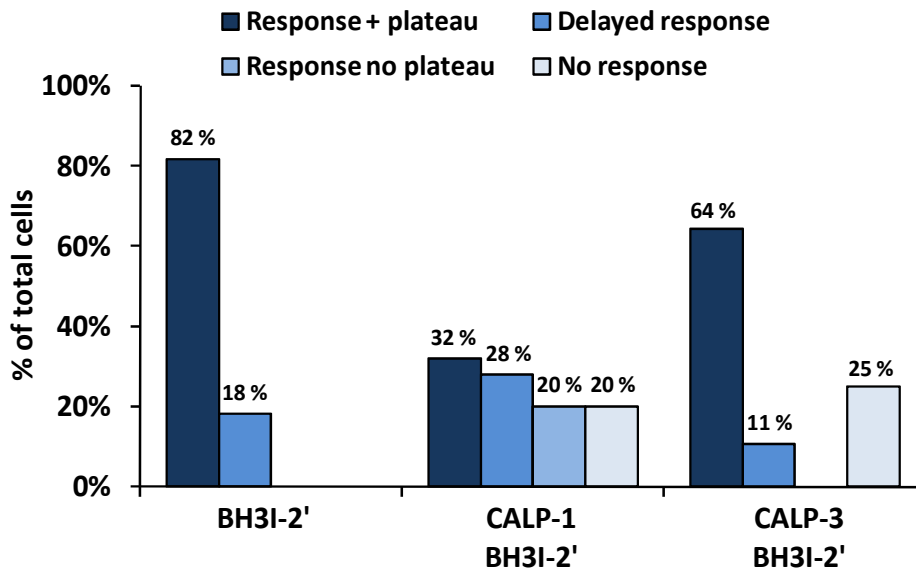
#### **4.2. Effects of Calcium-Like Peptides on BH3I-2'-related $\text{Ca}^{2+}$ responses**

Application of 5  $\mu\text{M}$  BH3I-2' on intact pancreatic acinar cells causes a CICR-type of response followed by sustained cytosolic  $\text{Ca}^{2+}$  plateau formation, as was already depicted in the previous chapter in *Fig. 3.4.A-B*. Here the effects of BH3I-2' on calcium homeostasis in pancreatic acinar cells were investigated in the presence or absence of CALP-1 or CALP-3. Freshly isolated pancreatic acinar cells were loaded with fura-2 and then preincubated for 200 s with 100  $\mu\text{M}$  CALP-1 ( $n = 25$ ) or CALP-3 ( $n = 28$ ). Control cells ( $n = 22$ ) were incubated for the same amount of time with NaHEPES (+ 1 mM  $\text{Ca}^{2+}$ ) only. Subsequently the cells were treated with 5  $\mu\text{M}$  BH3I-2' and calcium responses were compared. BH3I-2' alone induced  $\text{Ca}^{2+}$  responses in all treated cells: 82 % of cells developed major CICR-type of response followed by sustained  $\text{Ca}^{2+}$  plateau; and 18 % of cells responded with a delayed

---

increase in cytosolic  $\text{Ca}^{2+}$ , which also was followed by prolonged cytosolic  $\text{Ca}^{2+}$  elevation (*Fig. 4.2.A and B*). Pretreatment with 100  $\mu\text{M}$  CALP-1 resulted in substantial change in type of  $\text{Ca}^{2+}$  responses. Only 32 % of cells developed major  $\text{Ca}^{2+}$  responses (*Fig. 4.2.A*); however the amplitude of the responses was lower than those elicited by BH3I-2' only (*Fig. 4.2.C*). 28 % of cells responded with a delayed  $\text{Ca}^{2+}$  increase in the cytosol, which was concluded with sustained  $\text{Ca}^{2+}$  plateau (*Fig. 4.2.A and C*). Interestingly, 20 % of cells pretreated with CALP-1 responded with only transient cytosolic  $\text{Ca}^{2+}$  increase, which quickly returned to the basal level without plateau formation. Finally, a fraction of cells (20 %) did not respond in the time course of the experiment (*Fig. 4.2.A and C*). Preincubation with CALP-3 had a slightly different effect: it decreased the fraction of cells that developed major  $\text{Ca}^{2+}$  response to BH3I-2' from 82 % to 64 % (*Fig. 4.2.A*). Only 11 % of the cells developed a delayed  $\text{Ca}^{2+}$  response to treatment with the BH3 mimetic (*Fig. 4.2.A and D, trace b*). Importantly, 25 % of cells did not respond to BH3I-2' in the time course of the experiment (*Fig. 4.2.A and D, trace c*). *Fig. 4.2.E* shows average calcium responses to BH3I-2' in control cells and cells pretreated with 100  $\mu\text{M}$  CALP-1 or CALP-3. In order to quantitatively compare the effects of CALPs, the average areas under the traces were calculated between 400 s and 1000 s (*Fig. 4.2.F*). Also, the amplitudes were taken at 900 s of calcium traces, averaged and compared in *Fig. 4.2.G*. The results show that the presence of 100  $\mu\text{M}$  CALP-1 significantly reduces both the overall BH3I-2'-induced cytosolic  $\text{Ca}^{2+}$  elevation ( $p = 0.001$ , *Fig. 4.2.F*) and the amplitude of the response ( $p = 0.005$ , *Fig. 4.2.G*) as compared to control cells. In contrast, a slight reduction in both average BH3I-2'- elicited  $\text{Ca}^{2+}$  response ( $p = 0.4$ , *Fig. 4.2.F*) and the average amplitude of  $\text{Ca}^{2+}$  plateau

A.



B.

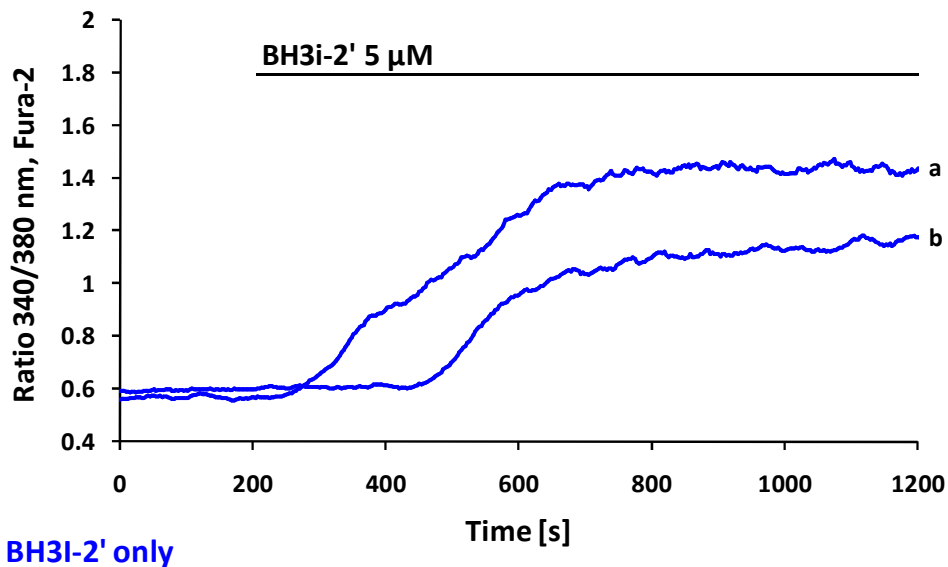
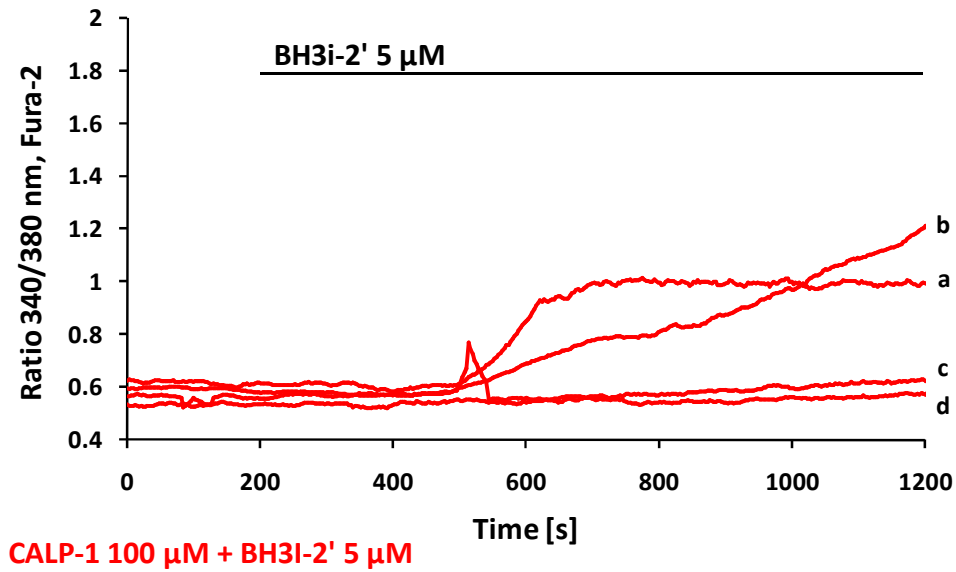


**Fig. 4.2. Effects of CALPs on BH3I-2'-induced calcium responses**

(A) The chart shows distribution of different types of Ca<sup>2+</sup> responses induced by treatment with 5 μM BH3I-2' in the presence / absence of 100 μM CALP-1 or 100 μM CALP-3. (B) Two sample traces showing immediate response to BH3I-2' followed by sustained Ca<sup>2+</sup> plateau (trace a) and a delayed response (trace b).

C.



D.

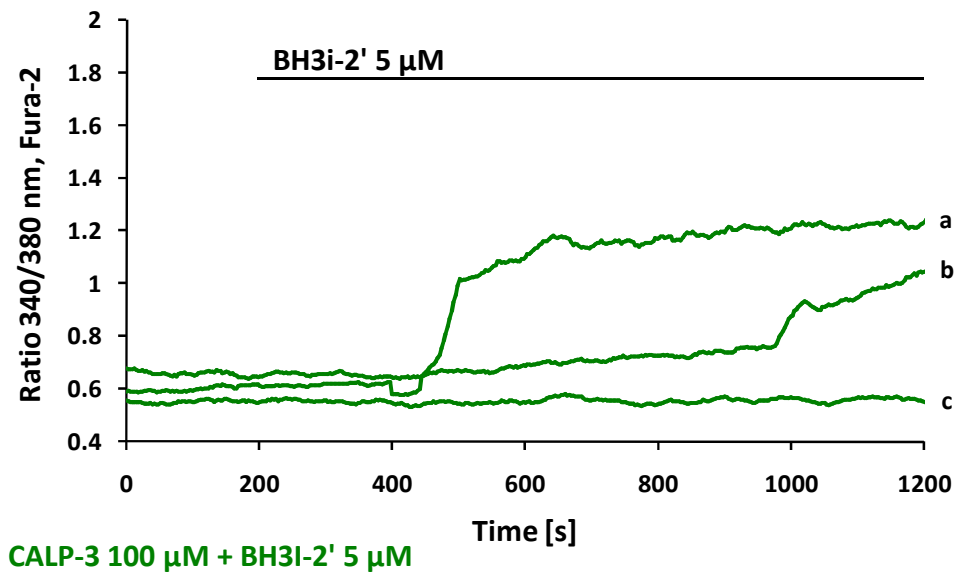
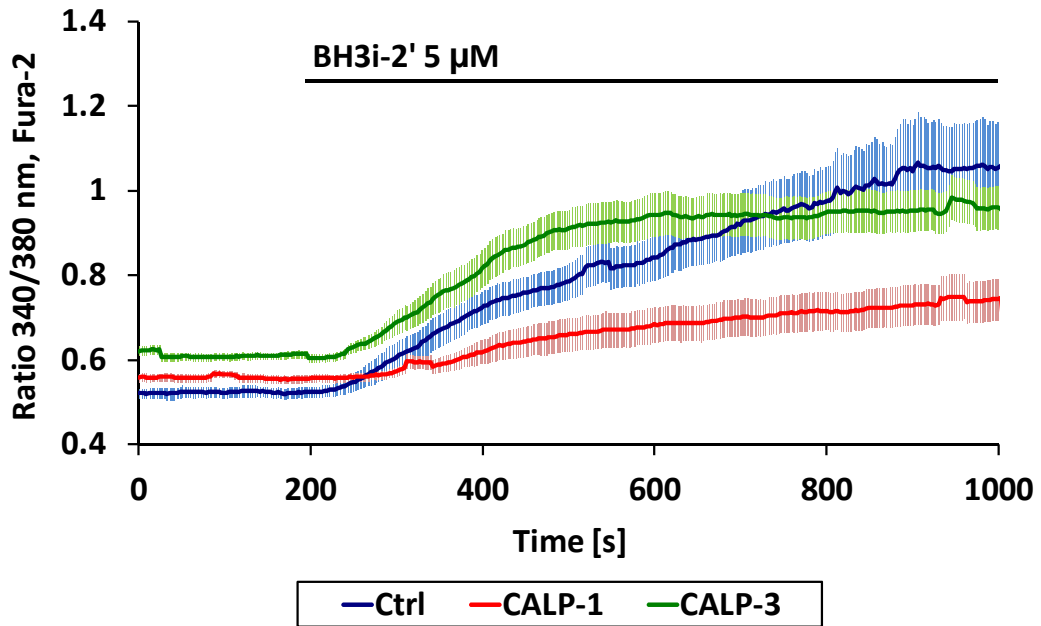


Fig. 4.2. (continues)

(C) Four sample traces showing different types of responses to BH3I-2' in the presence of CALP-1: a major response (trace a), a delayed response (trace b), transient  $\text{Ca}^{2+}$  increase without forming sustained cytosolic  $\text{Ca}^{2+}$  plateau (trace c), and no response (trace d). (D) Three sample traces showing responses to BH3I-2' in the presence of CALP-3: a major calcium response followed by sustained cytosolic  $\text{Ca}^{2+}$  plateau (trace a), a response delayed in time (trace b), and no response (trace c).

E.



F.

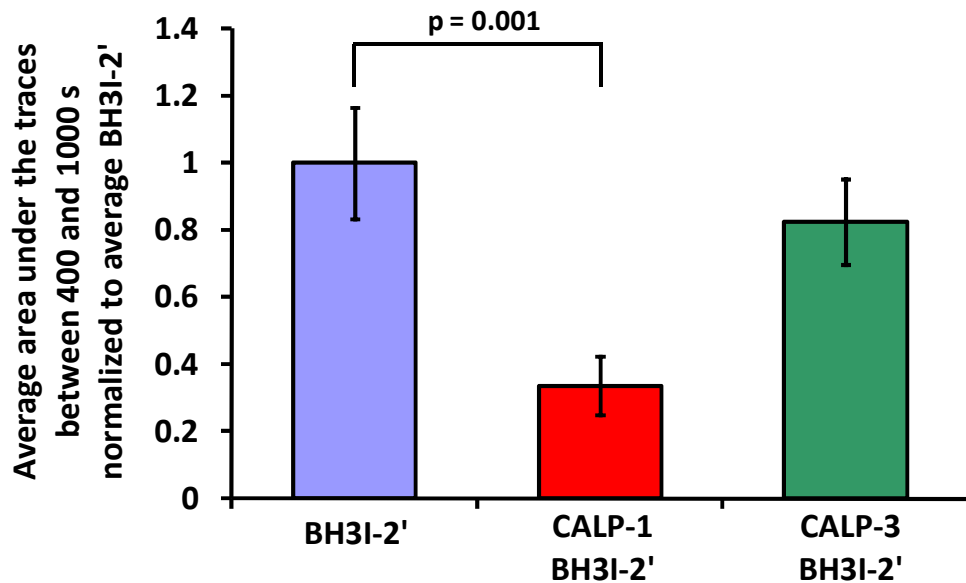


**Fig. 4.2.** (continues)

(E) Average traces of responses to 5  $\mu$ M BH3i-2' only ( $n = 22$ , blue trace), and to BH3i-2' in the presence of 100  $\mu$ M CALP-1 ( $n = 25$ , red trace) or 100  $\mu$ M CALP-3 ( $n = 28$ , green trace). Error bars represent standard errors of mean. (F) The bar chart shows average area under the traces depicted in E between 400 s and 1000 s of the recorded responses. Error bars represent standard error of mean.

G.

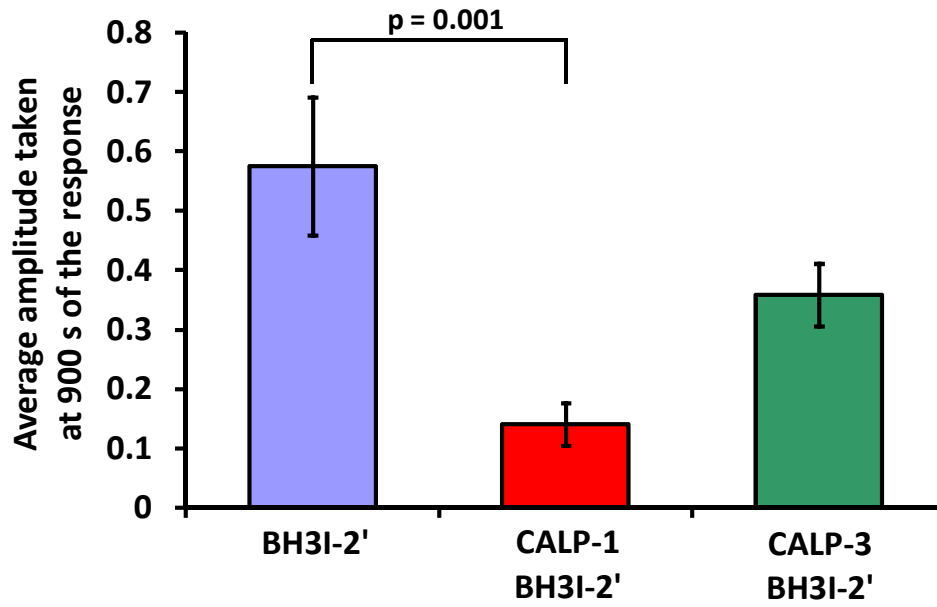


**Fig. 4.2.** (continues)

(G) The bar chart shows average amplitude obtained from the traces at 900 s of the recorded responses.

---

at 900 s ( $p = 0.1$ , *Fig. 4.2.G*) in the presence of CALP-3 were statistically non-significant. CALP-3 appears to interfere with  $\text{Ca}^{2+}$  release caused by BH3I-2', which is shown by the fraction of cells that did not respond to the treatment with the BH3 mimetic. However, its effects are not as strong as those evoked by CALP-1.

### **4.3. Effects of CALPs on BH3I-2'-induced cell death in pancreatic acinar cells**

CALPs modulate BH3I-2'-induced  $\text{Ca}^{2+}$  responses in pancreatic acinar cells. However, it is not clear whether induction of cell death is also affected. In order to address this issue the cell death assay was performed in pancreatic acinar cells. Pancreatic acinar cells were isolated as described above and were divided equally into 4 tubes. Two samples were pretreated with 100  $\mu\text{M}$  CALP-1 or CALP-3 for 15 min at room temperature. The other two were incubated for the same amount of time, but without any treatment. Subsequently the samples containing CALPs and one of the untreated samples were incubated with 5  $\mu\text{M}$  BH3I-2' for 30 min. 15 min before the end of the incubation annexin-V-FITC and propidium iodide were added to all samples in amounts defined by Apoptosis Detection Kit (Sigma). Apoptotic and necrotic cells were visualized with Leica confocal microscope. The assay was repeated three times on different days. The combined results of the experiment are shown in *Fig. 4.3*. In control sample most of the cells are alive and healthy; low levels of apoptosis and necrosis result from the process of isolation. Treatment with BH3I-2' substantially decreases the amount of live cells ( $p = 0.0003$ ), at the same time both apoptosis and necrosis are increased ( $p = 0.005$  and  $p = 0.01$ , respectively). Preincubation with 100  $\mu\text{M}$  CALP-1 does not change the fraction of live cells

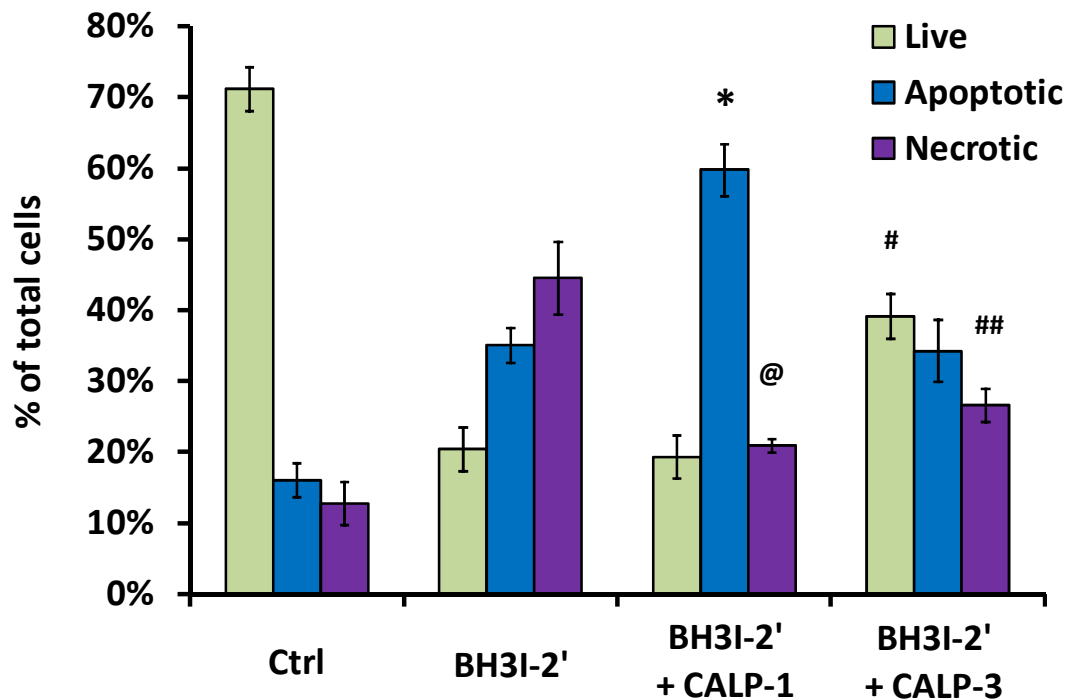


**Fig. 4.3. Effects of CALPs on BH3I-2'-induced cell death in acinar cells**

The results of cell death assay performed on pancreatic acinar cells preincubated for 15 min with 100  $\mu$ M CALP-1, 100  $\mu$ M CALP-3 or no CALPs and subsequently treated with 5  $\mu$ M BH3I-2'. Control cells were incubated without CALPs and BH3I-2'. Light green bars represent live cells, blue – apoptotic cells, and purple – necrotic. The chart is separated into four treatment groups, from the left: untreated control cells; cells treated with 5  $\mu$ M BH3I-2' only; cells preincubated with CALP-1 and treated with BH3I-2'; and cells preincubated with CALP-3 and treated with BH3I-2'. Black error bars represent standard error of mean. Apoptosis is significantly increased in CALP-1 + BH3I-2 sample as compared to BH3I-2' (\* $p = 0.007$ ); at the same time necrosis is substantially decreased (@ $p = 0.039$ ). In CALP-3 + BH3I-2' sample necrosis is reduced (## $p = 0.05$ ) as compared to BH3I-2' alone; and the fraction of live cells is significantly increased (# $p = 0.01$ ).

---

as compared to treatment with BH3I-2' alone ( $p = 0.82$ ); however in the presence of CALP-1 BH3I-2 induces substantially more apoptosis than BH3I-2' alone ( $*p = 0.007$ ) and at the same time necrosis is decreased ( $@p = 0.039$ ). In contrast, pretreatment with 100  $\mu$ M CALP-3 does not affect the levels of apoptosis as compared to BH3I-2' alone ( $p = 0.88$ ). However, in the presence of CALP-3, BH3I-2'-induced necrosis is reduced ( $##p = 0.05$ ), and the fraction of live cells is increased ( $#p = 0.01$ ) as compared to the BH3 mimetic alone. These results suggest that CALP-1 promotes apoptotic cell death over necrosis upon treatment with BH3I-2'; whereas CALP-3 does not affect apoptosis levels, but in turn promotes survival of the cells and reduces necrosis.

#### **4.4. The effects of gossypol on calcium homeostasis in pancreatic acinar cells**

Gossypol is a natural terpenoid aldehyde isolated from the seed, stem and root of the cotton plant (*Gossypium*). It is known to bind and inhibit anti-apoptotic proteins Bcl-2, Bcl-xL and Mcl-1<sup>228</sup>; it promotes conformational change of Bcl-2 and induces loss of mitochondrial potential in a Bax/Bak-independent manner<sup>229</sup>. Naturally isolated gossypol is a racemic mixture of (+)-gossypol and (-)-gossypol. (-)-Gossypol has been shown to be more potent than its (+) optic isomer, with  $K_i$  values of 320 nM and 480 nM for Bcl-2 and Bcl-xL, respectively<sup>230</sup>. Interestingly, its affinity to Mcl-1 is even higher ( $K_i = 180$  nM)<sup>230</sup>. Initially gossypol was used as anti-fertility agent in China in 1950s<sup>231</sup>. Currently gossypol is under clinical trials in order to evaluate its application as potential anti-cancer drug. It can be administered orally and is believed to have "acceptable and manageable toxicity"<sup>230</sup>. Therefore it represents a

---

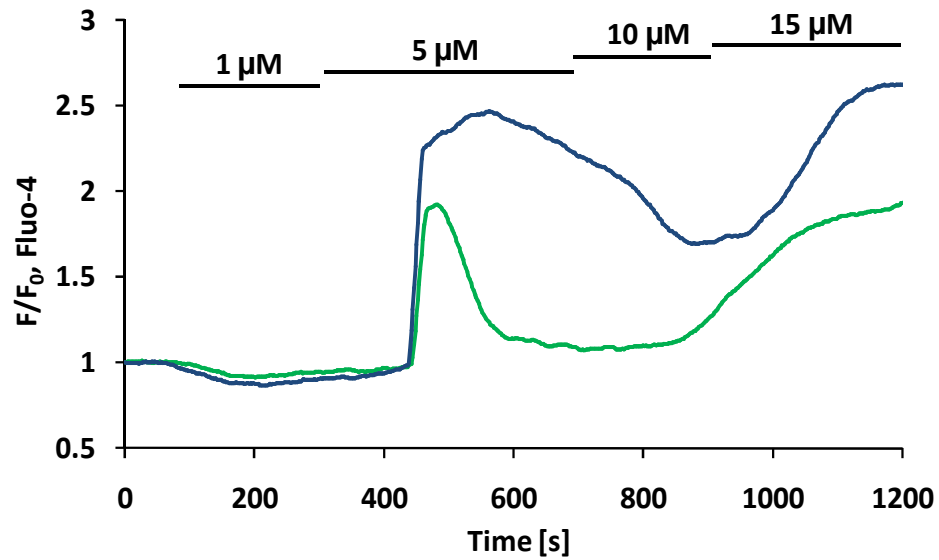
very promising compound that can give rise to a new class of anti-apoptotic Bcl-2 inhibitors.

However, up to now the effects of gossypol on intracellular calcium homeostasis in pancreatic acinar cells have not yet been investigated. Just like other BH3 mimetics gossypol is expected to induce  $\text{Ca}^{2+}$  release from the intracellular stores followed by cytosolic  $\text{Ca}^{2+}$  plateau formation. In order to test this notion the effects of different doses of gossypol were assessed in fluo-4-loaded pancreatic acinar cells. The cells were treated with increasing concentration of gossypol (1 - 15  $\mu\text{M}$ ) in the presence of 1 mM  $\text{Ca}^{2+}$  in order to determine the effective dose of the drug. *Fig. 4.4.A* shows two (out of 5) representative traces obtained in the experiment. Although the effects of gossypol on  $\text{Ca}^{2+}$  release in pancreatic acinar cells vary, 5  $\mu\text{M}$  concentration of the drug appears to be the lowest to induce a clear response (*Fig. 4.4.B*). Lower concentrations, such as 1  $\mu\text{M}$  in most cases have no apparent effect on cytosolic  $\text{Ca}^{2+}$  (82 % of cells did not respond to 1  $\mu\text{M}$  gossypol,  $n = 11$ , *Fig. 4.4.C*). However, 18 % of cells treated with low dose of gossypol developed small  $\text{Ca}^{2+}$  oscillations confined to the granular area ( $n = 11$ , *Fig. 4.4.C*). In conclusion, micromolar doses of gossypol have a very similar effect on intracellular calcium homeostasis in pancreatic acinar cells as observed with synthetic BH3 mimetics such as BH3I-2' or HA14-1.

#### **4.5. Effects of CALPs on gossypol-induced $\text{Ca}^{2+}$ responses**

As it has been shown above, treatment with gossypol induces  $\text{Ca}^{2+}$  release from the intracellular stores in pancreatic acinar cells followed by sustained  $\text{Ca}^{2+}$  plateau formation. Therefore use of gossypol as an anti-cancer drug will also be associated with toxic effects on pancreas, similarly to synthetic BH3 mimetics. Gossypol has

A.



B.

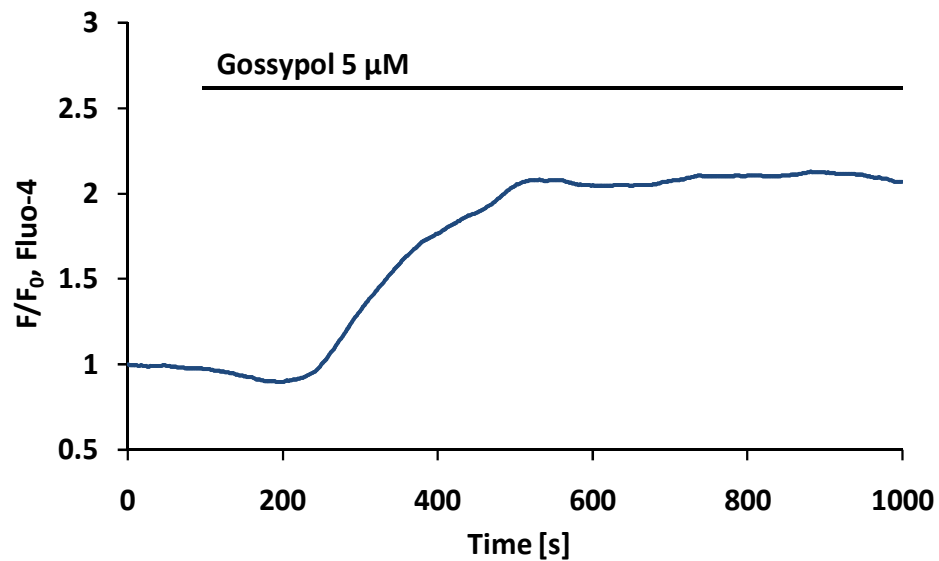


**Fig. 4.4. Calcium responses to gossypol in pancreatic acinar cells**

(A) Two sample traces showing responses of pancreatic acinar cells to increasing concentrations of gossypol (1 - 15  $\mu\text{M}$ ). (B) A representative trace demonstrating a typical  $\text{Ca}^{2+}$  response of pancreatic acinar cells to 5  $\mu\text{M}$  dose of gossypol; 5  $\mu\text{M}$  gossypol is the lowest dose capable of inducing cytosolic  $\text{Ca}^{2+}$  plateau in pancreatic acinar cells.

---

C.

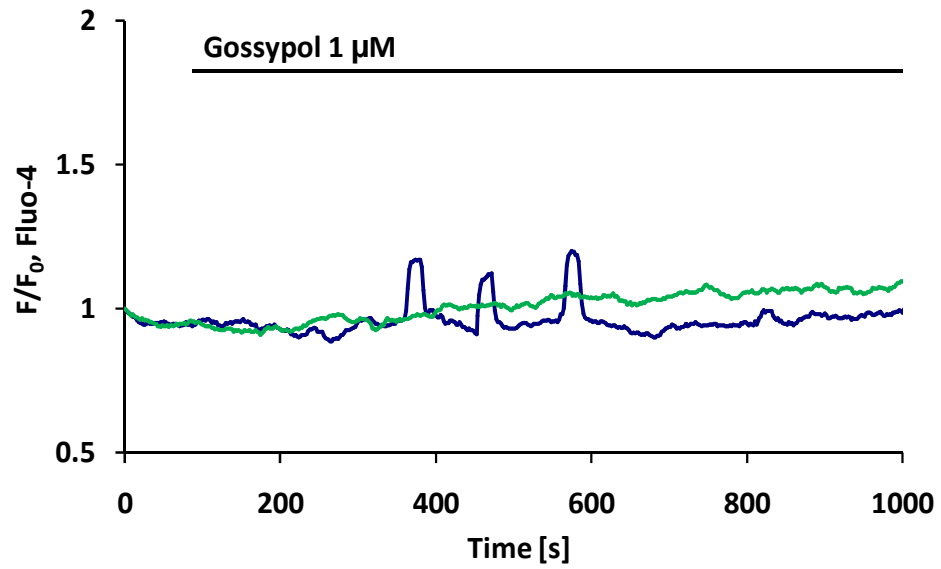


**Fig. 4.4.** (continues)

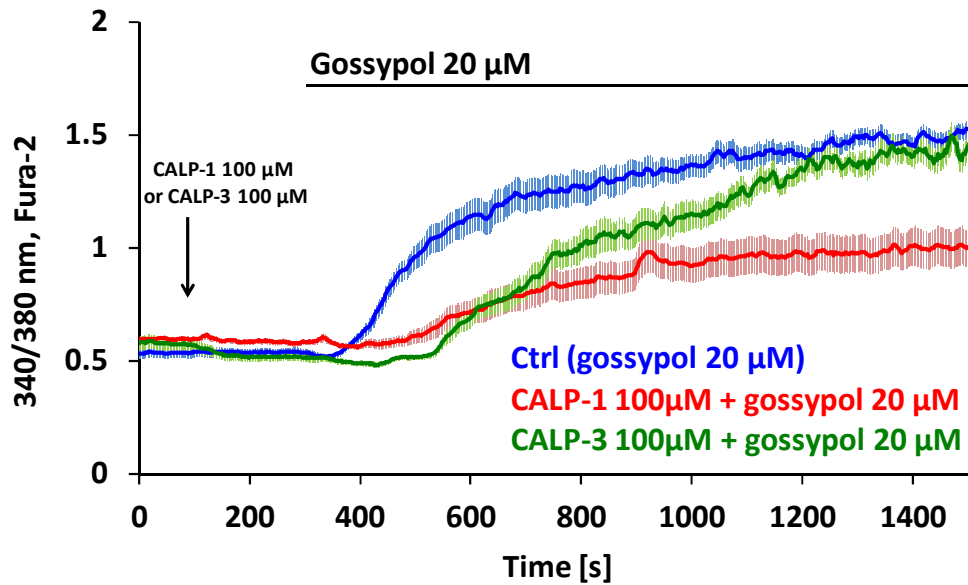
(C) Two sample traces obtained after treatment of pancreatic acinar cells with 1  $\mu\text{M}$  gossypol; blue trace shows oscillations in the granular area.

---

been shown to induce apoptosis as a result of its inhibitory effects on anti-apoptotic Bcl-2 proteins. However, it is also expected to induce high levels of necrosis because of its toxic effects leading to formation of prolonged elevation of cytosolic  $\text{Ca}^{2+}$ . The aim of the work presented in this chapter is to apply calcium-like peptides in order to reduce the toxicity of gossypol in the same way as it has been shown for BH3I-2'.

20  $\mu\text{M}$  dose of gossypol every time induces CICR-type of response followed by sustained cytosolic  $\text{Ca}^{2+}$  plateau in intact pancreatic acinar cells. Therefore here a 20  $\mu\text{M}$  dose was chosen to investigate the effects of gossypol on calcium homeostasis in pancreatic acinar cells in the presence or absence of CALP-1 or CALP-3. Freshly isolated pancreatic acinar cells were loaded with calcium sensitive dye fura-2 and then calcium responses to gossypol were recorded after 200 s of pretreatment with 100  $\mu\text{M}$  CALP-1 ( $n = 15$ ) or CALP-3 ( $n = 14$ ). Control cells ( $n = 20$ ) were preincubated for the same amount of time without CALPs. Subsequently, the cells were treated with 20  $\mu\text{M}$  gossypol and the average calcium responses were compared (*Fig. 4.5.A*). For quantitative comparison of the effects of CALPs, the average areas under the traces were calculated between 400 s and 1500 s (*Fig. 4.5.B*). Also, the amplitudes were taken at 800 s of calcium traces, averaged and compared in *Fig. 4.5.C*. The results show that pre-incubation with 100  $\mu\text{M}$  CALP-1 significantly reduces both the overall gossypol-induced cytosolic  $\text{Ca}^{2+}$  elevation ( $p < 0.0001$ , *Fig. 4.5.B*) and the amplitude of the response ( $p < 0.0001$ , *Fig. 4.5.C*) as compared to gossypol alone - treated cells. Interestingly, CALP-3 appears to delay the development of  $\text{Ca}^{2+}$  response to gossypol, which is reflected by reduction in average area under the trace as compared to control ( $p = 0.002$ , *Fig. 4.5.B*) as well as reduction in the average amplitude at 800 s

A.



B.

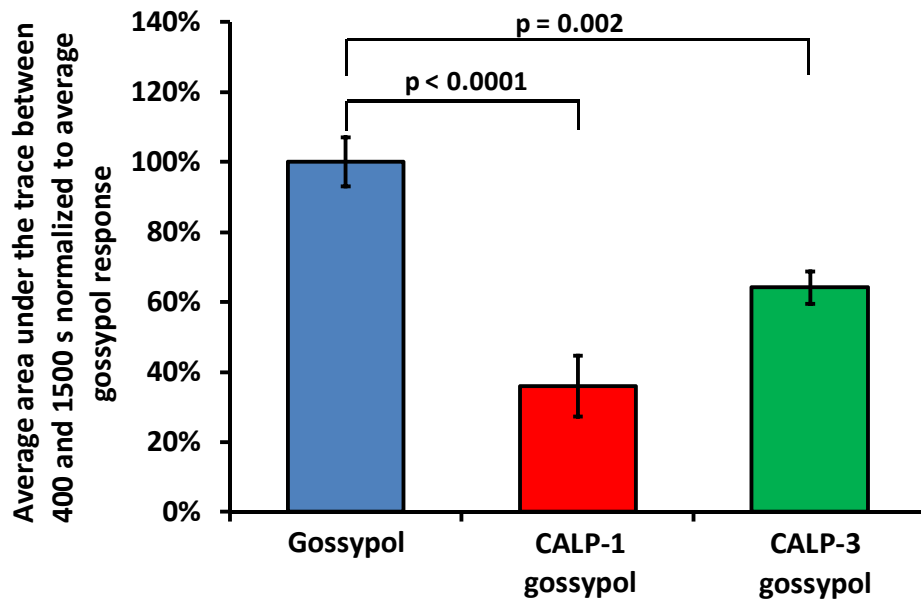


**Fig. 4.5. Effects of CALPs on gossypol-induced responses in acinar cells**

(A) The graph shows average Ca<sup>2+</sup> responses in pancreatic acinar cells induced by 20 μM gossypol only (n = 20), or 20 μM gossypol in the presence of 100 μM CALP-1 (n = 15) or 100 μM CALP-3 (n = 14). Error bars represent standard errors.

(B) The bar chart shows average area under the traces depicted in (A) between 400 s and 1500 s of the recorded responses. Error bars represent standard error of mean.

C.

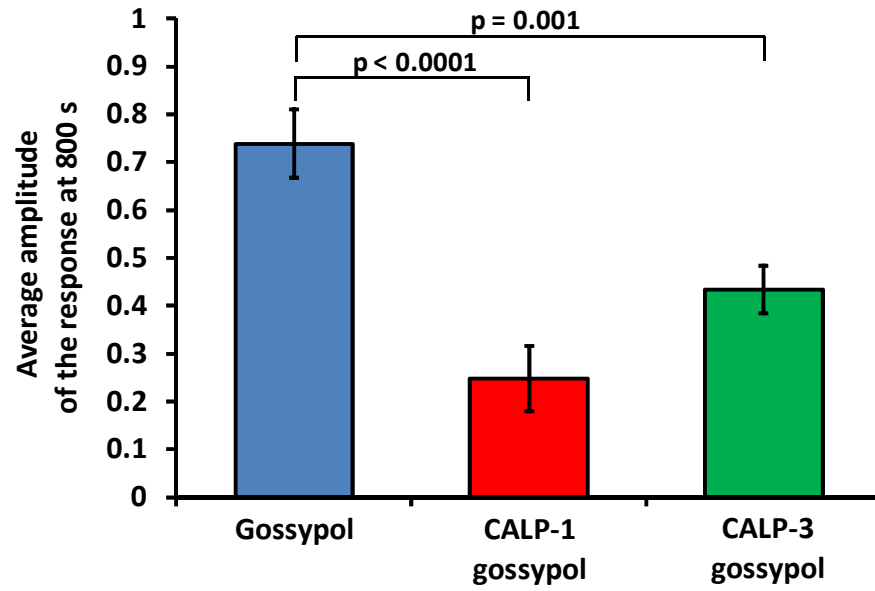


**Fig. 4.5.** (continues)

(C) The bar chart shows average amplitude obtained from the traces depicted in (A) at 800 s of the recorded responses.

---

( $p = 0.001$ , *Fig. 4.5.C*). Prolonged exposure to gossypol in the presence of CALP-3 leads to formation of cytosolic  $\text{Ca}^{2+}$  plateau with the average amplitude comparable to that of treatment with gossypol alone (*Fig. 4.5.A*). In conclusion both CALP-1 and CALP-3 interfere with action of gossypol on  $\text{Ca}^{2+}$  release from the intracellular stores, which is demonstrated by markedly reduced average amplitudes and areas under the traces of the responses in cells pretreated by one of the CALPs. However, the effect of CALP-1 on gossypol-induced responses appears more pronounced than the effect of CALP-3.

#### **4.6. Effects of CALPs on gossypol-induced cell death in pancreatic acinar cells**

As was shown above, CALPs modulate gossypol-induced  $\text{Ca}^{2+}$  responses in pancreatic acinar cells. However, in order to establish physiological significance of that observation, it is required to investigate the induction of cell death by combined treatment with gossypol and CALPs. Pancreatic acinar cells were isolated as described above and were divided equally into 4 tubes. Two samples were pretreated with 100  $\mu\text{M}$  CALP-1 or CALP-3 for 15 min. The other two were incubated for the same amount of time, but without any treatment. Subsequently, the samples containing CALPs and one of the untreated samples were incubated with relatively low dose of gossypol (5  $\mu\text{M}$ ) for 30 min. 15 min before the end of the incubation annexin-V-FITC and propidium iodide were added to all samples in amounts defined by Apoptosis Detection Kit (Sigma). Apoptotic and necrotic cells were visualized with Leica confocal microscope. The cell death assay was repeated three times in order to obtain independent values. The results of the experiment are presented in

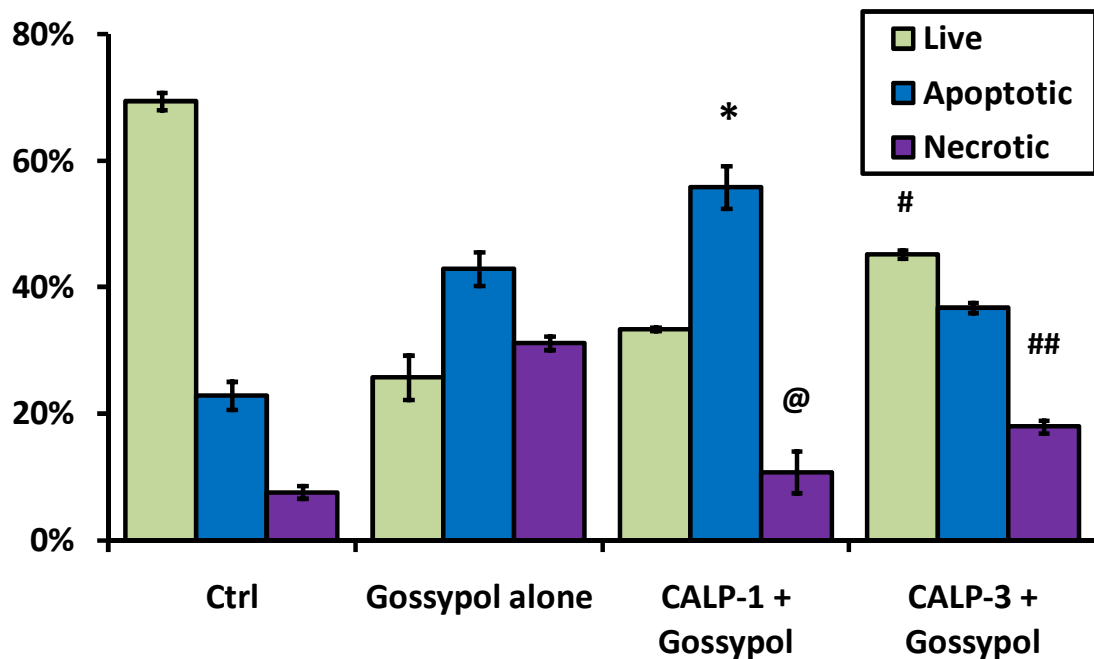


**Fig. 4.6. Effects of CALPs on gossypol-induced cell death in acinar cells**

The results of cell death assay performed on pancreatic acinar cells preincubated for 15 min with 100  $\mu$ M CALP-1, 100  $\mu$ M CALP-3 or no CALPs and subsequently treated with 5  $\mu$ M gossypol. Control cells were incubated without CALPs and gossypol. Light green bars represent live cells, blue – apoptotic cells, and purple – necrotic. The chart is separated into four treatment groups, from the left: untreated control cells; cells treated with 5  $\mu$ M gossypol only; cells preincubated with CALP-1 and treated with gossypol; and cells preincubated with CALP-3 and treated with gossypol. Black error bars represent standard error of mean. Apoptosis is significantly increased upon pre-treatment with CALP-1 as compared to gossypol alone (\* $p = 0.043$ ); at the same time necrosis is substantially decreased (@ $p = 0.017$ ). Pretreatment with CALP-3 reduces necrosis (## $p = 0.0008$ ) and increases the fraction of live cells (# $p = 0.028$ ) as compared to gossypol alone.

---

*Fig. 4.6.* In control sample most of the cells are alive; and low levels of apoptosis and necrosis are the result of the process of isolation. Treatment with gossypol alone substantially decreases the amount of live cells ( $p = 0.0028$ ), at the same time both apoptosis ( $p = 0.005$ ) and necrosis are increased ( $p = 0.0001$ ). The presence of 100  $\mu\text{M}$  CALP-1 does not significantly change the fraction of live cells as compared to the treatment with gossypol alone ( $p = 0.163$ ); however apoptosis is significantly increased ( $*p = 0.043$ ); and at the same time necrosis is substantially reduced ( $@p = 0.017$ ). Similarly to BH3I-2' data presented in Chapter 4.2, pretreatment with 100  $\mu\text{M}$  CALP-3 does not affect the levels of gossypol-induced apoptosis as compared to gossypol alone ( $p = 0.14$ ). However, CALP-3 markedly reduced gossypol-induced necrosis ( $###p = 0.0008$ ), increasing the fraction of life cells ( $\#p = 0.028$ ). The results suggest that CALP-1 promotes apoptotic cell death over necrosis upon treatment with gossypol; whereas CALP-3 does not affect apoptosis levels, but in turn promotes survival of the cells by reduction of necrosis. These effects are very similar to those obtained by induction of cell death by synthetic BH3 mimetic BH3I-2' in the presence of CALPs.

#### **4.7. CALPs do not affect physiological calcium responses to ACh in pancreatic acinar cells**

As was shown above, preincubation of pancreatic acinar cells with CALP-1 or CALP-3 leads to pre-activation of calmodulin, which modifies the pattern of pathological cytosolic  $\text{Ca}^{2+}$  responses and thus affects cell death induction. However, as promising as CALPs appear to be in reduction of pathological  $\text{Ca}^{2+}$  responses in life cells, their successful application as potential therapeutic agents can only be

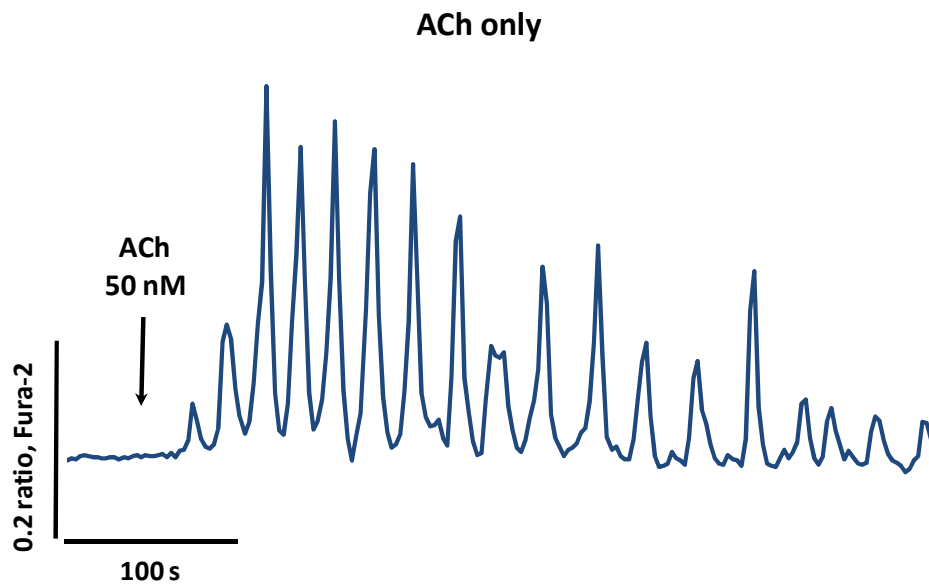
---

possible if physiological  $\text{Ca}^{2+}$  responses are not affected by the presence of calcium-like peptides. For pancreatic acinar cells the most important physiological stimuli are acetylcholine (ACh) and cholecystinin (CCK). As was described in detail in the introductory chapter, small doses of ACh induce  $\text{Ca}^{2+}$  oscillations in the cytosol and secretion of pancreatic enzymes. In order to investigate whether pre-activation of calmodulin with CALPs inhibits physiological  $\text{Ca}^{2+}$  signalling induced by ACh, freshly isolated pancreatic acinar cells were loaded with fura-2 and preincubated for 200 s with either 100  $\mu\text{M}$  CALP-1 or 100  $\mu\text{M}$  CALP-3. Control cells were incubated for 200 s without CALPs. Subsequently the cells were treated with relatively small concentration of ACh (50 nM). 50 nM ACh normally induces global cytosolic  $\text{Ca}^{2+}$  oscillations, which originate in the granular pole of pancreatic acinar cells and spread towards the basolateral area. The representative traces are presented in *Fig. 4.7.A-C*. All cells used in the experiment responded to ACh with repeated global cytosolic  $\text{Ca}^{2+}$  transients, which lasted for about 200 - 300 s. The major spikes were followed by tiny oscillations of the baseline. In all cases pretreatment with CALP-1 (n = 12) or CALP-3 (n = 10) did not block ACh-induced oscillations nor affected them substantially as compared to the responses of control cells (n = 15).

#### **4.8. CALPs have only a minor effect on CCK-induced calcium responses in pancreatic acinar cells**

Similarly to physiological doses of ACh, treatment with picomolar concentrations of CCK induces  $\text{Ca}^{2+}$  oscillations in pancreatic acinar cells, which are restricted to the apical area or spread towards the basolateral area as global  $\text{Ca}^{2+}$  spikes. In order to investigate whether pre-activation of calmodulin with CALPs inhibits physiological

A.



B.

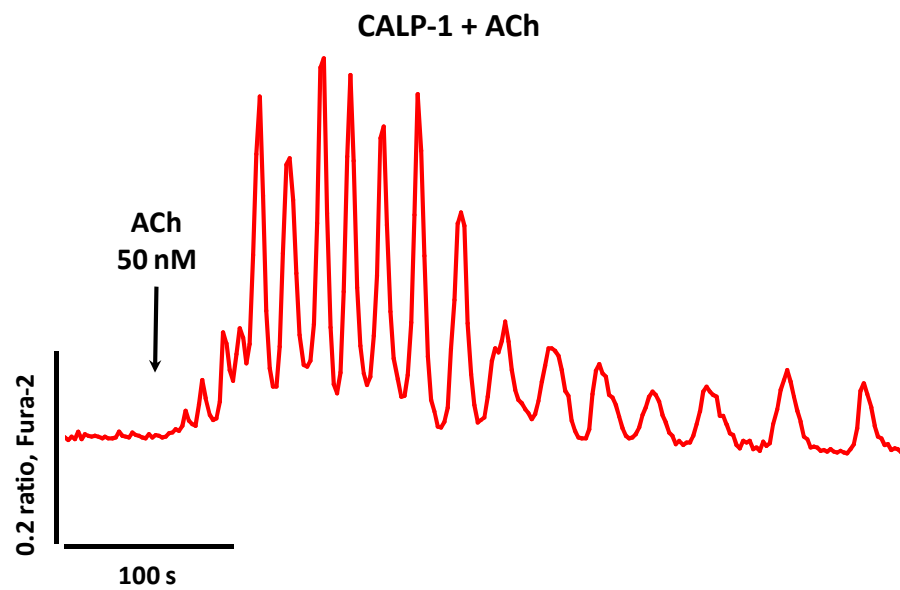


**Fig. 4.7. Effects of CALPs on ACh-induced calcium responses**

Representative traces obtained upon treatment of pancreatic acinar cells with: (A) 50 nM ACh and (B) 50 nM ACh after preincubation with 100  $\mu$ M CALP-1.

---

C.

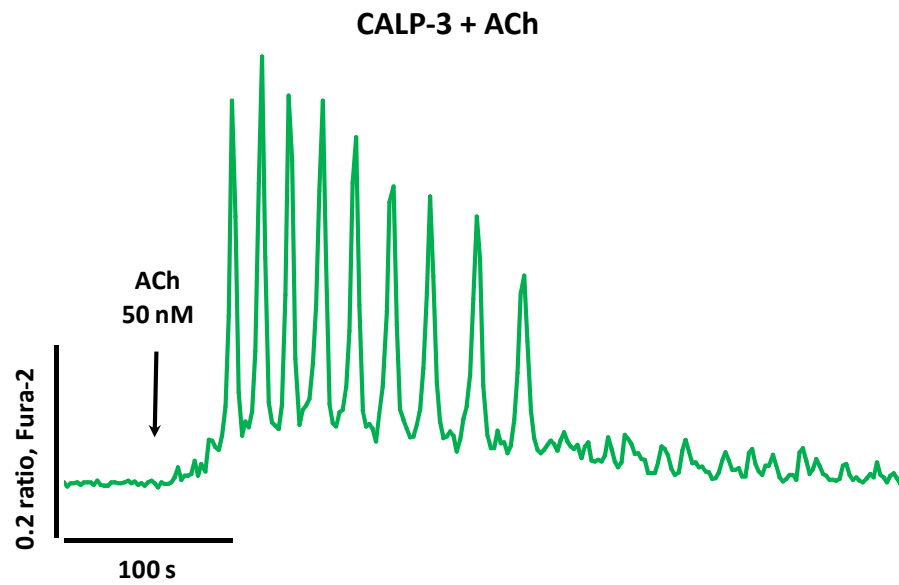


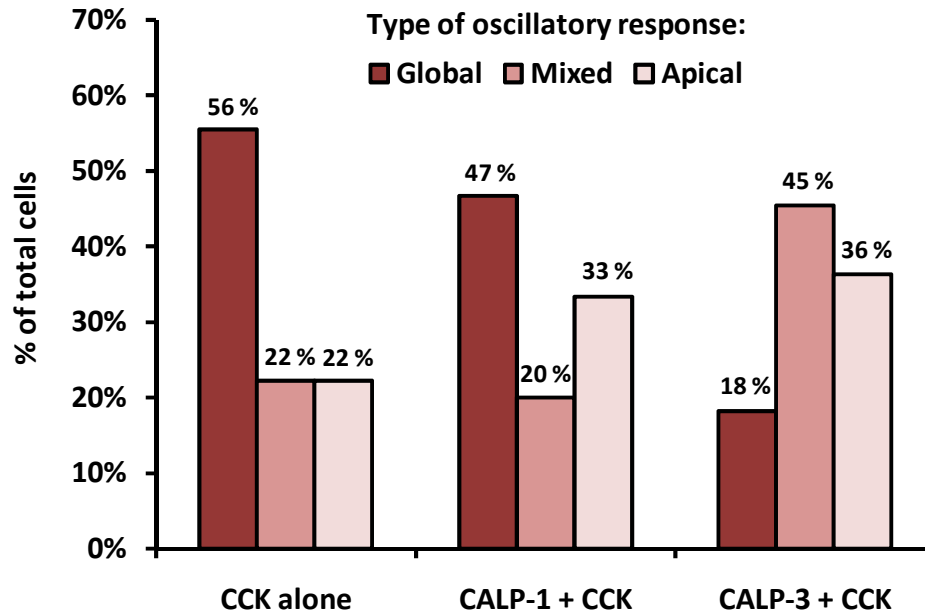
**Fig. 4.7.** (*continues*)

(C) A representative trace obtained upon treatment of pancreatic acinar cells with 50 nM ACh after preincubation with 100  $\mu$ M CALP-3.

---

Ca<sup>2+</sup> responses induced by CCK, freshly isolated pancreatic acinar cells were loaded with fura-2 and preincubated for 200 s with either 100 μM CALP-1 or 100 μM CALP-3. Control cells were incubated for 200 s without CALPs. Subsequently the cells were treated with 5 pM CCK. The responses obtained after treatment with CCK were classified into three different groups: (1) global Ca<sup>2+</sup> oscillations, (2) Ca<sup>2+</sup> oscillations confined to the apical area only, (3) and Ca<sup>2+</sup> oscillations consisting of mixture of both global and apical oscillations (*Fig. 4.8.A*). Treatment with CCK alone (without presence of CALPs) induced global Ca<sup>2+</sup> oscillations in most of the cells used in the experiment (56 %, 5 out of 9 cells, *Fig. 4.8.B*); 22 % of cells (2 out of 9) responded with small Ca<sup>2+</sup> oscillations restricted to the apical area; and the same amount of cells (22 %) responded with mixed type of oscillations, where propagation of Ca<sup>2+</sup> signal in some cases was restricted to the apical area, and in other cases spread throughout the basolateral region. Pretreatment with CALP-1 (n = 15) or CALP-3 (n = 11) did not block Ca<sup>2+</sup> responses to 5 pM CCK. However, the pattern of CCK-induced Ca<sup>2+</sup> responses in the presence of CALPs is not identical to responses induced by CCK alone. Preincubation with 100 μM CALP-1 led to a slight decrease in proportion of cells responding with global Ca<sup>2+</sup> oscillations (47 %, 7 out of 15 cells, *Fig. 4.8.A and C*); at the same time more cells responded with oscillations confined to the apical region only (33 %, 5 out of 15, *Fig. 4.8.A and D*); and similar proportion of cells produced mixed type of oscillations in response to CCK (20 %, 3 out of 15, *Fig. 4.8.A*). The effect of 100 μM CALP-3 was even more pronounced. In the presence of CALP-3 treatment with 5 pM CCK resulted in only few cells responding with global Ca<sup>2+</sup> oscillations (18 %, 2 out of 11, *Fig. 4.8.A and E*) and the amplitude of those Ca<sup>2+</sup> transients was substantially lower as compared to

A.



B.

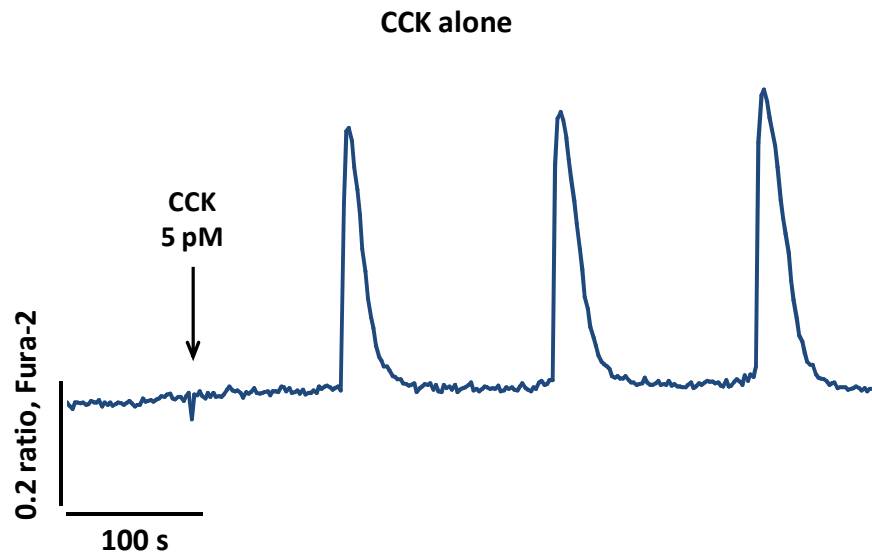
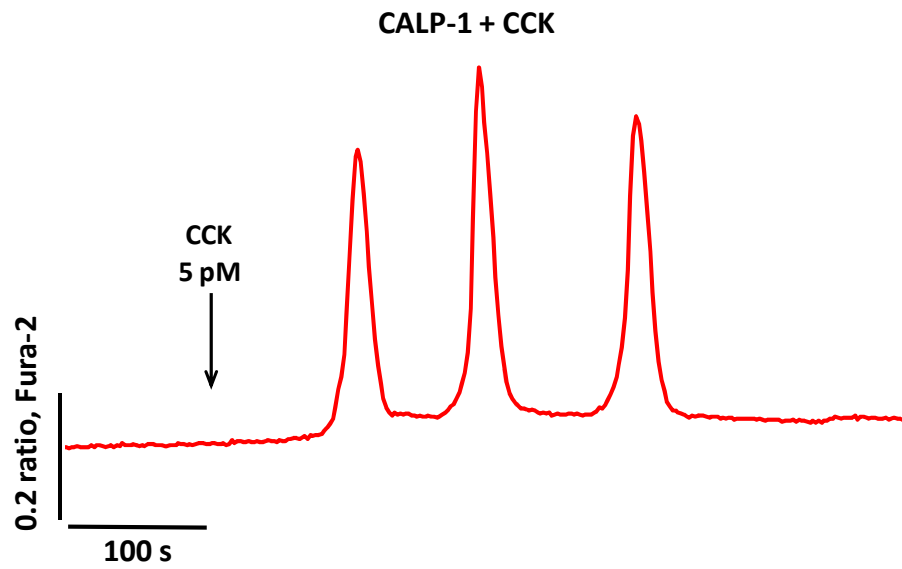


**Fig. 4.8. Effects of CALPs on CCK-induced calcium responses**

(A) The bar chart shows distribution of different types of oscillatory responses obtained in pancreatic acinar cells after treatment with 5 pM CCK. The responses are divided into three groups: global oscillations, mixed oscillations and apical oscillations. Treatment with CALPs promotes apical oscillations over global  $\text{Ca}^{2+}$  transients. (B) A sample trace showing typical global  $\text{Ca}^{2+}$  oscillations induced by treatment with 5 pM CCK in pancreatic acinar cells.

C.



D.

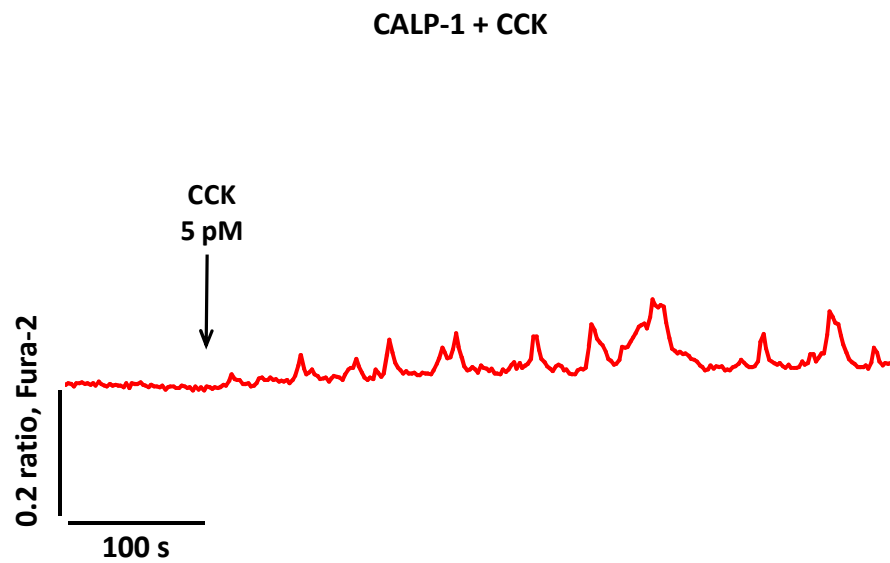
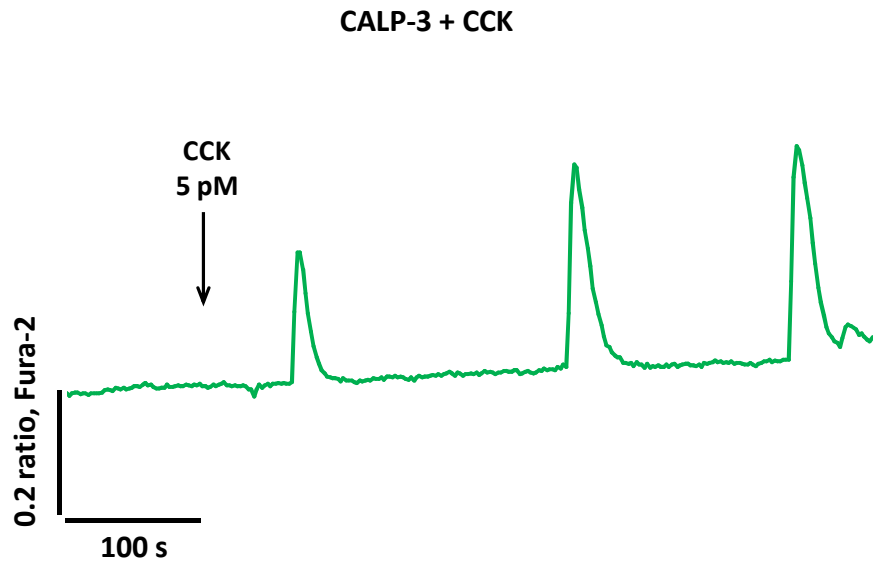


**Fig. 4.8.** (continues)

(C) A sample trace showing global  $\text{Ca}^{2+}$  oscillations induced by treatment with 5 pM CCK in pancreatic acinar cells pretreated with 100  $\mu\text{M}$  CALP-1. (D) A sample trace showing CCK-induced small  $\text{Ca}^{2+}$  oscillations confined to the apical area in pancreatic acinar cells pretreated with 100  $\mu\text{M}$  CALP-1.

E.



F.

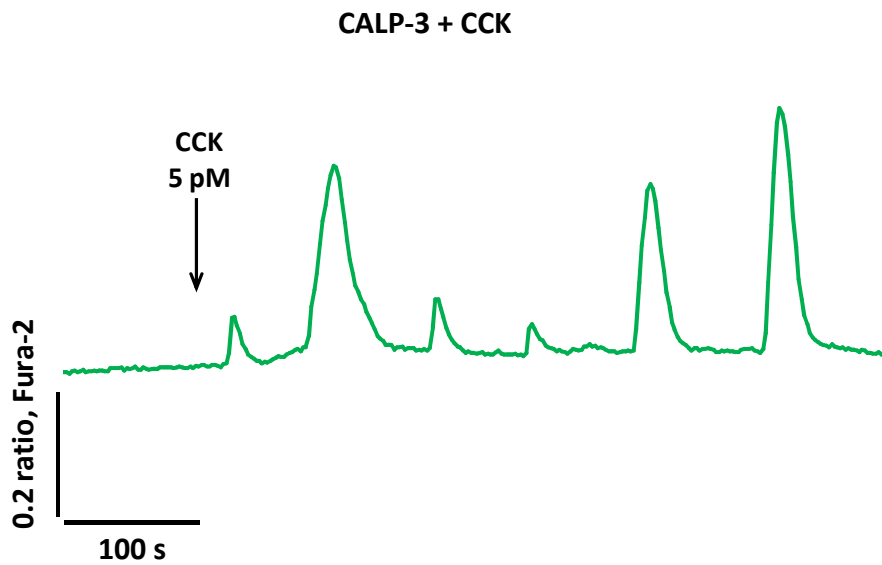


**Fig. 4.8.** (*continues*)

(E) A sample trace showing global  $\text{Ca}^{2+}$  oscillations induced by treatment with 5 pM CCK in pancreatic acinar cells pretreated with 100  $\mu\text{M}$  CALP-3. (F) A sample trace showing mixed  $\text{Ca}^{2+}$  oscillations induced by treatment with 5 pM CCK in pancreatic acinar cells pretreated with 100  $\mu\text{M}$  CALP-3.

---

G.

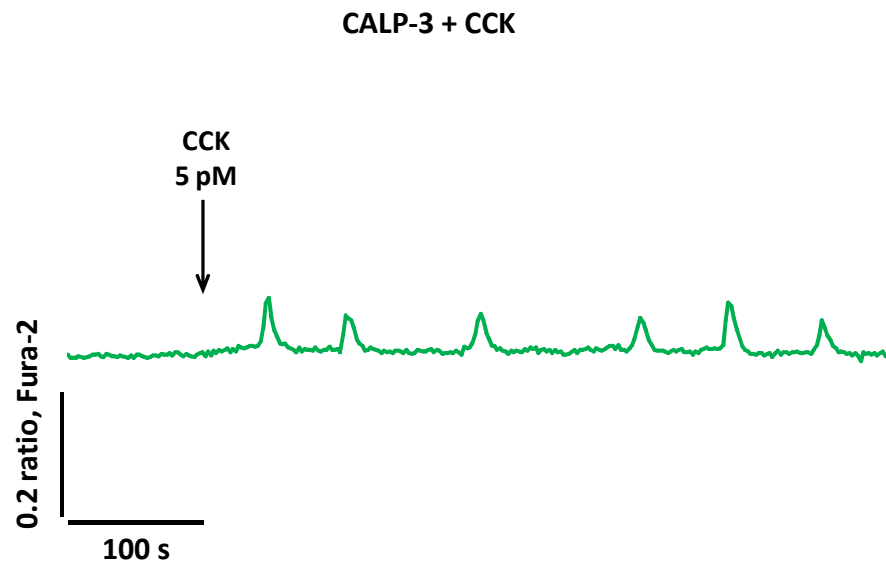


**Fig. 4.8.** (*continues*)

**(G)** A sample trace showing small apical  $\text{Ca}^{2+}$  oscillations induced by 5 pM CCK in pancreatic acinar cells pretreated with 100  $\mu\text{M}$  CALP-3.

---

treatment with CCK alone. Further, higher proportion of cells responded to CCK with apical oscillations only (36 %, 4 out of 11, *Fig. 4.8.A and G*) or mixed type of oscillations (45 %, 5 out of 11, *Fig. 4.8.A and F*). In summary, it appears that pretreatment with CALPs, particularly with CALP-3, promotes small  $\text{Ca}^{2+}$  oscillations confined to the apical area of pancreatic acinar cells over global  $\text{Ca}^{2+}$  increases. However, CALPs do not inhibit CCK signalling completely.

#### **4.9. Discussion**

CALP-1 and CALP-3 are relatively well established modulators of calmodulin. They can bind to the EF hand motifs of the protein leading to its activation even without the increase in cytosolic  $\text{Ca}^{2+}$ . Since calmodulin performs various functions in cells, its preactivation can affect many aspects of intracellular  $\text{Ca}^{2+}$  homeostasis. In this chapter it was tested whether preincubation with CALPs can protect cells against toxic increases in cytosolic  $\text{Ca}^{2+}$  induced by treatment with BH3 mimetics and thus decrease their necrotic effects in favour of apoptosis. Indeed it was demonstrated that preincubation with CALPs changed the pattern of  $\text{Ca}^{2+}$  responses induced by BH3I-2'. The BH3 mimetic alone in majority of the cases triggered quick and substantial  $\text{Ca}^{2+}$  release from the intracellular stores followed by a sustained  $\text{Ca}^{2+}$  plateau. Only few cells responded with a  $\text{Ca}^{2+}$  release signal that was delayed in time. Preincubation with CALP-1 led to an increase in the amount of cells showing delayed responses and, even more importantly, 20 % of investigated cells responded, but did not develop sustained  $\text{Ca}^{2+}$  plateau; and another 20 % did not respond at all. Interestingly, effects of CALP-3 were not that pronounced, but even in this case as many as 25 % of cells did not develop any responses to BH3I-2'. Even the typical

---

BH3 mimetic-elicited responses with a clear plateau phase were reduced in the presence of CALPs, which is reflected by decreased average amplitude; although in the case of CALP-3 this decrease is statistically non-significant.

CALPs showed very similar effects on  $\text{Ca}^{2+}$  responses induced by the natural Bcl-2 inhibitor gossypol. Both CALP-1 and CALP-3 reduced average  $\text{Ca}^{2+}$  release from the intracellular stores in response to gossypol as well as the average amplitude of the responses. CALP-1 again appeared to be more potent than CALP-3.

These effects of CALPs on BH3 mimetic-induced  $\text{Ca}^{2+}$  responses have a very important implication on induction of cell death. Reduced calcium responses to BH3 mimetics in the presence of CALP-1 are also reflected by increased apoptosis levels and decreased necrosis as compared to treatment with BH3I-2' or gossypol alone. In fact necrosis levels are only slightly elevated as compared to untreated controls. Pretreatment with CALP-3 also reduces levels of necrosis induced by BH3 mimetics. However, in contrast to CALP-1, CALP-3 does not markedly affect apoptosis, but in turn increases the amount of cells that survived the treatment.

It is not entirely clear why CALP-1 and CALP-3 have such different effects on  $\text{Ca}^{2+}$  responses induced by BH3 mimetics. CALP-3 has been designed as a complementary peptide to EF hand motif of calmodulin and thus has higher affinity to the protein than CALP-1, which was designed to interact with troponin C<sup>226</sup>. CALPs bind to C-terminal domain of calmodulin and induce conformational change of the protein, which is not identical to that caused by  $\text{Ca}^{2+}$  binding<sup>226</sup>. It is likely that slight differences in active conformation of calmodulin elicited by CALP-1 and CALP-3 are responsible for differences in effects of CALPs on BH3 mimetic-

---

dependent  $\text{Ca}^{2+}$  increases. What is more, since structure of CALP-1 is not absolutely complementary to EF hand motifs of calmodulin, the peptide might also interact with other intracellular targets containing EF hand motifs, such as  $\text{Ca}^{2+}$  channels. In that case, CALP-1 would not only activate calmodulin but also affect  $\text{Ca}^{2+}$  fluxes in calmodulin-independent mode. Therefore, the exact mechanism of CALP-mediated regulation of intracellular  $\text{Ca}^{2+}$  homeostasis requires further investigation. Resolving the mechanism is particularly important for development of effective therapeutic agents.

When speculating about potential use of CALPs as drugs, first of all it has to be noted that application of CALPs themselves is probably limited by their unfavourable pharmacological properties. Although the pharmacokinetic properties of CALPs have not yet been fully investigated, short peptides are usually characterised by poor cell permeability, bioavailability and metabolic stability. They are prone to degradation in digestive system, which means that oral administration would not be effective. Full assessment of the suitability of CALPs for therapeutic use exceeds the scope of this thesis. Here, it is reported that pre-activation of calmodulin decreases  $\text{Ca}^{2+}$  overload caused by BH3 mimetics and affects the type of cell death induced upon the treatment. From that perspective, the effects of  $\text{Ca}^{2+}$ -like peptides on  $\text{Ca}^{2+}$  responses are definitely worth attention and further investigation. The ultimate goal would be to develop compounds working similarly to CALPs, particularly CALP-1, which could potentially be used as attenuators of pathological calcium responses induced by BH3 mimetics and perhaps other drugs as well. Such compounds would be especially useful in situations where induction of apoptosis is beneficial, but necrosis is not, in particular in anti-cancer therapy.

---

Considering the vast spectrum of functions performed by calmodulin, it was important to test whether activation of calmodulin by CALPs affects physiological  $\text{Ca}^{2+}$  signalling. If physiological  $\text{Ca}^{2+}$  responses are inhibited in the same way or stronger than pathological responses, potential use of CALPs as therapeutic agents might be questioned. Course book examples of physiological responses in pancreatic acinar cells are ACh- and CCK-induced  $\text{Ca}^{2+}$  oscillations, which normally trigger pancreatic secretion. The results indicate that neither CALP-1 nor CALP-3 substantially change ACh signalling. In the presence of CALPs all investigated cells responded to 50 nM ACh with global oscillations. It would, however, be surprising if CALPs had no effects at all on physiological signalling and at the same time their influence on pathological  $\text{Ca}^{2+}$  increases was so substantial. Experiments with CCK demonstrate that  $\text{Ca}^{2+}$ -like peptides, particularly CALP-3, promote apical  $\text{Ca}^{2+}$  oscillations over global  $\text{Ca}^{2+}$  increases, but do not block CCK signalling completely. Slightly stronger effect of CALPs on CCK signalling is not entirely clear. CCK responses are predominantly dependent on  $\text{Ca}^{2+}$  release through RyRs; whereas ACh releases  $\text{Ca}^{2+}$  mainly through  $\text{IP}_3$ Rs. Both receptors are regulated by calmodulin and thus differences in the mechanisms of CaM-dependent regulation of RyRs and  $\text{IP}_3$ Rs can be responsible for stronger inhibitory effect of CALPs on CCK signalling.

Taken together, data shown in this chapter support the hypothesis that preactivation of calmodulin can protect cells from excessive  $\text{Ca}^{2+}$  increases in the cytosol caused by BH3 mimetics and thus extensive necrosis. Physiological  $\text{Ca}^{2+}$  responses might be slightly diminished by CALPs, but are not completely inhibited.

---

**CHAPTER 5:**  
**PROTECTIVE ROLE OF CALMODULIN AGAINST ETHANOL**  
**IN PANCREATIC ACINAR CELLS**

---

## **Chapter 5: Protective role of calmodulin against ethanol in pancreatic acinar cells**

### **5.1. Overview of ethanol actions on pancreas**

As was described in the introductory chapter, the incidence of acute pancreatitis is strongly associated with the level of alcohol intake. However, only a small percentage of heavy drinkers develop pancreatitis indicating that other factors are also important in the pathogenesis of this condition<sup>232</sup>. Repeated episodes of acute pancreatitis might result in chronic manifestation of the disease, which in turn increases the risk of pancreatic cancer<sup>41</sup>. The hallmark of pancreatitis is autodigestion of the organ, which is primarily initiated by intracellular activation of trypsin in pancreatic acinar cells. The main difference between chronic and acute pancreatitis lies in the extent and progression of necrosis in the organ.

Also, as was already pointed out in the Introduction, cytosolic calcium signals control physiological functions of pancreatic acinar cells, such as enzyme secretion. However, global increases in cytosolic calcium, especially when sustained, might be toxic for cells leading to premature activation of intracellular digestive enzymes, extensive vacuolization, activation of NFκB, inflammatory response and induction of cell death<sup>101,233-236</sup>. Since abnormal Ca<sup>2+</sup> signalling seems to play a crucial role in different models of acute pancreatitis, it is clear that either ethanol itself or some of its metabolites are responsible for induction of pathological Ca<sup>2+</sup> responses<sup>237</sup>. Interestingly, ethanol even in very high concentrations has only minor effects on

---

Ca<sup>2+</sup> homeostasis of pancreatic acinar cells<sup>100</sup>. Ethanol can be metabolised through two pathways: oxidative and non-oxidative. The main oxidative metabolite of ethanol, acetaldehyde, has been demonstrated to have no effect on cytosolic Ca<sup>2+</sup> in pancreatic acinar cells<sup>100</sup>. Fatty acid ethyl esters (FAEE) are the products of non-oxidative alcohol metabolism. They were found in high amounts in pancreas during post-mortem examination of individuals intoxicated with alcohol at the time of death<sup>238</sup>. Accumulating evidence supports the view that FAEE are the main mediators of ethanol toxicity in the pancreas. FAEE directly induce Ca<sup>2+</sup> release from the intracellular stores, which results in cytosolic Ca<sup>2+</sup> signals resembling those evoked by ACh or CCK. These signals can be blocked by caffeine, which clearly suggests involvement of IP<sub>3</sub>R in their generation (*Fig. 5.1*)<sup>108</sup>. Caffeine is a well known activator of RyRs, especially in cells characterised by high expression of these receptors, such as skeletal or cardiac muscle cells and neurons, where it increases Ca<sup>2+</sup> release from the ER<sup>239,240</sup>. However, in intact pancreatic acinar cells 20 mM caffeine does not induce Ca<sup>2+</sup> release and blocks IP<sub>3</sub>R-dependent Ca<sup>2+</sup> signals<sup>239,241</sup>. A recent study has demonstrated that palmitoleic acid ethyl ester (POAEE) induces Ca<sup>2+</sup> release from the intracellular stores, both the ER and the acid store; this release is dependent on type 2 and 3 IP<sub>3</sub>R and is associated with intracellular activation of trypsinogen in pancreatic acinar cells<sup>242</sup>. High doses of FAEEs can completely deplete the ER and consequently activate store-operated Ca<sup>2+</sup> entry mechanisms<sup>243</sup>. In contrast, non-esterified long chain fatty acids, such as palmitoleic acid, induce slow Ca<sup>2+</sup> release from the ER, which is predominantly dependent on inhibition of mitochondrial functions and decrease in cellular ATP content<sup>109</sup>. This effect, however, can also be responsible for intracellular activation of

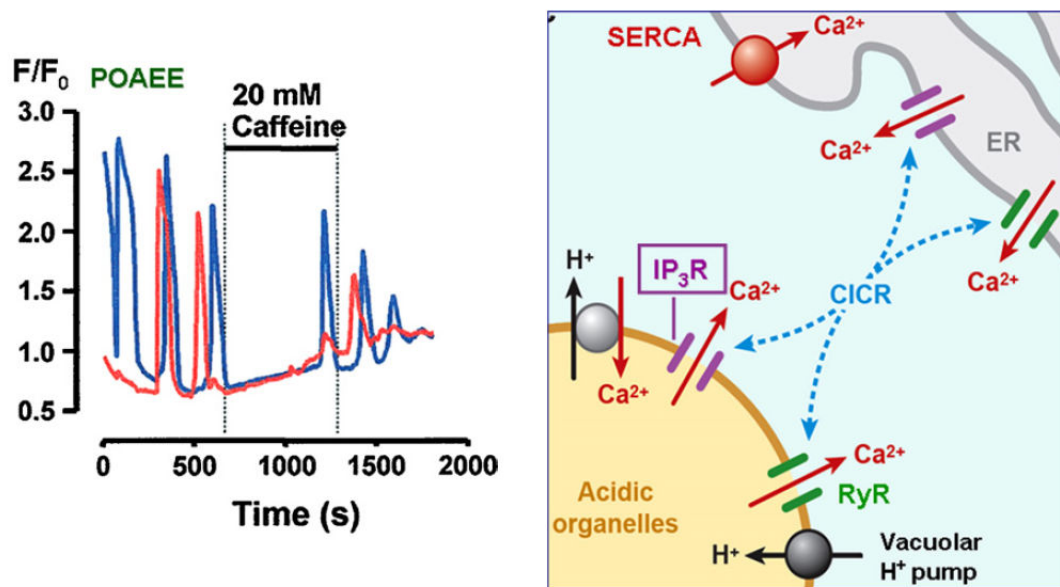


**Fig. 5.1. Calcium responses induced by POAEE**

Palmitoleic acid ethyl ester (POAEE) induces cytosolic  $\text{Ca}^{2+}$  oscillations, which can be blocked by caffeine. The traces (on left) demonstrate typical  $\text{Ca}^{2+}$  responses evoked by intracellular injection (via patch clamp pipette) of POAEE into a pancreatic acinar cell (blue trace) and responses of a neighbour cell (red trace). The schematic diagram (on right) illustrates possible mechanism of POAEE-induced cytosolic  $\text{Ca}^{2+}$  oscillations, which involves CICR and engagement of  $\text{IP}_3\text{Rs}$  and  $\text{RyRs}$  from the endoplasmic reticulum (ER) as well as from the acidic store. [Adapted from Criddle DN, 2006; Petersen OH, 2008 and Petersen OH, 2009]<sup>108,243,244</sup>.

---

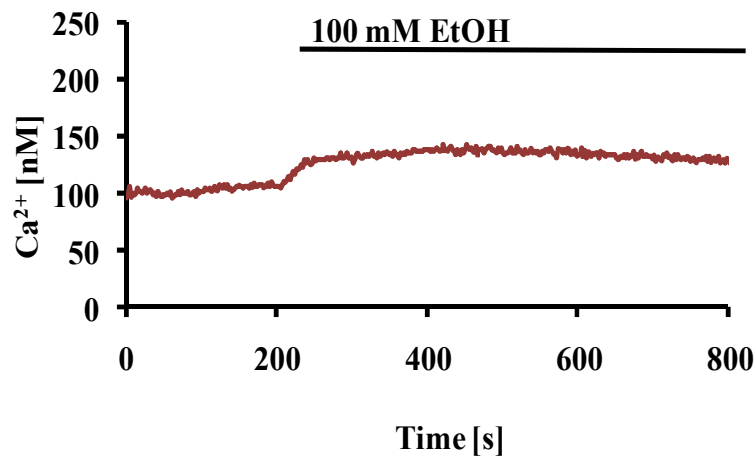
trypsinogen. Since mitochondria can hydrolyse FAEEs and thus generate FAs, interpreting the mechanism of action of FAEEs is not straightforward<sup>107</sup>. It appears that a considerable part of toxic effects of FAEEs might involve FAs generated by mitochondria. Such combined action of FAEEs and FAs on  $\text{Ca}^{2+}$  homeostasis is especially significant, since FAEEs induce rapid  $\text{Ca}^{2+}$  release from the intracellular stores and FAs affect mitochondrial functions decreasing ATP levels and thus ATP-dependent  $\text{Ca}^{2+}$  extrusion mechanisms<sup>243</sup>.

The evidence for FAEEs being the major mediators of ethanol toxicity does not, however, exclude other effects of alcohol on pancreas. Since ethanol induces only small and very variable responses of cytosolic  $\text{Ca}^{2+}$  in intact pancreatic acinar cells this chapter provides evidence and explanation for severe effects of ethanol in two photon permeabilized acinar cells.

## **5.2. Responses induced by ethanol in intact pancreatic acinar cells**

As was previously described by our group, even high concentrations of ethanol exert only very modest effects on intact pancreatic acinar cells<sup>243</sup>. The aim of this study is to present a detailed comparison of cytosolic  $\text{Ca}^{2+}$  responses in pancreatic acinar cells to 100 mM and 200 mM ethanol. Both concentrations are regarded as relatively moderate, with 100 mM being perfectly within the range of ethanol levels obtained from blood of individuals caught driving a vehicle while intoxicated with alcohol<sup>245</sup>. In the first experiment freshly isolated pancreatic acinar cells were loaded with calcium sensitive dye fura-2 and then exposed to 100 mM ethanol. 340/380 nm ratio values were recalculated to  $\text{Ca}^{2+}$  concentration in order to quantitatively compare the responses. Cytosolic calcium responses to 100 mM concentration of ethanol can be

A.



B.

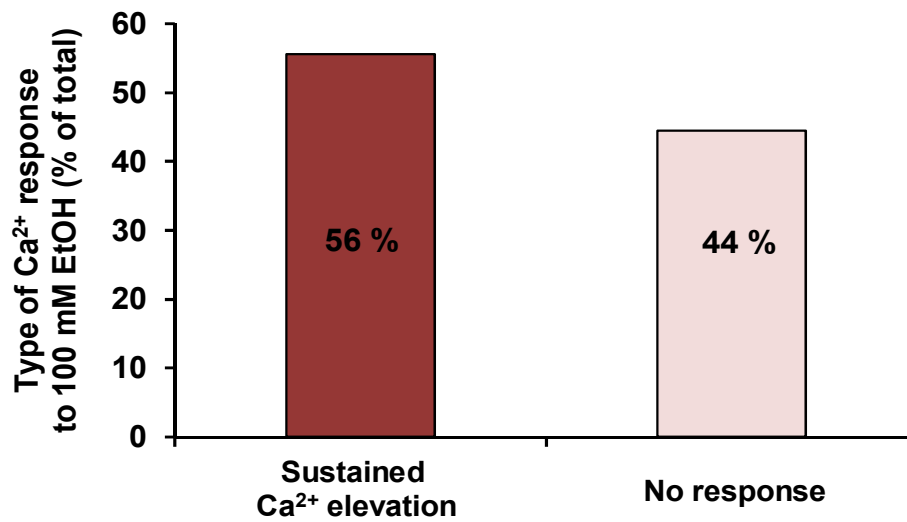
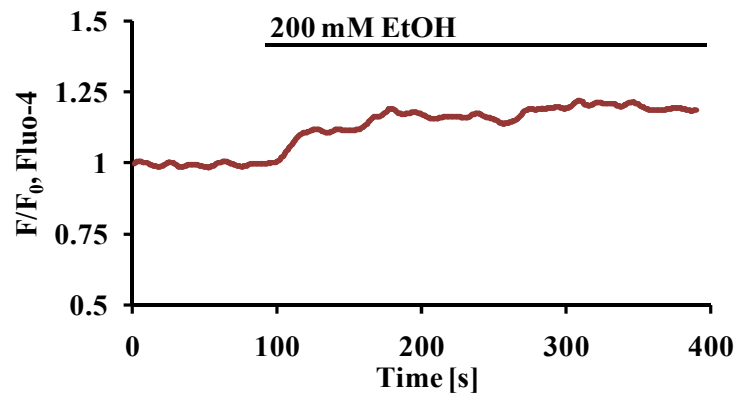


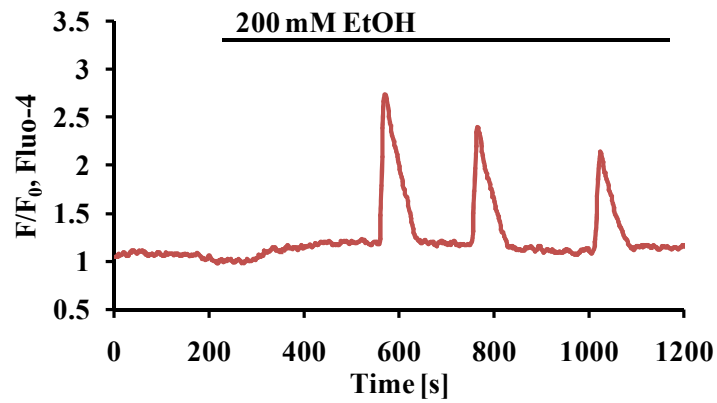
**Fig. 5.2. Calcium responses to ethanol in pancreatic acinar cells**

Cytosolic calcium responses of intact pancreatic acinar cells to ethanol: (A) typical trace that shows sustained cytosolic  $\text{Ca}^{2+}$  elevation upon treatment with 100 mM EtOH; (B) The chart compares frequencies of different types of cytosolic  $\text{Ca}^{2+}$  responses in pancreatic acinar cells to 100 mM EtOH (n = 18). [Adapted from *Gerasimenko JV, 2011*]<sup>246</sup>.

C.



D.



E.

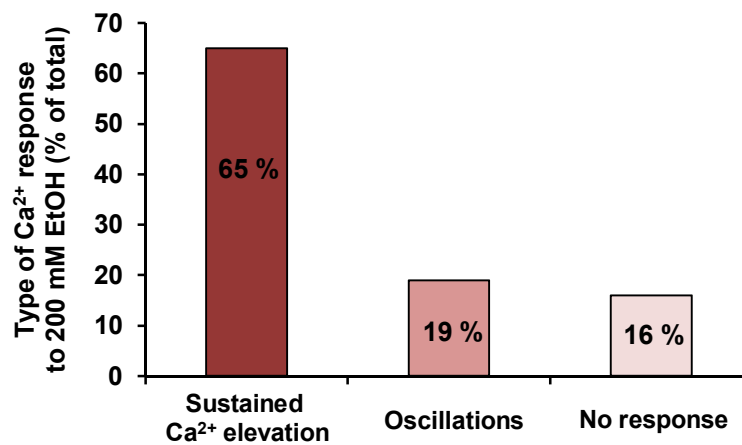


**Fig. 5.2.** (continues)

Typical traces showing (C) sustained cytosolic  $Ca^{2+}$  elevation and (D) oscillatory type of response to 200 mM EtOH; (E) The chart compares frequencies of different types of cytosolic  $Ca^{2+}$  responses in pancreatic acinar cells to 200 mM EtOH ( $n = 43$ ). [Adapted from *Gerasimenko JV, 2011*]<sup>246</sup>.

---

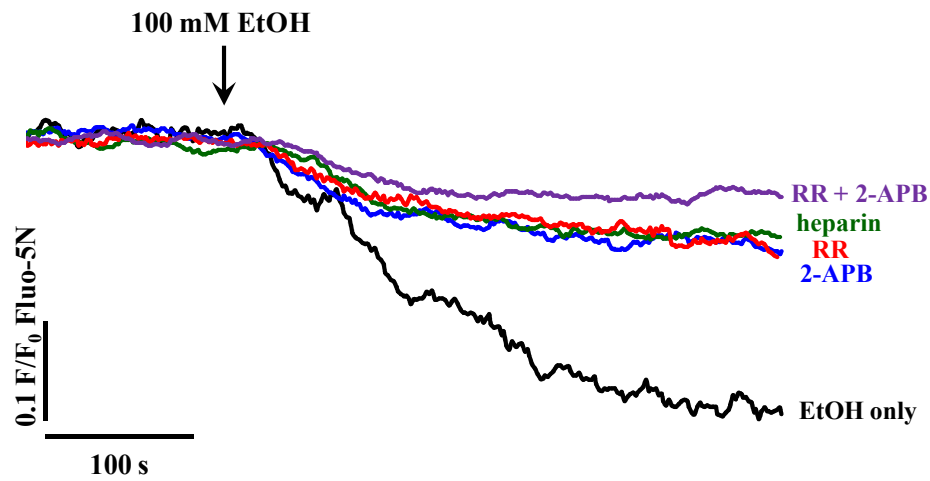
divided into two groups: 56 % of cells (10 out of 18) developed a small sustained elevation of cytosolic  $\text{Ca}^{2+}$ , just slightly higher than the baseline level. The average amplitude of the elevation was  $31 \text{ nM} \pm 6 \text{ nM}$  ( $n = 10$ ). The other 8 cells (44 %) used in the experiment did not respond to ethanol at all. The traces are shown in *Fig. 5.2.A* and the chart comparing different types of responses is presented in *Fig. 5.2.B*.

In the second experiment freshly isolated pancreatic acinar cells were loaded with calcium sensitive dye fluo-4 and subsequently were treated with 200 mM ethanol. Again, most of the cells (65 %, 28 out of 43) developed only a tiny sustained increase in cytosolic  $\text{Ca}^{2+}$  (*Fig. 5.2.C*); and small fraction of the cells (16 %, 7 out of 43) did not respond to ethanol. Interestingly, 19 % of the cells in the experiment (8 out of 43) developed delayed oscillatory type of response (*Fig. 5.2.D*). In these cells 200 mM ethanol caused the same small rise in cytosolic  $\text{Ca}^{2+}$  as in the other 65 % of cells, but after 200 - 400 s robust cytosolic  $\text{Ca}^{2+}$  oscillations appeared on the top of  $\text{Ca}^{2+}$  elevation. The results are summarized in *Fig. 5.2.E*.

### **5.3. Responses induced by ethanol in permeabilized pancreatic acinar cells**

It is surprising that even though ethanol intake is strongly correlated with acute pancreatitis, at the same time alcohol has only a minor effect on pancreatic acinar cells. In attempt to address this discrepancy the study was undertaken in order to test the exact effects of ethanol on the intracellular stores. For this purpose freshly isolated pancreatic acinar cells were loaded with a low affinity calcium sensitive indicator, fluo-5N, which preferentially locates into the intracellular stores. Subsequently, the cells were permeabilized by short application of two-photon light

A.



B.

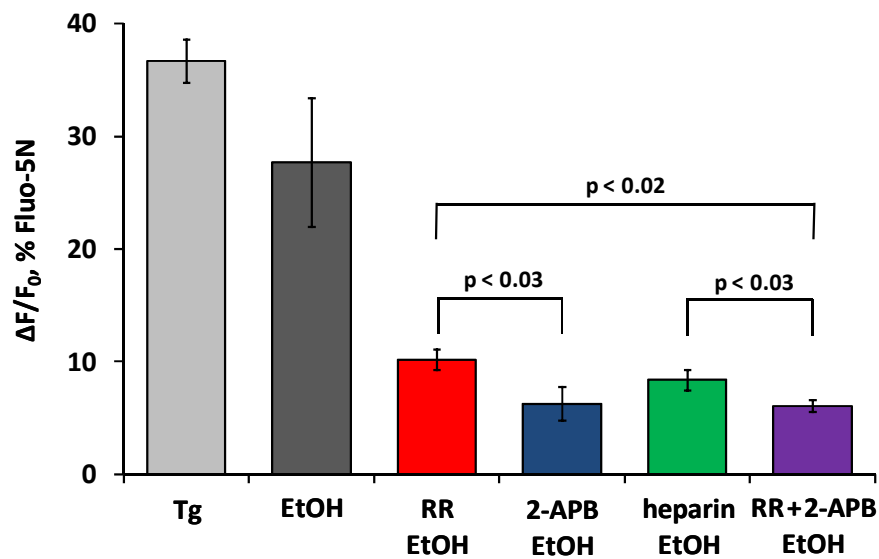


**Fig. 5.3. Responses of the intracellular stores in permeabilized pancreatic acinar cells to ethanol**

(A) Typical traces: 100 mM ethanol releases Ca<sup>2+</sup> from the intracellular stores, which is reflected by reduction in Fluo-5N fluorescence (black trace); responses to ethanol are reduced by pretreatment of cells with 10 μM ruthenium red (red trace), 100 μM 2-APB (blue trace), 250 μg/ml heparin (green trace), or mixture of 2-APB and ruthenium red (purple trace). (B) The chart compares the average amplitudes of responses to 100 mM ethanol in the presence of Ca<sup>2+</sup> release channel inhibitors. Colours of the bars correspond to the traces from (A). The error bars represent standard errors of mean. [Adapted from *Gerasimenko JV, 2011*]<sup>246</sup>.

C.

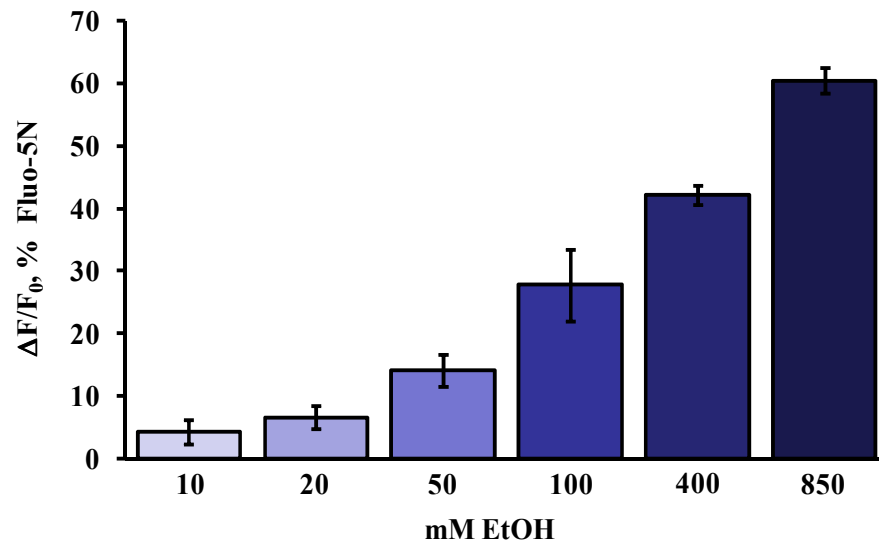


**Fig. 5.3.** (continues)

(C) The chart shows average responses of the intracellular stores in permeabilized pancreatic acinar cells to different doses of ethanol (10 - 850 mM,  $n \geq 6$ ). The error bars represent standard errors. [Adapted from *Gerasimenko JV, 2011*]<sup>246</sup>.

---

at a small region of the plasma membrane. This process led to disruption of illuminated region of the membrane and loss of cytosolic content. Successful permeabilization does not affect the intracellular stores. Application of 100 mM ethanol to permeabilized pancreatic acinar cells resulted in reduction in fluo-5N fluorescence of the intracellular stores, as depicted by the black trace in *Fig. 5.3.A*. A similar response has been previously recorded to palmitoleic acid ethyl ester<sup>242</sup>. Further, permeabilized pancreatic acinar cells were treated with different concentrations of ethanol (10 - 850 mM), all of which evoked marked dose-dependent responses (depicted in *Fig. 5.3.C*). Therefore permeabilized cells exhibit increased sensitivity to ethanol levels as compared with intact pancreatic acinar cells.

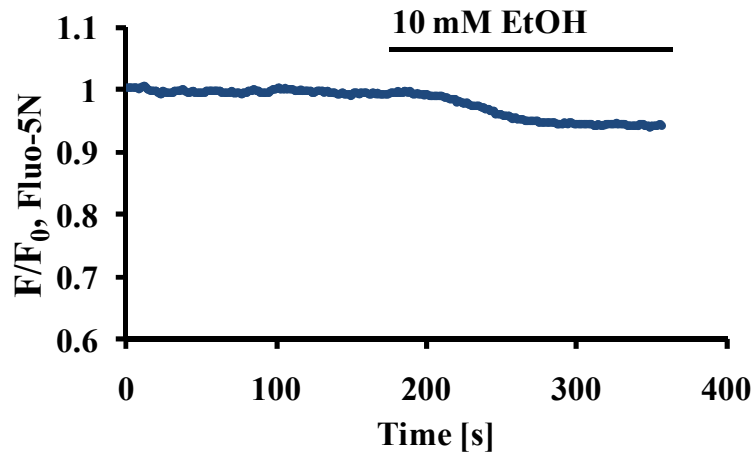
Average amplitudes of responses to ethanol ( $27.7\% \pm 5.7$  SE,  $n = 6$ , dark gray bar) and ethanol in the presence of  $\text{Ca}^{2+}$  receptor blockers are compared in *Fig. 5.3.B*, while typical traces are shown in *Fig. 5.3.A*. The responses evoked by ethanol in permeabilized cells were mediated by calcium release channels:  $\text{IP}_3\text{Rs}$  and  $\text{RyR}$ . Application of  $100\ \mu\text{M}$  2-aminoethoxydiphenyl borate (2-APB) or  $250\ \mu\text{g/ml}$  heparin, (both are effective blockers of  $\text{IP}_3\text{Rs}$ ), significantly reduced ethanol-elicited  $\text{Ca}^{2+}$  release from the intracellular stores (*Fig. 5.3.B*,  $6.3\% \pm 1.5$  SE,  $n = 9$  and  $8.4\% \pm 0.9$  SE,  $n = 7$ , for blue and green bar, respectively). Also, a reduction in  $\text{Ca}^{2+}$  release was obtained by inhibition of  $\text{RyRs}$  with  $10\ \mu\text{M}$  ruthenium red (*Fig. 5.3.B*,  $10.2\% \pm \text{SE}$ ,  $n = 6$ , red bar). Simultaneous inhibition of both receptors resulted in even more reduction of  $\text{Ca}^{2+}$  release induced by ethanol than inhibition of  $\text{RyRs}$  alone (*Fig. 5.3.B*,  $6.1\% \pm 0.5$  SE,  $n = 5$ , purple bar;  $p < 0.02$ ). Responses of the intracellular stores to  $10\ \mu\text{M}$  thapsigargin are provided for comparison (*Fig. 5.3.B*,  $36.7\% \pm 1.9$  SE,  $n = 10$ , light gray bar).

---

#### 5.4. Ethanol-induced responses are dependent on calmodulin

As described in Chapter 4, calmodulin is an important regulatory protein and an efficient intracellular  $\text{Ca}^{2+}$  sensor. Because of its relatively small size (17 kDa) it is very likely to be lost from the cytosol of permeabilized pancreatic acinar cells. Therefore calmodulin might be responsible for the difference to ethanol sensitivity between intact and permeabilized cells. To test this hypothesis experiments on fluo-5N-loaded and two-photon permeabilized pancreatic acinar cells were performed and the results are summarized in *Fig. 5.4.C*. 10 mM ethanol alone induces calcium release from the intracellular stores (*Fig. 5.4.A and C*,  $n = 8$ ). The presence of 2.5  $\mu\text{M}$  calmodulin in KHEPES solution effectively abolishes responses to 10 mM ethanol, but 100 mM ethanol is still able to release calcium from the intracellular stores, but the responses are markedly reduced (*Fig. 5.4.B and C*,  $n = 9$ ). The concentration of CaM in the cytoplasm of intact pancreatic acinar cells is close to 2.5  $\mu\text{M}$ <sup>247</sup> and thus the presence of 2.5  $\mu\text{M}$  calmodulin in KHEPES solution should compensate the loss of the intracellular protein. Pretreatment of permeabilized cells with both 2.5  $\mu\text{M}$  CaM and 20  $\mu\text{M}$  CaM inhibitor peptide led to restoration of the responses to 10 mM ethanol as seen in permeabilized pancreatic acinar cells treated with ethanol alone (*Fig. 5.4.C*,  $n = 8$ ). Additionally, the effects of calmodulin on  $\text{IP}_3\text{R}$ -dependent  $\text{Ca}^{2+}$  release from the intracellular stores were investigated. Treatment of permeabilized pancreatic acinar cells with 10  $\mu\text{M}$   $\text{IP}_3$  induced  $\text{Ca}^{2+}$  release from the stores (*Fig. 5.4.C*). Preincubation with 2.5  $\mu\text{M}$  CaM led to significant inhibition of  $\text{IP}_3$ -elicited responses (*Fig. 5.4.C*,  $n = 5$ ). The responses to  $\text{IP}_3$  were restored when permeabilized cells were preincubated with both 2.5  $\mu\text{M}$  calmodulin and 20  $\mu\text{M}$  CaM inhibitor peptide (*Fig. 5.4.C*,  $n = 5$ ).

A.



B.

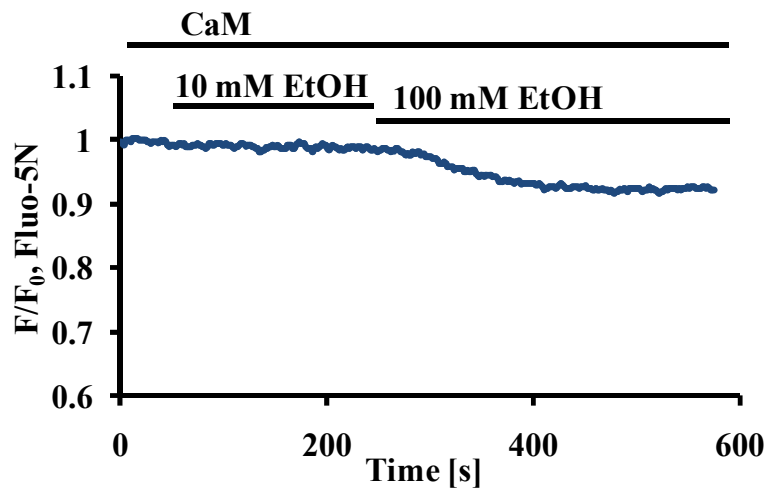


**Fig. 5.4. Effects of calmodulin on ethanol-induced responses in permeabilized pancreatic acinar cells**

Calmodulin reduces ethanol-induced responses of the intracellular stores in permeabilized pancreatic acinar cells. **(A)** Typical trace showing that 10 mM EtOH releases  $\text{Ca}^{2+}$  from the intracellular stores in permeabilized cells. **(B)** The trace demonstrates that in the presence of 2.5  $\mu\text{M}$  CaM responses to 10 mM EtOH are abolished and responses to 100 mM EtOH are substantially reduced. [Adapted from *Gerasimenko JV, 2011*]<sup>246</sup>.

C.

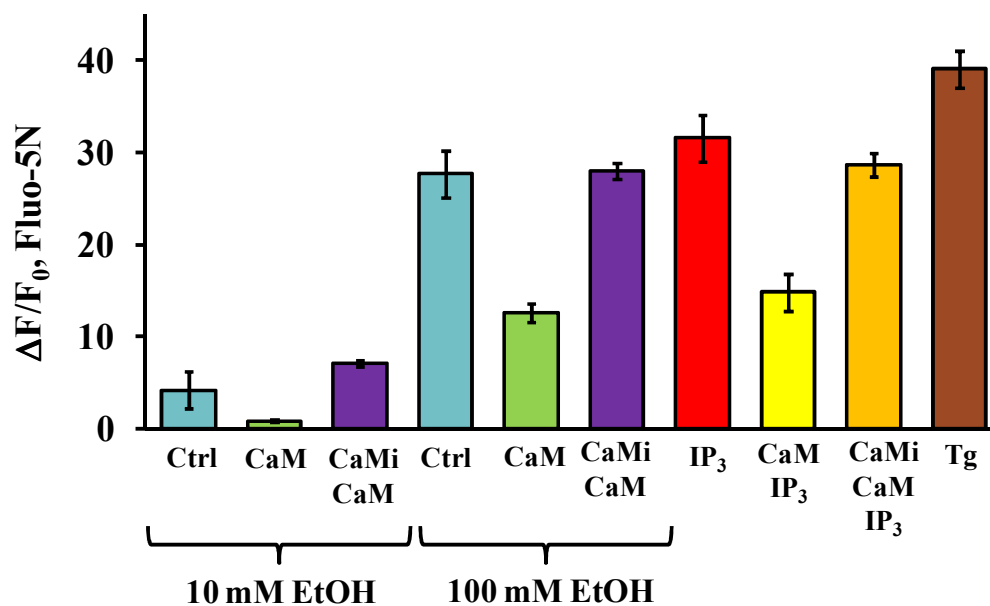


**Fig. 5.4.** (continues)

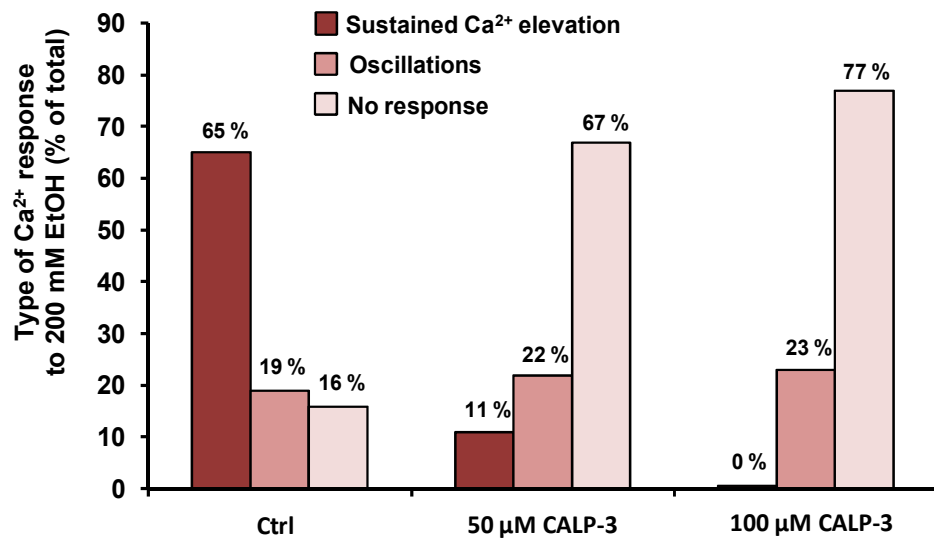
(C) Summary of the results showing inhibition of ethanol-elicited responses in permeabilized cells by CaM (full description in text). [Adapted from *Gerasimenko JV, 2011*]<sup>246</sup>.

---

## 5.5. Activation of calmodulin in intact cells protects against ethanol-induced responses

Since inhibition of calmodulin abolishes its protective effects on ethanol-induced responses in permeabilized pancreatic acinar cells, it can be hypothesised that specific activation of intracellular calmodulin in intact cells could potentially decrease sensitivity of cells to ethanol. The experiments were performed on freshly isolated fluo-4-loaded pancreatic acinar cells. Control cells were treated with 200 mM EtOH, which induced three types of responses. As was described above, the majority of cells (65 %) responded with clear sustained elevation of baseline; 19 % of cells developed robust calcium oscillations on the top of the plateau; and 16 % did not respond (*Fig. 5.2.E* and *Fig. 5.5.A*). Preincubation with 50  $\mu$ M calmodulin activator CALP-3 resulted in a dramatic decrease in sustained elevation type of responses (from 65 % in control to 11 %); whereas the levels of oscillatory responses (22 % of cells) remained on the similar level; and as many as 67 % of cell did not respond at all (*Fig. 5.5.A-C*). Further, 100  $\mu$ M CALP-3 had even stronger effect on 200 mM ethanol-induced responses. It completely abolished ethanol-elicited sustained elevations of baseline; 23 % of cells still developed oscillations, but the amplitudes of the transients were dramatically reduced as compared to those observed in control cells; finally, 77 % of the cell pretreated with 100  $\mu$ M CALP-3 showed no response at all (*Fig. 5.5.A and D*). *Fig. 5.5.E* compares the average responses in pancreatic acinar cells to 200 mM ethanol (dark blue trace, n = 10) and to ethanol in the presence of 100  $\mu$ M CALP-3 (red trace, n = 18). CALP-3 substantially reduces alcohol-induced calcium responses in pancreatic acinar cells.

A.



B.

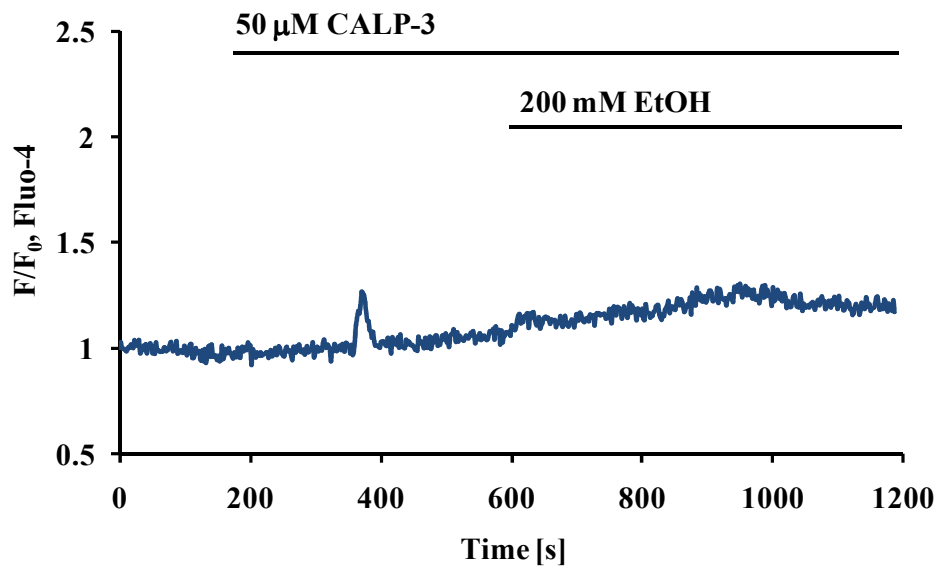
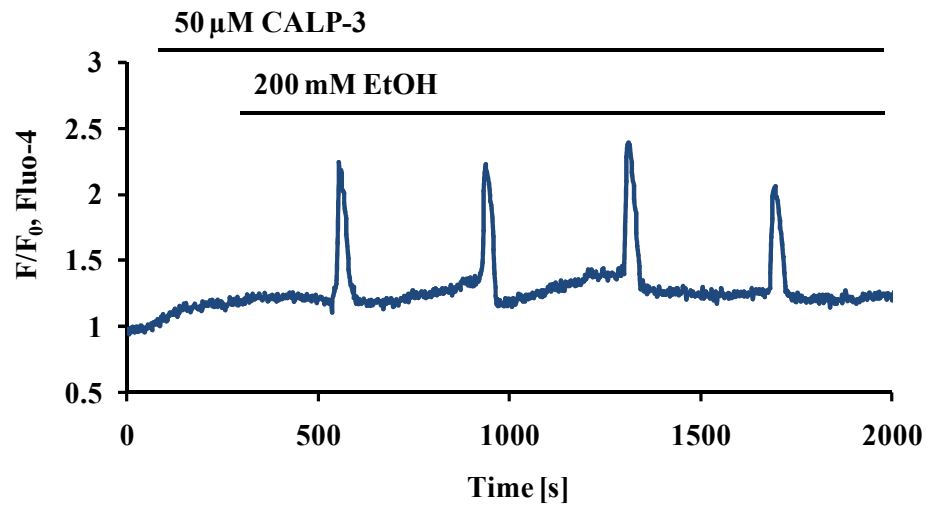


**Fig. 5.5. Activation of CaM by CALP-3 reduces 200 mM EtOH-induced responses in intact pancreatic acinar cells**

(A) The chart compares frequencies of different types of cytosolic Ca<sup>2+</sup> responses in pancreatic acinar cells to 200 mM EtOH, and ethanol in the presence of 50 μM CALP-3 or 100 μM CALP-3. (B) Typical trace showing a sustained elevation type of calcium response to 200 mM ethanol in the presence of 50 μM CALP-3.

C.



D.

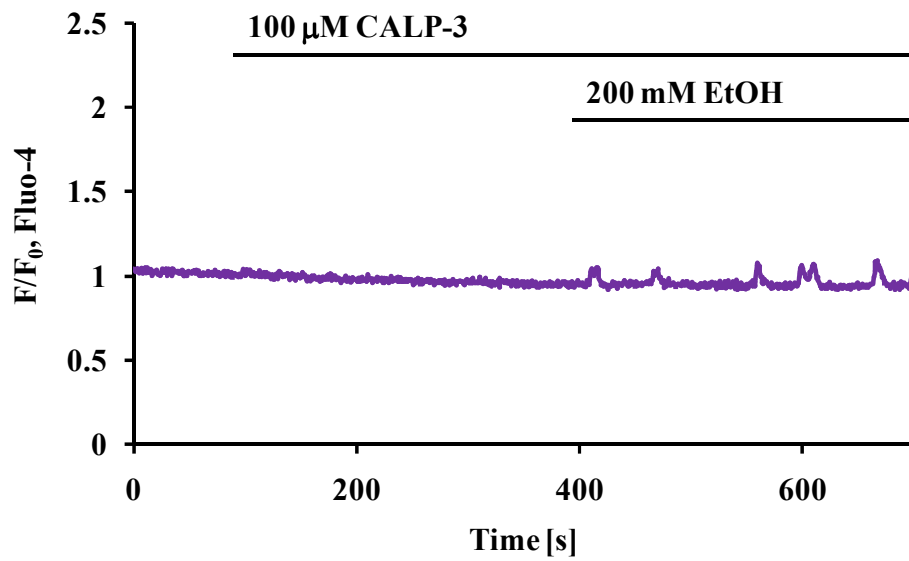


**Fig. 5.5.** (*continues*)

(C) Typical trace showing an oscillatory type of calcium response to 200 mM ethanol in the presence of 50  $\mu\text{M}$  CALP-3. (D) Typical trace showing small oscillations induced by 200 mM ethanol in the presence of 100  $\mu\text{M}$  CALP-3.

E.

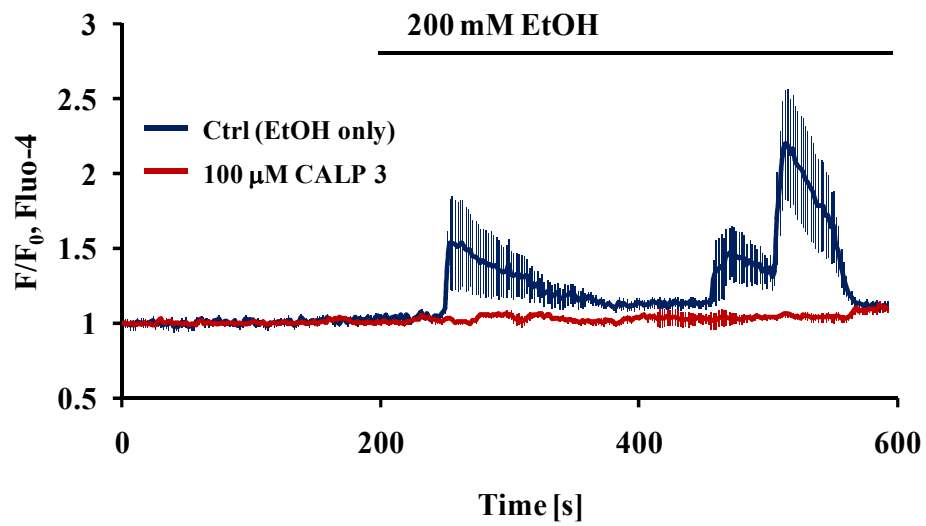


**Fig. 5.5.** (continues)

(E) Average responses to 200 mM EtOH alone ( $n = 10$ , dark blue trace) and EtOH in the presence of 100  $\mu\text{M}$  CALP-3 ( $n = 18$ , red trace). [Adapted from *Gerasimenko JV, 2011*]<sup>246</sup>.

---

## 5.6. Involvement of the acidic stores in ethanol-induced $\text{Ca}^{2+}$ release

The endoplasmic reticulum is the major calcium store in all cell types. However, accumulating evidence indicates that the acidic compartment might also have an important input in cytosolic  $\text{Ca}^{2+}$  responses<sup>53,248</sup>. The acidic compartment is particularly significant in pancreatic acinar cells, which contain zymogen granules, where substantial amounts of  $\text{Ca}^{2+}$  and  $\text{Zn}^{2+}$  are stored<sup>249</sup>. Interestingly, it is known that  $\text{Zn}^{2+}$  uptake into zymogen granules is facilitated by a specific transporter named as ZnT2<sup>249</sup>; in contrast, pathways of  $\text{Ca}^{2+}$  transport are still not fully understood, but the evidence shows that they are dependent on vacuolar  $\text{H}^+$  pumps<sup>202</sup>.

In order to investigate the involvement of the acidic store in calcium responses induced by ethanol, pancreatic acinar cells were loaded with fluo-5N and permeabilized using two-photon laser. Application of 10  $\mu\text{M}$  thapsigargin inhibited the SERCA and led to depletion of the ER store. After calcium baseline levels were stabilized, the cells were treated with 100 mM ethanol. Interestingly, ethanol had no effect in the basal region of the cell, where the ER is located. In contrast, a substantial decrease in fluo-5N fluorescence was observed in the granular area, which can be explained as  $\text{Ca}^{2+}$  release from the acidic compartment (*Fig. 5.6.A*). This experiment demonstrates that the acidic store is involved in ethanol-induced calcium responses.

Subsequently, experiments were designed to further characterise ethanol-elicited calcium release from the acidic compartment. First, it was tested whether liberation of  $\text{Ca}^{2+}$  is dependent on low pH of the acidic store. For that purpose 100 nM bafilomycin A1 was applied to fluo-5N-loaded permeabilized pancreatic acinar cells

---

in order to inhibit the vacuolar type H<sup>+</sup> ATPase. After 30 min preincubation with bafilomycin A1 and after emptying the ER with thapsigargin, the cells were treated with 100 mM ethanol, which failed to induce any response (gray trace, *Fig. 5.6.B*). Importantly, it was previously demonstrated that the presence of bafilomycin A1 does not affect ER store depletion caused by thapsigargin<sup>250</sup>. The results of the experiment indicate that calcium release requires low pH of the acidic store.

Further, involvement of calcium channels in ethanol-elicited responses was investigated on permeabilized pancreatic acinar cells, whose ER store was depleted by thapsigargin. The cells were pretreated with inhibitors of IP<sub>3</sub>Rs: 250 μg/ml heparin (n = 6) or 100 μM 2-APB (n = 5) and then 100 mM ethanol was applied. The results presented in *Fig. 5.6.B* (blue and green traces) indicate that IP<sub>3</sub>Rs are involved in Ca<sup>2+</sup> release from the acidic store, as upon IP<sub>3</sub>R inhibition the responses to ethanol were substantially reduced. When the cells were pretreated with 10 μM ruthenium red in order to block RyRs (n = 5), Ca<sup>2+</sup> responses to ethanol were also reduced, but not as much as in case of preincubation with heparin or 2-APB (red trace, *Fig. 5.6.B*). Finally, simultaneous inhibition of IP<sub>3</sub>Rs and RyRs by pretreatment with a mixture of 100 μM 2-APB and 10 μM ruthenium red (n = 5) completely abolished Ca<sup>2+</sup> release from the acidic store in response to 100 mM ethanol (purple trace, *Fig. 5.6.B*). The average amplitudes of responses are compared in *Fig. 5.6.C*. The pharmacological data accumulated on permeabilized pancreatic acinar cells suggest that alcohol-induced Ca<sup>2+</sup> release from the acidic compartment is mediated by both IP<sub>3</sub>Rs and RyRs.

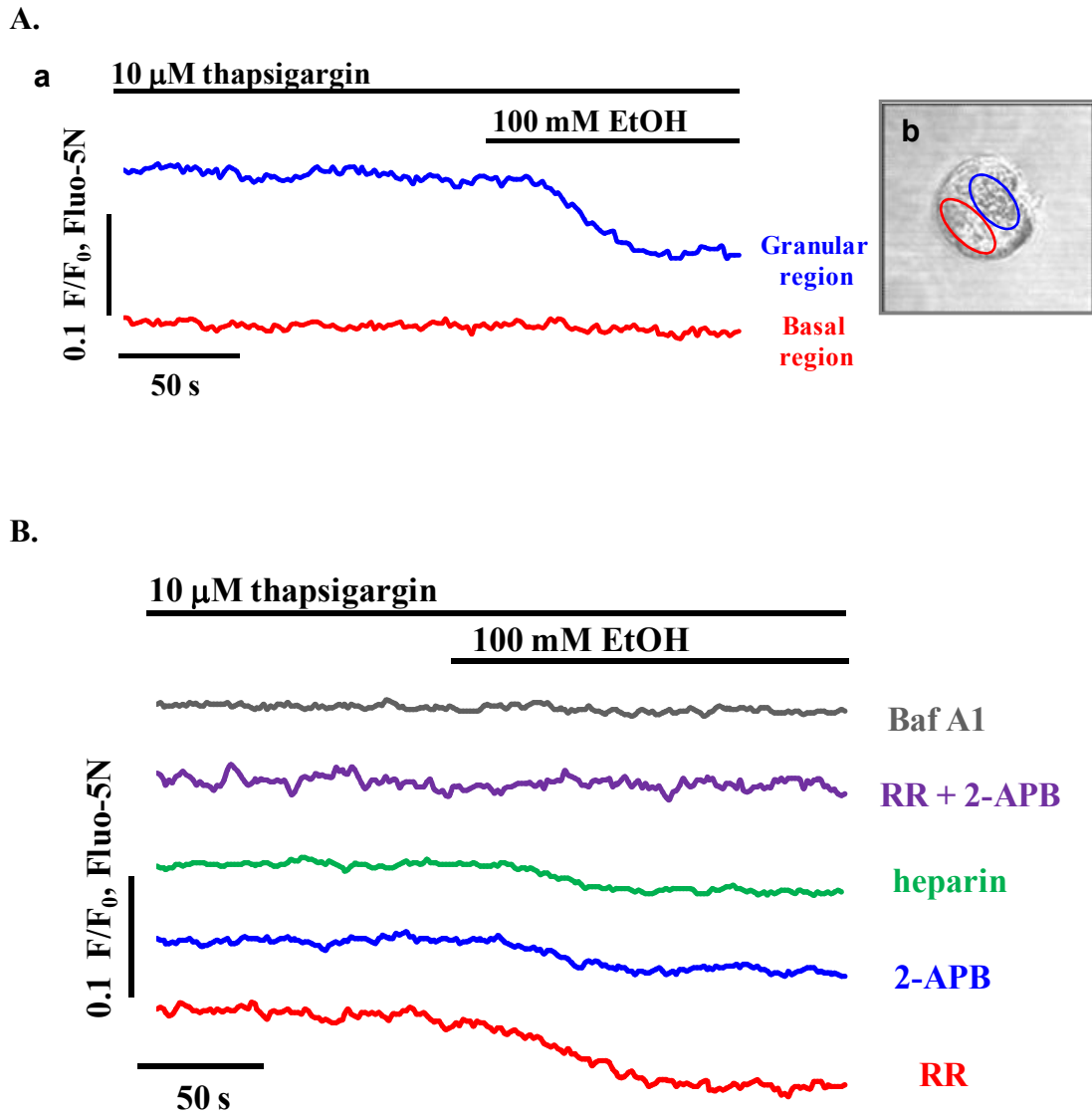


**Fig. 5.6. Ethanol releases  $\text{Ca}^{2+}$  from thapsigargin-insensitive acidic store in permeabilized pancreatic acinar cells**

(A) The figure compares  $\text{Ca}^{2+}$  release in the basolateral area (**b**, red region) and the apical area (**b**, blue region). After depletion of the ER stores with 10  $\mu\text{M}$  thapsigargin, 100 mM EtOH releases  $\text{Ca}^{2+}$  from the granular area containing zymogen granules (**a**, blue trace) but not from the basolateral region, which contains mainly the ER (**a**, red trace). (B) Typical traces showing the effects of 100 mM EtOH on the acidic store (granular area), after depletion of the ER with 10  $\mu\text{M}$  thapsigargin. 100 mM EtOH is accompanied by various inhibitors: 100 nM bafilomycin A1 (gray trace), 10  $\mu\text{M}$  ruthenium red (red trace), 100  $\mu\text{M}$  2-APB (blue trace), 250  $\mu\text{g/ml}$  heparin (green trace) and both 10  $\mu\text{M}$  ruthenium red and 100  $\mu\text{M}$  2-APB (purple trace). [Adapted from *Gerasimenko JV, 2011*]<sup>246</sup>.

C.

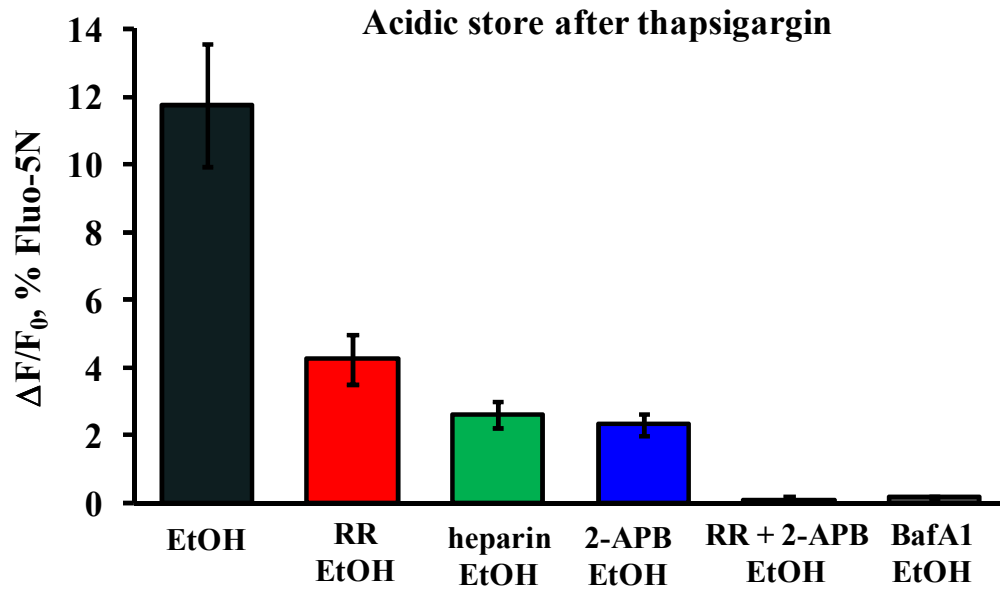


**Fig. 5.6.** (continues)

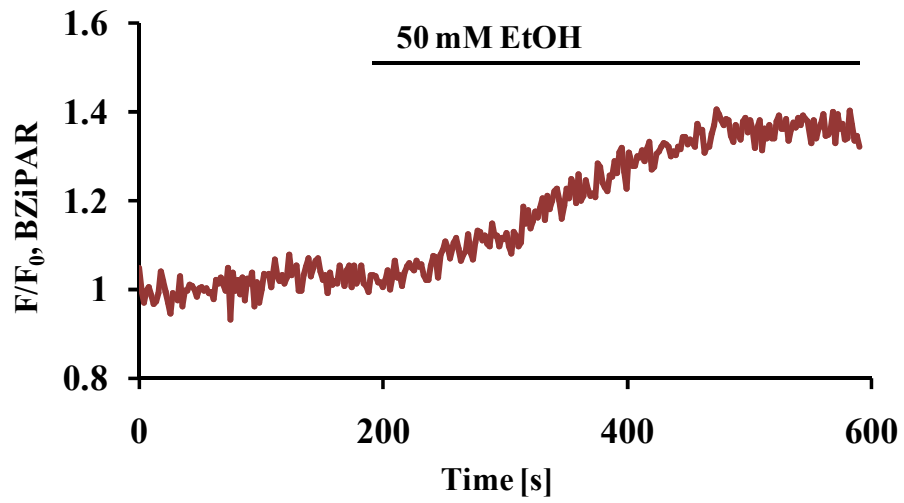
(C) The chart compares the average amplitudes of the responses from (B). The error bars represent standard errors of mean. [Adapted from *Gerasimenko JV, 2011*]<sup>246</sup>.

---

### 5.7. Ethanol induces activation of trypsinogen

Intracellular conversion of trypsinogen to trypsin is one of the main hallmarks of acute pancreatitis. BZiPAR (Rhodamine 110, bis-(N-CBZ-L-isoleucyl-L-prolyl-L-arginine amide), dihydrochloride) is a synthetic substrate for trypsin, which becomes fluorescent when the enzyme cleaves two oligopeptide residues. It has been used in the past for monitoring of the time course of trypsin activation<sup>251</sup>. Here it has been applied as a useful tool for investigation of trypsinogen activation upon treatment with ethanol in permeabilized pancreatic acinar cells. BZiPAR was added to the perfusion chamber after cell permeabilization and could enter the cytosol of cells with disrupted plasma membrane. The cells were exposed to different concentrations of ethanol: 10 mM, 50 mM and 100 mM and fluorescence of BZiPAR was measured. The results summarized in *Fig. 5.7.C* show that ethanol induced a dose-dependent activation of trypsin. Untreated control cells had only low background activity of trypsin (n = 7). Treatment with 10 mM ethanol was associated with small but clear activation of trypsin (n = 8); 50 mM ethanol induced higher activity of trypsin, which was reflected by increased fluorescence of BZiPAR (n = 5, *Fig. 5.7.A*); and treatment with 100 mM ethanol led to respectively increased activation of trypsin (n = 10) as compared to lower doses of alcohol (*Fig. 5.7.C*). Trypsin activity induced by 100 mM ethanol treatment was completely abolished in the presence of 0.01 % trypsin inhibitor from soybean (n = 6, *Fig. 5.7.C*). Further, in order to investigate whether trypsin activation is dependent on Ca<sup>2+</sup> signals, treatment with 100 mM ethanol was performed in strong Ca<sup>2+</sup> buffering conditions, where cytosolic Ca<sup>2+</sup> was clamped to physiological levels by application of 2 mM CaCl<sub>2</sub> and 10 mM BAPTA. Under conditions of clamped calcium 100 mM ethanol did not induce trypsinogen

A.



B.

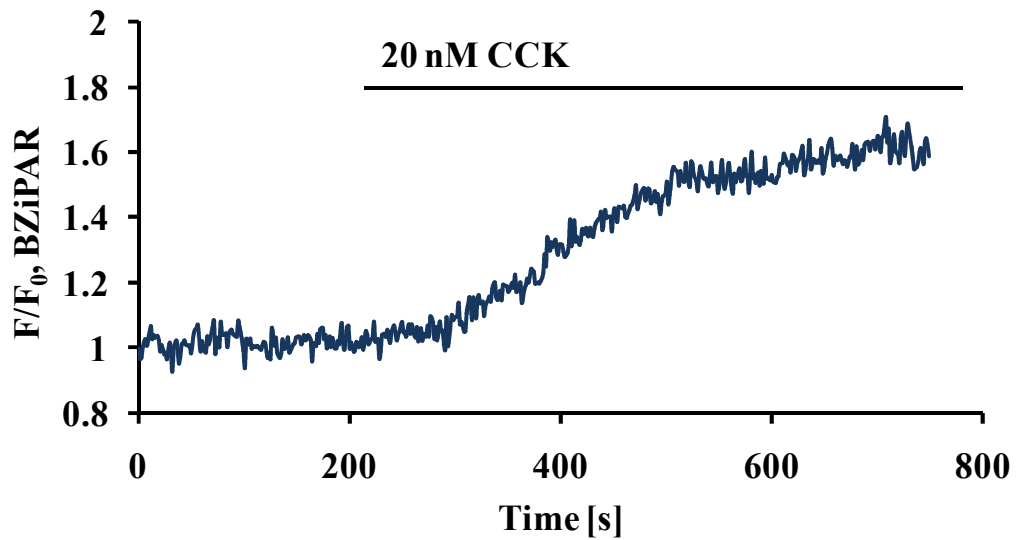


**Fig. 5.7. Ethanol induces trypsinogen activation**

(A) Typical trace showing trypsinogen activation induced by 50 mM ethanol in permeabilized cells. (B) Typical trace demonstrating trypsinogen activation upon treatment with 20 nM CCK.

C.\

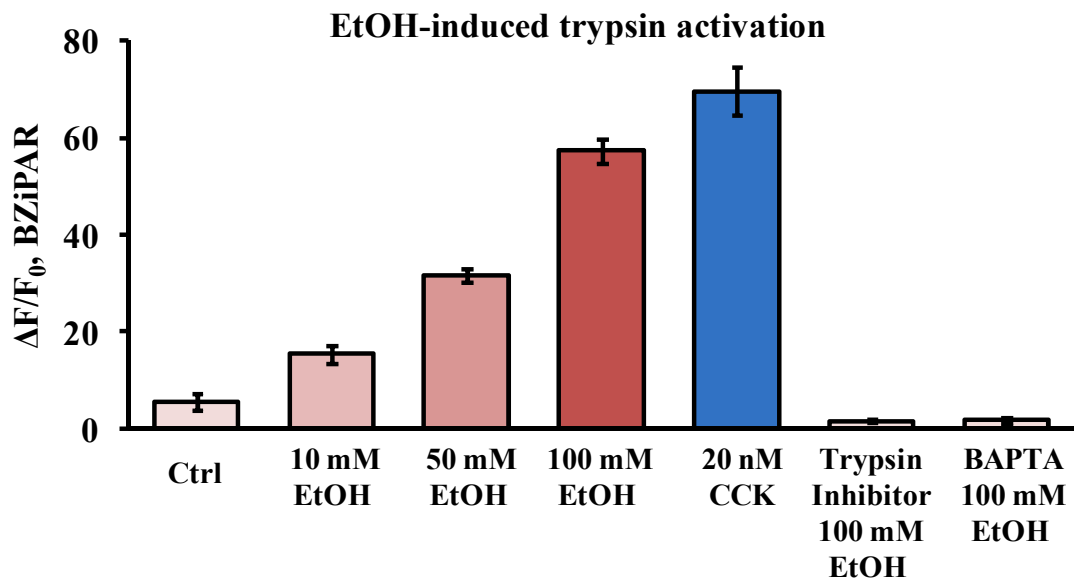


**Fig. 5.7.** (continues)

(C) The bar chart shows trypsin activation in untreated permeabilized pancreatic acinar cells ( $n = 7$ , left bar); cells treated with different concentrations of ethanol: 10 mM ( $n = 8$ ), 50 mM ( $n = 5$ ), 100 mM ( $n = 10$ ); cells stimulated with 20 nM CCK ( $n = 5$ , blue bar); trypsin activation by 100 mM ethanol in the presence of 0.01% trypsin inhibitor from soybean ( $n = 6$ ); and trypsin activation by 100 mM ethanol in conditions of clamped calcium: 10 mM BAPTA and 2 mM  $\text{CaCl}_2$  ( $n = 6$ ). Black error bars represent standard errors. [Adapted from *Gerasimenko JV, 2011*]<sup>246</sup>.

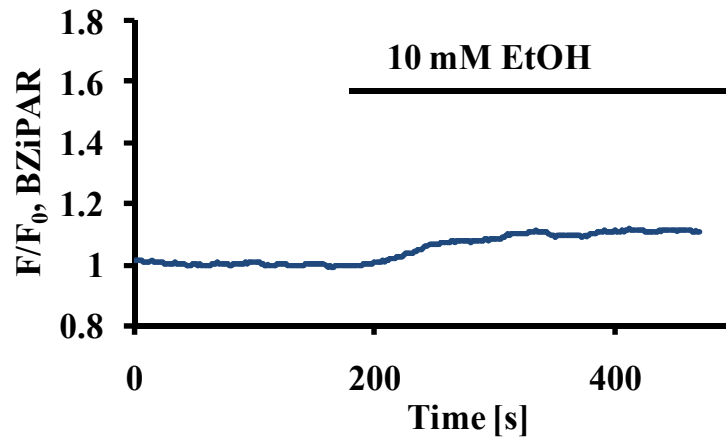
---

conversion to trypsin (n = 6, *Fig. 5.7.C*). In contrast, supra-maximal dose of CCK (20 nM), which is known to induce quick Ca<sup>2+</sup> release from the intracellular stores, was associated with very strong induction of trypsin activity seen as substantial increase in BZiPAR fluorescence (n = 5, *Fig. 5.7.B and C*).

### **5.8. Trypsinogen activation by ethanol is inhibited by calmodulin**

As was described above, ethanol-induced Ca<sup>2+</sup> responses are inhibited by calmodulin. Since trypsin activation is dependent on Ca<sup>2+</sup> release from the acidic store, it is expected that conversion of trypsinogen to trypsin should also be blocked by calmodulin. Therefore experiments were performed to test the effects of CaM on trypsinogen activation in BZiPAR-loaded permeabilized pancreatic acinar cells. In control cells 10 mM ethanol (n = 8) induced noticeable trypsin activity (*Fig. 5.8.A and D*). Similar degree of trypsinogen activation by 10 mM ethanol was observed in the presence of 2.5 μM CaM and 20 μM CaM inhibitor peptide (n = 5, *Fig. 5.8.D*). In contrast, preincubation of cells with 2.5 μM CaM alone effectively abolished trypsinogen activation by 10 mM ethanol (n = 6, *Fig. 5.8.B and D*). 100 mM ethanol induced substantial trypsinogen activation in permeabilized pancreatic acinar cells (n = 10, *Fig. 5.8.D*) and in cells preincubated with both 2.5 μM CaM and 20 μM CaM inhibitor peptide (n = 5, *Fig. 5.8.D*). This effect was markedly reduced in the presence of 2.5 μM CaM alone (n = 6, *Fig. 5.8.B and D*); however, it was not abolished. Almost complete inhibition of ethanol-induced trypsinogen activation was observed in cells pretreated with 2.5 μM CaM and 100 μM CALP-3 (n = 10, *Fig. 5.8.C and D*). Treatment with 10 μM IP<sub>3</sub> results in similar degree of trypsinogen activation to that observed upon application of 10 mM ethanol alone (n = 7,

A.



B.

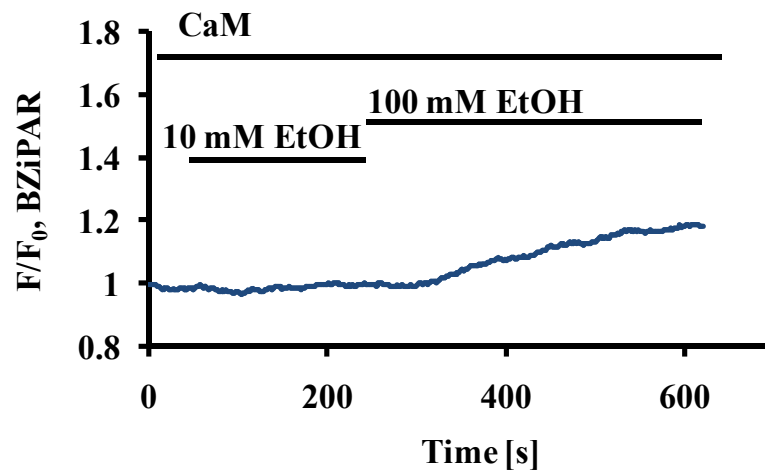
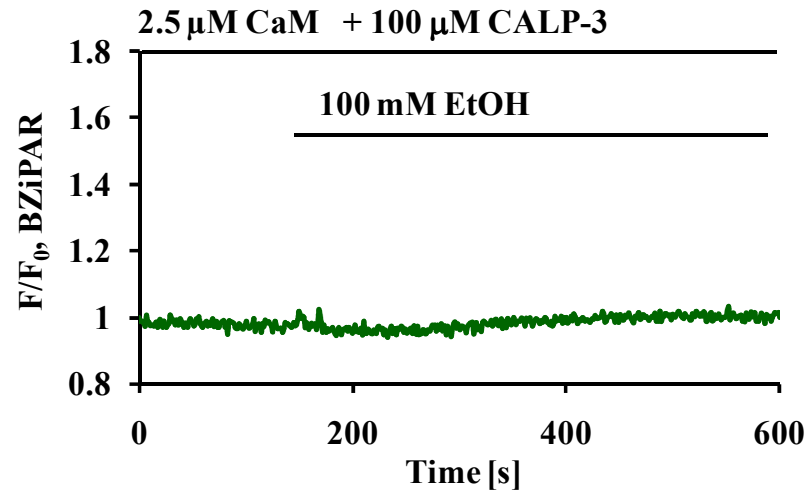


**Fig. 5.8. Calmodulin inhibits ethanol-mediated activation of trypsinogen**

(A) Typical trace showing 10 mM ethanol-induced trypsinogen activation in premeabilized pancreatic acinar cells. (B) Typical trace showing that the presence of 2.5  $\mu$ M calmodulin completely abolishes 10 mM ethanol-induced trypsinogen activation and substantially reduces 100 mM ethanol-elicited trypsinogen activation in permeabilized pancreatic acinar cells. [Adapted from *Gerasimenko JV, 2011*]<sup>246</sup>.

C.



D.

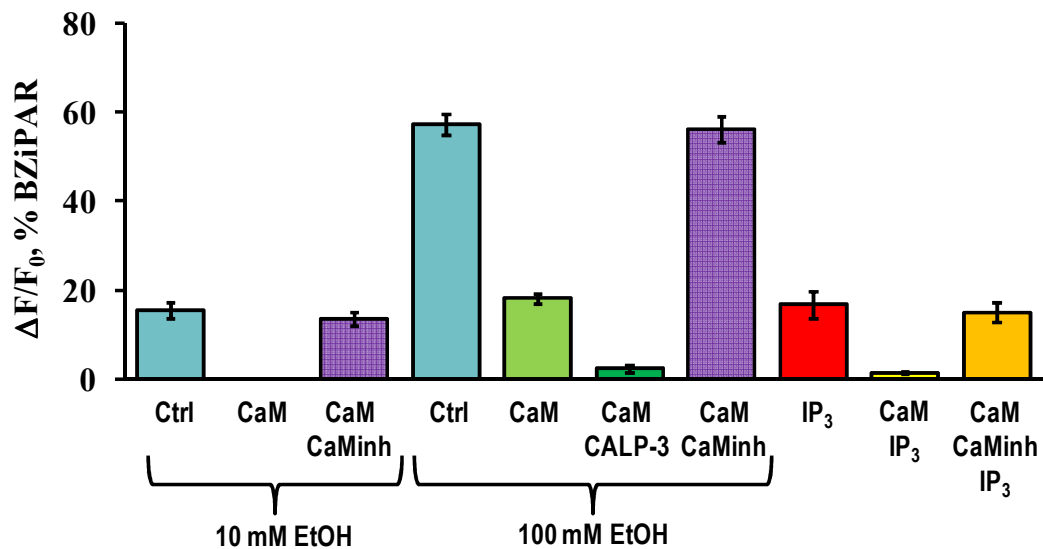


**Fig. 5.8.** (continues)

(C) Typical trace showing that in the presence of 2.5  $\mu\text{M}$  calmodulin and 100  $\mu\text{M}$  CALP-3 trypsinogen activation induced by 100 mM ethanol is substantially reduced. (D) The chart compares trypsinogen activation in permeabilized pancreatic acinar cells upon treatment with 10 mM or 100 mM ethanol in the presence / absence of 2.5  $\mu\text{M}$  CaM or 20  $\mu\text{M}$  CaM inhibitor peptide; or upon treatment with IP<sub>3</sub> in the presence / absence of CaM or CaM inhibitor peptide (full description in text). Black error bars represent standard error. [Adapted from *Gerasimenko JV, 2011*]<sup>246</sup>.

---

*Fig. 5.8.D*). This effect was inhibited in the presence of 2.5  $\mu\text{M}$  CaM ( $n = 6$ ), but again restored when CaM was accompanied by 20  $\mu\text{M}$  CaM inhibitor peptide ( $n = 7$ , *Fig. 5.8.D*).

The importance of  $\text{Ca}^{2+}$  release from the acidic store for the process of trypsinogen activation is underlined by the fact, that 10  $\mu\text{M}$   $\text{IP}_3$  induces significantly less trypsinogen activation than 100 mM ethanol, even though  $\text{IP}_3$  has much stronger effect on  $\text{Ca}^{2+}$  release from the stores. However,  $\text{IP}_3$  releases  $\text{Ca}^{2+}$  mainly from the ER; its effects on the acidic store are much weaker<sup>242</sup>.

## **5.9. Discussion**

Excessive alcohol consumption is strongly correlated with acute pancreatitis. However, so far even very high doses of ethanol have been demonstrated to exert only minor effects on pancreatic acinar cells<sup>100</sup>. Accumulating evidence supports the view that metabolites of ethanol, fatty acid ethyl esters, are the main mediators of ethanol toxicity in the pancreas.

In this chapter it has been shown that ethanol in moderate concentration (100 mM) releases  $\text{Ca}^{2+}$  from the intracellular stores, both the ER and the acidic stores in the apical area. Although the effect of ethanol on intact cells is very modest, in permeabilized cells ethanol causes substantial dose-dependent  $\text{Ca}^{2+}$  release from both the ER and the acidic store. Further, the results presented in this chapter demonstrate that ethanol-induced  $\text{Ca}^{2+}$  release is crucial for pathological intracellular trypsinogen activation. This  $\text{Ca}^{2+}$  release is mediated and amplified by both RyRs and  $\text{IP}_3$ R<sub>s</sub>. The apparent discrepancy between modest effects of alcohol on intact pancreatic acinar

---

cells and its powerful effects on permeabilized cells has been here addressed. It is now clear that high levels of calmodulin in pancreatic acinar cells act inhibitory against ethanol actions on  $\text{Ca}^{2+}$  release from the intracellular stores in intact cells. In permeabilized cells calmodulin is lost and thus its protective effect abates. However, the exact mechanism of calmodulin-dependent inhibition of ethanol toxic effects is still unclear. It could be speculated that CaM can control  $\text{Ca}^{2+}$  release through regulation of  $\text{IP}_3\text{R}$  opening, which has been previously reported<sup>252,253</sup>.

What is more, the exact effects of calmodulin in the granular region of pancreatic acinar cells attract growing interest. It has been already reported that calmodulin is recruited from the basolateral cytoplasm to the apical region upon physiological stimulation that generates local calcium spikes in the apical pole<sup>247</sup>. Since calmodulin attenuates  $\text{Ca}^{2+}$  release from the intracellular stores and thus inhibits trypsinogen activation in zymogen granules, recruitment of CaM to the apical region might be viewed as protective mechanism that evolved in pancreatic acinar cells<sup>254,255</sup>. Interestingly, activation of calmodulin differs between physiological and pathological responses. It was observed that physiological  $\text{Ca}^{2+}$  oscillations in the granular region recruit calmodulin during each  $\text{Ca}^{2+}$  spike; in contrast excessive doses of CCK or ACh result in sustained calcium elevations with only one transient phase, and consistently calmodulin is recruited to the apical region only once<sup>247</sup>. That suggests importance of increasing phase of  $\text{Ca}^{2+}$  oscillations in calmodulin recruitment to the apical region.

This study also provides important observations from medical point of view. The results on permeabilized cells demonstrate that specific pre-activation of calmodulin by calcium-like peptide CALP-3 results in even stronger inhibition of ethanol-

---

mediated  $\text{Ca}^{2+}$  release from the stores and trypsinogen activation than does the presence of calmodulin alone in intact cells. Consistently, in Chapter 4 it was shown that CALP-3 reduces pathological  $\text{Ca}^{2+}$  responses, a side effect of BH3 mimetic application, and thus promotes pancreatic acinar cell survival. Taken these observations together it is conceivable that calmodulin activators might find their application as potential therapeutic approach for treatment of pancreatitis or perhaps for reduction of adverse effects of ethanol poisoning.

---

**CHAPTER 6:**  
**BCL-2 FAMILY PROTEINS AND PASSIVE CALCIUM LEAK**  
**FROM THE ENDOPLASMIC RETICULUM**

---

## Chapter 6: Bcl-2 family proteins and passive calcium leak from the endoplasmic reticulum

### 6.1. Overview of passive calcium leak from the ER

Passive calcium leak from the ER is probably the most enigmatic process in calcium signalling field. Although it is unnoticeable in physiological conditions it can be unmasked by inhibition of the SERCA pump by thapsigargin (*Fig. 6.1*), which results in slow release of  $[Ca^{2+}]$  from the ER, which often is amplified by the opening of IP<sub>3</sub>Rs and RyRs in CICR process. The leak itself, however, is not affected by inhibition of IP<sub>3</sub>Rs, RyRs or Ca<sup>2+</sup> release by NAADP<sup>175,256</sup>. Up to now the nature of passive calcium leak from the ER remains elusive, since it does not appear to be mediated by any of the major Ca<sup>2+</sup>-releasing channels and thus the clear-cut evidence of the mechanism is still missing.

However, in the literature data can be found, which demonstrates that passive calcium leak at least in some cell types is potentiated by ATP or glutathione<sup>256,257</sup>, and inhibited by Ni<sup>2+</sup>, which also blocks certain channels in the plasma membrane<sup>258</sup>. Also, the leak shows some temperature dependency, which suggests it might be mediated by an unidentified Ca<sup>2+</sup> channel<sup>258</sup>. Interestingly, the leak rate is maintained relatively constant throughout a wide range of calcium concentration in the ER, but suddenly decreases when  $[Ca^{2+}]_{ER}$  drops to micromolar range<sup>174</sup>. The leak rates, however, differ in different cell types. In pancreatic acinar cells the leak is relatively

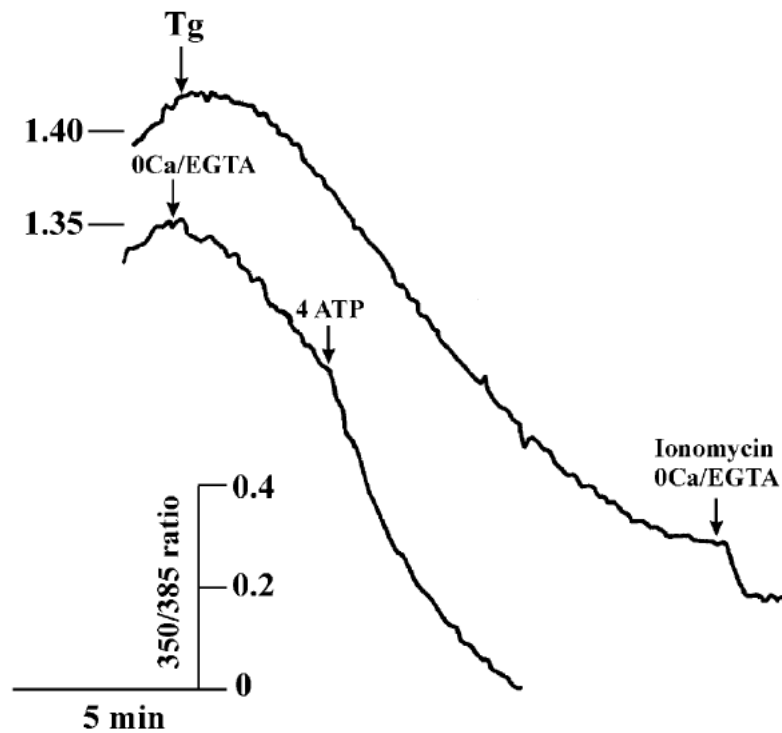


**Fig. 6.1. Passive calcium leak from the intracellular stores**

Recordings of the leak from mag-fura-2-loaded BHK-21 cells, permeabilized with streptolysin-O.  $\text{Ca}^{2+}$  leak can be unmasked either by treatment with thapsigargin (upper trace) or by lowering of external calcium (lower trace). [Adapted from *Hofer AM, 1996*]<sup>256</sup>

---

slow, up to  $19 \mu\text{M}/\text{min}^{259}$ ; much higher values were found in sensory neurons:  $90 \mu\text{M}/\text{min}^{260}$ , or in HeLa cells:  $200 \mu\text{M}/\text{min}^{261}$ .

Recently, potential candidate channels for passive  $\text{Ca}^{2+}$  leak have been attracting a lot of attention. Accumulating evidence does not point to one channel; instead few candidates and mechanisms have been postulated. It is possible that what is perceived as passive ER  $\text{Ca}^{2+}$  leak is in fact a sum of effects mediated by more than one family of membrane proteins.

One of the candidates includes the translocons, which are protein conducting channels present in rough ER membranes. The idea originated from the observation that the passive ER calcium leak was stimulated by treatment of pancreatic acinar cells with puromycin – an antibiotic that inhibits protein synthesis by premature termination of growing polypeptide chain in the ribosome<sup>175</sup>. This indicates that at least one component of passive calcium leak could be mediated by translocon complex. However, translocon should not be permeable for  $\text{Ca}^{2+}$  during the translocation process, when the channel pore is occupied by growing polypeptide chain<sup>262</sup>. Also, when the translocon channel is not engaged in protein synthesis, it is closed by the BiP protein at the ER lumen, which excludes the possibility of ion transfer<sup>263</sup>. A possible explanation is that  $\text{Ca}^{2+}$  leak is a consequence of imperfections in translocation system, which allows  $\text{Ca}^{2+}$  ions to escape from the ER.

Presenilins (PS1 and PS2) are extensively studied proteins due to their involvement in pathogenesis of Alzheimer's disease. Mutations in the genes encoding presenilins are responsible for the most of familial Alzheimer disease cases<sup>264-267</sup>. Presenilins are aspartic proteases, which together with other proteins form  $\gamma$ -secretase complex

---

responsible for regulated intramembrane proteolysis.  $\gamma$ -secretase complex is transported to the plasma membrane or endosomes, where it cleaves type I transmembrane proteins including amyloid precursor protein. Mutations in presenilins might result in a shift in the proteolysis pattern of the latter leading to generation of hydrophobic fragments of amyloid, which tend to spontaneously aggregate. Some data suggest that presenilins can also function as channels in the ER membranes and thus mediate passive  $\text{Ca}^{2+}$  leak<sup>268</sup>. Therefore, mutations in presenilin genes not only affect their proteolytic properties but also might block  $\text{Ca}^{2+}$  leak leading to  $\text{Ca}^{2+}$  overload in the ER and potentiated release of  $\text{Ca}^{2+}$  from the store upon treatment<sup>269,270</sup>. Hydrophilic catalytic cavity of presenilins could also serve as the  $\text{Ca}^{2+}$  conductance pore<sup>266</sup>.

Another potential targets responsible for ER  $\text{Ca}^{2+}$  are polycystins: polycystin-1 (PKD1) and polycystin-2 (PKD2). Mutations in the genes encoding these proteins result in Autosomal Dominant Polycystic Kidney disease characterised by formation of cysts in kidney tubules<sup>271</sup>. Both polycystins are transmembrane proteins located to the ER membranes as well as the plasma membrane at the primary cilia<sup>272</sup>. PKD1 is larger in size with 11 transmembrane domains, as compared to 6 transmembrane domains of PKD2. The latter, however, bears substantial similarity to transient receptor potential (TRP) channels, and thus it functions as a cation channel and perhaps can sustain ER  $\text{Ca}^{2+}$  leak<sup>273</sup>. What is more, PKD2 was demonstrated to interact with  $\text{IP}_3\text{Rs}$  and prolong the  $\text{IP}_3$ -elicited  $\text{Ca}^{2+}$  release<sup>274</sup>. PKD1, on the other hand, was shown to bind to STIM1, which caused inhibition of store operated  $\text{Ca}^{2+}$  entry<sup>275</sup> and increased STIM1 interaction with  $\text{IP}_3\text{R}$ <sup>276</sup>.

---

Further, a strong link exists between ER  $\text{Ca}^{2+}$  leak and Bcl-2 family proteins. It was demonstrated that overexpression of Bcl-2 protein is associated with a decrease in calcium content of the ER, which was explained by increased leakiness of the intracellular stores<sup>157,204</sup>. However, the exact mechanism of Bcl-2-dependent  $\text{Ca}^{2+}$  leak has not yet been clarified. One of the explanations assumes that Bcl-2 can function as an ion channel and thus increased expression of the protein simply introduces more leak channels in the ER<sup>204</sup>. Indeed, some members of Bcl-2 family, particularly Bcl-xL and Bax, exhibit substantial structural similarities with pore-forming bacterial toxins<sup>277,278</sup>. Bcl-2 itself was demonstrated to form channels in artificial lipid bilayers, capable of conducting  $\text{Na}^+$ , but not  $\text{Ca}^{2+}$ , leaving the mechanism unclear<sup>279</sup>. Alternatively, Bcl-2 family members instead of being  $\text{Ca}^{2+}$  channels themselves might be involved in the regulation of other proteins mediating the leak. This chapter provides preliminary data demonstrating possible involvement of Bcl-2 family members in the regulation of passive  $\text{Ca}^{2+}$  leak from the ER in pancreatic acinar cells.

## **6.2. Loss of Bax protein inhibits BH3 mimetic-induced calcium release**

Data presented in Chapter 3 show that treatment with BH3 mimetics BH3I-2' and HA14-1 cause slow  $\text{Ca}^{2+}$  release from the intracellular stores, which eventually is amplified by  $\text{IP}_3\text{Rs}$  and  $\text{RyRs}$ . Although  $\text{Ca}^{2+}$  release was decreased upon inhibition of  $\text{IP}_3\text{Rs}$  and  $\text{RyRs}$ , it was not completely blocked, which suggests the involvement of other  $\text{Ca}^{2+}$  channels in the response to BH3 mimetics. In an attempt to understand the nature of the leak and the exact mechanism of its regulation by Bcl-2 family proteins the effects of loss of Bcl-2, Bak or Bax proteins on BH3I-2'- or HA14-1-

---

induced calcium plateau were investigated. Pancreatic acinar cells were isolated from C57BL/6J wild type mice and from transgenic mice having loss-of-function mutation of one of the following genes: *bcl-2*, *bax* or *bak*. The cells were loaded with AM ester form of calcium sensitive fluorescent dye fluo-4, plated into a perfusion chamber and perfused with 5  $\mu$ M BH3I-2' or 30  $\mu$ M HA14. All experiments were performed in NaHEPES solution, which contained no  $\text{Ca}^{2+}$ ; therefore all changes in cytosolic calcium were dependent only on calcium release from the intracellular stores. The results are presented in *Fig. 6.2*. Upon treatment with 5  $\mu$ M BH3I-2' wild type (n = 12), *bak*<sup>-/-</sup> (n = 27) and *bcl-2*<sup>-/-</sup> (n = 28) cells responded with a substantial increase in cytosolic calcium followed by sustained  $\text{Ca}^{2+}$  plateau, whereas *bax*<sup>-/-</sup> (n = 20) cells showed significant resistance to the treatment with BH3I-2' and did not develop dramatic  $\text{Ca}^{2+}$  responses (*Fig. 6.2.A*). In order to quantitatively compare  $\text{Ca}^{2+}$  responses the areas under the traces were calculated between 602 and 1000 s of the recorded signals, averaged, normalized to the baseline and presented in *Fig. 6.2.B*.  $\text{Ca}^{2+}$  responses in pancreatic acinar cells lacking functional Bax were almost completely abolished as compared to the wild type cells (p < 0.0001) and other knockouts.

Similarly, treatment with 30  $\mu$ M HA14-1 led to  $\text{Ca}^{2+}$  release from the intracellular stores and cytosolic  $\text{Ca}^{2+}$  responses concluded with sustained plateau in wild type cells (n = 25), *bak*<sup>-/-</sup> (n = 43) and *bcl-2*<sup>-/-</sup> (n = 23), but not in *bax*<sup>-/-</sup> (n = 17) cells (*Fig. 6.2.C*). The same quantitative analysis was performed as for BH3I-2' treatment - the areas under the traces were calculated between 602 and 1000 s of the recorded responses, averaged and normalized to the baseline as shown in *Fig. 6.2.D*. Again,

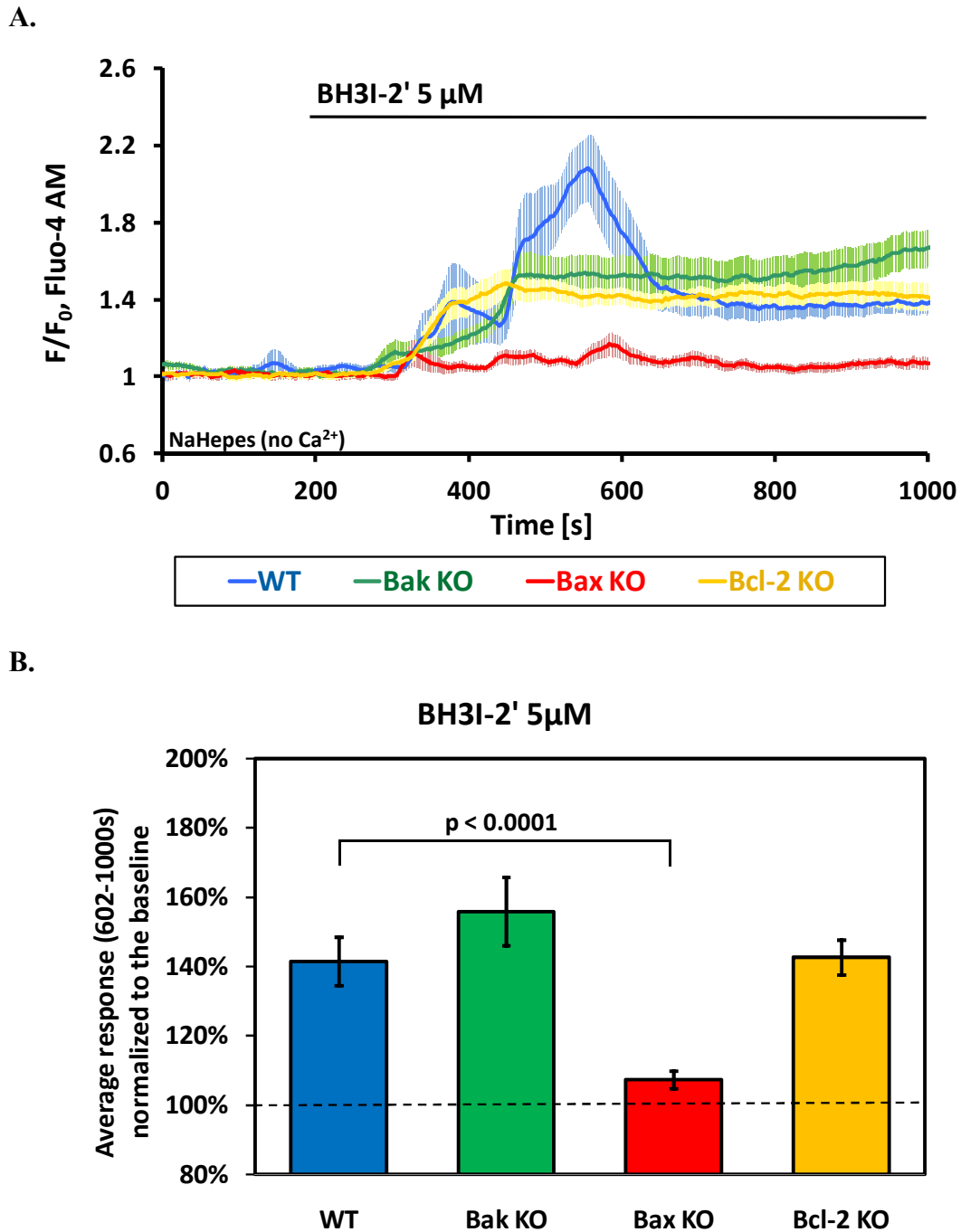


**Fig. 6.2. Loss of Bax inhibits calcium release caused by BH3I-2' and HA14-1**

(A) The graph shows average calcium responses to 5  $\mu$ M BH3I-2' in pancreatic acinar cells isolated from C57BL6/J wild type (n = 12) mice and animals lacking functional Bak (n = 27), Bax (n = 20) or Bcl-2 (n = 28). Error bars represent standard errors. (B) The responses to 5  $\mu$ M BH3I-2' were compared as the average sums of relative fluorescence values recorded between 602 and 1000, which corresponds to the areas under the curves. Black error bars represent standard errors.

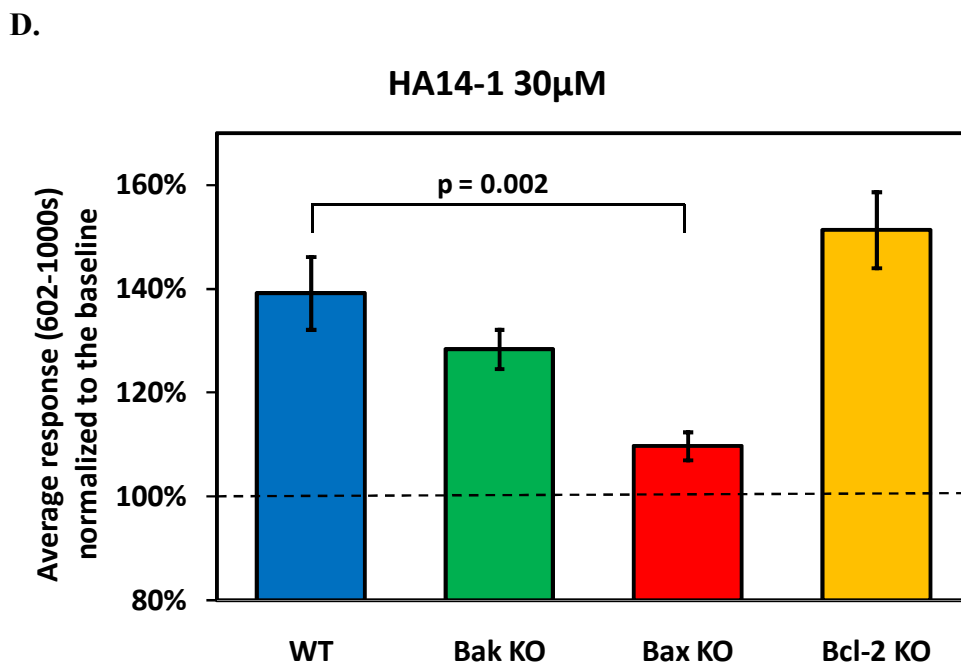
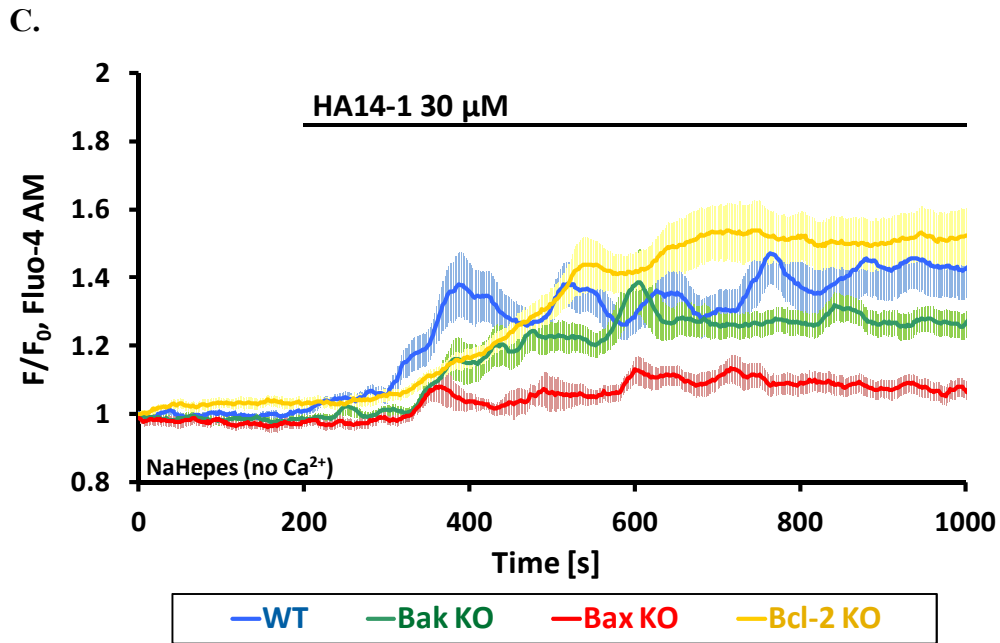


**Fig. 6.2.** (*continues*)

(C) The graph shows average calcium responses to 30  $\mu$ M HA14-1 in pancreatic acinar cells isolated from C57BL6/J wild type (n = 25) mice and animals lacking functional Bak (n = 43), Bax (n = 17) or Bcl-2 (n = 23). Error bars represent standard errors. (B) The responses to 30  $\mu$ M HA14-1 were compared as the average sums of relative fluorescence values recorded between 602 and 1000 s, which corresponds to the areas under the curves. Black error bars represent standard errors.

---

Ca<sup>2+</sup> responses in pancreatic acinar cells lacking functional Bax were dramatically lower as compared to the wild type cells (p = 0.002) and other knockouts.

The results clearly indicate that loss of Bax protein blocks Ca<sup>2+</sup> responses induced by inhibition of anti-apoptotic Bcl-2 members by BH3 mimetics.

### **6.3. BH3 mimetic-induced Ca<sup>2+</sup> release is only partially mediated by IP<sub>3</sub>Rs or RyRs**

As was described in the Introduction, IP<sub>3</sub>Rs and RyRs are the major types of channels responsible for calcium release from the ER in pancreatic acinar cells. In permeabilized pancreatic acinar cells inhibition of IP<sub>3</sub>Rs by 2-APB, or RyRs by ruthenium red was associated with a marked decrease in BH3 mimetic-induced Ca<sup>2+</sup> release from the intracellular stores. Combined inhibition of both receptors reduced responses even more, but did not block them completely (see Chapter 3). Here, experiments on freshly isolated intact pancreatic acinar cells were performed. The cells were loaded with fluo-4, and then simultaneous inhibition of IP<sub>3</sub>Rs and RyRs together with inhibition of anti-apoptotic Bcl-2 protein with BH3 mimetics was applied. It is already well established that in acinar cells 20 mM caffeine and 10 μM ruthenium red efficiently block IP<sub>3</sub>Rs and RyRs, respectively. Therefore, as predicted, perfusion of the cells with a mixture of caffeine and ruthenium red completely abolishes 10 pM CCK-induced calcium spikes (*Fig. 6.3.A*).

In the main experiment pancreatic acinar cells isolated from C57BL6/J wild type and *bax*<sup>-/-</sup> mice were loaded with fluo-4 AM and then treated with 5 μM BH3I-2' or 30 μM HA14-1 after short preincubation with 20 mM caffeine and 10 μM ruthenium

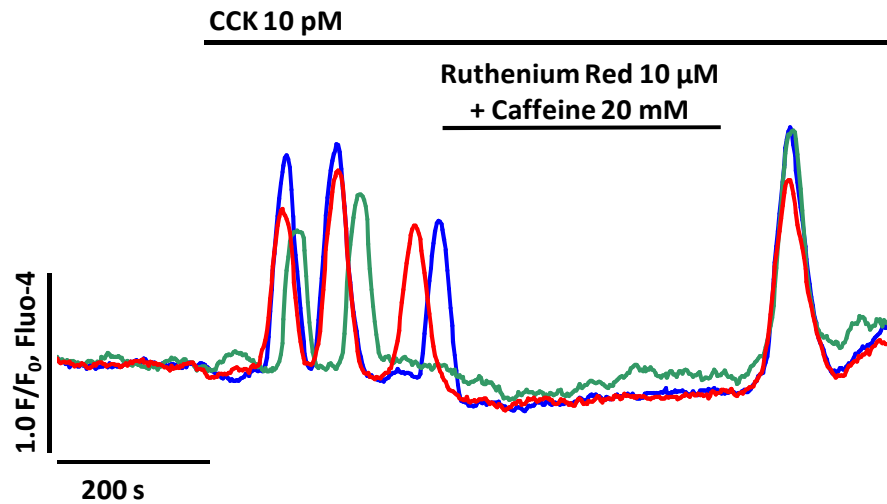
---

red. All experiments were performed in NaHEPES solution, which contained no  $\text{Ca}^{2+}$ , in order to exclude  $\text{Ca}^{2+}$  influx from the extracellular environment. The results demonstrate that even upon inhibition of both  $\text{IP}_3\text{Rs}$  and  $\text{RyRs}$  treatment with 5  $\mu\text{M}$  BH3I-2' induces cytosolic calcium plateau in wild type cells ( $n = 8$ , *Fig. 6.3.B*). As predicted, cells lacking functional Bax protein did not develop any responses to BH3I-2' in the conditions of the experiment ( $n = 8$ ). The responses were compared as the average sums of relative fluorescence values recorded between 802 and 1200 s, which corresponds to the average area under the traces (*Fig. 6.3.C*). In condition of blocked  $\text{IP}_3\text{Rs}$  and  $\text{RyRs}$  treatment with BH3I-2' caused substantial responses in wild type cells, whereas *bax*<sup>-/-</sup> cells were completely resistant to the BH3 mimetic ( $p = 0.0028$ ).

Treatment with 30  $\mu\text{M}$  HA14-1 in the presence of caffeine and ruthenium red still led to formation of cytosolic calcium plateau in wild type cells ( $n = 10$ ); however, in *bax*<sup>-/-</sup> cells ( $n = 9$ ) the responses were completely abolished (*Fig. 6.3.D*). The comparison of the average areas under the traces recorded between 802 and 1200 s demonstrates that the significant difference between responses induced by HA14-1 in wild type cells and Bax KOs remains under condition of inhibited  $\text{IP}_3\text{Rs}$  and  $\text{RyRs}$  (*Fig. 6.3.E*,  $p < 0.0001$ ).

The results presented here, together with the data from Chapter 3, indicate that BH3 mimetics, BH3I-2' and HA14-1, release calcium from the intracellular stores primary not through  $\text{IP}_3\text{Rs}$  /  $\text{RyRs}$  (*Fig. 3.6.A-G*) but through a novel mechanism, which is dependent on Bax protein.  $\text{IP}_3\text{Rs}$  and  $\text{RyRs}$  only potentiate BH3 mimetic-dependent calcium release through the phenomenon of CICR. Since Bcl-2 family proteins were suggested to be involved in the regulation of passive  $\text{Ca}^{2+}$  leak from the ER, it might

A.



B.

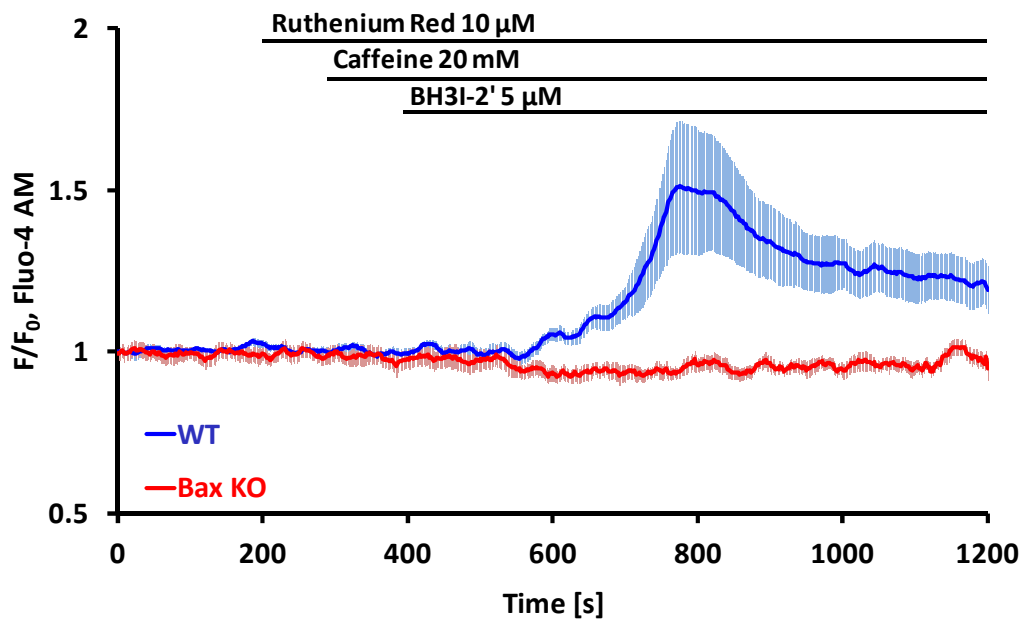
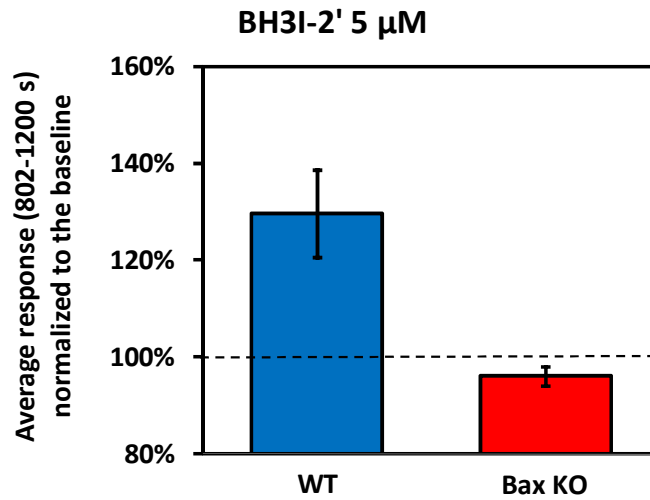


**Fig. 6.3. BH3 mimetic-induced  $Ca^{2+}$  release is mediated by  $IP_3Rs$  and  $RyRs$**

(A) Sample traces showing inhibition of 10 pM CCK-induced  $Ca^{2+}$  oscillations by application of 20 mM caffeine and 10  $\mu$ M ruthenium red. Caffeine and ruthenium red are efficient blockers of  $IP_3Rs$  and  $RyRs$ , respectively. (B) Average traces showing effects of 5  $\mu$ M BH3I-2' on  $Ca^{2+}$  homeostasis in pancreatic acinar cells isolated from wild type mice (blue trace,  $n = 8$ ) and Bax knockouts (red trace,  $n = 8$ ) under inhibition of  $IP_3Rs$  and  $RyRs$ . Error bars represent standard errors.

C.



D.

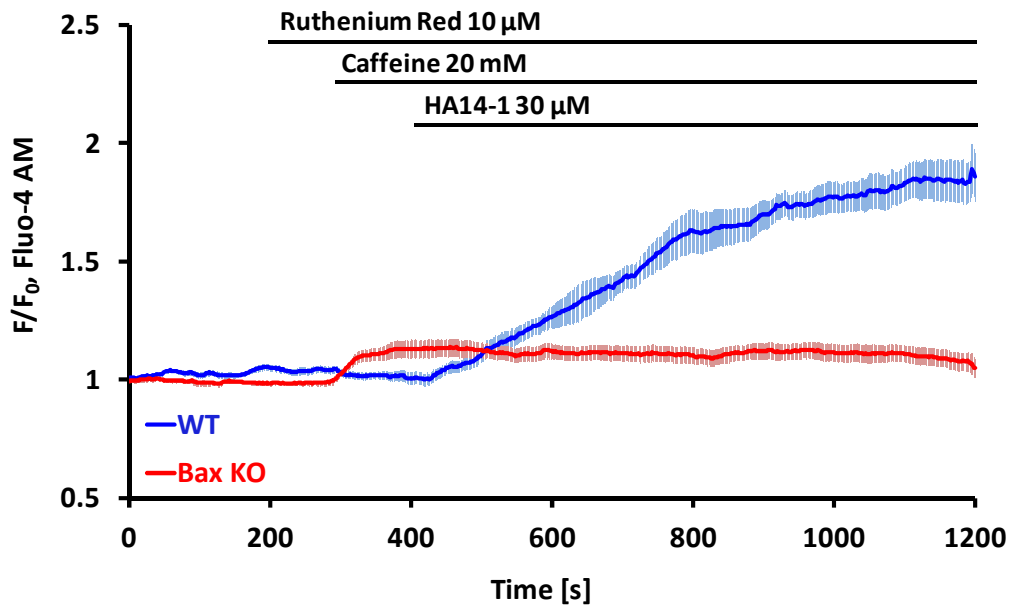


**Fig. 6.3.** (continues)

(C) The bar chart shows comparison of the average sums of relative fluorescence values recorded between 802 and 1000 ( $p = 0.0028$ ) in WT and *bax*<sup>-/-</sup> cells treated with 5  $\mu$ M BH3I-2' under inhibition of IP<sub>3</sub>R and RyR (shown in (B)). Black error bars represent standard errors of mean. (D) Average traces showing effects of 30  $\mu$ M HA14-1 on Ca<sup>2+</sup> homeostasis in pancreatic acinar cells isolated from wild type mice (blue trace,  $n = 10$ ) and Bax knockouts (red trace,  $n = 9$ ) under inhibition of IP<sub>3</sub>R and RyR. Error bars represent standard errors.

---

E.

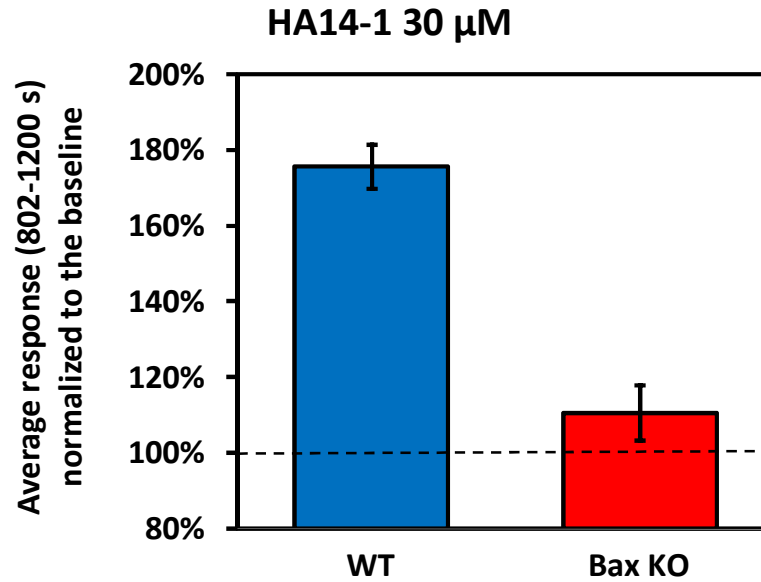


**Fig. 6.3.** (continues)

(E) The bar chart shows comparison of the average sums of relative fluorescence values recorded between 802 and 1000 ( $p < 0.0001$ ) in WT and *bax*<sup>-/-</sup> cells treated 30  $\mu$ M HA14-1 under inhibition of IP<sub>3</sub>Rs and RyRs (shown in (D)). Black error bars represent standard errors of mean.

---

be speculated that treatment with BH3 mimetics increases release of  $\text{Ca}^{2+}$  through the leak channels.

#### **6.4. Discussion**

In Chapter 3 it was demonstrated that BH3 mimetics: BH3I-2' and HA14-1 induce release of calcium from the intracellular stores, which leads to formation of sustained cytosolic calcium plateau in both pancreatic acinar cells as well as in AR42J cells.  $\text{Ca}^{2+}$  release caused by BH3 mimetic was shown not to be exclusively dependent on  $\text{IP}_3\text{Rs}$  or  $\text{RyR}$ , because inhibition of both receptors did not block cytosolic calcium plateau formation in wild type pancreatic acinar cells. This finding is particularly surprising, since it indicates that other  $\text{Ca}^{2+}$  channels have to mediate  $\text{Ca}^{2+}$  release from the intracellular stores in response to treatment with BH3I-2' and HA14-1. Therefore the aim of this chapter was to provide more insights into the mechanism of BH3 mimetic-dependent  $\text{Ca}^{2+}$  responses. Here it has been tested how loss of certain Bcl-2 family proteins, Bax, Bak and Bcl-2 itself, would affect responses to pharmacological inhibition of anti-apoptotic Bcl-2 protein members. The data presented in this chapter reveal that loss of Bax, but not Bak or Bcl-2, has a profound effect on  $\text{Ca}^{2+}$  responses to BH3 mimetic. The responses were markedly reduced and in most of the cases BH3I-2' as well as HA14-1 failed to induce any  $\text{Ca}^{2+}$  release in *bax*<sup>-/-</sup> cells. At the same time wild type cells developed substantial responses even under conditions of inhibited  $\text{IP}_3\text{Rs}$  and  $\text{RyRs}$ .

The results described here provide a very important observation that could potentially be linked to the enigmatic  $\text{Ca}^{2+}$  leak channel. It seems apparent that loss of Bax inhibits  $\text{Ca}^{2+}$  release in response to BH3 mimetic treatment. The simplest

---

explanation of this phenomenon is that Bax could form a channel, which upon inhibition of anti-apoptotic Bcl-2 members mediates slow  $\text{Ca}^{2+}$  leak from the ER, further amplified by main  $\text{Ca}^{2+}$  release channels:  $\text{IP}_3\text{Rs}$  and  $\text{RyRs}$ . This suggestion is supported by the observations that Bax has a similar structure to pore-forming bacterial toxins and thus in principle should be able to form ion channels in membranes<sup>204,280</sup>. To be able to form a channel permeable to ions, a protein needs to have amphipathic helices long enough to span lipid bilayer. Indeed Bax has seven helices. Helices  $\alpha_2$ ,  $\alpha_3$  and  $\alpha_4$  form a hydrophobic groove; helix  $\alpha_1$  is connected to  $\alpha_2$  by a long unstructured loop; and helix  $\alpha_9$  binds to the hydrophobic groove of the protein hiding both hydrophobic residues of the groove and its own residues inside the structure, which increases Bax solubility and makes it possible for the protein to be present as a monomer in the cytosol<sup>281</sup>. The two remaining helices  $\alpha_5$  and  $\alpha_6$  meet the criteria for transmembrane fragments and are considered to be a putative pore-forming domain<sup>282,283</sup>.  $\alpha_5$ - $\alpha_6$  region is positioned in the core of the protein and is characteristic not only for Bax but also for other members of Bcl-2 family such as Bcl-2 and Bcl-xL. It has been demonstrated that deletion of homological region to  $\alpha_5$ - $\alpha_6$  in Bcl-2 protein abolishes its ability to form ion conducting channels in artificial lipid bilayers<sup>277</sup>. Two  $\alpha$ -helices are obviously insufficient to create an aqueous pore; and therefore it is unlikely that a single Bax monomer could conduct ions across membranes. However, Bax could potentially form dimers or oligomers, so  $\alpha_5$ - $\alpha_6$  regions from more than one protein might efficiently contribute to the pore of Bax membrane channel<sup>282</sup>.

Somewhat in contrast to its ability to form ion pores, it was demonstrated that Bax overexpression increases resting  $\text{Ca}^{2+}$  levels in the ER<sup>204</sup>. It was shown that this

---

effect of Bax is independent on its presumed channel-forming region, as the insertion of homological  $\alpha 5$ - $\alpha 6$  fragment from other Bcl-2 members protein did not change the above mentioned effect of Bax on ER  $\text{Ca}^{2+}$  content<sup>283</sup>. Considering this finding, an alternative mechanism might be postulated, which would explain Bax-dependent BH3 mimetic-induced  $\text{Ca}^{2+}$  release from the intracellular stores. Rather than acting as a channel itself, Bax could directly or indirectly activate  $\text{Ca}^{2+}$  leak from the ER mediated by other proteins. According to that mechanism application of BH3 mimetics such as BH3I-2' or HA14-1 increases unbound and activated fraction of Bax protein, which in turn acts on a calcium channel in the ER membrane and potentiates calcium release from the ER (*Fig. 6.4*). Importantly, Bcl-2 inhibition is absolutely crucial to reveal Bax-dependent  $\text{Ca}^{2+}$  leak. This indicates that under normal conditions anti-apoptotic Bcl-2 members suppress Bax functions related to the leak, most likely via sequestration of Bax by Bcl-2 / Bcl-xL.

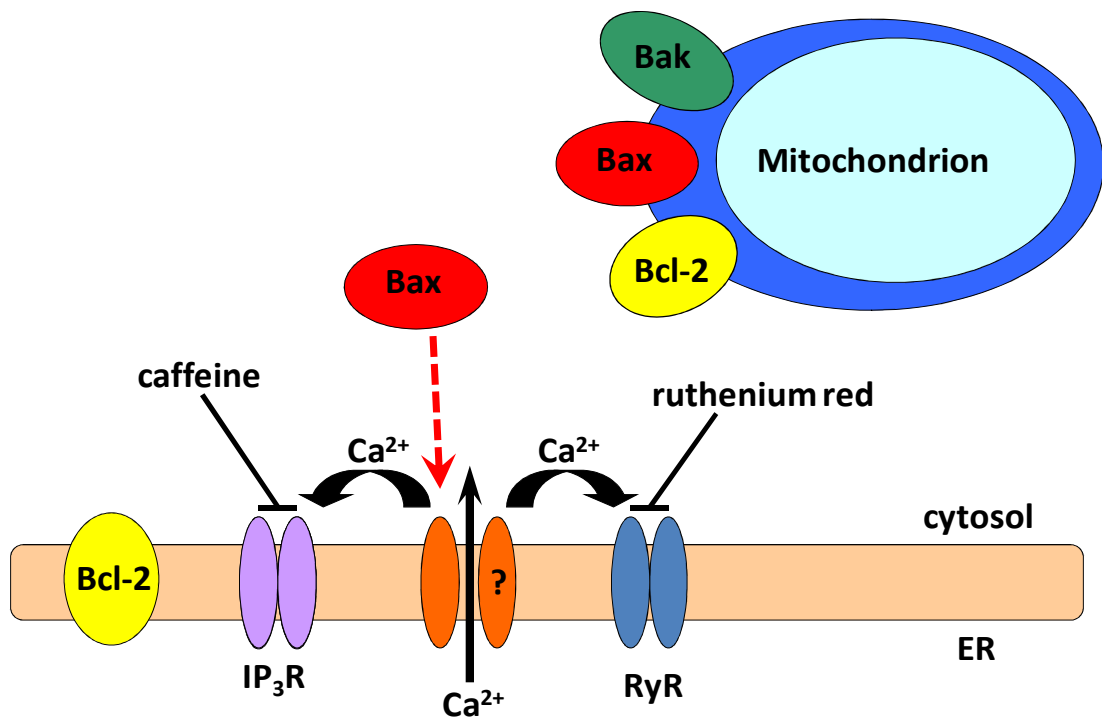


**Fig. 6.4. Schematic illustration of possible interactions between Bcl-2 family members and calcium channels / pumps**

Bax, which is activated by treatment with BH3 mimetics, either forms a channel in the ER membrane or acts on a channel formed by another protein. As a result calcium release is induced and subsequently amplified by RyRs and IP<sub>3</sub>Rs. Inhibition of IP<sub>3</sub>Rs and RyRs by caffeine and ruthenium red eliminates CICR-type of response; however calcium leak persists.

---

**CHAPTER 7:**  
**THE ROLE OF BCL-2 PROTEIN IN REGULATION**  
**OF CALCIUM FLUXES ACROSS THE PLASMA MEMBRANE**

---

## **Chapter 7: The role of Bcl-2 protein in regulation of calcium fluxes across the plasma membrane**

### **7.1. Overview of calcium extrusion mechanisms through the plasma membrane**

As described in the introduction, movement of  $\text{Ca}^{2+}$  ions across the plasma membrane is strictly regulated and crucial for maintenance of cell functions. In all eukaryotic cells calcium extrusion from the cytosol to the extracellular space is mainly facilitated by the PMCA, which is a P-type plasma membrane  $\text{Ca}^{2+}$  pump.  $\text{Na}^+/\text{Ca}^{2+}$  exchanger is an alternative  $\text{Ca}^{2+}$  extrusion pathway, which is especially important in excitable cells, where it exports calcium even more efficiently than the PMCA.

$\text{Na}^+/\text{Ca}^{2+}$  exchangers are membrane transporters that utilize  $\text{Na}^+/\text{K}^+$  gradient across the plasma membrane to export cytosolic  $\text{Ca}^{2+}$ . They can be divided into two main types depending on stoichiometry and nature of exported cations. The transporter commonly present in neurons and cardiac cells facilitates exchange of three  $\text{Na}^+$  for one  $\text{Ca}^{2+}$  and is referred as  $\text{NCX}^{284}$ . The other type was originally discovered in retinal rods and cones and is named  $\text{NCKX}$ , since it exchanges four  $\text{Na}^+$  ions from the extracellular space for one  $\text{Ca}^{2+}$  and  $\text{K}^+$  from cytosol<sup>285</sup>.

The  $\text{NCX}$  transporter has three known isoforms encoded by different genes ( $\text{NCX1}$ ,  $\text{NCX2}$  and  $\text{NCX3}$ )<sup>286,287</sup>; however, they exhibit only minor differences in their

---

biochemical properties. They all have nine transmembrane domains and cytosolic  $\text{Ca}^{2+}$ -binding domain located in the middle of the polypeptide. NCX is mainly present in heart and neurons, where it is engaged in regulation of intracellular  $\text{Ca}^{2+}$  homeostasis. It also prevents pathological  $\text{Ca}^{2+}$  overload, and thus protects against cell death. The NCKX transporter can be found in retinal photoreceptors. Interestingly, NCX and NCKX are characterised by different affinity for  $\text{Ca}^{2+}$ . NCKX has high affinity and thus controls  $\text{Ca}^{2+}$  levels at nanomolar range. On the other hand, NCX transports large amounts of  $\text{Ca}^{2+}$  out of the cell but with low affinity, which means it efficiently reduces cytosolic  $\text{Ca}^{2+}$  overload leaving the fine tuning of intracellular  $\text{Ca}^{2+}$  to the PMCA<sup>288</sup>.

The PMCA is closely related to the SERCA, which is present in the ER membranes and functions as the  $\text{Ca}^{2+}$  store replenishment mechanism. Both  $\text{Ca}^{2+}$  pumps have similar topology - they are single polypeptides with ten transmembrane domains and four main cytosolic domains that catalyse phosphorylation of a conserved aspartate residue in the core of the pump. This phosphorylation forms a high-energy aspartyl-phosphoranhidride intermediate required for the conversion between two different conformations described as E1 and E2. In E1 state the pumps have high affinity to  $\text{Ca}^{2+}$  ions at the cytosolic site, whereas conformational change in E2 promotes opening of the pumps on the luminal / extracellular site and release of bound  $\text{Ca}^{2+}$ . In contrast to the SERCA, which transports two  $\text{Ca}^{2+}$  ions per one hydrolyzed ATP molecule, the PMCA transports only one  $\text{Ca}^{2+}$  ion per cycle<sup>289</sup>. This is because the PMCA has only one  $\text{Ca}^{2+}$ -binding site instead of two<sup>290</sup>. However, the PMCA has been reported to be more efficient than the SERCA in decreasing cytosolic  $[\text{Ca}^{2+}]$ <sup>291</sup>.

---

Just like all the other P-type pumps, the PMCA can be inhibited by orthovanadate and by lanthanum.

In mammalian cells four PMCA isoforms can be found, each of which is encoded by a separate gene and has a specific expression pattern. PMCA1 and PMCA4 are more ubiquitously expressed, whereas PMCA2 and PMCA3 are characteristic for neurons. Another level of complexity is introduced by alternative PMCA mRNA splicing, which generates additional pump variants. There are two main splicing sites: in the first intracellular loop (referred as site A) and in the C-terminus of the pump (site C). Splicing at site A most likely influences the membrane targeting of the PMCA<sup>292</sup>; whereas C splicing variants might exhibit different sensitivity to calmodulin regulation and could specifically interact with additional regulatory proteins<sup>293,294</sup>.

Under normal physiological conditions the PMCA has very low affinity for Ca<sup>2+</sup> ( $K_d > 10 \mu\text{M}$ ); and therefore it is effectively inactive. Interestingly, the C-terminal region of the pump contains a calmodulin-binding domain (CaM-BD), which has an autoinhibitory functions. The CaM-BD domain simultaneously interacts with two different sites in the main body of the pump: one is located on the second intracellular domain, and the other - on the third domain<sup>295</sup>. The binding of calmodulin to the CaM-BD disrupts that interaction and abolishes autoinhibition leading to the decrease of the  $K_d$  to 0.4 - 0.5  $\mu\text{M}$ <sup>296</sup>. Interestingly, certain isoforms of the PMCA have higher affinity for calmodulin than the others; for example PMCA2 binds this regulatory protein 5 - 10 times stronger than PMCA4<sup>297</sup>. Calmodulin appears to be the main activator of the PMCA. Other mechanisms of activation include for instance phosphorylation at serine, threonine and tyrosine residues. The main kinases involved in that process are protein kinase A (PKA), protein kinase C

---

(PKC) and the focal adhesion kinase (FAK)<sup>298-300</sup>. Phosphorylation on its own (in the absence of calmodulin) can decrease the  $K_d$  to values around 1  $\mu$ M. What is more, modification of a Thr residue in the CaM-BD of the pump by PKC efficiently prevents autoinhibition. Another interesting mechanism that modulates PMCA activity is based on oligomerization of the pump via the CaM-BDs. It abolishes autoinhibition and makes the PMCA insensitive to calmodulin. Such process, however, requires relatively high concentration of the pump in the membrane and thus is believed to occur only in the caveolae<sup>301</sup>. Finally, phospholipids present in the surrounding plasma membrane can influence PMCA activity. Acidic phospholipids and polyunsaturated fatty acids interact with two sites of the pump: one is located on the CaM-BD, and the other lies within the first cytosolic domain<sup>302</sup>. That leads to decrease of the  $K_d$  to values close to physiological  $Ca^{2+}$  concentration (about 100 nM).

In this chapter it is postulated that Bcl-2 family proteins could potentially be novel regulators of calcium extrusion across the plasma membrane. This notion is based on (1) the fact that Bcl-2 family proteins play crucial roles in the intracellular calcium homeostasis by regulating  $Ca^{2+}$  fluxes across the ER membrane; and therefore they could be expected to influence calcium fluxes across the plasma membrane as well; (2) and preliminary data depicted in *Fig. 7.1* demonstrating that pancreatic acinar cells lacking functional Bcl-2 protein exhibit increased cytosolic  $Ca^{2+}$  extrusion across the plasma membrane in comparison to control cells.

Pancreatic acinar cells for the above mentioned experiment were isolated from pancreas of wild type and *bcl-2*<sup>-/-</sup> mice on C57BL6/J x 129S background. The cells were subsequently loaded with AM form of calcium sensitive dye fluo-4, as

---

described in Material and Methods. Combined treatment with 10  $\mu$ M ACh and 10  $\mu$ M thapsigargin was applied in order to quickly empty the intracellular stores and inhibit SERCA-dependent  $\text{Ca}^{2+}$  clearance. Under these conditions  $\text{Ca}^{2+}$  can only be removed from the cytosol through extrusion mechanism of the plasma membrane. High dose of ACh makes calcium release mainly dependent on  $\text{IP}_3\text{Rs}$  and potentiated by CICR process. Importantly, since fluo-4 measurements are non-ratiometric, obtained fluorescence values were normalized to the initial values, which fixed the baselines at  $F/F_0 = 1$ . Therefore this approach allows for comparison of amplitudes and rates of increase / decrease of calcium responses. However, comparison of baseline cytosolic  $\text{Ca}^{2+}$  concentration is impossible due to the nature of the fluorescent dye and normalization of the obtained traces. Nevertheless, the results in *Fig. 7.1.A*, which represent average responses of pancreatic acinar cells from wild type mice (blue trace,  $n = 11$ ) and from Bcl-2 knockout mice (red trace,  $n = 23$ ) clearly show that the latter extrude cytosolic  $\text{Ca}^{2+}$  much quicker than the wild type cells. *Fig. 7.1.B* compares  $\text{Ca}^{2+}$  responses in a form of a bar chart. Areas between 200 s and 400 s under the traces from *Fig. 7.1.A* were calculated. Baseline values correspond to 100 % and any increase above it represents the actual calcium response. Since  $\text{Ca}^{2+}$  remains elevated for longer in wild type cells, their cytosolic calcium responses to combined treatment with Tg and ACh appear significantly larger than the responses in *bcl-2<sup>-/-</sup>* pancreatic acinar cells ( $p = 0.002$ ). Elevated  $\text{Ca}^{2+}$  returned to the baseline levels after about 300 s in wild type cells and after 150 s in *bcl-2<sup>-/-</sup>* cells. This chapter aims to describe the detailed investigation of that interesting phenomenon.

A.

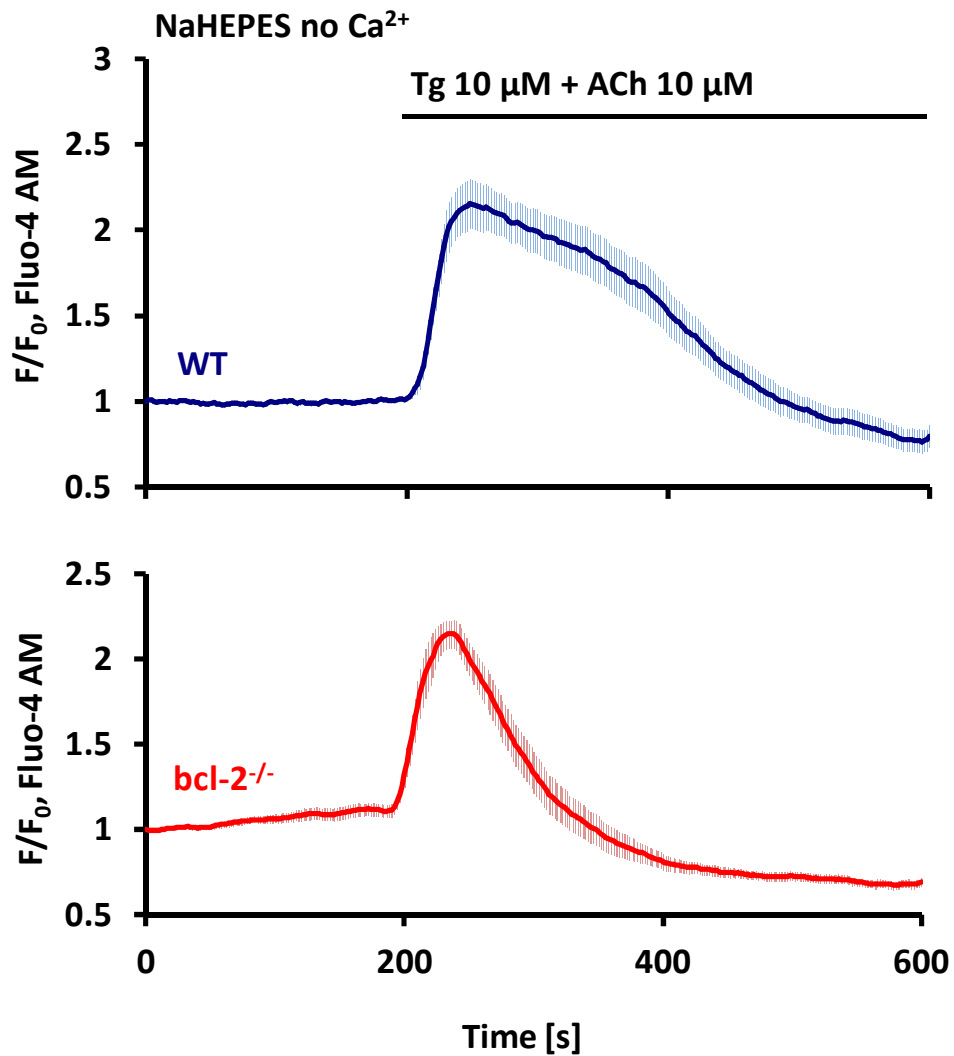


**Fig. 7.1. Loss of Bcl-2 affects Tg-induced Ca<sup>2+</sup> responses**

(A) Average traces (with standard errors) showing cytosolic calcium responses to a mixture 10 μM ACh and 10 μM thapsigargin in pancreatic acinar cells isolated from wild type (blue trace, n = 11) and *bcl-2*<sup>-/-</sup> (red trace, n = 23) mice and loaded with a calcium sensitive dye fluo-4.

---

**B.**

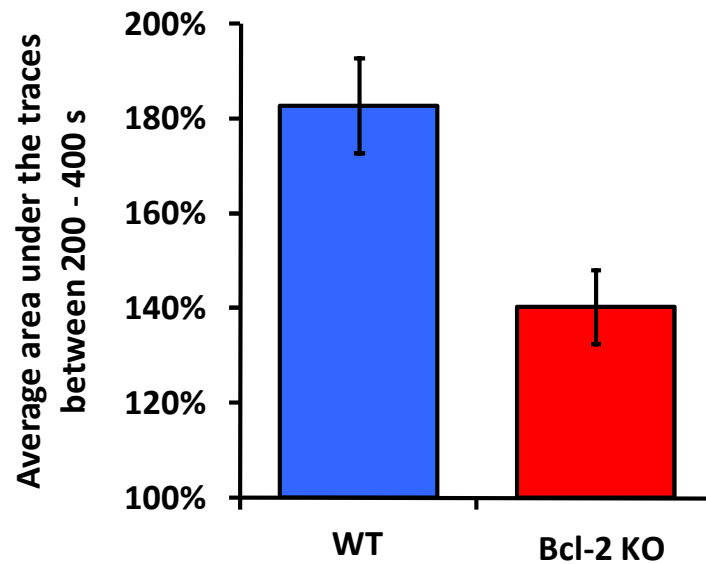


**Fig. 7.1.** (continues)

**(B)** The responses from (A) are shown as average sums of fluo-4 fluorescence values obtained in the experiment between 200 and 400 s and normalized to the baseline (100%), which reflects the difference in areas under the traces from (A) ( $p = 0.002$ ).

---

## 7.2. Loss of Bcl-2 affects calcium release from the intracellular stores and calcium extrusion from the cytosol

In order to perform more detailed investigation of the interesting phenomenon indicated by the preliminary data, calcium sensitive dye fura-2 was applied instead of fluo-4 for fluorescent  $\text{Ca}^{2+}$  measurements in freshly isolated pancreatic acinar cells. In contrast to fluo-4, fura-2 is used for ratiometric measurement of cytosolic calcium changes, which enables more reliable comparison of baseline values. What is more, together with specific calibration techniques and mathematical calculation (see Material and Methods for reference) fura-2 is a dye of choice for estimation of free calcium concentrations within the cells.

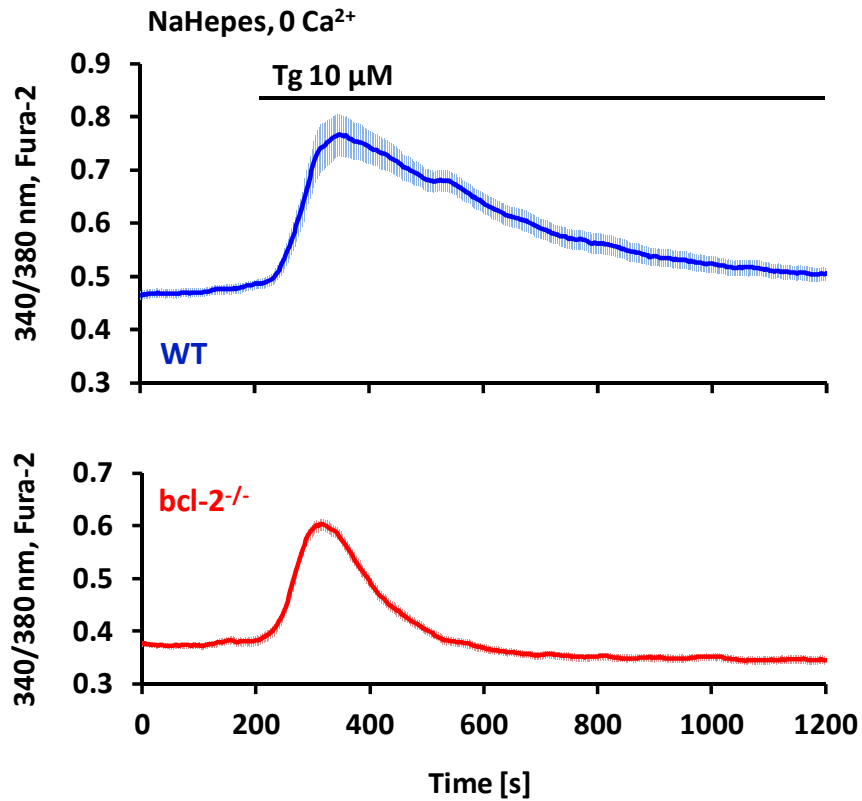
In the first experiment fura-2-loaded pancreatic acinar cells were treated with 10  $\mu\text{M}$  Tg in order to inhibit the SERCA, empty the ER and induce cytosolic calcium increase due to passive  $\text{Ca}^{2+}$  leak. Average responses with standard errors are depicted in *Fig. 7.2.A*, where blue trace represents responses of wild type pancreatic acinar cells ( $n = 35$ ) and red trace refers to cells isolated from Bcl-2 knockout mice ( $n = 27$ ). The data immediately bring to attention three important observations. First of all, similarly to the preliminary results, cytosolic  $\text{Ca}^{2+}$  extrusion in *bcl-2<sup>-/-</sup>* pancreatic acinar cells is more efficient than in wild type cells. Secondly, baseline cytosolic  $\text{Ca}^{2+}$  values appear to be decreased in *bcl-2<sup>-/-</sup>* pancreatic acinar cells as compared to the wild type cells, which is indicated by average initial 340/380 ratio values. And finally, the average amplitude of the Tg-elicited responses in *bcl-2<sup>-/-</sup>* cells is slightly lower than the amplitude of the same responses in wild type cells. Since the ER stores are empty and the SERCA is inhibited, potentiated cytosolic

---

$\text{Ca}^{2+}$  extrusion and decreased resting  $\text{Ca}^{2+}$  levels in  $bcl-2^{-/-}$  cells suggest increased  $\text{Ca}^{2+}$  efflux across the plasma membrane. On the other hand, decreased amplitude of the responses to Tg might indicate substantial changes of ER calcium content of  $bcl-2^{-/-}$  pancreatic acinar cells.

In order to provide a rough comparison of the rates of cytosolic calcium clearance in wild type and  $bcl-2^{-/-}$  cells, decrease of 340/380 nm-induced fluorescence ratio per unit of time was calculated. These values are referred in text as  $-d(\text{Ratio})/dt$  and were obtained from  $\text{Ca}^{2+}$  extrusion phases of the average wild type and  $bcl-2^{-/-}$  traces shown in *Fig. 7.2.A*.  $-d(\text{Ratio})/dt$  values were then plotted against corresponding temporal cytosolic fluorescence ratio values recorded in pancreatic acinar cells. The results are presented as a graph in *Fig. 7.2.B*, where blue and red points represent values obtained from wild type trace and  $bcl-2^{-/-}$  trace from *Fig. 7.2.A*, respectively. Linear fits were calculated using linear regression least square method. The difference between the series is reflected in the equations of the linear fits:  $y = ax + b$ . Wild type linear equation is  $y = 0.0019x - 0.0008$  and  $bcl-2^{-/-}$  is  $y = 0.0081x - 0.0027$ . Comparing coefficients  $a$  allows for assessment of the rates of cytosolic  $\text{Ca}^{2+}$  extrusion in pancreatic cells isolated from wild type and  $bcl-2^{-/-}$  mice. Clearly  $a_{bcl2^{-/-}} > a_{WT}$ , therefore for the same ratio values the rate of ratio decrease is higher in  $bcl-2^{-/-}$  cells than in wild type cells. And since the changes of ratio reflect the changes of cytosolic  $\text{Ca}^{2+}$ ,  $bcl-2^{-/-}$  cells clear intracellular  $\text{Ca}^{2+}$  faster than wild type cells.

A.



B.

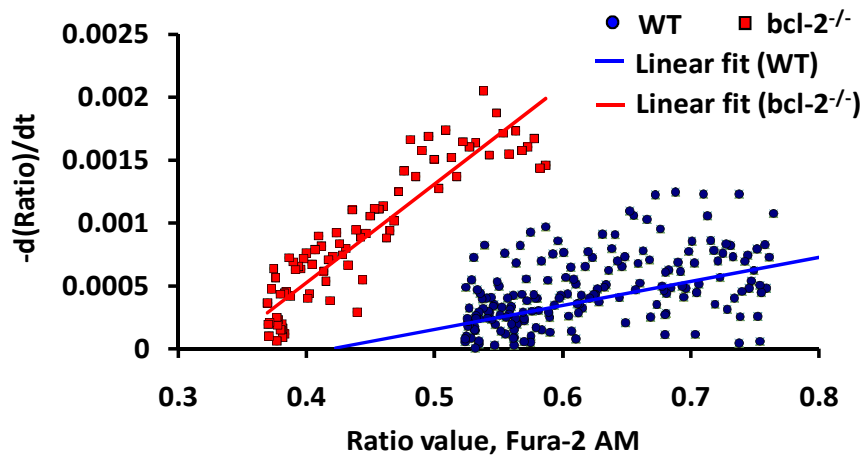


**Fig. 7.2. Loss of Bcl-2 increases Ca<sup>2+</sup> clearance from the cytosol**

(A) Average cytosolic Ca<sup>2+</sup> responses (with standard errors) to 10 μM thapsigargin in pancreatic acinar cells isolated from wild type (blue trace, n = 35) and *bcl-2*<sup>-/-</sup> (red traces, n = 27) mice and loaded with fura-2. (B) The dependence of rate of fura-2 ratio decrease on the temporal ratio values in wild type (shown in blue) and *bcl-2*<sup>-/-</sup> (shown in red) pancreatic acinar cells, which directly corresponds to calcium clearance from the cytosol. -d(Ratio)/dt values were calculated from the average traces depicted in (A).

---

### 7.3. Bcl-2 regulates calcium extrusion across the plasma membrane in pancreatic acinar cells.

In order to fully understand the difference in handling of cytosolic  $\text{Ca}^{2+}$  elevation between *bcl-2*<sup>-/-</sup> and wild type pancreatic acinar cells, detailed analysis of calcium fluxes in acinar cells was required. That analysis should be based on multiple experiments, high n number, and application of mathematical methods in order to accurately trace  $\text{Ca}^{2+}$  changes in the cytosol of the cells. Just like in the previous experiment, *bcl-2*<sup>-/-</sup> and wild type pancreatic acinar cells were loaded with fura-2 dye in order to perform ratiometric calcium measurements. At the beginning of each experiment the cells were perfused with 2  $\mu\text{M}$  Tg in the absence of extracellular  $\text{Ca}^{2+}$  to inhibit the SERCA and empty the ER stores. Once cytosolic  $\text{Ca}^{2+}$  returned to the basal levels, the extracellular solution (NaHEPES) was rapidly changed from nominal 0  $\text{Ca}^{2+}$  to 1 mM, 5 mM or 10 mM  $\text{Ca}^{2+}$ . That induced immediate  $\text{Ca}^{2+}$  influx to the cytosol. After the stable cytosolic  $\text{Ca}^{2+}$  plateau was reached, extracellular  $\text{Ca}^{2+}$  was again removed, causing  $\text{Ca}^{2+}$  efflux from the cytosol via plasma membrane extrusion mechanisms. As a result cytosolic calcium concentration returned to the baseline values. Examples of the traces recorded in this experiment for both wild type and *bcl-2*<sup>-/-</sup> acinar cells are shown in *Fig. 7.3.A* ( $n_{\text{WT}} = 45$ ,  $n_{\text{bcl2-/-}} = 109$ ). In order to assess differences in calcium fluxes between wild type and *bcl-2*<sup>-/-</sup> cells, the recovery phase of the high calcium transient from every trace was fitted with exponential decay function using Origin Pro 8 and the non-linear least-squares method:

$$y = y_0 + A \times \exp[-(x - x_0) / \tau]$$

---

Symbols:

$x_0$  – time at the peak

$y_0$  – resting calcium concentration

$\tau$  – the decay time constant

A – the amplitude associated to each exponential component

Further, the derivatives  $-d[Ca^{2+}]/dt$  were calculated from the fits and then plotted as functions of  $[Ca^{2+}]$  values obtained from the exponential fits. Initial  $-d[Ca^{2+}]/dt$  values obtained for the highest cytosolic  $[Ca^{2+}]$  from each trace were collected and plotted together on a separate graph as single points. Each point referred to a different cell. Then linear regression fits were found, one for wild type and the other for *bcl-2<sup>-/-</sup>* cells (*Fig. 7.3.B*). The results clearly demonstrate that calcium elevations in the cytosol induce much quicker calcium extrusion in *bcl-2<sup>-/-</sup>* cells as compared to wild type cells.

Above presented results indicate that Bcl-2 protein plays a role in regulation of calcium extrusion in pancreatic acinar cells. It could also be suspected that Bcl-2 simultaneously controls calcium influx to the cytosol from the extracellular space in the process of store-operated  $Ca^{2+}$  entry; however this notion requires further investigation. In this experimental setup upon inhibition of the SERCA and with nominal 0  $Ca^{2+}$  in the extracellular solution, influx component was removed and all changes in cytosolic  $Ca^{2+}$  were solely dependent on extrusion mechanism across the plasma membrane. Therefore it can be concluded that Bcl-2 protein is involved in regulation of calcium extrusion across the plasma membrane of pancreatic acinar cells.

A.

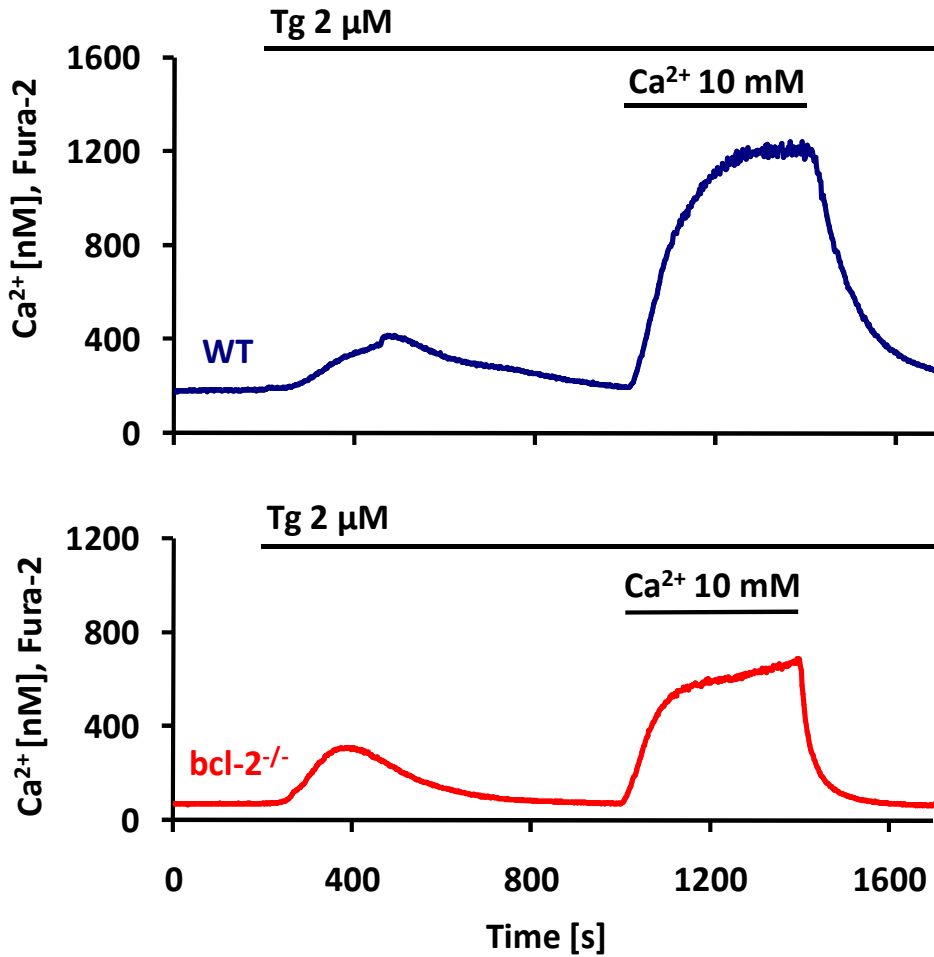


**Fig. 7.3. Bcl-2 regulates  $Ca^{2+}$  extrusion across the plasma membrane**

(A) Example traces showing cytosolic calcium extrusion after removal of high  $Ca^{2+}$  from the external solution. The ER store was initially depleted with 2  $\mu$ M thapsigargin in the absence of external  $Ca^{2+}$  and then cells were exposed for 400 s to 10 mM  $CaCl_2$ , which caused an increase in cytosolic  $Ca^{2+}$ . Cytosolic  $Ca^{2+}$  returned towards basal values after removal of extracellular  $Ca^{2+}$ . Responses of wild type cells are shown in blue and *bcl-2*<sup>-/-</sup> in red.

B.

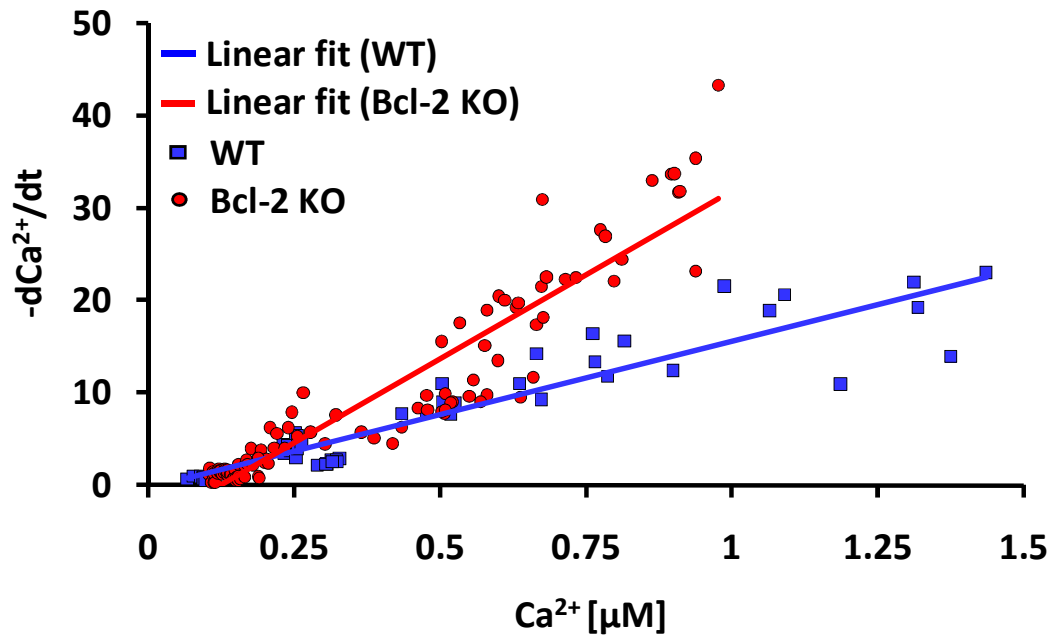


**Fig. 7.3.** (*continues*)

(B) The dependence of initial rate of cytosolic calcium extrusion (calcium decrease in time) on the cytosolic Ca<sup>2+</sup> plateau levels in wild type (blue, n = 34) and *bcl-2*<sup>-/-</sup> (red, n = 109) pancreatic acinar cells. High cytosolic Ca<sup>2+</sup> is cleared faster in pancreatic acinar cells lacking Bcl-2 as compared to wild type cells.

---

#### **7.4. Cytosolic calcium extrusion in pancreatic acinar cells is mainly dependent on the plasma membrane calcium-activated ATPase**

The role of Bcl-2 protein in regulation of cytosolic  $\text{Ca}^{2+}$  has been clearly demonstrated. However, the exact mechanism is yet to be determined. In general, cytosolic  $\text{Ca}^{2+}$  can be extruded across the plasma membrane by two proteins: the plasma membrane calcium-activated ATPase (PMCA) and the sodium-calcium exchanger (NCX)<sup>288</sup>. Therefore it is crucial to understand, (1) what the input of each of these mechanisms is in the overall cytosolic  $\text{Ca}^{2+}$  clearance in pancreatic acinar cells; (2) and which of those mechanisms is influenced by Bcl-2. In the literature it has already been stated that in  $\text{Ca}^{2+}$  transport in acinar cells  $\text{Na}^+/\text{Ca}^{2+}$  exchange plays only a minor role, if any at all<sup>303</sup>. In this case calcium export across the plasma membrane should be mainly facilitated by the PMCA; and therefore the PMCA should also be the target for the Bcl-2-dependent regulation. However, this notion requires experimental confirmation, which is the main task of this chapter.

In order to assess the input of  $\text{Na}^+/\text{Ca}^{2+}$  exchange in the overall  $\text{Ca}^{2+}$  extrusion in pancreatic acinar cells two different experiments were designed. The first experiment aimed to inhibit the NCX without affecting PMCA functions. Unfortunately, up to now there is no specific inhibitor available, which would selectively target the NCX. Some compounds have been synthesised such as SEA400 and KB-R7943; however they are not suitable for complete blockage of all isoforms of the NCX<sup>288</sup>. Since the NCX functions are dependent on the presence of extracellular  $\text{Na}^+$ , indirect inhibition of the exchanger could be achieved by complete substitution of  $\text{Na}^+$  with  $\text{NMDG}^+$

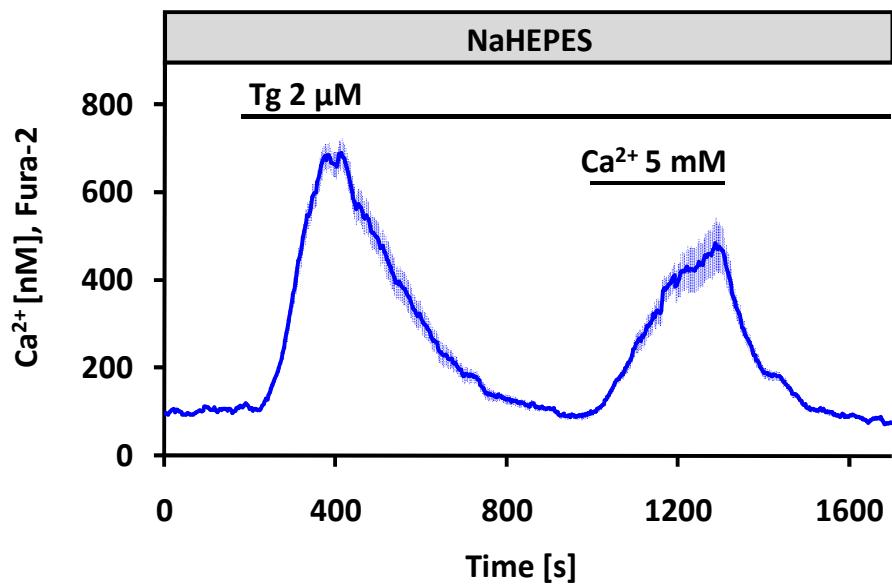
---

(N-methyl D-glucamine) in the extracellular solution. In fact, this approach was frequently used in the past<sup>304,305</sup>.

Freshly isolated pancreatic acinar cells were loaded with calcium sensitive dye fura-2. Similarly to the previous experiments, the cells were initially perfused with NaHEPES solution containing no  $\text{Ca}^{2+}$ ; and that was followed by treatment with 2  $\mu\text{M}$  Tg in order to block the SERCA and empty the ER. After Tg-induced cytosolic  $\text{Ca}^{2+}$  elevation returned to the resting levels, extracellular NaHEPES solution was replaced by NMDG-HEPES with no  $\text{Ca}^{2+}$ . Then, the cells were exposed to 5 mM  $\text{Ca}^{2+}$ , which induced rapid influx of  $\text{Ca}^{2+}$  to the cytosol. Abrupt removal of extracellular  $\text{Ca}^{2+}$  resulted in cytosolic  $\text{Ca}^{2+}$  clearance. *Fig. 7.4.A* shows the average control trace ( $n = 18$ ) and *Fig. 7.4.B* depicts the average trace under conditions of  $\text{Na}^+$  substitution with  $\text{NMDG}^+$  ( $n = 24$ ). In both cases removal of 5 mM  $\text{CaCl}_2$  from the extracellular solution results in comparable average rates of cytosolic calcium extrusion (shown in *Fig. 7.4.C*).

The second experiment aimed to specifically inhibit the PMCA without affecting NCX functions. As it was mentioned in Chapter 7.1, P-type pumps can be efficiently inhibited by orthovanadate and by lanthanum. However, this inhibition targets many proteins, not just the PMCA. Recently a novel class of selective PMCA inhibitors has been developed. They are called caloxins, and are peptide-based inhibitors selective for different PMCA isoforms<sup>306</sup>. Unfortunately, they are characterised by relatively low affinity for the pump and thus their application in this study would be limited. Therefore  $\text{La}^{3+}$  appears to be a much better choice, although it targets other P-type pumps in the cells.

A.



B.

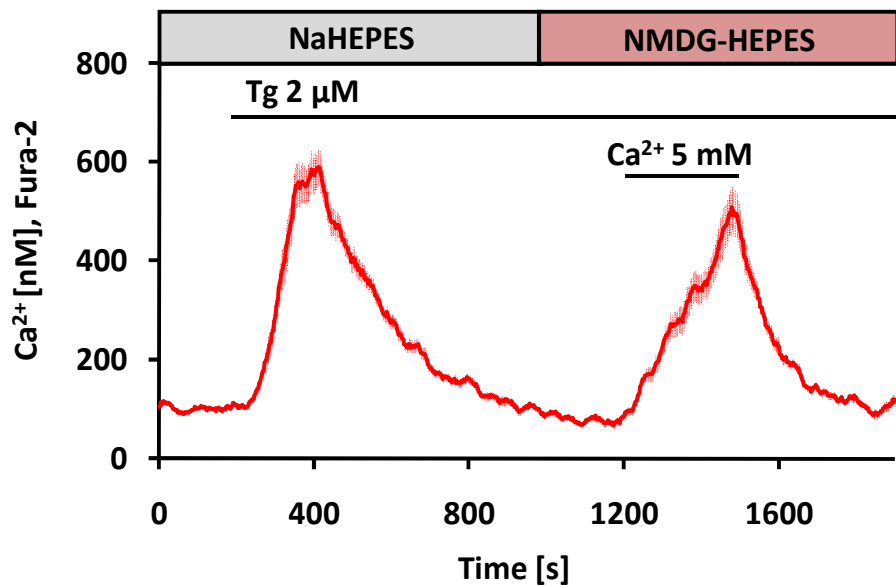
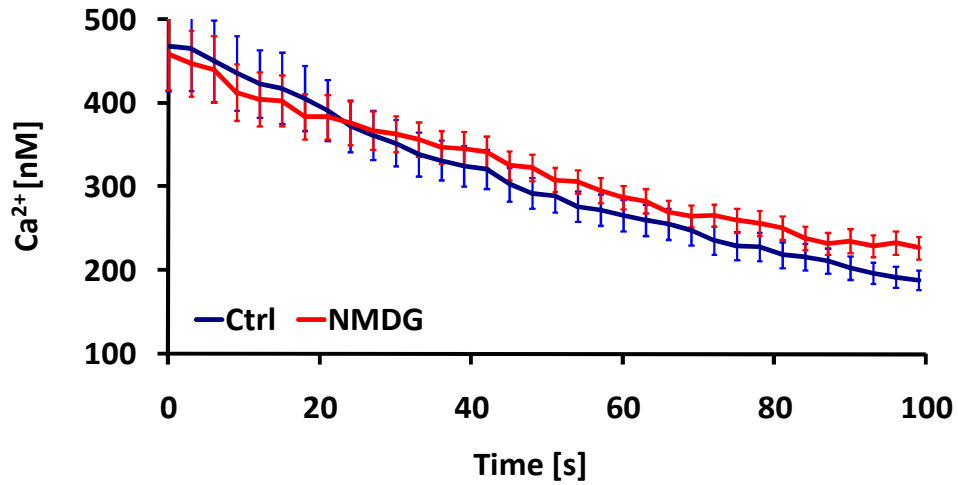


**Fig. 7.4. Involvement of the PMCA and the NCX in  $\text{Ca}^{2+}$  extrusion in pancreatic acinar cells**

(A) Average trace showing cytosolic calcium extrusion in pancreatic acinar cells after removal of high extracellular  $\text{Ca}^{2+}$  in the presence of external  $\text{Na}^+$  ( $n = 18$ ; bars are standard errors). Initially the ER store was depleted with 2  $\mu\text{M}$  thapsigargin in the absence of external  $\text{Ca}^{2+}$ . (B) Average trace recorded in pancreatic acinar cells using similar protocol as in (A); however here extracellular  $\text{Na}^+$  was substituted by NMDG $^+$  200 s before application of 5 mM  $\text{Ca}^{2+}$  in order to inhibit the NCX ( $n = 24$ ; bars are standard errors).

C.



D.

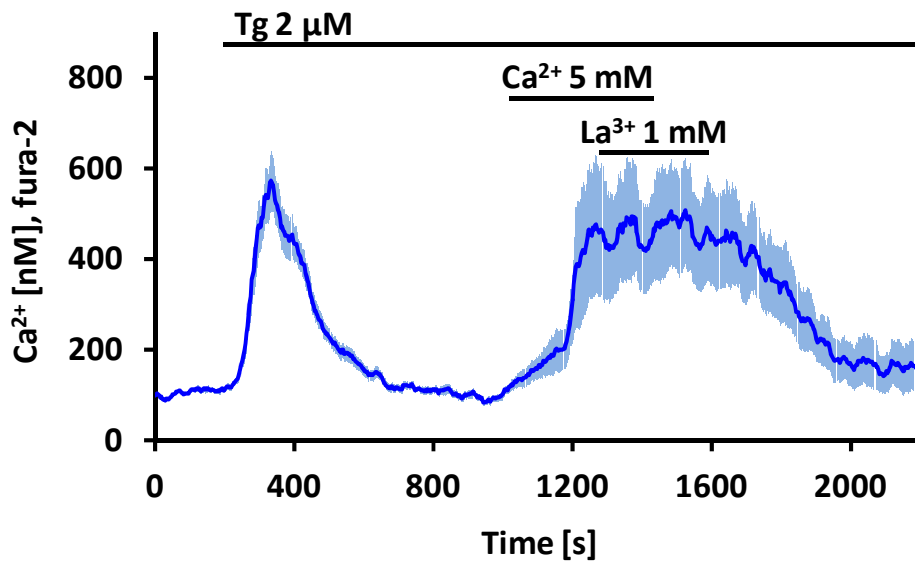


**Fig. 7.4.** (continues)

(C) The comparison of calcium extrusion phases from traces depicted on (A) and (B). Cytosolic calcium extrusion across the plasma membrane in pancreatic acinar cells is independent on the presence of  $\text{Na}^+$  in the extracellular solution. Therefore  $\text{Na}^+/\text{Ca}^{2+}$  exchange does not play a major role in  $\text{Ca}^{2+}$  export. (D) Average trace showing inhibition of cytosolic calcium extrusion in pancreatic acinar cells upon treatment with 1 mM  $\text{La}^{3+}$ , which is a blocker of the PMCA. ( $n = 12$ ; bars represent standard errors). Similarly to (A) and (B) the ER was emptied by thapsigargin and the cells were exposed to 5 mM  $\text{Ca}^{2+}$ . 1 mM  $\text{La}^{3+}$  was applied on top of cytosolic  $\text{Ca}^{2+}$  plateau.

---

For the purpose of the experiment, the cells were loaded with fura-2 dye and the ER was depleted by application of 2  $\mu\text{M}$  Tg in NaHEPES solution with no  $\text{Ca}^{2+}$ . When Tg-elicited  $\text{Ca}^{2+}$  elevation was completely cleared, 5 mM  $\text{CaCl}_2$  was used to induce high cytosolic calcium plateau. Then 1 mM  $\text{LaCl}_3$  was applied. In such high concentration lanthanum is a very potent blocker of the PMCA. Indeed its presence effectively inhibited all cytosolic calcium extrusion after removal of 5 mM  $\text{CaCl}_2$  (*Fig. 7.4.D*). Removal of lanthanum by perfusion with fresh NaHEPES solution led to recovery of  $\text{Ca}^{2+}$  extrusion and caused the return of cytosolic  $\text{Ca}^{2+}$  to the resting levels.

Both above described approaches, PMCA inhibition and  $\text{Na}^+$  substitution for  $\text{NMDG}^+$ , independently confirm that  $\text{Na}^+/\text{Ca}^{2+}$  exchange plays very little role in cytosolic  $\text{Ca}^{2+}$  extrusion in pancreatic acinar cells. Therefore effects of Bcl-2 on calcium extrusion are associated with PMCA functions.

### **7.5. Bcl-2 regulates calcium extrusion independently on its roles in mitochondria**

Bcl-2 localizes both to mitochondria and to the ER, and is widely recognized for its anti-apoptotic functions associated with mitochondria. Further, mitochondria are engaged in regulation of many cell processes; they generate most of intracellular ATP; they are involved in cell death, growth and differentiation; what is more, they are known to efficiently buffer cytosolic calcium<sup>307</sup>. Loss of Bcl-2 protein might potentially affect mitochondrial functions; therefore it is possible that observed differences in calcium extrusion between wild type pancreatic cells and *bcl-2*<sup>-/-</sup> cells are in fact a result of changes in conditions of mitochondria or ATP metabolism. In

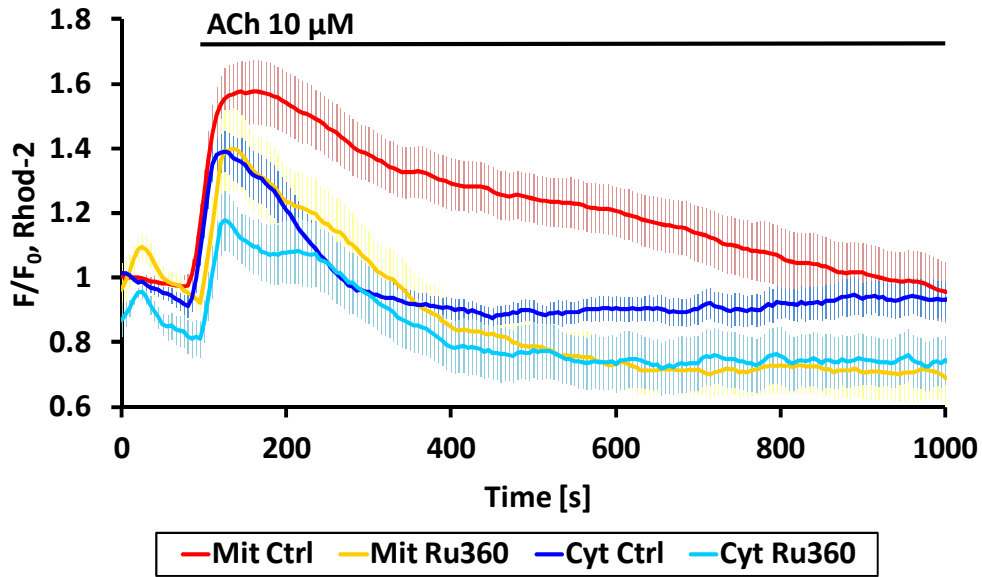
---

order to exclude this possibility, cytosolic calcium clearance was investigated under conditions, where mitochondrial  $\text{Ca}^{2+}$  buffering functions were abolished. This can be achieved by selective inhibition of mitochondrial  $\text{Ca}^{2+}$  uniporter by a compound called Ru360.

First, a control experiment was performed, which aimed to test whether Ru360 can eliminate mitochondria involvement in  $\text{Ca}^{2+}$  responses. Freshly isolated pancreatic acinar cells were loaded with rhod-2, a calcium sensitive dye, which preferentially localizes to mitochondria. Since the measurements were performed in intact cells, a fraction of the dye was also present in the cytosol and thus recorded mitochondrial  $\text{Ca}^{2+}$  responses in fact contained both mitochondrial and cytosolic components. Pancreatic acinar cells were preincubated with 10  $\mu\text{M}$  Ru360 to block mitochondrial  $\text{Ca}^{2+}$  uniporter; and 10  $\mu\text{M}$  ACh was used to induce rapid  $\text{Ca}^{2+}$  release from the stores. Mitochondrial and cytosolic responses to ACh were recorded in both Ru360-treated cells and control (untreated) cells. The results are presented in *Fig. 7.5.A*. Mitochondrial responses of control cells (red trace,  $n = 9$ ) are markedly longer with delayed clearance phase than cytosolic responses (dark blue trace,  $n = 6$ ). Preincubation with Ru360 eliminates the actual mitochondrial component from the responses recorded on mitochondria (yellow trace,  $n = 6$ ), leaving only cytosolic component similar to the responses recorded in the cytosol in the presence of Ru360 (light blue trace,  $n = 5$ ) (*Fig. 7.5.A*). This control experiment demonstrates that Ru360 is a potent blocker of mitochondrial  $\text{Ca}^{2+}$  uniporter and can indeed exclude the involvement of mitochondria in cytosolic  $\text{Ca}^{2+}$  responses.

In order to investigate  $\text{Ca}^{2+}$  fluxes under inhibition of mitochondrial  $\text{Ca}^{2+}$  uniporter, pancreatic acinar cells were loaded with fura-2. After preincubation for 200 s with

A.



B.

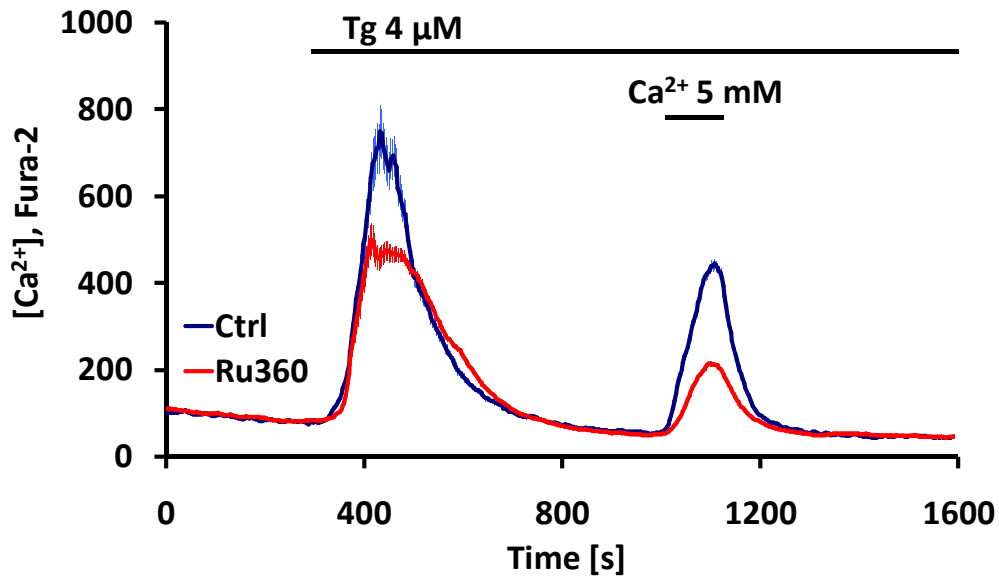


**Fig. 7.5. Condition of mitochondria does not markedly affect  $Ca^{2+}$  extrusion**

(A) Average traces showing calcium responses in mitochondria and in the cytosol to 10 μM acetylcholine in control cells and cells pretreated with 10 μM Ru360. Responses of control cells are presented as red (mitochondria,  $n = 9$ ) and dark blue (cytosol,  $n = 6$ ) traces; whereas responses of Ru360-pretreated cells are shown in yellow (mitochondria,  $n = 6$ ) and light blue (cytosol,  $n = 5$ ). Bars represent standard errors. (B) Average traces comparing cytosolic calcium responses after store depletion with 4 μM thapsigargin in control cells ( $n = 19$ , blue trace) and cells pretreated with 10 μM Ru360 ( $n = 19$ , red trace). Bars are standard errors.

C.

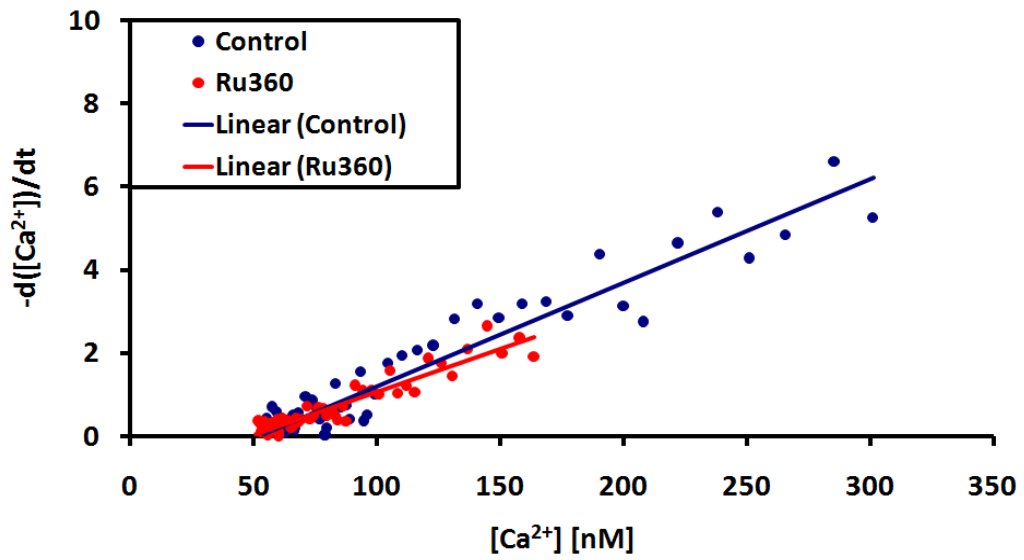


**Fig. 7.5.** (continues)

(C) The dependence of rate of cytosolic  $Ca^{2+}$  extrusion on the temporal  $Ca^{2+}$  level in control (blue line) and Ru360-pretreated (red line) pancreatic acinar cells.  $-d[Ca^{2+}]/dt$  values were obtained from average traces depicted in (B).

---

10  $\mu\text{M}$  Ru360, the ER was emptied by application of 4  $\mu\text{M}$  Tg in NaHEPES solution containing no  $\text{Ca}^{2+}$ . After the return of Tg-induced cytosolic  $\text{Ca}^{2+}$  increase to the basal levels, extracellular  $\text{Ca}^{2+}$  concentration was changed from 0 to 5 mM  $\text{CaCl}_2$ , which induced rapid  $\text{Ca}^{2+}$  influx to the cytosol. Then the extracellular solution was changed again to NaHEPES with no  $\text{Ca}^{2+}$  leading to  $\text{Ca}^{2+}$  extrusion from the cytosol. *Fig. 7.5.B* shows response patterns recorded in control cells and cells treated with Ru360. Although the amplitudes of cytosolic  $\text{Ca}^{2+}$  elevations clearly differ, the rates of  $\text{Ca}^{2+}$  extrusion (calculated as described in Chapter 7.3) are similar for both control conditions and inhibition of mitochondrial calcium uniporter (*Fig. 7.5.C*). In summary this experiment demonstrates that although mitochondria are involved in cytosolic  $\text{Ca}^{2+}$  responses, they do not substantially affect  $\text{Ca}^{2+}$  export across the plasma membrane. Therefore it is very unlikely that increased rate of cytosolic calcium extrusion in *bcl-2<sup>-/-</sup>* is a result of changed mitochondrial functions by loss of Bcl-2 protein.

## **7.6. Bcl-2 regulates resting calcium levels in the cytosol and in the ER**

One of the observations from calcium extrusion experiments described in Chapter 7.2. was the clear difference in the resting cytosolic  $\text{Ca}^{2+}$  levels between *bcl-2<sup>-/-</sup>* cells and wild type cells. Detailed comparison of the baseline calcium levels from wild type and *bcl-2<sup>-/-</sup>* traces revealed that loss of Bcl-2 protein in pancreatic acinar cells was associated with significantly lower basal cytosolic calcium concentration ( $57.5 \text{ nM} \pm 3 \text{ SE}$ ) as compared to wild type cells ( $100.3 \text{ nM} \pm 5.6 \text{ SE}$ ). The difference is illustrated in *Fig. 7.6.A*. Calcium extrusion is one of the main mechanisms responsible for the maintenance of cytosolic calcium levels<sup>303</sup>.

---

Therefore one of the possible explanations of this phenomenon is increased activity of calcium pumps in *bcl-2*<sup>-/-</sup> pancreatic acinar cells, which obviously would be in agreement with observed differences in cytosolic calcium clearance between the Bcl-2 KO cells and wild type cells. Additionally, resting cytosolic calcium concentration can be influenced by changes in calcium content and release from the ER. In the literature there is an established agreement that Bcl-2 protein indeed regulates Ca<sup>2+</sup> levels in the ER; however the exact mechanism appears to be complex and we only begin to understand some of the aspects of Bcl-2-dependent regulation. The most popular approach of [Ca<sup>2+</sup>]<sub>ER</sub> assessment is indirect, since it is based on comparison of Ca<sup>2+</sup> release from the intracellular stores. The aim of this part of the study was to present direct and thus more accurate measurements of Ca<sup>2+</sup> in the ER. For this purpose an independent analysis of ER calcium concentration in stabilized rat pancreatic cancer cell line AR42J was conducted. Although morphologically slightly different from freshly isolated pancreatic acinar cells, AR42J cell line is a relatively good model of pancreatic cells, which was frequently used by our research group on multiple occasions<sup>44,207</sup>. For accurate [Ca<sup>2+</sup>]<sub>ER</sub> measurements AR42J cells were transfected with ER-targeted cameleon plasmid, which is a calcium sensitive probe. ER-cameleon consists of two fluorescent components: CFP and YFP, separated by Ca<sup>2+</sup>-responsive motif constructed from modified calmodulin and calmodulin binding peptide M13<sup>83,308,309</sup>. Calcium binding leads to conformational change of ER-cameleon probe resulting in a new orientation of its fluorescent components CFP and YFP, which increases fluorescence resonance energy transfer (FRET) between them. That leads to decrease in cyan fluorescence and increase in yellow fluorescence, which allows ratiometric measurements of calcium changes in the ER.

---

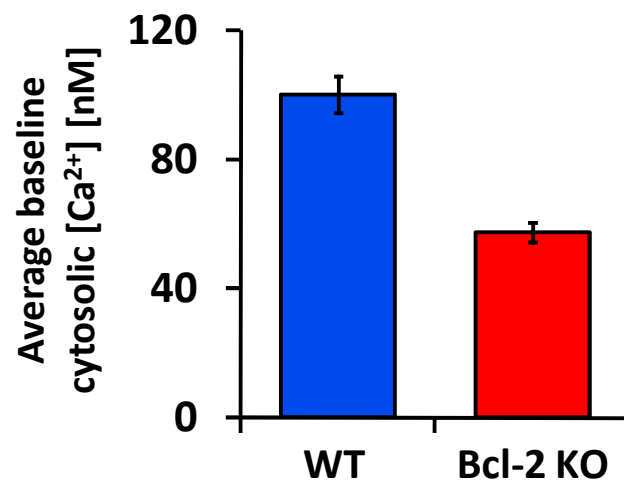
Exclusive expression of cameleon probe in the ER is accomplished both by (1) N-terminal calreticulin signal sequence that targets the protein to the ER on the first place and (2) C-terminal ER retention sequence KDEL, which ensures that the probe will remain in the ER. The expression pattern of ER-cameleon in AR42J cells is shown in *Fig. 7.6.B*. Blue colour represents cyan component and yellow - YFP fluorescence.

In order to test the effects of Bcl-2 overexpression on ER calcium levels, AR42J cells were stably transfected with pcDNA3 plasmid with human *bcl-2* insert. At the same time transient transfection with Bcl-2 siRNA was performed to attenuate Bcl-2 expression in AR42J cells. For the purpose of experiments untransfected AR42J cells were used as a control for the effects of overexpression; whereas cells transiently transfected with scrambled siRNA served as reference for Bcl-2 silencing. All the cells were plated on small 60 mm<sup>3</sup> glass-bottom petri dishes and transiently transfected with ER-targeted cameleon plasmid. In fact transfections with the plasmid and siRNAs were performed simultaneously. In each group cells expressing cameleon plasmid were visualized using Leica confocal microscope. Images of yellow and cyan fluorescence were taken from a number of untreated cells (from 62 to 97 per group) and YFP/CFP ratio was calculated. The ratio directly reflects the resting ER calcium levels in AR42J cells. Additionally, in each group some of the cells were treated with 20 μM cyclopiazonic acid (CPA), a fungal toxin that similarly to thapsigargin blocks the SERCA. CPA causes inhibition of store replenishment; and since the passive Ca<sup>2+</sup> leak continues, treatment with CPA leads to ER depletion of calcium. Therefore application of CPA allows for assessment of the total amount of releasable Ca<sup>2+</sup> in the ER. *Fig. 7.6.C* shows average YFP/CFP ratio values

---

obtained in resting conditions and after CPA treatment in untransfected AR42J cells (dark gray and light blue bar, respectively); and in AR42J cells overexpressing Bcl-2 (dark green and light green bar). *Fig. 7.6.D* shows average YFP/CFP ratio values obtained in resting conditions and after CPA treatment in AR42J cells transfected with Bcl-2 siRNA (presented as red bars) or control (scrambled) siRNA (blue bars). Bcl-2-dependent differences in resting  $[Ca^{2+}]_{ER}$  are presented as  $\Delta YFP/CFP$  ratio values obtained by subtraction of average "after CPA" values in each group from resting YFP/CFP ratio values; normalized to the appropriate controls (*Fig. 7.6.E*). Overexpression of Bcl-2 caused a statistically significant decrease in resting  $Ca^{2+}$  concentration in the ER (untransfected AR42J  $1.00 \pm 0.018$  SE,  $n = 78$ ; Bcl-2-overexpressing AR42J  $0.83 \pm 0.013$  SE,  $n = 97$ ,  $p < 0.001$ ). In contrast, silencing of Bcl-2 expression in AR42J cells resulted in elevated levels of resting  $Ca^{2+}$  in the ER (AR42J cells transfected with control siRNA:  $1.00 \pm 0.015$  SE,  $n = 69$ ; cells transfected with Bcl-2 siRNA:  $1.10 \pm 0.014$  SE,  $n = 62$ ,  $p < 0.001$ ). These results demonstrate that attenuated expression of Bcl-2 protein causes opposite effects on the resting  $Ca^{2+}$  levels in different cell compartments: a decrease in the cytosol and an increase in the ER. Therefore it seems unlikely that changes in cytosolic calcium are only a secondary effect to Bcl-2-dependent changes in the ER calcium. At this point it might be speculated that Bcl-2 regulates both  $Ca^{2+}$  pumps: the PMCA in the plasma membrane and the SERCA in the ER membranes. Loss of Bcl-2 protein results in increased activity of both pumps, leading to potentiated  $Ca^{2+}$  uptake to the intracellular stores and increased  $Ca^{2+}$  export from the cell.

A.



B.

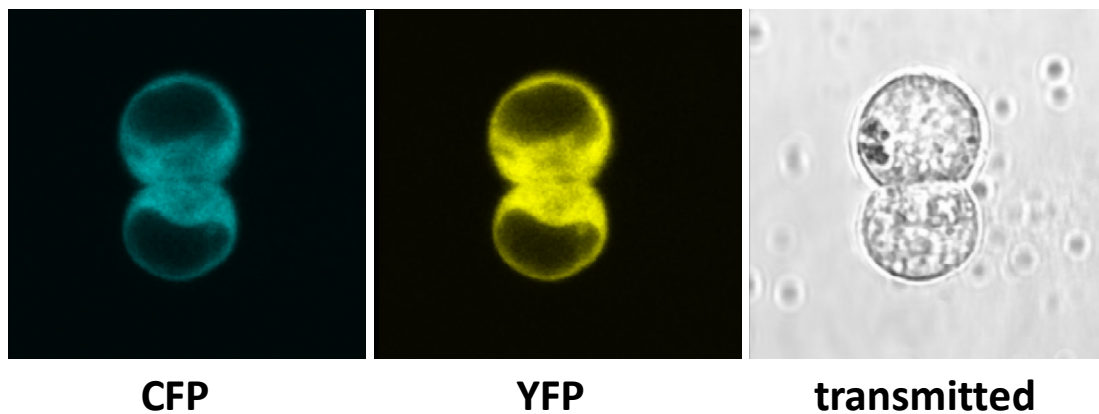
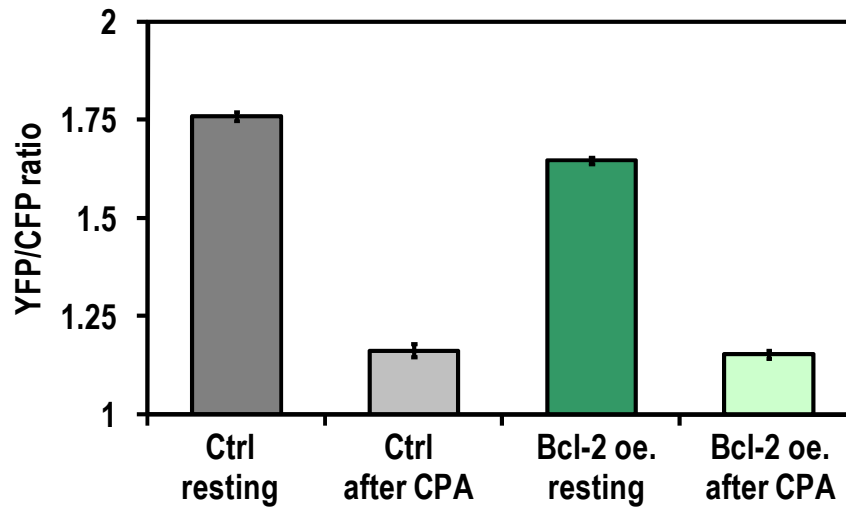


**Fig. 7.6. Bcl-2 regulates resting Ca<sup>2+</sup> levels in the cytosol and in the ER**

(A) Comparison of the initial (resting, baseline) cytosolic calcium levels in wild type pancreatic acinar cells (blue bar, n = 34) and *bcl-2*<sup>-/-</sup> cells (red bar, n = 109, p < 0.0001). The values were obtained from the experiment depicted in Fig. 7.3.

(B) Two AR42J cells transfected with ER-targeted cameleon. Blue colour represents CFP fluorescence and yellow colour - YFP. On the right: a transmitted light image of the AR42J cell doublet.

C.



D.

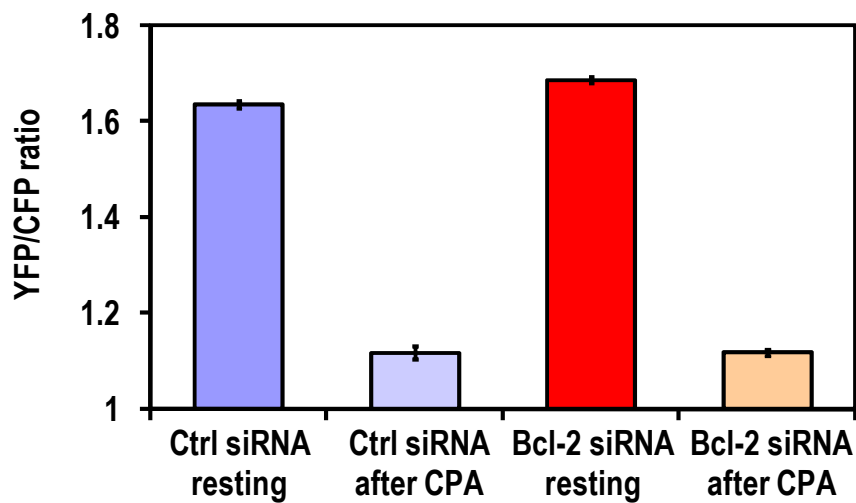


**Fig. 7.6. (continues)**

The charts show initial YFP/CFP ratio values reflecting resting  $\text{Ca}^{2+}$  concentration in the ER and final YFP/CFP ratio values obtained upon treatment with 20  $\mu\text{M}$  CPA, which corresponds to the ER depleted of calcium. The experiments were performed in (C) untransfected AR42J cells (dark gray bar for initial and light gray bar for final ratio values) and in AR42J cells stably overexpressing Bcl-2 (dark and light green, respectively); (D) AR42J cells transfected with scrambled siRNA (dark and light blue bars) and in AR42J cells transfected with Bcl-2 siRNA (dark and light red).

E.

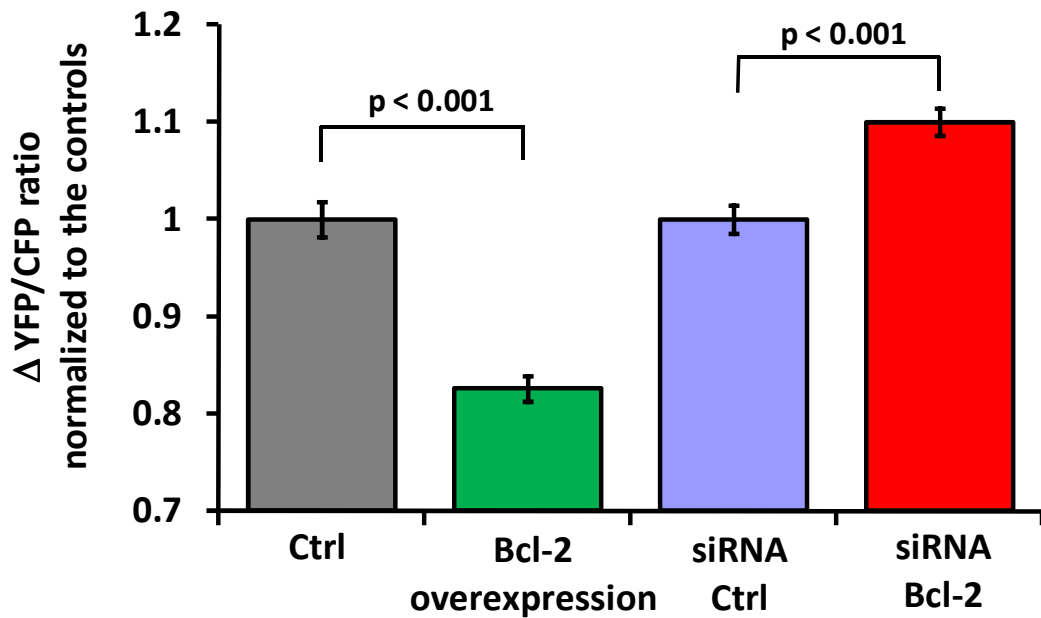


**Fig. 7.6.** (continues)

(E) Bar chart shows differences in resting levels of  $\text{Ca}^{2+}$  in the ER (full description in text). From the left: gray bar represents control (untransfected) AR42J cells ( $n = 78$ ); green bar refers to stably transfected cells, which overexpress Bcl-2 ( $n = 97$ ); blue bar – AR42J cells transiently transfected with control siRNA ( $n = 69$ ); red bar – AR42J cells transiently transfected with siRNA against Bcl-2 ( $n = 62$ ).

---

### **7.7. Bcl-2 is present in close proximity to the plasma membrane**

The results presented so far in this chapter strongly support the hypothesis that Bcl-2 protein regulates activity of the PMCA. However, the exact mechanism still remains obscure. There is not enough data in the literature to state whether regulation of the PMCA by Bcl-2 requires direct interaction of the proteins, or is indirect, which means that other factors mediate Bcl-2 dependent effects on PMCA activity. Direct interaction mechanism could only be postulated if both proteins can be found in close proximity that allows binding. Since the proteins are present in different cell compartments (the PMCA is localized to the plasma membrane and Bcl-2 is associated with mitochondrial and ER membranes) their interaction might seem unlikely. However, ER membranes can potentially be found close to the plasma membrane and direct interactions between ER and plasmalemmal proteins were already demonstrated in the past<sup>310,311</sup>. What is more, cytosolic localization of Bcl-2 is also a possibility. In order to test whether Bcl-2 might interact with the PMCA, intracellular distribution of fluorescently labelled Bcl-2 was investigated. For this purpose different approaches based on fluorescent imaging were applied.

AR42J cells were transfected with pEGFP-Bcl-2 protein as described above. On the second day after transfection RPMI medium was replaced with NaHEPES containing 1.5  $\mu$ M dextran conjugated with AlexaFluor 647. Dextran does not penetrate into the cells, but instead stains the extracellular environment in red. This simple method should allow for indirect visualization of the plasma membrane, which obviously should be found on the border of red colour from extracellular dextran. Since Bcl-2 is known to mainly localize to mitochondria, these structures were specifically

---

stained with 50 nM TMRE. Images of AR42J cells were obtained using Leica confocal microscope and Leica software. *Fig. 7.7.A* shows the staining and Bcl-2 expression pattern in an AR42J cell. It is clear that Bcl-2-GFP is predominantly localized to mitochondria, which is shown by the yellow colour on the overlay of green fluorescence from GFP and red TMRE (*Fig. 7.7.A.e*). However, Bcl-2 is also present throughout the cell (with exception of the nucleus), which corresponds to the ER localization (for comparison see *Fig. 3.2.B*). A fraction of that Bcl-2 from the ER is present very close to the plasma membrane, which is shown by the overlay of red and green fluorescence (*Fig. 7.7.A.f,i*).

In order to stain the plasma membrane more specifically, AR42J cells were transfected with Bcl-2-GFP and simultaneously infected with baculovirus expressing RFP targeted to the plasma membrane (Invitrogen, BacMam 2.0 - RFP). On the third day after transfection / infection, cell medium was removed and replaced with NaHEPES supplemented with 1 mM  $\text{Ca}^{2+}$ . AR42J cells were visualized using Leica confocal system. *Fig. 7.7.B* shows an image of two AR42J cells expressing both Bcl-2-GFP and RFP at the plasma membrane, which is depicted by green and red colour, respectively. The overlay of green and red fluorescence (*Fig. 7.7.B.c*) demonstrates that Bcl-2-GFP is expressed close enough to the plasma membrane that allows green and red colour on the picture to merge into yellow. Further, Bcl-2-GFP and RFP fluorescence values were obtained from a cell cross-section (see white line in *Fig. 7.7.B.c*) and presented on the graph as function of distance (*Fig. 7.7.C*). Peaks at the red trace (RFP fluorescence) indicate localization of the plasma membrane. Importantly, these red peaks overlap with green peaks from Bcl-2-GFP traces, which

**A.**

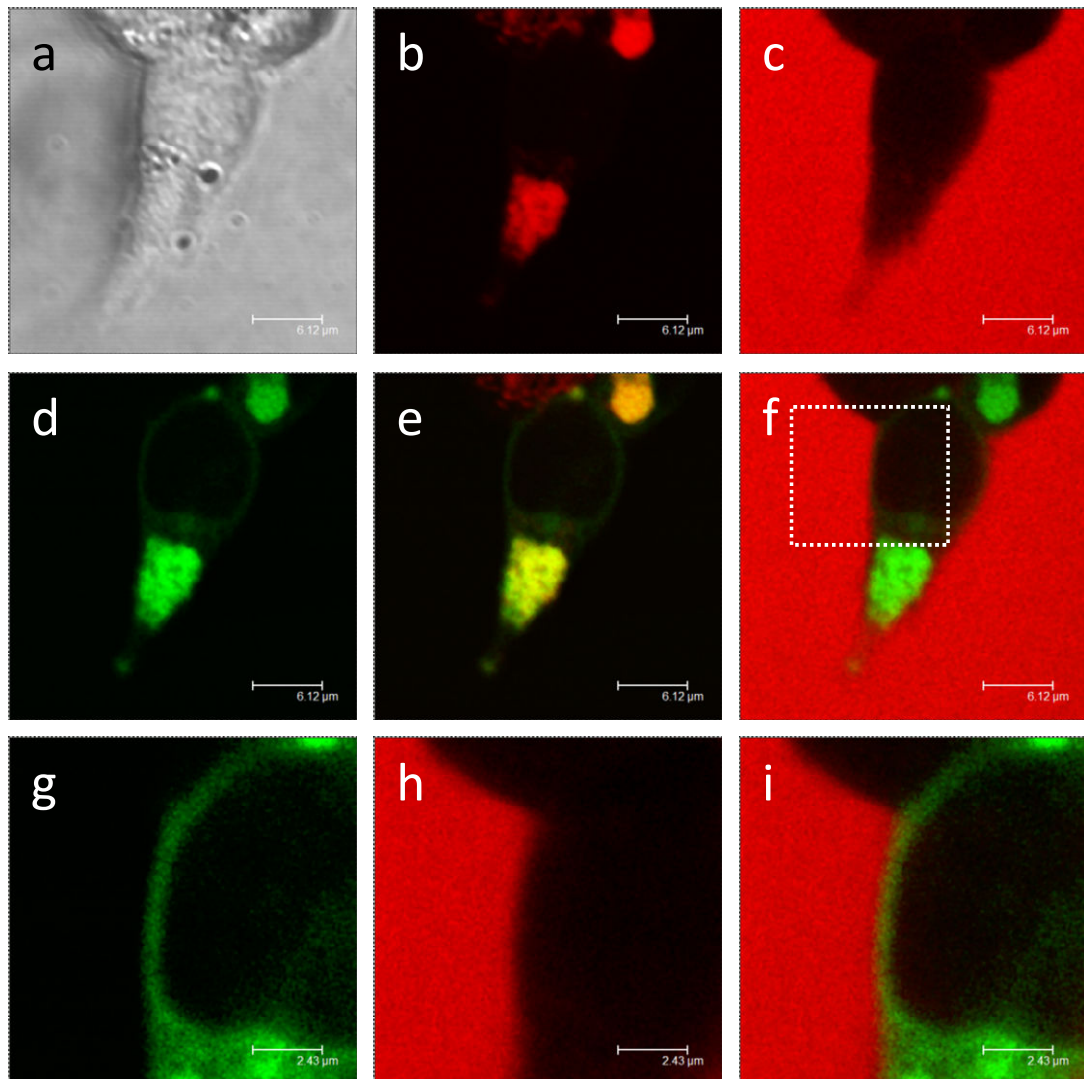
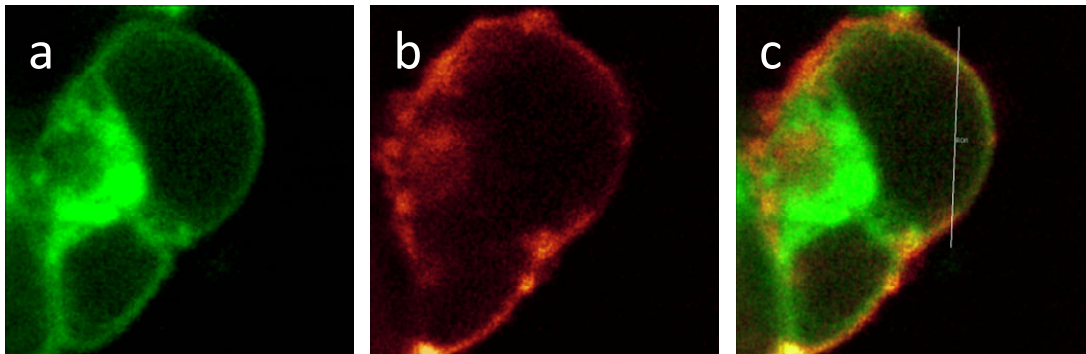


**Fig. 7.7. Bcl-2 is present in close proximity to the plasma membrane**

(A) A single AR42J cell transfected overexpressing Bcl-2-GFP. (A.a) Transmitted light image of the cell. (A.b) Mitochondria were visualized using 50 nM TMRE (red colour). (A.c) Extracellular space was stained with 1.5  $\mu$ M dextran AlexaFluor (red colour). (A.d) Expression of Bcl-2-GFP is shown in green. (A.e) Overlay of fluorescence of TMRE (red) and Bcl-2-GFP (green) shows that most of Bcl-2 is concentrated in mitochondria. (A.f) Overlay of fluorescence of dextran AlexaFluor (red) and Bcl-2-GFP (green). (A.g-i) Magnification of the marked part of the cluster from (f): (A.g) shows Bcl-2-GFP fluorescence (green) of the marked fragment; (A.h) shows red dextran fluorescence; and (A.i) is an overlay of (g) and (h), where yellow colour demonstrates that fraction of Bcl-2-GFP is located close to the plasma membrane.

B.



C.

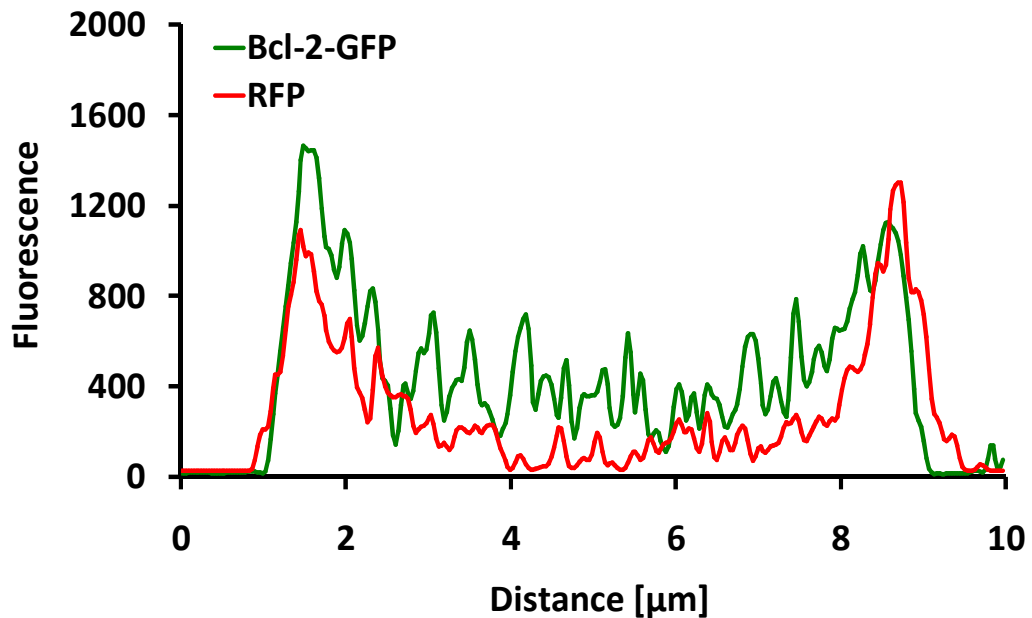


**Fig. 7.7. (continues)**

**(B)** Two AR42J cells transfected with pcDNA3 Bcl-2-GFP plasmid and infected with baculovirus (BacMam 2.0) expressing RFP targeted to the plasma membrane. **(B.a)** Expression of Bcl-2-GFP is shown in green and **(B.b)** RFP fluorescence is shown in red. **(B.c)** Overlay of red fluorescence of membrane RFP and green Bcl-2-GFP results in yellow colour at the plasma membrane. **(C)** The graph shows fluorescence of Bcl-2-GFP (green trace) and RFP (red trace) collected from the cross-section depicted by the white line on image (B.c). RFP peaks indicate location of the plasma membrane and they overlap with Bcl-2-GFP.

---

**D.**

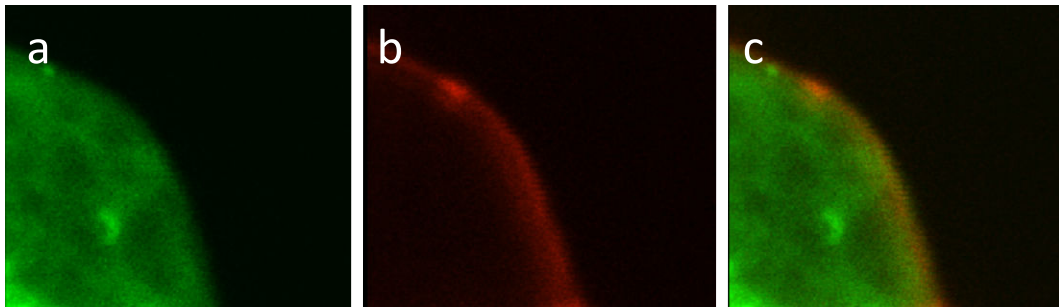


**Fig. 7.7. (continues)**

**(D)** Figure shows a section of a pancreatic acinar cell transiently expressing Bcl-2-GFP: **(D.a)** green colour represents fluorescence of Bcl-2-GFP; **(D.b)** red colour at the edge of the cell comes from FM 1-64 dye, which specifically stains the plasma membrane. **(D.c)** Overlay of green and red fluorescence demonstrates close localization of Bcl-2-GFP and the plasma membrane (yellow colour).

---

can be explained as accumulation of Bcl-2 protein in close proximity to the plasma membrane in AR42J cells.

Demonstrating close localization of Bcl-2 and the plasma membrane is particularly challenging in pancreatic acinar cells due to their very low efficiency of transfection as well as short lifespan when cultured. Nevertheless, the attempts were undertaken to express GFP-tagged Bcl-2 protein in overnight cultured acinar cells. Transfection of pancreatic acinar cells with Bcl-2-GFP plasmid was performed by electroporation using Amaxa Kit and following the manufacturer's protocol. Subsequently the cells were plated onto 5 cm<sup>3</sup> glass bottom petri dishes. After overnight incubation at 32°C, the cell membrane was stained with FM 1-64 dye and images of the cells exhibiting green fluorescence were taken. On average there was at least one transfected cell per petri dish. In *Fig. 7.7.D* a section of a live pancreatic acinar cell expressing Bcl-2-GFP is presented, which shows that green fluorescence from the fusion protein partially overlaps with red fluorescence of the plasma membrane. That makes possible the speculation of direct interaction between Bcl-2 and the PMCA in pancreatic acinar cells.

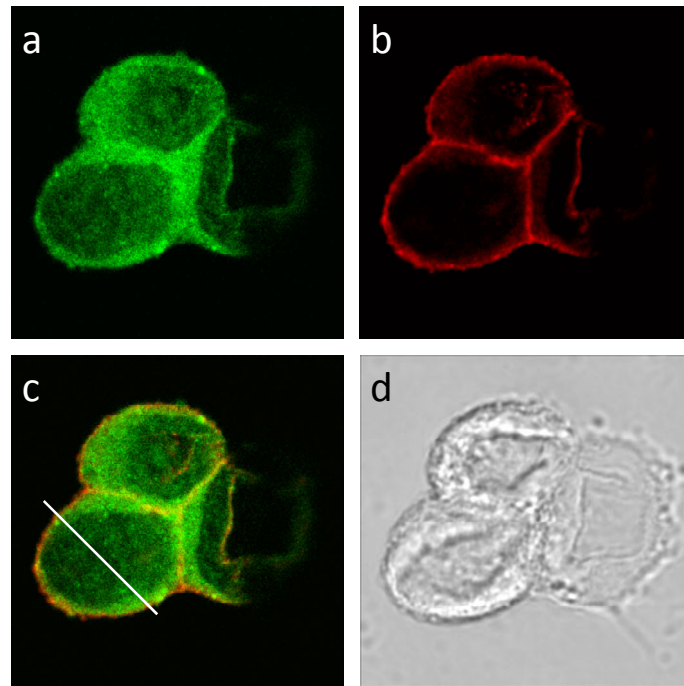
### **7.8. Bcl-2 is localized in close proximity to the PMCA at the plasma membrane in AR42J cells**

As it was demonstrated above, Bcl-2 can localize in close proximity to the plasma membrane in live AR42J cells as well as in pancreatic acinar cells. For confirmation of those results, immunostaining in fixed cells was performed. AR42J cells were plated onto 13 mm glass cover slips, which were placed at the bottom of separate wells in 24-well plate. The cells were transiently transfected with Bcl-2-GFP plasmid

---

using PromoFectin 2000 as described above and incubated in tissue culture incubator for 24 h in order to allow the cells to attach and produce detectable levels of Bcl-2-GFP fluorescence. On the second day after transfection the cells were fixed with ice-cold methanol for immunostaining as described in Chapter 2. The PMCA was specifically stained with primary mouse anti-PMCA antibody followed by secondary goat anti-mouse antibody conjugated to AlexaFluor 635. After 24 h incubation at 4°C the cells were visualized using confocal imaging system. A small cluster of AR42J cells is shown in *Fig. 7.8.A*, where green colour demonstrates the fluorescence of GFP and thus distribution of Bcl-2 protein; and the PMCA staining is depicted in red. The overlay in *Fig. 7.8.A.c* shows close localization of Bcl-2 and the PMCA. *Fig. 7.8.A.d* presents transmitted image of the cells. Just like in the example in Chapter 7.7., Bcl-2-GFP and AlexaFluor 635 fluorescence values were obtained from a cell cross-section (see white line in *Fig. 7.8.A.c*) and presented on the graph as function of distance (*Fig. 7.8.B*). Peaks at the red trace indicate localization of the PMCA and they overlap with green traces of Bcl-2-GFP fluorescence. Finally, immunostaining in fixed pancreatic acinar cells was performed. Following methanol fixation and removal of unspecific binding sites (as described in Materials and Methods) Bcl-2 was stained with primary rabbit anti-Bcl-2 antibody and secondary goat anti-rabbit antibody conjugated to Alexa Fluor 488; whereas for the detection of the PMCA primary mouse and secondary anti-mouse (AlexaFluor 635-conjugated) antibodies were used. After 24 h incubation at 4°C the cells were visualized using Leica confocal imaging system. The results are presented in *Fig. 7.8.C-G*. *Fig. 7.8.C* shows a doublet of pancreatic acinar cells; and *Fig. 7.8.D* - a single cell, where green colour demonstrates the distribution of Bcl-2 protein (*a*); and

A.



B.

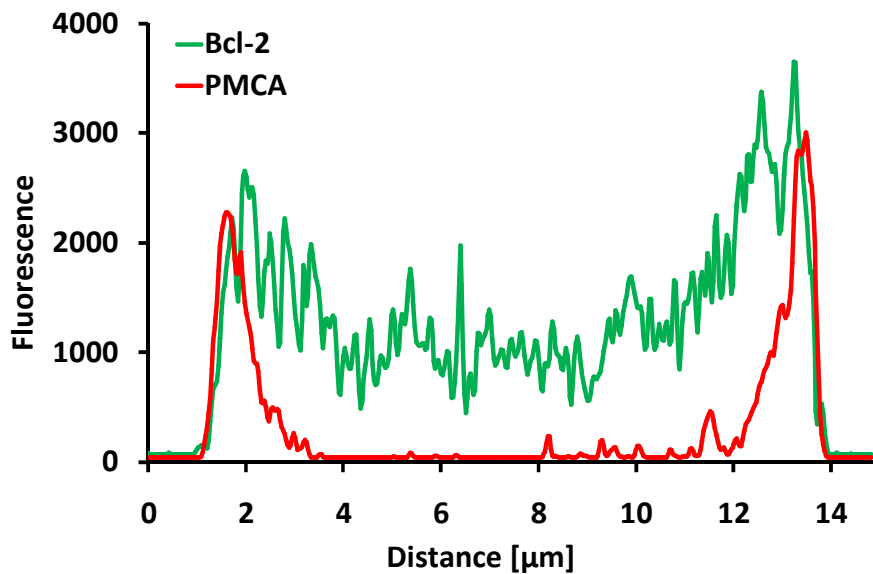
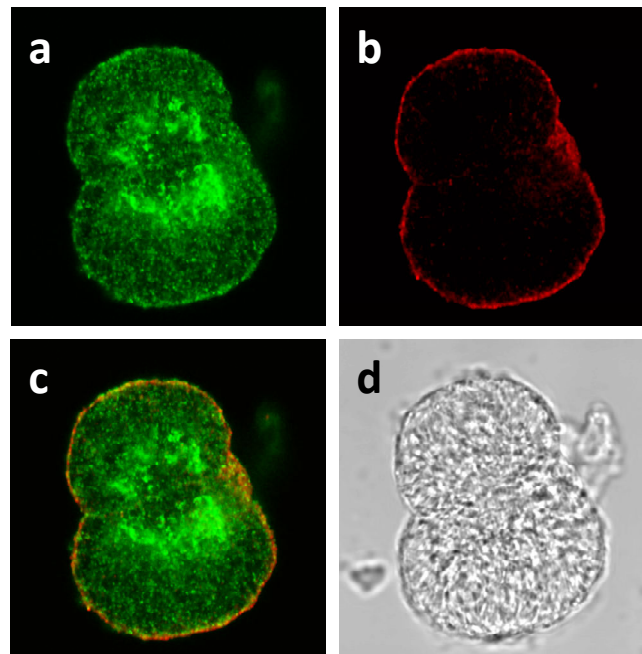


**Fig. 7.8. Bcl-2 is present in close proximity to the PMCA in AR42J cells**

(A) A small cluster of fixed AR42J cells overexpressing Bcl-2-GFP and immunostained with antibody against the PMCA: (A.a) Expression pattern of Bcl-2-GFP is shown in green and (A.b) localization of the PMCA is depicted by red colour. (A.c) Overlay of red fluorescence of the PMCA and green Bcl-2-GFP results in yellow colour at the plasma membrane. (B) The graph shows fluorescence of Bcl-2-GFP (green trace) and AlexaFluor 635 form the PMCA staining (red trace) collected at the cross-section depicted by the white line on image (A.c).

C.



D.

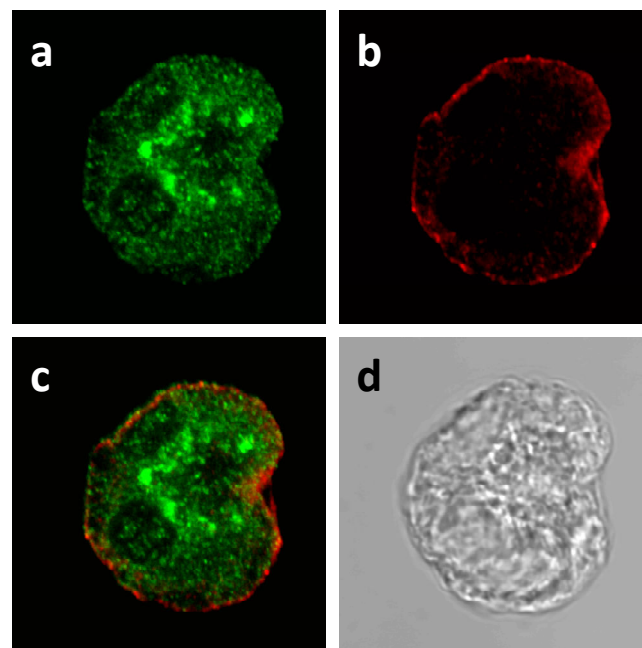
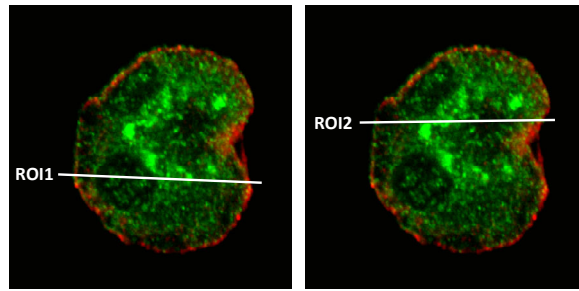


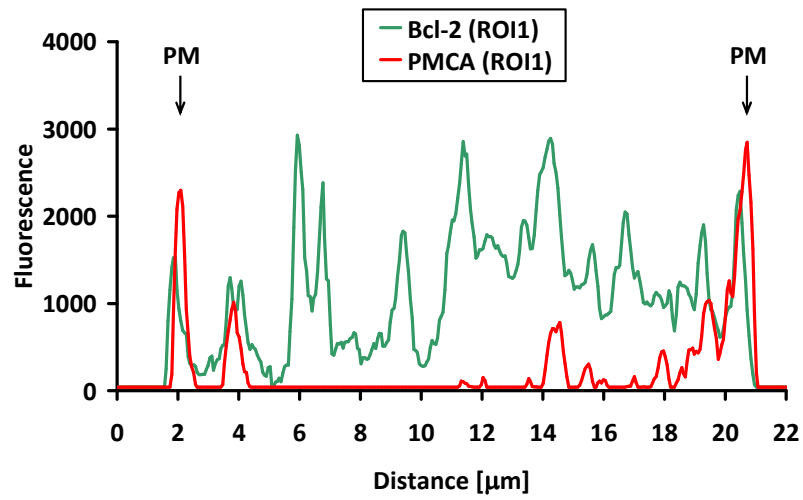
**Fig. 7.8.** (*continues*)

(C) A doublet of fixed pancreatic acinar cells immunostained with antibody against Bcl-2 (green) and the PMCA (red): (C.a) expression pattern of Bcl-2; (C.b) localization of the PMCA; (C.c) overlay of red and green fluorescence; (C.d) transmitted light image. (D) A single fixed pancreatic acinar cell immunostained with antibody against Bcl-2 (green) and the PMCA (red): (D.a) expression pattern of Bcl-2; (D.b) localization of the PMCA; (D.c) overlay of red and green fluorescence; (D.d) transmitted light image.

E.



F.



G.

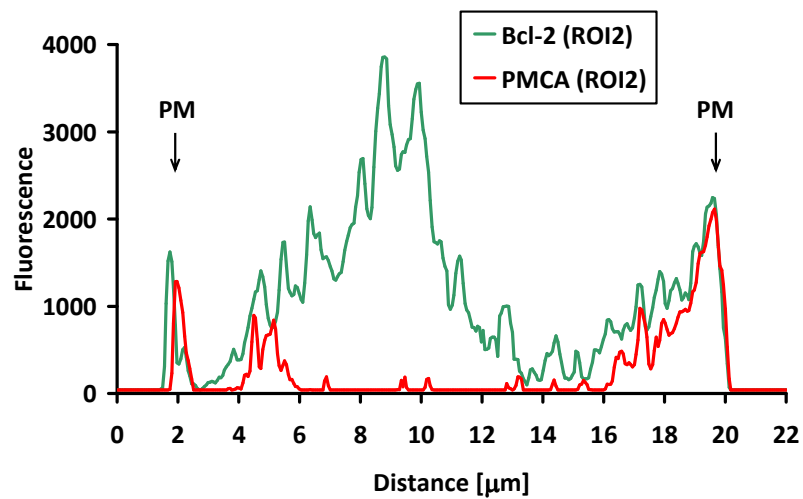


**Fig. 7.8.** (continues)

(E) The same cell as in (D.c) with marked two regions of interest (white lines). (F-G) The graphs show fluorescence of AlexaFluor 488 from Bcl-2 (green traces) and AlexaFluor 635 from the PMCA staining (red traces) collected at (F) region of interest 1 (ROI1) and (G) region of interest 2 (ROI2) as depicted by the white lines on image (E).

---

the PMCA staining is depicted in red (*b*). The overlay (*c*) demonstrates close localization of Bcl-2 and the PMCA. Transmitted light images of the cells are presented in (*d*). Green and red fluorescence values were obtained from cross-sections depicted in *Fig. 7.8.E* (see white lines) and presented on the graphs as function of distance (*Fig. 7.8.F and G*, for ROI1 and ROI2, respectively). Peaks at the red trace indicate localization of the PMCA and they overlap with peaks at the green traces of Bcl-2 fluorescence. According to the staining of a single pancreatic acinar cell, the PMCA is present in both basolateral and apical membranes; however it appears to be more concentrated in the neighbourhood of the granular area, which is also shown as higher and wider peaks in *Fig. 7.8.F and G*.

In conclusion immunolocalization data from fixed cells support the results obtained from live cells, and thus together demonstrate the accumulation of Bcl-2 protein in close proximity to the plasma membrane and the PMCA. Since Bcl-2 protein can be present very close to the PMCA, it makes feasible the speculation of direct interaction between the PMCA and Bcl-2, which is important in regulation of the activity of the pump and thus cytosolic calcium extrusion.

### **7.9. Loss of Bcl-2 promotes apoptosis and protects against necrosis**

Bcl-2 is well known for its anti-apoptotic functions. Interestingly, data presented in this chapter suggest that Bcl-2 decreases activity of the PMCA, which leads to slower calcium extrusion from the cytosol that might promote cell death. Therefore the pathophysiological importance of Bcl-2-dependent regulation of the PMCA seems counterintuitive. In order to explain this phenomenon cell death assays on pancreatic acinar cells were performed. The cells were isolated from wild type and

---

*bcl-2*<sup>-/-</sup> mice and challenged with (1) 30 μM menadione, which promotes production of reactive oxygen species and induces apoptosis via intrinsic pathway; (2) high Ca<sup>2+</sup> (5 mM) in order to increase calcium gradient across the plasma membrane and potentiate calcium influx, which could reveal effects dependent on different PMCA regulation; (3) menadione and high Ca<sup>2+</sup> together. The cells were incubated for 30 min at room temperature with gentle agitation. This also includes control groups, which were incubated in the same conditions but without any treatment. Then cells were spun, resuspended in binding buffer and incubated with annexin-V-FITC and propidium iodide according to the protocol of apoptosis kit (Sigma). Multiple images of the cells were taken using Leica confocal system and the numbers of live / apoptotic / necrotic cells were obtained based on the staining pattern with annexin-V-FITC and propidium iodide. Annexin binds to phosphatidylserine exposed on the outer leaflet of the plasma membrane in apoptotic cells. Propidium iodide can only label cells when the plasma membrane has been compromised; therefore it is a good indicator of necrotic cells. The results are presented in *Fig. 7.9.A-B*. Untreated wild type and *bcl-2*<sup>-/-</sup> cells have very similar percentages of apoptosis and necrosis. Treatment with 5 mM Ca<sup>2+</sup> led to a decrease in wild type live cells as compared to untreated wild type cells ( $p = 0.019$ ) as well as in comparison to *bcl-2*<sup>-/-</sup> cells challenged with the same concentration of extracellular calcium ( $p = 0.05$ ). Cells lacking Bcl-2 protein appear to have a slightly higher tolerance for conditions of high extracellular calcium. Treatment with menadione resulted in significant reduction in percentage of live wild type cells as compared to the untreated wild type control ( $p < 0.001$ ); at the same time apoptosis ( $p < 0.001$ ) as well as necrosis ( $p = 0.01$ ) were markedly increased. Wild type cells challenged with both menadione and 5 mM

---

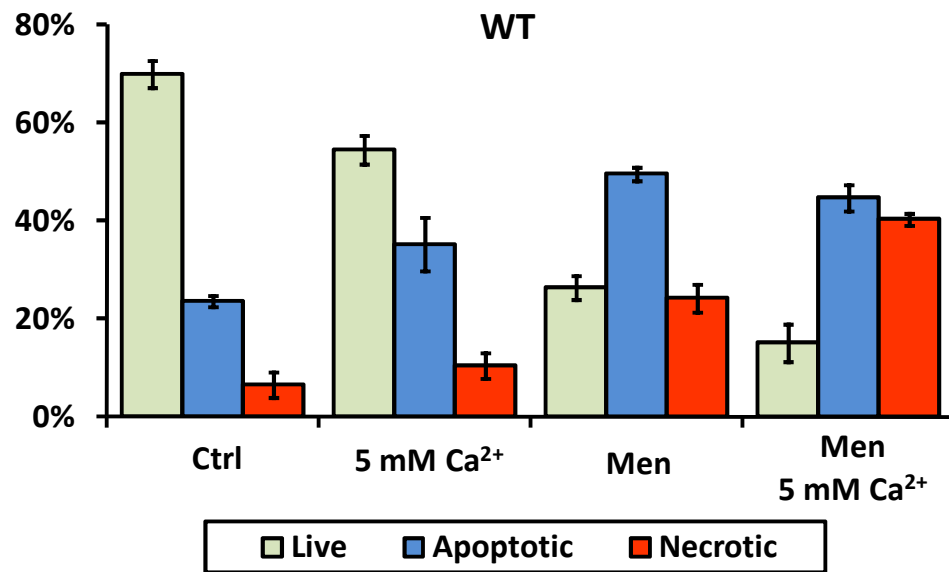
calcium had their necrosis levels increased even more substantially when compared to treatment with menadione alone ( $p = 0.018$ ). Cells lacking Bcl-2 responded to menadione with a decrease in percentage of live cells ( $p = 0.001$ ). Interestingly, their apoptosis levels were substantially increased over control *bcl-2*<sup>-/-</sup> values ( $p = 0.003$ ), but percentage of necrosis was not significantly different from untreated *bcl-2*<sup>-/-</sup> cells ( $p = 0.138$ ). Further, combined treatment of *bcl-2*<sup>-/-</sup> cells with menadione and high calcium did not increase their necrosis levels over treatment with menadione alone ( $p = 0.282$ ), which is a major difference from wild type cells. Also important to note is that menadione had dramatically different effects on wild type cells than on *bcl-2*<sup>-/-</sup> cells. Cells lacking Bcl-2 developed markedly more apoptosis ( $p = 0.002$ ) and substantially less necrosis ( $p = 0.016$ ) than wild type cells treated in the same way. Finally, difference in necrosis levels between *bcl-2*<sup>-/-</sup> and wild type cells is even more pronounced upon combined treatment with menadione and 5 mM Ca<sup>2+</sup> ( $p = 0.008$ ). Taken together these results confirm that loss of Bcl-2 promotes apoptosis induction under conditions of oxidative stress. Also, consistently with the hypothesis that Bcl-2 decreases PMCA activity, *bcl-2*<sup>-/-</sup> cells seem to exhibit better survival against the adverse effects of high extracellular calcium. Both wild type and *bcl-2*<sup>-/-</sup> cells are sensitive to oxidative stress induced by menadione, which is well depicted by decreased levels of live cells that are comparable in both groups (26.33 %  $\pm$  2.50 % in wild type group and 27.39 %  $\pm$  1.14 % in *bcl-2*<sup>-/-</sup>). However, striking is the fact that although cells in both groups die, they utilize different cell death mechanisms. Loss of Bcl-2 strongly promotes apoptosis and protects against necrosis upon oxidative stress. Additionally, oxidative stress in combination with high extracellular calcium induces even more necrosis in wild type cells; whereas menadione-

---

dependent cell death of *bcl-2*<sup>-/-</sup> cells does not seem to be affected by the presence of high extracellular calcium.

In order to fully understand the effects of Bcl-2 protein on cell death induction, cytosolic calcium responses to 5 mM Ca<sup>2+</sup>, and 30 μM menadione in the presence of 1 mM or 5 mM extracellular Ca<sup>2+</sup> were investigated in fura-2-loaded wild type and *bcl-2*<sup>-/-</sup> pancreatic acinar cells. Typical traces are shown in *Fig. 7.9.C-D*. In the presence of 5 mM CaCl<sub>2</sub> in the extracellular environment wild type pancreatic acinar cells developed a slow elevation of cytosolic Ca<sup>2+</sup> (n = 18). In contrast, increased extracellular calcium had no effect on *bcl-2*<sup>-/-</sup> cells (*Fig. 7.9.C-D*, n = 12). WT as well as *bcl-2*<sup>-/-</sup> cells responded to menadione with an elevation of cytosolic Ca<sup>2+</sup> (n<sub>WT</sub> = 23 and n<sub>bcl-2</sub> = 14). However, wild type cells additionally developed robust oscillations on top of the increasing calcium baseline (*Fig. 7.9.C*). What is more, menadione-induced oscillations were substantially potentiated in wild type cells in the presence of 5 mM Ca<sup>2+</sup> (*Fig. 7.9.C*, n = 22). Interestingly, pancreatic acinar cells lacking Bcl-2 did not develop such robust Ca<sup>2+</sup> oscillations in response to menadione (*Fig. 7.9.D*). The presence of high extracellular calcium had no further effect on responses evoked by menadione in those cells (*Fig. 7.9.D*, n = 12). The effects of menadione and high extracellular calcium on WT and *bcl-2*<sup>-/-</sup> cells are summarized in *Fig. 7.9.E*. The results are shown as average areas under the traces calculated between 200 s (upon treatment with menadione) and 1200 s, and normalized to the average values obtained for treatment with 5 mM Ca<sup>2+</sup> in wild type cells. Since 5 mM Ca<sup>2+</sup> has only a minor effect on wild type cells, the responses are not statistically significant from those recorded in *bcl-2*<sup>-/-</sup> cells (p = 0.105), although the difference is noticeable. Treatment with 30 μM menadione in the presence

A.



B.

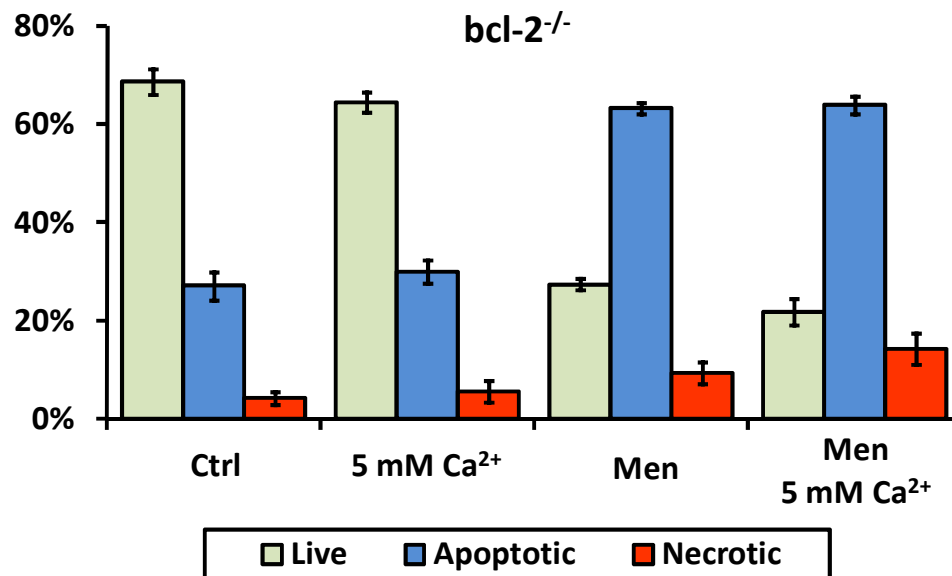
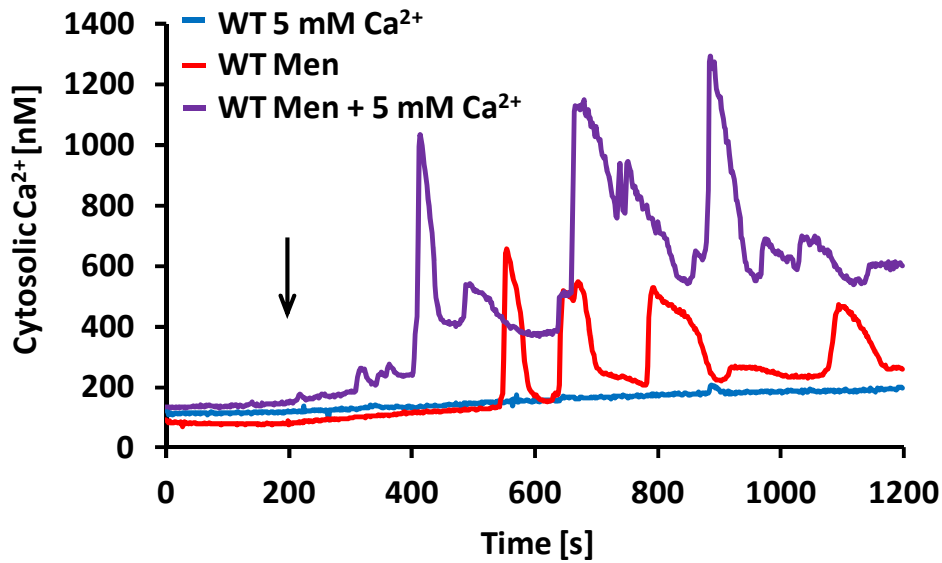


**Fig. 7.9. Loss of Bcl-2 promotes apoptosis and protects against necrosis**

(A) The chart shows the results of cell death assays performed on WT cells. Green bars represent percentage of live cells, blue – percentage of apoptotic cells, and red – percentage of necrotic cells. Four treatment groups are presented from left to right: control cells (no treatment); cells exposed to 5 mM Ca<sup>2+</sup>; cells treated with 30 μM menadione; and cells treated with 30 μM menadione in the presence of 5 mM Ca<sup>2+</sup>. (B) The results of cell death assays in *bcl-2*<sup>-/-</sup> pancreatic acinar cell are presented in the same way as in (A). Cells with no functional Bcl-2 develop substantially more apoptosis and markedly less necrosis than WT cells upon treatment with 30 μM menadione or menadione in the presence of high calcium.

C.



D.

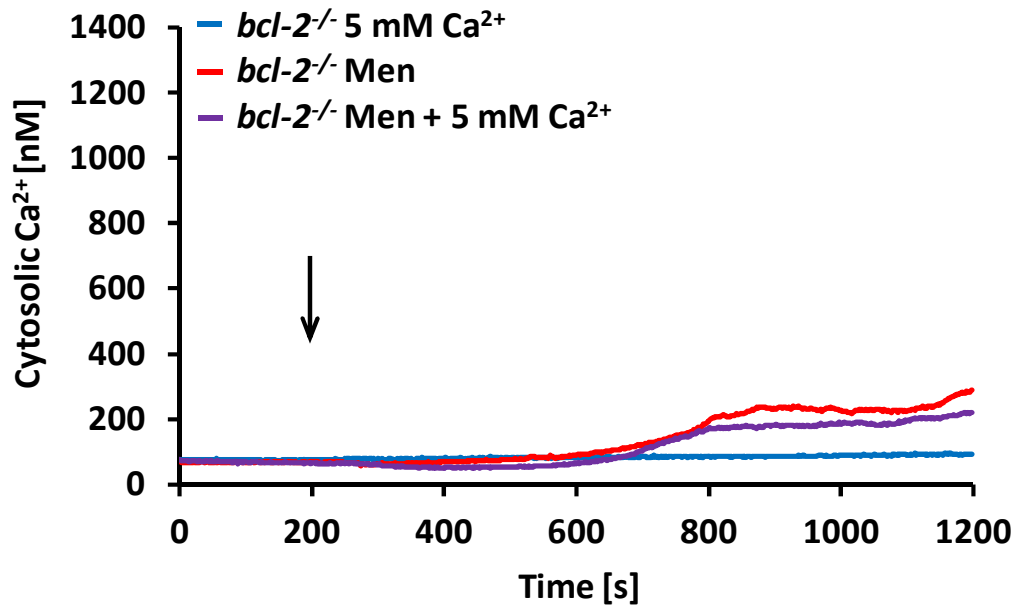
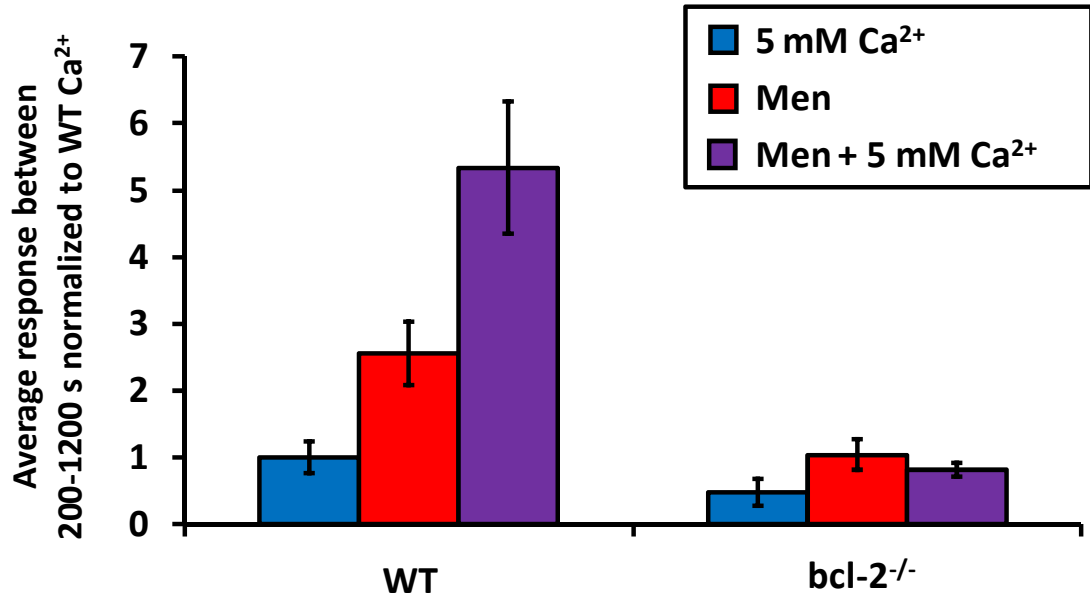


Fig. 7.9. (continues)

(C) The figure shows typical calcium responses in WT pancreatic acinar cells to 5 mM  $\text{Ca}^{2+}$  (blue trace,  $n = 18$ ), to 30  $\mu\text{M}$  menadione in 1 mM  $\text{Ca}^{2+}$  (red trace,  $n = 23$ ) and 30  $\mu\text{M}$  menadione in the presence of 5 mM  $\text{Ca}^{2+}$  (violet trace,  $n = 22$ ). (D) The figure shows typical calcium responses in  $bcl-2^{-/-}$  pancreatic acinar cells to 5 mM  $\text{Ca}^{2+}$  (blue trace,  $n = 12$ ), to 30  $\mu\text{M}$  menadione in 1 mM  $\text{Ca}^{2+}$  (red trace,  $n = 14$ ) and 30  $\mu\text{M}$  menadione in the presence of 5 mM  $\text{Ca}^{2+}$  (violet trace,  $n = 12$ ). In both figures black arrows indicate the time point of treatment application.

E.



**Fig. 7.9.** (continues)

(E) The figure shows average calcium responses recorded between 200 and 1200 s to 5 mM extracellular Ca<sup>2+</sup>, 30  $\mu$ M menadione, and menadione in high extracellular Ca<sup>2+</sup>. The responses were normalized to the average values obtained for 5 mM Ca<sup>2+</sup> in WT cells. Blue bars represent cells exposed to 5 mM Ca<sup>2+</sup>, red bars refer to cells treated with 30  $\mu$ M menadione, and violet bars represent cells challenged with 30  $\mu$ M menadione in the presence of 5 mM Ca<sup>2+</sup>. The responses of WT cells to menadione are clearly greater than those of *bcl-2*<sup>-/-</sup> cells, and are even more potentiated by the presence of high extracellular calcium in the external solution.

---

of 1 mM as well as 5 mM extracellular  $\text{Ca}^{2+}$  resulted in substantially greater responses in WT cells as compared to cells lacking Bcl-2 ( $p = 0.007$  and  $p \ll 0.001$ , for 1 mM and 5 mM  $\text{Ca}^{2+}$  respectively). In wild type cells responses to menadione in the presence of 5 mM extracellular  $\text{Ca}^{2+}$  were significantly greater than those caused by menadione alone ( $p = 0.017$ ). In contrast, increased extracellular  $\text{Ca}^{2+}$  did not affect menadione-dependent responses in *bcl-2*<sup>-/-</sup> ( $p = 0.38$ ).

Taken together, loss of Bcl-2 in pancreatic acinar cells protects against the adverse effects of increased external calcium, since such cells can extrude cytosolic calcium across the plasma membrane more efficiently than WT cells. In contrast to WT cells, *bcl-2*<sup>-/-</sup> cells respond with increased levels of apoptosis and are protected against excessive necrosis, when challenged with 30  $\mu\text{M}$  menadione. This protective effect is even more pronounced, when menadione treatment is combined with high extracellular calcium.

## 7.10. Discussion

Bcl-2 family proteins are very well known as the crucial regulators of apoptosis and mitochondrial integrity. However, recently their roles associated with other cell compartments have been attracting gradually more interest. Currently it is widely accepted that Bcl-2 proteins have heterogeneous intracellular distribution; they can be found not only at the outer mitochondrial membrane, but also at the ER, nuclear envelope and even in the cytosol<sup>153,312,313</sup>. The presence of Bcl-2 in the ER is especially interesting, since  $\text{Ca}^{2+}$  released from the intracellular stores can affect mitochondrial functions. Having calcium uniporter, mitochondria easily take up and accumulate increased cytosolic  $\text{Ca}^{2+}$ , which in turn can trigger radically different

---

effects. Beneficial role of calcium in mitochondria is associated with activation of  $\text{Ca}^{2+}$ -dependent enzymes of Krebs cycle, which leads to stimulation of aerobic metabolism and thus an increase in ATP production<sup>314</sup>. In contrast, calcium overload of mitochondria induces opening of permeability transition pore (PTP), which is involved in the release of proapoptotic factors<sup>315</sup>. It has been demonstrated by our group that apoptosis induction via intrinsic pathway indeed requires calcium responses in pancreatic acinar cells<sup>45</sup>. Therefore, Bcl-2 proteins seem to be involved in regulation of life and death signals at different cell compartments.

Roles of Bcl-2 family members, however, are not limited to their proapoptotic / prosurvival functions. These proteins have been found to regulate many aspects of calcium signalling of profound importance for cell homeostasis. They are known to be involved in the regulation of calcium release from the intracellular stores<sup>213,215</sup> as well as CICR process<sup>207</sup> (which has been shown in Chapter 3). The role of Bcl-2 proteins in controlling  $\text{Ca}^{2+}$  fluxes across the plasma membrane is less clear. It has been reported that Bcl-2 could be involved in the regulation of  $\text{Ca}^{2+}$  influx and store operated calcium entry<sup>316</sup>. Up to now the function of Bcl-2 protein in the regulation of calcium efflux from the cytosol across the plasma membrane has not been addressed.

In this chapter some aspects of calcium signalling have been compared between wild type and *bcl-2*<sup>-/-</sup> pancreatic acinar cells. Additionally, AR42J cell line has been used in order to manipulate the levels of intracellular Bcl-2 through transient or stable overexpression and RNA interference approach. The study originated from the initial observation described in Chapter 7.1., that loss of Bcl-2 protein resulted in increased cytosolic  $\text{Ca}^{2+}$  clearance in pancreatic acinar cells treated with a mixture of 10  $\mu\text{M}$

---

and 10  $\mu\text{M}$  ACh. In the literature it has been suggested that Bcl-2 might affect  $\text{Ca}^{2+}$  entry to the cytosol<sup>316,317</sup>; however its effects on calcium extrusion have not been previously described. Therefore the comprehensive study was undertaken in order to investigate this phenomenon in more detail. The results demonstrate that loss of Bcl-2 protein has significant implications for cellular calcium homeostasis. Pancreatic acinar cells without functional Bcl-2 protein export cytosolic calcium across the plasma membrane more efficiently than wild type cells. In pancreatic acinar cells calcium extrusion across the plasma membrane is mainly facilitated by the PMCA<sup>303</sup>. Indeed,  $\text{Na}^+$  substitution by NMDG<sup>+</sup> in the extracellular solution did not affect  $\text{Ca}^{2+}$  export from pancreatic acinar cells, whereas lanthanum almost completely blocked it. Since  $\text{Na}^+/\text{Ca}^{2+}$  exchange is negligible in pancreatic acinar cells, it is clear that the effects of Bcl-2 loss are associated with the PMCA. Bcl-2 appears to negatively regulate the PMCA, leading to increased activity of the latter in *bcl-2*<sup>-/-</sup> cells and thus more efficient  $\text{Ca}^{2+}$  extrusion from the cytosol. Further, calcium extrusion is one of the main mechanisms maintaining cytoplasmic calcium levels. Therefore pancreatic acinar cells lacking Bcl-2 exhibit significantly lower resting calcium levels in the cytosol as compared to wild type cells. Studies on AR42J cell line revealed that Bcl-2 overexpression led to reduced resting levels of calcium in the ER; and silencing Bcl-2 expression resulted in increased resting  $[\text{Ca}^{2+}]_{\text{ER}}$ . These suppressive effects of Bcl-2 overexpression on resting  $[\text{Ca}^{2+}]$  in the ER have also been observed by other research groups in different cell types<sup>83,157,158</sup>. In contrast, group of C. Distelhorst failed to find any differences in ionomycin-releasable intracellular store calcium between cells with and without functional Bcl-2<sup>318,319</sup>. One of the possible explanations of this apparent discrepancy could imply that the regulation

---

might slightly vary in different cell types. Additionally, previous measurements of ER calcium content were indirect, based on assessment of released  $\text{Ca}^{2+}$  from the ER. Here, more accurate direct measurement of resting  $\text{Ca}^{2+}$  levels in the ER has been applied by transient transfection of the AR42J cell line with ER-targeted cameleon plasmid.

The results provide some general insights into a potential mechanism of Bcl-2-dependent regulation of the PMCA, although they do not explain it completely. It is not clear whether this regulation is direct or indirect. Here, the possibility of the direct regulation was tested by analysing the distribution of Bcl-2 in AR42J cells and in acinar cells. While the substantial amount of Bcl-2 was localized to mitochondria, a fraction of it was also found in the ER in close proximity to the plasma membrane. Immunostaining of fixed cells demonstrated that at least small proportion of Bcl-2 can be localized very close to the PMCA. This confirms that direct interaction is potentially feasible and cannot be excluded.

Finally, the patho-physiological consequences of PMCA regulation by Bcl-2 protein have been investigated. Importantly, increase in extracellular calcium concentration to 5 mM leads to substantial increase in necrosis in wild type cells and wild type cells treated with menadione, but not in *bcl-2*<sup>-/-</sup> cells. Cells lacking Bcl-2 are not affected by increased extracellular calcium and are more likely to die of apoptosis when challenged with menadione alone. Necrosis remains at low levels even upon combined treatment with menadione and high calcium. These results provide novel insights into understanding of the functions of Bcl-2 protein. On one hand, by its anti-apoptotic actions it promotes cell survival; and negative regulation of the PMCA might help preserving cellular energy resources. On the other hand, loss of Bcl-2

---

makes apoptosis the cell death mechanism of choice under cytotoxic conditions, which at the same time serves as protection against excessive necrosis.

---

**CHAPTER 8:**  
**CONCLUDING REMARKS**

---

## Chapter 8: Concluding remarks

### 8.1. Summary

The present study aimed to investigate roles of Bcl-2 family proteins as well as some aspects of calmodulin actions on  $\text{Ca}^{2+}$  homeostasis in pancreatic acinar cells. Calmodulin is an ubiquitous regulatory protein engaged in regulation of multiple signalling pathways and cellular processes dependent on calcium<sup>195,220-223</sup>. And the roles of Bcl-2 proteins in regulation of intracellular calcium homeostasis have been recently gaining increasing attention<sup>157,160,204</sup>. Briefly, this thesis demonstrated that pharmacological inhibition of anti-apoptotic Bcl-2 and Bcl-xL by BH3 mimetics led to  $\text{Ca}^{2+}$  release from the intracellular stores followed by sustained cytosolic  $\text{Ca}^{2+}$  plateau formation. This  $\text{Ca}^{2+}$  release was only partially and not primarily dependent on  $\text{IP}_3\text{Rs}$  and  $\text{RyRs}$ , and it was almost completely abolished by loss of Bax protein. Anti-apoptotic Bcl-2 proteins were demonstrated to control sensitivity to CICR in pancreatic acinar cells. Simultaneously, Bcl-2 protein was shown to be involved in regulation of PMCA activity in pancreatic acinar cells and thus regulation of cytosolic  $\text{Ca}^{2+}$  extrusion across the plasma membrane. Further, the effects of calmodulin pre-activation by  $\text{Ca}^{2+}$ -like peptides CALP-1 and CALP-3 have been assessed. Application of CALPs, particularly CALP-1, reduced toxic effects of BH3 mimetics, which decreased levels of necrosis in favour of apoptosis in treated cells. Finally, the present study showed toxic effects of ethanol on intracellular  $\text{Ca}^{2+}$  homeostasis. Ethanol induced  $\text{Ca}^{2+}$  release from the ER and the acidic store, which

---

subsequently led to premature trypsinogen activation within the cells. These toxic effects of alcohol were inhibited by calmodulin and even more substantially - by calmodulin preactivation with CALP-3.

## **8.2. The effects of BH3 mimetics on calcium homeostasis in pancreatic acinar cells and their consequences**

It is generally accepted that the balance between pro- and anti-apoptotic Bcl-2 proteins regulates the fate of cells: death and survival<sup>116,166</sup>. This regulation is mediated by specific protein interactions. Anti-apoptotic Bcl-2 members possess a characteristic hydrophobic groove formed by BH1, BH2 and BH3 domains<sup>126</sup>. The BH3 domain of pro-apoptotic proteins Bax and Bak specifically binds to that groove, which neutralizes their apoptotic functions. Upon reception of death or stress signals, BH3-only proteins are activated and competitively displace Bax and Bak from the anti-apoptotic Bcl-2 members<sup>320</sup>. Displacement of Bax and Bak leads to their oligomerization followed by mitochondrial outer membrane permeabilization. Simultaneously, evidence suggests that several BH3-only proteins (such as Bid, Bim and PUMA) might also directly bind and activate Bax and Bak<sup>134,140</sup>. Since overexpression of anti-apoptotic Bcl-2 family members appears to be a very common feature of distinct cancer types, application of agents that inhibit their pro-survival functions is a promising anti-cancer approach. One of the first attempts to block anti-apoptotic Bcl-2 members was application of antisense-based strategies<sup>321</sup>. Antisense oligodeoxynucleotides target and bind to specific mRNA sequences, which leads to the RNaseH-mediated degradation of DNA-RNA heteroduplexes. This approach, however, had only very little therapeutic success.

---

BH3 mimetics are compounds that bear structural similarity to BH3 domain from pro-apoptotic Bcl-2 members, which is responsible for interaction with hydrophobic groove in anti-apoptotic proteins. Treatment with BH3 mimetics aims to disrupt the interaction between anti- and pro-apoptotic Bcl-2 members, inhibit pro-survival functions of Bcl-2 and Bcl-xL, and thus sensitize cells to apoptosis induction. BH3 mimetics are mainly synthetic chemicals such as HA14-1 and BH3I-2' that were generated by computer modelling. Some are natural theaflavins and epigallocatechins, such as gossypol, which can be found in cotton seeds. Gossypol also acts as an inhibitor of anti-apoptotic Bcl-2 members, exhibiting high affinity to Bcl-2, Bcl-xL and Mcl-1<sup>322</sup>. Its anti-cancer effects have been demonstrated in various cell types<sup>323-325</sup>.

Previously it has been demonstrated that HA14-1 is capable of displacing Bax protein from Bcl-2 and induce apoptosis in cultured cells<sup>167</sup>. Similarly, members of BH3I family of synthetic BH3 mimetics were shown to displace Bak peptide from Bcl-xL and promote cell death<sup>170</sup>. However, it was proved that a substantial proportion of the cytotoxic effects of HA14-1 and BH3I-2' was not due to specific inhibition of anti-apoptotic Bcl-2 members, since the BH3 mimetics are able to kill cells also in a manner independent on Bax and Bak<sup>326</sup>.

In the present study it has been observed that application of BH3 mimetics in pancreatic acinar cells is associated with Ca<sup>2+</sup> release from the intracellular stores followed by sustained Ca<sup>2+</sup> plateau<sup>207</sup>. These effects of BH3 mimetics were shown independent on mitochondrial functions, since inhibition of ATP synthesis by combined application of rotenone and oligomycin did not affect BH3 mimetic-induced Ca<sup>2+</sup> release from the intracellular stores. Surprisingly, the results presented

---

here indicate that the main ER channels responsible for  $\text{Ca}^{2+}$  release - IP<sub>3</sub>Rs and RyRs - are not primarily responsible for BH3 mimetic-induced  $\text{Ca}^{2+}$  release. Pharmacological inhibition of these receptors both in intact and permeabilized cells substantially reduced  $\text{Ca}^{2+}$  release from the intracellular stores, but did not completely abolish it, which suggests that the role of IP<sub>3</sub>Rs and RyRs is mainly restricted to amplification of already existing  $\text{Ca}^{2+}$  leak.

At the same time results from Chapter 3 led to formulation of hypothesis that anti-apoptotic Bcl-2 members regulate CICR process by sensitizing IP<sub>3</sub>Rs and RyRs for activation by  $\text{Ca}^{2+}$ . The hypothesis is strongly supported by the previous studies, which clearly demonstrate that Bcl-2 and Bcl-xL can physically interact with the IP<sub>3</sub>R affecting its  $\text{Ca}^{2+}$  releasing abilities<sup>213-215</sup>. Recently, BH4 domain of Bcl-2 protein was shown to bind to the regulatory domain of the IP<sub>3</sub>R, which decreased both  $\text{Ca}^{2+}$  release from the ER and apoptosis<sup>215</sup>. Those finding are further supported by experiments on AR42J cells, where overexpression of Bcl-2 protein attenuates both CICR and cytosolic  $\text{Ca}^{2+}$  plateau induced by BH3I-2'. Therefore application of BH3 mimetics affects cellular  $\text{Ca}^{2+}$  homeostasis in multiple ways. First, it potentiates passive  $\text{Ca}^{2+}$  leak from the ER, which, as shown in the present study, is dependent on pro-apoptotic Bax protein. Further, it increases sensitivity of  $\text{Ca}^{2+}$  release channels - IP<sub>3</sub>Rs and RyRs - for activation by  $\text{Ca}^{2+}$ . These two effects explain CICR type of responses caused by BH3 mimetics. Finally, prolonged cytosolic  $\text{Ca}^{2+}$  increase, which is sustained even in the absence of extracellular calcium, is indeed unexpected and difficult to explain immediately. It appears that application of BH3 mimetics and thus anti-apoptotic Bcl-2 inhibition reveals important and previously unknown functions of Bcl-2 proteins in regulation of  $\text{Ca}^{2+}$  release from the ER as well as in

---

Ca<sup>2+</sup> extrusion across the plasma membrane. These functions are investigated in more detail and described in the present study.

Although the anti-cancer actions of BH3 mimetics have been extensively investigated in the past, this study demonstrates their adverse effects on Ca<sup>2+</sup> homeostasis. Global Ca<sup>2+</sup> release followed by sustained cytosolic Ca<sup>2+</sup> plateau is toxic and might explain previously observed induction of cell death by BH3 mimetics in the manner independent on pro-apoptotic Bcl-2 members. Importantly, observed actions of BH3 mimetics on Ca<sup>2+</sup> homeostasis in normal cells, particularly pancreatic acinar cells, are serious side effects that need to be taken care of before these compounds can be safely used as potential therapeutic agents. Therefore this study identifies previously overlooked problem associated with the application of small molecular weight BH3 mimetic compounds for anti-cancer therapy.

### **8.3. The effects of ethanol on calcium homeostasis in pancreatic acinar cells**

Although the awareness of harmful impacts of alcohol drinking on health appears to have been increasing in recent years in the UK, mortality directly related to alcohol in 2008 showed an increase of 24 % as compared to 2001 (Statistics on Alcohol: England, 2010, NHS). Excessive alcohol consumption often leads to alcoholic liver disease and is strongly correlated with pancreatitis. Despite the clinical data indicating substantial toxicity of ethanol to pancreas, so far no major effects of alcohol on pancreatic acinar cells have been observed<sup>100</sup>. Therefore now it is accepted that the main mediators of ethanol toxicity in the pancreas are its metabolites<sup>243</sup>. Non-oxidative metabolites of ethanol – fatty acid ethyl esters – were

---

shown to induce a slow but substantial increase in cytosolic  $\text{Ca}^{2+}$  in pancreatic acinar cells. Also fatty acids cause a delayed dose-dependent  $\text{Ca}^{2+}$  rise in the cytosol, which is not mediated by  $\text{IP}_3\text{Rs}$ ; and induce severe cell damage indicated by uptake of propidium iodide<sup>100,108</sup>.

In the present study it has been demonstrated that ethanol alone in high concentrations (10 mM - 100 mM) releases  $\text{Ca}^{2+}$  from the intracellular stores. The effects of ethanol on intact cells are very modest and cannot alone explain severe impacts of heavy alcohol drinking on health. However, the effects of ethanol in permeabilized cells are far more substantial. The results show that treatment of two-photon permeabilized pancreatic acinar cells with ethanol causes  $\text{Ca}^{2+}$  release from both the ER and the acidic store in dose-dependent manner. This  $\text{Ca}^{2+}$  release is strongly associated with intracellular trypsinogen activation, which is the hallmark of pancreatitis. Activation of trypsin is crucial in pathogenesis of pancreatitis and the research shows this process is mediated by cathepsin B, a cysteine protease found in lysosomes<sup>41,327</sup>. Accumulating evidence suggests that autophagy might play a role in premature trypsinogen activation<sup>328,329</sup>. The mechanism of ethanol-mediated toxicity in pancreatic acinar cells is not yet fully understood and requires further investigation. This study provides only some insights into ethanol-related effects on pancreas.

The difference in  $\text{Ca}^{2+}$  responses to ethanol between intact and permeabilized pancreatic acinar cells comes from calmodulin content. Intact pancreatic acinar cells have exceptionally high levels of calmodulin, which is inevitably lost upon cell permeabilization. High calmodulin content acts protectively against ethanol toxicity diminishing its effects on  $\text{Ca}^{2+}$  release from the intracellular stores. Therefore this

---

study provides important evidence for protective functions of calmodulin. Further investigation of the exact mechanism of calmodulin-dependent inhibition of ethanol mediated  $\text{Ca}^{2+}$  release and trypsinogen activation might provide us with an invaluable weapon in fight against ethanol toxicity and pancreatitis.

#### **8.4. Calcium-like peptides as a potential tool against toxic effects of calcium**

Calcium-like peptides (CALPs) show no structural resemblance to  $\text{Ca}^{2+}$  ion. Instead their name indicates functional similarities. Complementary surface contour to EF-hand  $\text{Ca}^{2+}$ -binding motifs allows them to interact with the  $\text{Ca}^{2+}$  binding sites and thus mimic or block effects of calcium<sup>226</sup>. EF-hand motifs are present in various proteins, whose activity is regulated by  $\text{Ca}^{2+}$ , such as calmodulin and certain calcium channels.

Four different  $\text{Ca}^{2+}$ -like peptides have been designed by Villain et al<sup>226</sup>. Octamers CALP-1 and CALP-3 mimic the effects of  $\text{Ca}^{2+}$  binding to the carboxy-terminal EF-hands in calmodulin. Binding of CALP-1 and CALP-3 to calmodulin is associated with conformational change of the protein, which differs from that observed for  $\text{Ca}^{2+}$ -CaM. In contrast 12-mers CALP-2 and CALP-4 act as calmodulin antagonists and, consistently, do not induce active conformation of calmodulin<sup>226</sup>.

In order to exert their functions CALPs have to be able to enter cells efficiently. This property of CALPs has been previously tested with a modified version of CALP-1, which was conjugated to fluorescein maleimide. Using fluorescent microscopy the molecule was demonstrated to accumulate in different cell types: rat neocortical

---

neurons and Jurkat T cells<sup>227</sup>. In contrast, a hydrophilic control peptide modified in the same way was not taken up by the cells<sup>227</sup>.

In this study CALP-1 and CALP-3 were used for specific pre-activation of calmodulin both in intact pancreatic acinar cells and permeabilized cells (CALP-3 only). However the actions of Ca<sup>2+</sup>-like peptides seem to extend even further. They can act as inhibitors on certain channels affecting their Ca<sup>2+</sup> sensing mechanisms. This inhibitory effect can be exerted either by direct interaction of the peptide with the EF-hand motif of the channel, or it can be indirect - mediated through calmodulin<sup>227</sup>. It has been postulated that the channel blocking function of CALPs can inhibit Ca<sup>2+</sup> influx to the cytosol and therefore apoptosis dependent on Ca<sup>2+</sup> influx<sup>227</sup>.

This study focuses on calmodulin-dependent functions of Ca<sup>2+</sup>-like peptides. CALPs have been applied here in order to reduce toxic effects of elevated cytosolic Ca<sup>2+</sup> induced by treatment with BH3 mimetics as well as toxic effects of ethanol on Ca<sup>2+</sup> homeostasis in pancreatic acinar cells. Sustained cytosolic Ca<sup>2+</sup> elevation induced by BH3 mimetics or treatment with high doses of ethanol leads to intracellular trypsinogen activation in pancreatic acinar cells and further to induction of necrosis<sup>243</sup>. Necrosis results in loss of cell integrity and release of intracellular content, which promotes inflammation.

The results presented here demonstrate that Ca<sup>2+</sup>-like peptides acting on calmodulin are capable of reducing pathological Ca<sup>2+</sup> signals of different origin. Preincubation with CALP-1 or CALP-3 on average decreased the amplitude of Ca<sup>2+</sup> responses induced by BH3 mimetics: BH3I-2' and gossypol; and that was also reflected by the

---

results of cell death assays. CALP-1 appeared to protect against necrotic cell death promoting apoptosis; whereas CALP-3 reduced necrosis and increased the numbers of cells that survived the treatment. Experiments on permeabilized cells show that not only re-admission of calmodulin has a protective effect on ethanol-induced  $\text{Ca}^{2+}$  release, but more importantly pre-activation of calmodulin by calcium-like peptide CALP-3 brings even stronger inhibitory effect on both ethanol-mediated  $\text{Ca}^{2+}$  release from the stores and trypsinogen activation<sup>246</sup>. The mechanisms of  $\text{Ca}^{2+}$  release induced by high doses of ethanol and by treatment with BH3 mimetics markedly differ. BH3 mimetics release  $\text{Ca}^{2+}$  mainly from the ER and they do so in both intact and permeabilized cells. In contrast, ethanol induces  $\text{Ca}^{2+}$  release from the ER as well as from the acidic store. Ethanol-elicited effects are, however, strongly dependent on the presence of calmodulin. Consistently, ethanol has only a minor effect on intact cells, whereas in permeabilized cells, which have lost most of their calmodulin, ethanol induced substantial  $\text{Ca}^{2+}$  release from the intracellular stores. Taken together, the results indicate that  $\text{Ca}^{2+}$ -like peptides are effective against pathological  $\text{Ca}^{2+}$  signals induced in different ways.

In the present study it has also been tested whether  $\text{Ca}^{2+}$ -like peptides could interfere with physiological  $\text{Ca}^{2+}$  signals. The results indicate that neither CALP-1 nor CALP-3 substantially affect ACh signalling. Further, CALPs have only a minor effect on CCK signalling reducing global  $\text{Ca}^{2+}$  spikes in favour of apical oscillations. The latter might be beneficial, since localized oscillations are sufficient to induce exocytosis of digestive enzymes and secretion of fluid<sup>244</sup>.

---

Although CALPs have been designed more than 10 years ago, surprisingly they have not been extensively used in research. The current study rediscovers these compounds by providing important evidence that specific pre-activation of calmodulin by  $\text{Ca}^{2+}$ -like peptides is protective against pathological  $\text{Ca}^{2+}$  responses. This application of CALPs has not yet been previously suggested. And the data presented in this study demonstrate that CALPs could potentially be used as drugs against pancreatitis by reducing pathological  $\text{Ca}^{2+}$  responses resulting in intracellular trypsinogen activation and extensive cell death. Moreover, CALPs might find their application in cancer therapy, as agents modulating toxicity of BH3 mimetics. Treatment with CALP-like drugs together with a BH3 mimetic would protect healthy cells from adverse effects of the latter and would increase the levels of apoptosis induced by BH3 mimetics in cancer cells reducing levels of necrosis and thus inflammation. As was described in Chapter 4, peptides are not ideal drugs, since they are usually characterised by poor pharmacokinetic properties and are prone to degradation. However, development of synthetic compounds of structure and functions resembling that of CALPs might contribute to the development of therapeutic agents against acute pancreatitis as well as support BH3 mimetic-based anti-cancer therapy. From that perspective compounds analogical to CALP-3 would serve better for the first purpose, as they improve cell survival and decrease necrosis. On the other hand, CALP-1-based compounds could be applied for reduction of BH3 mimetic-induced toxicity, as they decrease necrosis but promote apoptosis.

---

## 8.5. Novel roles of Bcl-2 family protein in cellular Ca<sup>2+</sup> homeostasis

Bcl-2 protein was identified in 80s during analysis of a frequent chromosomal translocation in B cell lymphoma<sup>122,330</sup>, and gave rise to a novel family of proteins. Initially believed to be present exclusively in mitochondria<sup>313</sup>, Bcl-2 has been subsequently found in other intracellular compartments such as the ER, the nuclear envelope and even a small fraction of it could be found in the cytosol<sup>153,207,312</sup>. Functionally, Bcl-2 proteins are well known regulators of apoptotic cell death; they either promote cell survival (Bcl-2, Bcl-xL, Bcl-w, Mcl-1, A1 ) or cell death (Bax, Bak, and BH3-only proteins such as Bid, Bim, PUMA and many others)<sup>118,331</sup>. Additionally, they regulate integrity of mitochondria and promote or antagonize formation of the permeability transition pore (PTP)<sup>332,333</sup>.

Although apoptosis-related functions of Bcl-2 family proteins are very well established, accumulating evidence suggests that the proteins perform additional functions. For example in the ER Bcl-2 family proteins play a role in unfolded protein response, induced by protein misfolding. Bax and Bak proteins were shown to interact with IRE1 – one of the ER stress sensor protein<sup>154</sup>. Even more importantly Bcl-2 family members are involved in the regulation of intracellular calcium homeostasis including Ca<sup>2+</sup> release from the stores<sup>158,159,204</sup>. The exact nature of this regulation remains controversial and is a subject of interest of many world leading research groups. Bcl-2 has been previously suggested to decrease Ca<sup>2+</sup> concentration in the ER<sup>157,158</sup>. At the same time, several studies reported the opposite effects of Bcl-2 on ER calcium content: preservation of ER calcium by upregulation of the SERCA<sup>176</sup>. Finally, some studies showed no effects of Bcl-2 on ER Ca<sup>2+</sup> content<sup>334</sup>. Interaction between Bcl-2 and IP<sub>3</sub>Rs is already well established and is associated

---

with the inhibition of  $\text{Ca}^{2+}$  release from the ER<sup>160</sup>. Further, overexpression of Bax and Bak leads to mobilization of  $\text{Ca}^{2+}$  from the ER to mitochondria during apoptosis<sup>161</sup>. And loss of the two proteins results in dramatically reduced calcium concentration in the ER and decreased  $\text{Ca}^{2+}$  uptake by mitochondria. It appears that Bcl-2 proteins have complex roles in calcium signalling, which might depend on cell types and even experimental conditions, such as extracellular  $\text{Ca}^{2+}$  concentration.

In the current study different aspects of Bcl-2 functions were investigated, which particular focus on calcium release from the intracellular stores and cytosolic calcium extrusion in pancreatic acinar cells as well as on pharmacological Bcl-2 inhibition by BH3 mimetics. The results suggest that Bcl-2 family members are crucial for proper maintenance of intracellular  $\text{Ca}^{2+}$  homeostasis. This thesis provides data indicating that anti-apoptotic Bcl-2 members such as Bcl-2 and Bcl-xL are involved in regulation of CICR in pancreatic acinar cells. It has been postulated here that pharmacological inhibition of Bcl-2 and Bcl-xL can sensitize  $\text{IP}_3\text{Rs}$  and  $\text{RyRs}$  for activation by  $\text{Ca}^{2+}$ . Although Bcl-2 proteins have been suspected to influence  $\text{Ca}^{2+}$  release from the ER, their role in regulation of CICR has not been previously addressed. Inhibition of anti-apoptotic Bcl-2 members has profound consequences for the intracellular  $\text{Ca}^{2+}$  homeostasis. As described above, pharmacological blockade of anti-apoptotic functions of Bcl-2 leads to  $\text{Ca}^{2+}$  release from the intracellular stores and causes formation of sustained cytosolic  $\text{Ca}^{2+}$  plateau even in the absence of extracellular calcium. Interestingly, the data presented in this study demonstrate that BH3 mimetic-induced  $\text{Ca}^{2+}$  release from the intracellular stores is dependent on the presence of Bax protein. Loss of Bax substantially increases resistance of pancreatic acinar cells to treatment with BH3 mimetics. This

---

unexpected role of Bax might shed some light to the enigmatic process of passive  $\text{Ca}^{2+}$  leak. Bax appears to play a role in regulation of ER leakiness, most likely by interaction with ER calcium channels other than  $\text{IP}_3\text{Rs}$  or  $\text{RyRs}$ .

Importantly, formation of sustained cytosolic  $\text{Ca}^{2+}$  plateau in pancreatic acinar cells upon Bcl-2 inhibition immediately suggests that anti-apoptotic Bcl-2 members might be involved in regulation of  $\text{Ca}^{2+}$  extrusion from the cytosol across the plasma membrane. This notion has been further investigated and the results indicate that loss of Bcl-2 protein enhances  $\text{Ca}^{2+}$  extrusion through the plasma membrane. The PMCA is the major  $\text{Ca}^{2+}$  extrusion mechanism in non-excitabile cells, and pancreatic acinar cells are considered to have very little, if any, NXC activity. Therefore it has been postulated here that Bcl-2 is involved in the regulation of the PMCA. This notion is supported by the studies of subcellular distribution of GFP-tagged Bcl-2 in life cells and immunostaining in fixed cells. The data demonstrate close localization of Bcl-2 and the PMCA, which potentially enables direct interaction between the proteins. Although in the literature there is some evidence of Bcl-2 controlling the SERCA, the potential link to the PMCA has not yet been demonstrated. Regulation of the PMCA has very important patho-physiological implications. It appears that cells lacking functional Bcl-2 protein are much less affected by increased extracellular calcium and have been shown to die mainly of apoptosis when challenged with menadione (an inducer of ROS production), or menadione and high calcium simultaneously. These results provide novel insights into the understanding of the functions of Bcl-2 protein. So far, anti-apoptotic Bcl-2 was generally considered as purely protective and pro-survival, since it antagonizes apoptotic cell death. By negative regulation of the PMCA, Bcl-2 might also help to preserve

---

cellular energy resources. However, at the same time inhibition of the PMCA can promote  $\text{Ca}^{2+}$  overload under pathological conditions. It appears that the cells heavily challenged with toxic agents or increased extracellular calcium are more likely to die via necrosis. Therefore loss of Bcl-2 under certain conditions might protect cells from extensive necrosis by promotion of more desirable apoptotic cell death.

---

## REFERENCES

---

## References

1. Leung,P.S. & Ip,S.P. Pancreatic acinar cell: its role in acute pancreatitis. *Int. J. Biochem. Cell Biol.* **38**, 1024-1030 (2006).
2. Gittes,G.K. Developmental biology of the pancreas: a comprehensive review. *Dev. Biol.* **326**, 4-35 (2009).
3. Puri,S. & Hebrok,M. Cellular plasticity within the pancreas--lessons learned from development. *Dev. Cell* **18**, 342-356 (2010).
4. Fishman,M.P. & Melton,D.A. Pancreatic lineage analysis using a retroviral vector in embryonic mice demonstrates a common progenitor for endocrine and exocrine cells. *Int. J. Dev. Biol.* **46**, 201-207 (2002).
5. Pictet,R.L., Clark,W.R., Williams,R.H. & Rutter,W.J. An ultrastructural analysis of the developing embryonic pancreas. *Dev. Biol.* **29**, 436-467 (1972).
6. Shen,C.N., Horb,M.E., Slack,J.M. & Tosh,D. Transdifferentiation of pancreas to liver. *Mech. Dev.* **120**, 107-116 (2003).
7. Wasle,B. & Edwardson,J.M. The regulation of exocytosis in the pancreatic acinar cell. *Cell Signal.* **14**, 191-197 (2002).
8. Sollner,T.H. Regulated exocytosis and SNARE function (Review). *Mol. Membr. Biol.* **20**, 209-220 (2003).
9. Toonen,R.F. & Verhage,M. Munc18-1 in secretion: lonely Munc joins SNARE team and takes control. *Trends Neurosci.* **30**, 564-572 (2007).
10. Gerber,S.H. & Sudhof,T.C. Molecular determinants of regulated exocytosis. *Diabetes* **51 Suppl 1**, S3-11 (2002).
11. Jahn,R. & Scheller,R.H. SNAREs--engines for membrane fusion. *Nat. Rev. Mol. Cell Biol.* **7**, 631-643 (2006).
12. Gerber,S.H. & Sudhof,T.C. Molecular determinants of regulated exocytosis. *Diabetes* **51 Suppl 1**, S3-11 (2002).
13. Hanson,P.I., Heuser,J.E. & Jahn,R. Neurotransmitter release - four years of SNARE complexes. *Curr. Opin. Neurobiol.* **7**, 310-315 (1997).
14. Jahn,R. & Sudhof,T.C. Membrane fusion and exocytosis. *Annu. Rev. Biochem.* **68**, 863-911 (1999).
15. Weber,T. *et al.* SNAREpins: minimal machinery for membrane fusion. *Cell* **92**, 759-772 (1998).

- 
16. Verhage, M. *et al.* Synaptic assembly of the brain in the absence of neurotransmitter secretion. *Science* **287**, 864-869 (2000).
  17. Gaisano, H.Y., Sheu, L., Foskett, J.K. & Trimble, W.S. Tetanus toxin light chain cleaves a vesicle-associated membrane protein (VAMP) isoform 2 in rat pancreatic zymogen granules and inhibits enzyme secretion. *J. Biol. Chem.* **269**, 17062-17066 (1994).
  18. Gaisano, H.Y. *et al.* Distinct cellular locations of the syntaxin family of proteins in rat pancreatic acinar cells. *Mol. Biol. Cell* **7**, 2019-2027 (1996).
  19. Gaisano, H.Y., Sheu, L., Wong, P.P., Klip, A. & Trimble, W.S. SNAP-23 is located in the basolateral plasma membrane of rat pancreatic acinar cells. *FEBS Lett.* **414**, 298-302 (1997).
  20. Gaisano, H.Y. *et al.* Snare protein expression and adenoviral transfection of amphicrine AR42J. *Biochem. Biophys. Res. Commun.* **260**, 781-784 (1999).
  21. Hodel, A. *et al.* Cholesterol-dependent interaction of syncollin with the membrane of the pancreatic zymogen granule. *Biochem. J.* **356**, 843-850 (2001).
  22. Edwardson, J.M., An, S. & Jahn, R. The secretory granule protein syncollin binds to syntaxin in a Ca<sup>2+</sup>(+)-sensitive manner. *Cell* **90**, 325-333 (1997).
  23. Rizzuto, R. *et al.* Ca<sup>2+</sup> transfer from the ER to mitochondria: when, how and why. *Biochim. Biophys. Acta* **1787**, 1342-1351 (2009).
  24. Putney, J.W., Jr. A model for receptor-regulated calcium entry. *Cell Calcium* **7**, 1-12 (1986).
  25. Putney, J.W., Jr. New molecular players in capacitative Ca<sup>2+</sup> entry. *J. Cell Sci.* **120**, 1959-1965 (2007).
  26. Feske, S. *et al.* A mutation in Orai1 causes immune deficiency by abrogating CRAC channel function. *Nature* **441**, 179-185 (2006).
  27. Lis, A. *et al.* CRACM1, CRACM2, and CRACM3 are store-operated Ca<sup>2+</sup> channels with distinct functional properties. *Curr. Biol.* **17**, 794-800 (2007).
  28. Roberts-Thomson, S.J., Peters, A.A., Grice, D.M. & Monteith, G.R. ORAI-mediated calcium entry: mechanism and roles, diseases and pharmacology. *Pharmacol. Ther.* **127**, 121-130 (2010).
  29. Penna, A. *et al.* The CRAC channel consists of a tetramer formed by Stim-induced dimerization of Orai dimers. *Nature* **456**, 116-120 (2008).
  30. Parker, N.J., Begley, C.G., Smith, P.J. & Fox, R.M. Molecular cloning of a novel human gene (D11S4896E) at chromosomal region 11p15.5. *Genomics* **37**, 253-256 (1996).

- 
31. Roos,J. *et al.* STIM1, an essential and conserved component of store-operated Ca<sub>2</sub><sup>+</sup> channel function. *J. Cell Biol.* **169**, 435-445 (2005).
  32. Liou,J. *et al.* STIM is a Ca<sub>2</sub><sup>+</sup> sensor essential for Ca<sub>2</sub><sup>+</sup>-store-depletion-triggered Ca<sub>2</sub><sup>+</sup> influx. *Curr. Biol.* **15**, 1235-1241 (2005).
  33. Cahalan,M.D. STIMulating store-operated Ca(2+) entry. *Nat. Cell Biol.* **11**, 669-677 (2009).
  34. Lopez,J.J., Salido,G.M., Pariente,J.A. & Rosado,J.A. Interaction of STIM1 with endogenously expressed human canonical TRP1 upon depletion of intracellular Ca<sub>2</sub><sup>+</sup> stores. *J. Biol. Chem.* **281**, 28254-28264 (2006).
  35. Jardin,I., Lopez,J.J., Salido,G.M. & Rosado,J.A. Orai1 mediates the interaction between STIM1 and hTRPC1 and regulates the mode of activation of hTRPC1-forming Ca<sub>2</sub><sup>+</sup> channels. *J. Biol. Chem.* **283**, 25296-25304 (2008).
  36. Salido,G.M., Jardin,I. & Rosado,J.A. The TRPC ion channels: association with Orai1 and STIM1 proteins and participation in capacitative and non-capacitative calcium entry. *Adv. Exp. Med. Biol.* **704**, 413-433 (2011).
  37. Brandman,O., Liou,J., Park,W.S. & Meyer,T. STIM2 is a feedback regulator that stabilizes basal cytosolic and endoplasmic reticulum Ca<sub>2</sub><sup>+</sup> levels. *Cell* **131**, 1327-1339 (2007).
  38. Soboloff,J. *et al.* STIM2 is an inhibitor of STIM1-mediated store-operated Ca<sub>2</sub><sup>+</sup> Entry. *Curr. Biol.* **16**, 1465-1470 (2006).
  39. Parekh,A.B. Store-operated CRAC channels: function in health and disease. *Nat. Rev. Drug Discov.* **9**, 399-410 (2010).
  40. Sutton,R., Petersen,O.H. & Pandol,S.J. Pancreatitis and calcium signalling: report of an international workshop. *Pancreas* **36**, e1-14 (2008).
  41. Pandol,S.J., Saluja,A.K., Imrie,C.W. & Banks,P.A. Acute pancreatitis: bench to the bedside. *Gastroenterology* **133**, 1056 (2007).
  42. Toescu,E.C., Gallacher,D.V. & Petersen,O.H. Identical regional mechanisms of intracellular free Ca<sub>2</sub><sup>+</sup> concentration increase during polarized agonist-evoked Ca<sub>2</sub><sup>+</sup> response in pancreatic acinar cells. *Biochem. J.* **304** ( Pt 1), 313-316 (1994).
  43. Kasai,H., Li,Y.X. & Miyashita,Y. Subcellular distribution of Ca<sub>2</sub><sup>+</sup> release channels underlying Ca<sub>2</sub><sup>+</sup> waves and oscillations in exocrine pancreas. *Cell* **74**, 669-677 (1993).
  44. Baumgartner,H.K. *et al.* Calcium elevation in mitochondria is the main Ca<sub>2</sub><sup>+</sup> requirement for mitochondrial permeability transition pore (mPTP) opening. *J. Biol. Chem.* **284**, 20796-20803 (2009).

- 
45. Gerasimenko, J.V. *et al.* Menadione-induced apoptosis: roles of cytosolic Ca<sup>2+</sup> elevations and the mitochondrial permeability transition pore. *J. Cell Sci.* **115**, 485-497 (2002).
  46. Criddle, D.N. *et al.* Calcium signalling and pancreatic cell death: apoptosis or necrosis? *Cell Death. Differ.* **14**, 1285-1294 (2007).
  47. Gerasimenko, O.V., Gerasimenko, J.V., Petersen, O.H. & Tepikin, A.V. Short pulses of acetylcholine stimulation induce cytosolic Ca<sup>2+</sup> signals that are excluded from the nuclear region in pancreatic acinar cells. *Pflugers Arch.* **432**, 1055-1061 (1996).
  48. Petersen, O.H. & Sutton, R. Ca<sup>2+</sup> signalling and pancreatitis: effects of alcohol, bile and coffee. *Trends Pharmacol. Sci.* **27**, 113-120 (2006).
  49. Cancela, J.M. Specific Ca<sup>2+</sup> signaling evoked by cholecystokinin and acetylcholine: the roles of NAADP, cADPR, and IP<sub>3</sub>. *Annu. Rev. Physiol* **63**, 99-117 (2001).
  50. Williams, J.A. Intracellular signaling mechanisms activated by cholecystokinin-regulating synthesis and secretion of digestive enzymes in pancreatic acinar cells. *Annu. Rev. Physiol* **63**, 77-97 (2001).
  51. Lee, H.C. Mechanisms of calcium signaling by cyclic ADP-ribose and NAADP. *Physiol Rev.* **77**, 1133-1164 (1997).
  52. Chini, E.N., Beers, K.W. & Dousa, T.P. Nicotinate adenine dinucleotide phosphate (NAADP) triggers a specific calcium release system in sea urchin eggs. *J. Biol. Chem.* **270**, 3216-3223 (1995).
  53. Churchill, G.C. *et al.* NAADP mobilizes Ca<sup>2+</sup> from reserve granules, lysosome-related organelles, in sea urchin eggs. *Cell* **111**, 703-708 (2002).
  54. Genazzani, A.A. & Galione, A. Nicotinic acid-adenine dinucleotide phosphate mobilizes Ca<sup>2+</sup> from a thapsigargin-insensitive pool. *Biochem. J.* **315** ( Pt 3), 721-725 (1996).
  55. Galione, A. & Petersen, O.H. The NAADP receptor: new receptors or new regulation? *Mol. Interv.* **5**, 73-79 (2005).
  56. Chini, E.N. & Dousa, T.P. Nicotinate-adenine dinucleotide phosphate-induced Ca<sup>2+</sup>-release does not behave as a Ca<sup>2+</sup>-induced Ca<sup>2+</sup>-release system. *Biochem. J.* **316** ( Pt 3), 709-711 (1996).
  57. Petersen, O.H., Petersen, C.C. & Kasai, H. Calcium and hormone action. *Annu. Rev. Physiol* **56**, 297-319 (1994).
  58. Liddle, R.A. Cholecystokinin cells. *Annu. Rev. Physiol* **59**, 221-242 (1997).

- 
59. Williams, J.A. Intracellular regulatory mechanisms in pancreatic acinar cellular function. *Curr. Opin. Gastroenterol.* **15**, 385-391 (1999).
  60. Matozaki, T. *et al.* Two functionally distinct cholecystokinin receptors show different modes of action on Ca<sup>2+</sup> mobilization and phospholipid hydrolysis in isolated rat pancreatic acini. Studies using a new cholecystokinin analog, JMV-180. *J. Biol. Chem.* **265**, 6247-6254 (1990).
  61. Yamasaki, M. *et al.* Role of NAADP and cADPR in the induction and maintenance of agonist-evoked Ca<sup>2+</sup> spiking in mouse pancreatic acinar cells. *Curr. Biol.* **15**, 874-878 (2005).
  62. Cancela, J.M. & Petersen, O.H. The cyclic ADP ribose antagonist 8-NH<sub>2</sub>-cADP-ribose blocks cholecystokinin-evoked cytosolic Ca<sup>2+</sup> spiking in pancreatic acinar cells. *Pflugers Arch.* **435**, 746-748 (1998).
  63. Ashby, M.C. & Tepikin, A.V. Polarized calcium and calmodulin signaling in secretory epithelia. *Physiol Rev.* **82**, 701-734 (2002).
  64. Montell, C. The latest waves in calcium signaling. *Cell* **122**, 157-163 (2005).
  65. Thorn, P., Lawrie, A.M., Smith, P.M., Gallacher, D.V. & Petersen, O.H. Local and global cytosolic Ca<sup>2+</sup> oscillations in exocrine cells evoked by agonists and inositol trisphosphate. *Cell* **74**, 661-668 (1993).
  66. Nathanson, M.H., Fallon, M.B., Padfield, P.J. & Maranto, A.R. Localization of the type 3 inositol 1,4,5-trisphosphate receptor in the Ca<sup>2+</sup> wave trigger zone of pancreatic acinar cells. *J. Biol. Chem.* **269**, 4693-4696 (1994).
  67. Leite, M.F., Dranoff, J.A., Gao, L. & Nathanson, M.H. Expression and subcellular localization of the ryanodine receptor in rat pancreatic acinar cells. *Biochem. J.* **337** ( Pt 2), 305-309 (1999).
  68. Straub, S.V., Giovannucci, D.R. & Yule, D.I. Calcium wave propagation in pancreatic acinar cells: functional interaction of inositol 1,4,5-trisphosphate receptors, ryanodine receptors, and mitochondria. *J. Gen. Physiol* **116**, 547-560 (2000).
  69. Ashby, M.C. *et al.* Localized Ca<sup>2+</sup> uncaging reveals polarized distribution of Ca<sup>2+</sup>-sensitive Ca<sup>2+</sup> release sites: mechanism of unidirectional Ca<sup>2+</sup> waves. *J. Cell Biol.* **158**, 283-292 (2002).
  70. Park, M.K., Tepikin, A.V. & Petersen, O.H. What can we learn about cell signalling by combining optical imaging and patch clamp techniques? *Pflugers Arch.* **444**, 305-316 (2002).
  71. Morrison, L.E. Basic principles of fluorescence and energy transfer. *Methods Mol. Biol.* **429**, 3-19 (2008).

- 
72. Knot,H.J. *et al.* Twenty years of calcium imaging: cell physiology to dye for. *Mol. Interv.* **5**, 112-127 (2005).
  73. Grynkiewicz,G., Poenie,M. & Tsien,R.Y. A new generation of Ca<sup>2+</sup> indicators with greatly improved fluorescence properties. *J. Biol. Chem.* **260**, 3440-3450 (1985).
  74. Gee,K.R. *et al.* Chemical and physiological characterization of fluo-4 Ca(2+)-indicator dyes. *Cell Calcium* **27**, 97-106 (2000).
  75. SHIMOMURA,O., JOHNSON,F.H. & SAIGA,Y. Extraction, purification and properties of aequorin, a bioluminescent protein from the luminous hydromedusan, Aequorea. *J. Cell Comp Physiol* **59**, 223-239 (1962).
  76. Cody,C.W., Prasher,D.C., Westler,W.M., Prendergast,F.G. & Ward,W.W. Chemical structure of the hexapeptide chromophore of the Aequorea green-fluorescent protein. *Biochemistry* **32**, 1212-1218 (1993).
  77. Ormo,M. *et al.* Crystal structure of the Aequorea victoria green fluorescent protein. *Science* **273**, 1392-1395 (1996).
  78. Margolin,W. Green fluorescent protein as a reporter for macromolecular localization in bacterial cells. *Methods* **20**, 62-72 (2000).
  79. Gerdes,H.H. & Kaether,C. Green fluorescent protein: applications in cell biology. *FEBS Lett.* **389**, 44-47 (1996).
  80. Chalfie,M., Tu,Y., Euskirchen,G., Ward,W.W. & Prasher,D.C. Green fluorescent protein as a marker for gene expression. *Science* **263**, 802-805 (1994).
  81. Miyawaki,A. *et al.* Fluorescent indicators for Ca<sup>2+</sup> based on green fluorescent proteins and calmodulin. *Nature* **388**, 882-887 (1997).
  82. Miyawaki,A., Griesbeck,O., Heim,R. & Tsien,R.Y. Dynamic and quantitative Ca<sup>2+</sup> measurements using improved cameleons. *Proc. Natl. Acad. Sci. U. S. A* **96**, 2135-2140 (1999).
  83. Palmer,A.E., Jin,C., Reed,J.C. & Tsien,R.Y. Bcl-2-mediated alterations in endoplasmic reticulum Ca<sup>2+</sup> analyzed with an improved genetically encoded fluorescent sensor. *Proc. Natl. Acad. Sci. U. S. A* **101**, 17404-17409 (2004).
  84. Nagai,T., Sawano,A., Park,E.S. & Miyawaki,A. Circularly permuted green fluorescent proteins engineered to sense Ca<sup>2+</sup>. *Proc. Natl. Acad. Sci. U. S. A* **98**, 3197-3202 (2001).
  85. Miyawaki,A., Mizuno,H., Nagai,T. & Sawano,A. Development of genetically encoded fluorescent indicators for calcium. *Methods Enzymol.* **360**, 202-225 (2003).

- 
86. Ghaneh,P., Costello,E. & Neoptolemos,J.P. Biology and management of pancreatic cancer. *Postgrad. Med. J.* **84**, 478-497 (2008).
  87. Cancer Research UK. Pancreatic cancer risk factors. 4-11-2008. Internet Communication
  88. Sutton,R. *et al.* Signal transduction, calcium and acute pancreatitis. *Pancreatology.* **3**, 497-505 (2003).
  89. Lowenfels,A.B., Sullivan,T., Fiorianti,J. & Maisonneuve,P. The epidemiology and impact of pancreatic diseases in the United States. *Curr. Gastroenterol. Rep.* **7**, 90-95 (2005).
  90. Swaroop,V.S., Chari,S.T. & Clain,J.E. Severe acute pancreatitis. *JAMA* **291**, 2865-2868 (2004).
  91. Uhl,W. *et al.* IAP Guidelines for the Surgical Management of Acute Pancreatitis. *Pancreatology.* **2**, 565-573 (2002).
  92. Armstrong,C.P. & Taylor,T.V. Pancreatic-duct reflux and acute gallstone pancreatitis. *Ann. Surg.* **204**, 59-64 (1986).
  93. Vonlaufen,A., Wilson,J.S. & Apte,M.V. Molecular mechanisms of pancreatitis: current opinion. *J. Gastroenterol. Hepatol.* **23**, 1339-1348 (2008).
  94. Kim,J.Y. *et al.* Transporter-mediated bile acid uptake causes Ca<sup>2+</sup>-dependent cell death in rat pancreatic acinar cells. *Gastroenterology* **122**, 1941-1953 (2002).
  95. DiMagno,E.P., Shorter,R.G., Taylor,W.F. & Go,V.L. Relationships between pancreaticobiliary ductal anatomy and pancreatic ductal and parenchymal histology. *Cancer* **49**, 361-368 (1982).
  96. Durbec,J.P., Bidart,J.M. & Sarles,H. Risks of chronic pancreatitis, hepatocirrhosis and pancreas cancer. Role of alcohol consumption, results of 3 retrospective studies (cases-controls). *Mater. Med. Pol.* **13**, 10-14 (1981).
  97. Steinberg,W. & Tenner,S. Acute pancreatitis. *N. Engl. J. Med.* **330**, 1198-1210 (1994).
  98. Werner,J. *et al.* Alcoholic pancreatitis in rats: injury from nonoxidative metabolites of ethanol. *Am. J. Physiol Gastrointest. Liver Physiol* **283**, G65-G73 (2002).
  99. Pandol,S.J. *et al.* Ethanol diet increases the sensitivity of rats to pancreatitis induced by cholecystikinin octapeptide. *Gastroenterology* **117**, 706-716 (1999).

- 
100. Criddle,D.N. *et al.* Ethanol toxicity in pancreatic acinar cells: mediation by nonoxidative fatty acid metabolites. *Proc. Natl. Acad. Sci. U. S. A* **101**, 10738-10743 (2004).
  101. Gukovskaya,A.S. *et al.* Ethanol metabolism and transcription factor activation in pancreatic acinar cells in rats. *Gastroenterology* **122**, 106-118 (2002).
  102. Haber,P.S. *et al.* Non-oxidative metabolism of ethanol by rat pancreatic acini. *Pancreatology*. **4**, 82-89 (2004).
  103. Lugea,A., Gukovsky,I., Gukovskaya,A.S. & Pandol,S.J. Nonoxidative ethanol metabolites alter extracellular matrix protein content in rat pancreas. *Gastroenterology* **125**, 1845-1859 (2003).
  104. Haber,P.S., Wilson,J.S., Apte,M.V., Korsten,M.A. & Pirola,R.C. Chronic ethanol consumption increases the fragility of rat pancreatic zymogen granules. *Gut* **35**, 1474-1478 (1994).
  105. Haber,P.S., Wilson,J.S., Apte,M.V. & Pirola,R.C. Fatty acid ethyl esters increase rat pancreatic lysosomal fragility. *J. Lab Clin. Med.* **121**, 759-764 (1993).
  106. Hungund,B.L., Goldstein,D.B., Villegas,F. & Cooper,T.B. Formation of fatty acid ethyl esters during chronic ethanol treatment in mice. *Biochem. Pharmacol.* **37**, 3001-3004 (1988).
  107. Lange,L.G. & Sobel,B.E. Mitochondrial dysfunction induced by fatty acid ethyl esters, myocardial metabolites of ethanol. *J. Clin. Invest* **72**, 724-731 (1983).
  108. Criddle,D.N. *et al.* Fatty acid ethyl esters cause pancreatic calcium toxicity via inositol trisphosphate receptors and loss of ATP synthesis. *Gastroenterology* **130**, 781-793 (2006).
  109. Criddle,D.N., Sutton,R. & Petersen,O.H. Role of Ca<sup>2+</sup> in pancreatic cell death induced by alcohol metabolites. *J. Gastroenterol. Hepatol.* **21 Suppl 3**, S14-S17 (2006).
  110. Kloppel,G. & Maillet,B. Pathology of acute and chronic pancreatitis. *Pancreas* **8**, 659-670 (1993).
  111. Bhatia,M. Apoptosis of pancreatic acinar cells in acute pancreatitis: is it good or bad? *J. Cell Mol. Med.* **8**, 402-409 (2004).
  112. Bhatia,M. *et al.* Induction of apoptosis in pancreatic acinar cells reduces the severity of acute pancreatitis. *Biochem. Biophys. Res. Commun.* **246**, 476-483 (1998).

- 
113. Shibue,T. & Taniguchi,T. BH3-only proteins: integrated control point of apoptosis. *Int. J. Cancer* **119**, 2036-2043 (2006).
  114. Melino,G., Knight,R.A. & Nicotera,P. How many ways to die? How many different models of cell death? *Cell Death. Differ.* **12 Suppl 2**, 1457-1462 (2005).
  115. Willis,S.N. *et al.* Apoptosis initiated when BH3 ligands engage multiple Bcl-2 homologs, not Bax or Bak. *Science* **315**, 856-859 (2007).
  116. Danial,N.N. & Korsmeyer,S.J. Cell death: critical control points. *Cell* **116**, 205-219 (2004).
  117. Boldin,M.P., Goncharov,T.M., Goltsev,Y.V. & Wallach,D. Involvement of MACH, a novel MORT1/FADD-interacting protease, in Fas/APO-1- and TNF receptor-induced cell death. *Cell* **85**, 803-815 (1996).
  118. Youle,R.J. & Strasser,A. The BCL-2 protein family: opposing activities that mediate cell death. *Nat. Rev. Mol. Cell Biol.* **9**, 47-59 (2008).
  119. Veis,D.J., Sorenson,C.M., Shutter,J.R. & Korsmeyer,S.J. Bcl-2-deficient mice demonstrate fulminant lymphoid apoptosis, polycystic kidneys, and hypopigmented hair. *Cell* **75**, 229-240 (1993).
  120. Motoyama,N. *et al.* Massive cell death of immature hematopoietic cells and neurons in Bcl-x-deficient mice. *Science* **267**, 1506-1510 (1995).
  121. Ross,A.J. *et al.* Testicular degeneration in Bclw-deficient mice. *Nat. Genet.* **18**, 251-256 (1998).
  122. Tsujimoto,Y., Finger,L.R., Yunis,J., Nowell,P.C. & Croce,C.M. Cloning of the chromosome breakpoint of neoplastic B cells with the t(14;18) chromosome translocation. *Science* **226**, 1097-1099 (1984).
  123. Muchmore,S.W. *et al.* X-ray and NMR structure of human Bcl-xL, an inhibitor of programmed cell death. *Nature* **381**, 335-341 (1996).
  124. Chipuk,J.E., Moldoveanu,T., Llambi,F., Parsons,M.J. & Green,D.R. The BCL-2 family reunion. *Mol. Cell* **37**, 299-310 (2010).
  125. Willis,S.N. *et al.* Proapoptotic Bak is sequestered by Mcl-1 and Bcl-xL, but not Bcl-2, until displaced by BH3-only proteins. *Genes Dev.* **19**, 1294-1305 (2005).
  126. Sattler,M. *et al.* Structure of Bcl-xL-Bak peptide complex: recognition between regulators of apoptosis. *Science* **275**, 983-986 (1997).
  127. Huang,D.C. & Strasser,A. BH3-Only proteins-essential initiators of apoptotic cell death. *Cell* **103**, 839-842 (2000).

- 
128. Petros,A.M. *et al.* Rationale for Bcl-xL/Bad peptide complex formation from structure, mutagenesis, and biophysical studies. *Protein Sci.* **9**, 2528-2534 (2000).
  129. Liu,X., Dai,S., Zhu,Y., Marrack,P. & Kappler,J.W. The structure of a Bcl-xL/Bim fragment complex: implications for Bim function. *Immunity.* **19**, 341-352 (2003).
  130. Denisov,A.Y. *et al.* Structural model of the BCL-w-BID peptide complex and its interactions with phospholipid micelles. *Biochemistry* **45**, 2250-2256 (2006).
  131. Chou,J.J., Li,H., Salvesen,G.S., Yuan,J. & Wagner,G. Solution structure of BID, an intracellular amplifier of apoptotic signaling. *Cell* **96**, 615-624 (1999).
  132. Lama,D. & Sankararamakrishnan,R. Anti-apoptotic Bcl-XL protein in complex with BH3 peptides of pro-apoptotic Bak, Bad, and Bim proteins: comparative molecular dynamics simulations. *Proteins* **73**, 492-514 (2008).
  133. Letai,A. *et al.* Distinct BH3 domains either sensitize or activate mitochondrial apoptosis, serving as prototype cancer therapeutics. *Cancer Cell* **2**, 183-192 (2002).
  134. Kuwana,T. *et al.* BH3 domains of BH3-only proteins differentially regulate Bax-mediated mitochondrial membrane permeabilization both directly and indirectly. *Mol. Cell* **17**, 525-535 (2005).
  135. Chen,L. *et al.* Differential targeting of prosurvival Bcl-2 proteins by their BH3-only ligands allows complementary apoptotic function. *Mol. Cell* **17**, 393-403 (2005).
  136. Szegezdi,E., Macdonald,D.C., Ni,C.T., Gupta,S. & Samali,A. Bcl-2 family on guard at the ER. *Am. J. Physiol Cell Physiol* **296**, C941-C953 (2009).
  137. Zong,W.X., Lindsten,T., Ross,A.J., MacGregor,G.R. & Thompson,C.B. BH3-only proteins that bind pro-survival Bcl-2 family members fail to induce apoptosis in the absence of Bax and Bak. *Genes Dev.* **15**, 1481-1486 (2001).
  138. Wang,K., Yin,X.M., Chao,D.T., Milliman,C.L. & Korsmeyer,S.J. BID: a novel BH3 domain-only death agonist. *Genes Dev.* **10**, 2859-2869 (1996).
  139. Harada,H., Quearry,B., Ruiz-Vela,A. & Korsmeyer,S.J. Survival factor-induced extracellular signal-regulated kinase phosphorylates BIM, inhibiting its association with BAX and proapoptotic activity. *Proc. Natl. Acad. Sci. U. S. A* **101**, 15313-15317 (2004).
  140. Cartron,P.F. *et al.* The first alpha helix of Bax plays a necessary role in its ligand-induced activation by the BH3-only proteins Bid and PUMA. *Mol. Cell* **16**, 807-818 (2004).

- 
141. Puthalakath,H., Huang,D.C., O'Reilly,L.A., King,S.M. & Strasser,A. The proapoptotic activity of the Bcl-2 family member Bim is regulated by interaction with the dynein motor complex. *Mol. Cell* **3**, 287-296 (1999).
  142. Puthalakath,H. *et al.* Bmf: a proapoptotic BH3-only protein regulated by interaction with the myosin V actin motor complex, activated by anoikis. *Science* **293**, 1829-1832 (2001).
  143. Puthalakath,H. & Strasser,A. Keeping killers on a tight leash: transcriptional and post-translational control of the pro-apoptotic activity of BH3-only proteins. *Cell Death. Differ.* **9**, 505-512 (2002).
  144. Hsu,Y.T., Wolter,K.G. & Youle,R.J. Cytosol-to-membrane redistribution of Bax and Bcl-X(L) during apoptosis. *Proc. Natl. Acad. Sci. U. S. A* **94**, 3668-3672 (1997).
  145. Hsu,Y.T. & Youle,R.J. Bax in murine thymus is a soluble monomeric protein that displays differential detergent-induced conformations. *J. Biol. Chem.* **273**, 10777-10783 (1998).
  146. Nechushtan,A., Smith,C.L., Lamensdorf,I., Yoon,S.H. & Youle,R.J. Bax and Bak coalesce into novel mitochondria-associated clusters during apoptosis. *J. Cell Biol.* **153**, 1265-1276 (2001).
  147. Wei,M.C. *et al.* Proapoptotic BAX and BAK: a requisite gateway to mitochondrial dysfunction and death. *Science* **292**, 727-730 (2001).
  148. Wei,M.C. *et al.* tBID, a membrane-targeted death ligand, oligomerizes BAK to release cytochrome c. *Genes Dev.* **14**, 2060-2071 (2000).
  149. Moldoveanu,T. *et al.* The X-ray structure of a BAK homodimer reveals an inhibitory zinc binding site. *Mol. Cell* **24**, 677-688 (2006).
  150. Oltvai,Z.N., Milliman,C.L. & Korsmeyer,S.J. Bcl-2 heterodimerizes in vivo with a conserved homolog, Bax, that accelerates programmed cell death. *Cell* **74**, 609-619 (1993).
  151. Cheng,E.H., Sheiko,T.V., Fisher,J.K., Craigen,W.J. & Korsmeyer,S.J. VDAC2 inhibits BAK activation and mitochondrial apoptosis. *Science* **301**, 513-517 (2003).
  152. Oakes,S.A., Lin,S.S. & Bassik,M.C. The control of endoplasmic reticulum-initiated apoptosis by the BCL-2 family of proteins. *Curr. Mol. Med.* **6**, 99-109 (2006).
  153. Krajewski,S. *et al.* Investigation of the subcellular distribution of the bcl-2 oncoprotein: residence in the nuclear envelope, endoplasmic reticulum, and outer mitochondrial membranes. *Cancer Res.* **53**, 4701-4714 (1993).

- 
154. Hetz,C. *et al.* Proapoptotic BAX and BAK modulate the unfolded protein response by a direct interaction with IRE1alpha. *Science* **312**, 572-576 (2006).
  155. Liang,X.H. *et al.* Protection against fatal Sindbis virus encephalitis by beclin, a novel Bcl-2-interacting protein. *J. Virol.* **72**, 8586-8596 (1998).
  156. Pattingre,S. *et al.* Bcl-2 antiapoptotic proteins inhibit Beclin 1-dependent autophagy. *Cell* **122**, 927-939 (2005).
  157. Pinton,P. *et al.* Reduced loading of intracellular Ca(2+) stores and downregulation of capacitative Ca(2+) influx in Bcl-2-overexpressing cells. *J. Cell Biol.* **148**, 857-862 (2000).
  158. Foyouzi-Youssefi,R. *et al.* Bcl-2 decreases the free Ca<sup>2+</sup> concentration within the endoplasmic reticulum. *Proc. Natl. Acad. Sci. U. S. A* **97**, 5723-5728 (2000).
  159. Kuo,T.H. *et al.* Modulation of endoplasmic reticulum calcium pump by Bcl-2. *Oncogene* **17**, 1903-1910 (1998).
  160. Rong,Y.P. *et al.* Targeting Bcl-2-IP3 receptor interaction to reverse Bcl-2's inhibition of apoptotic calcium signals. *Mol. Cell* **31**, 255-265 (2008).
  161. Nutt,L.K. *et al.* Bax and Bak promote apoptosis by modulating endoplasmic reticular and mitochondrial Ca<sup>2+</sup> stores. *J. Biol. Chem.* **277**, 9219-9225 (2002).
  162. Oakes,S.A. *et al.* Proapoptotic BAX and BAK regulate the type 1 inositol trisphosphate receptor and calcium leak from the endoplasmic reticulum. *Proc. Natl. Acad. Sci. U. S. A* **102**, 105-110 (2005).
  163. Vogelstein,B., Lane,D. & Levine,A.J. Surfing the p53 network. *Nature* **408**, 307-310 (2000).
  164. Vogler,M., Dinsdale,D., Dyer,M.J. & Cohen,G.M. Bcl-2 inhibitors: small molecules with a big impact on cancer therapy. *Cell Death. Differ.* **16**, 360-367 (2009).
  165. Adams,J.M. & Cory,S. The Bcl-2 apoptotic switch in cancer development and therapy. *Oncogene* **26**, 1324-1337 (2007).
  166. Zhang,L., Ming,L. & Yu,J. BH3 mimetics to improve cancer therapy; mechanisms and examples. *Drug Resist. Updat.* **10**, 207-217 (2007).
  167. Wang,J.L. *et al.* Structure-based discovery of an organic compound that binds Bcl-2 protein and induces apoptosis of tumor cells. *Proc. Natl. Acad. Sci. U. S. A* **97**, 7124-7129 (2000).

- 
168. Lessene,G., Czabotar,P.E. & Colman,P.M. BCL-2 family antagonists for cancer therapy. *Nat. Rev. Drug Discov.* **7**, 989-1000 (2008).
169. Walensky,L.D. *et al.* Activation of apoptosis in vivo by a hydrocarbon-stapled BH3 helix. *Science* **305**, 1466-1470 (2004).
170. Degterev,A. *et al.* Identification of small-molecule inhibitors of interaction between the BH3 domain and Bcl-xL. *Nat. Cell Biol.* **3**, 173-182 (2001).
171. Shangary,S. & Johnson,D.E. Recent advances in the development of anticancer agents targeting cell death inhibitors in the Bcl-2 protein family. *Leukemia* **17**, 1470-1481 (2003).
172. Hao,J.H., Yu,M., Liu,F.T., Newland,A.C. & Jia,L. Bcl-2 inhibitors sensitize tumor necrosis factor-related apoptosis-inducing ligand-induced apoptosis by uncoupling of mitochondrial respiration in human leukemic CEM cells. *Cancer Res.* **64**, 3607-3616 (2004).
173. Hanahan,D. & Weinberg,R.A. The hallmarks of cancer. *Cell* **100**, 57-70 (2000).
174. Camello,C., Lomax,R., Petersen,O.H. & Tepikin,A.V. Calcium leak from intracellular stores--the enigma of calcium signalling. *Cell Calcium* **32**, 355-361 (2002).
175. Lomax,R.B., Camello,C., Van Coppenolle,F., Petersen,O.H. & Tepikin,A.V. Basal and physiological Ca(2+) leak from the endoplasmic reticulum of pancreatic acinar cells. Second messenger-activated channels and translocons. *J. Biol. Chem.* **277**, 26479-26485 (2002).
176. Wang,N.S., Unkila,M.T., Reineks,E.Z. & Distelhorst,C.W. Transient expression of wild-type or mitochondrially targeted Bcl-2 induces apoptosis, whereas transient expression of endoplasmic reticulum-targeted Bcl-2 is protective against Bax-induced cell death. *J. Biol. Chem.* **276**, 44117-44128 (2001).
177. Yamamoto,K., Ichijo,H. & Korsmeyer,S.J. BCL-2 is phosphorylated and inactivated by an ASK1/Jun N-terminal protein kinase pathway normally activated at G(2)/M. *Mol. Cell Biol.* **19**, 8469-8478 (1999).
178. Knudson,C.M., Tung,K.S., Tourtellotte,W.G., Brown,G.A. & Korsmeyer,S.J. Bax-deficient mice with lymphoid hyperplasia and male germ cell death. *Science* **270**, 96-99 (1995).
179. The Jackson Laboratory. Coat color of Baxtm1Sjk mice. The Jackson Laboratory Website . 2012.  
Electronic Citation

- 
180. Maruyama, Y. & Petersen, O.H. Delay in granular fusion evoked by repetitive cytosolic Ca<sup>2+</sup> spikes in mouse pancreatic acinar cells. *Cell Calcium* **16**, 419-430 (1994).
  181. Gerasimenko, J.V., Sherwood, M., Tepikin, A.V., Petersen, O.H. & Gerasimenko, O.V. NAADP, cADPR and IP<sub>3</sub> all release Ca<sup>2+</sup> from the endoplasmic reticulum and an acidic store in the secretory granule area. *J. Cell Sci.* **119**, 226-238 (2006).
  182. Tirlapur, U.K. & Konig, K. Targeted transfection by femtosecond laser. *Nature* **418**, 290-291 (2002).
  183. Henke, W., Cetinsoy, C., Jung, K. & Loening, S. Non-hyperbolic calcium calibration curve of Fura-2: implications for the reliability of quantitative Ca<sup>2+</sup> measurements. *Cell Calcium* **20**, 287-292 (1996).
  184. Hirst, R.A., Harrison, C., Hirota, K. & Lambert, D.G. Measurement of [Ca<sup>2+</sup>]<sub>i</sub> in whole cell suspensions using fura-2. *Methods Mol. Biol.* **114**, 31-39 (1999).
  185. Saluja, A. *et al.* In vivo rat pancreatic acinar cell function during supramaximal stimulation with caerulein. *Am. J. Physiol* **249**, G702-G710 (1985).
  186. Saluja, A. *et al.* Subcellular redistribution of lysosomal enzymes during caerulein-induced pancreatitis. *Am. J. Physiol* **253**, G508-G516 (1987).
  187. Mareninova, O.A. *et al.* Cell death in pancreatitis: caspases protect from necrotizing pancreatitis. *J. Biol. Chem.* **281**, 3370-3381 (2006).
  188. Iino, M. Calcium dependent inositol trisphosphate-induced calcium release in the guinea-pig taenia caeci. *Biochem. Biophys. Res. Commun.* **142**, 47-52 (1987).
  189. Parys, J.B. *et al.* Isolation, characterization, and localization of the inositol 1,4,5-trisphosphate receptor protein in *Xenopus laevis* oocytes. *J. Biol. Chem.* **267**, 18776-18782 (1992).
  190. Marshall, I.C. & Taylor, C.W. Biphasic effects of cytosolic Ca<sup>2+</sup> on Ins(1,4,5)P<sub>3</sub>-stimulated Ca<sup>2+</sup> mobilization in hepatocytes. *J. Biol. Chem.* **268**, 13214-13220 (1993).
  191. Hamilton, S.L. Ryanodine receptors. *Cell Calcium* **38**, 253-260 (2005).
  192. Hirota, J. *et al.* Kinetics of calcium release by immunoaffinity-purified inositol 1,4,5-trisphosphate receptor in reconstituted lipid vesicles. *J. Biol. Chem.* **270**, 19046-19051 (1995).

- 
193. Sienaert, I. *et al.* Characterization of a cytosolic and a luminal Ca<sup>2+</sup> binding site in the type I inositol 1,4,5-trisphosphate receptor. *J. Biol. Chem.* **271**, 27005-27012 (1996).
  194. Sienaert, I. *et al.* Molecular and functional evidence for multiple Ca<sup>2+</sup>-binding domains in the type 1 inositol 1,4,5-trisphosphate receptor. *J. Biol. Chem.* **272**, 25899-25906 (1997).
  195. Meissner, G. & Henderson, J.S. Rapid calcium release from cardiac sarcoplasmic reticulum vesicles is dependent on Ca<sup>2+</sup> and is modulated by Mg<sup>2+</sup>, adenine nucleotide, and calmodulin. *J. Biol. Chem.* **262**, 3065-3073 (1987).
  196. Taylor, C.W., da Fonseca, P.C. & Morris, E.P. IP(3) receptors: the search for structure. *Trends Biochem. Sci.* **29**, 210-219 (2004).
  197. Rossi, A.M. & Taylor, C.W. Ca<sup>2+</sup> regulation of inositol 1,4,5-trisphosphate receptors: can Ca<sup>2+</sup> function without calmodulin? *Mol. Pharmacol.* **66**, 199-203 (2004).
  198. Michikawa, T. *et al.* Calmodulin mediates calcium-dependent inactivation of the cerebellar type 1 inositol 1,4,5-trisphosphate receptor. *Neuron* **23**, 799-808 (1999).
  199. Park, M.K., Petersen, O.H. & Tepikin, A.V. The endoplasmic reticulum as one continuous Ca(2+) pool: visualization of rapid Ca(2+) movements and equilibration. *EMBO J.* **19**, 5729-5739 (2000).
  200. Park, M.K., Ashby, M.C., Erdemli, G., Petersen, O.H. & Tepikin, A.V. Perinuclear, perigranular and sub-plasmalemmal mitochondria have distinct functions in the regulation of cellular calcium transport. *EMBO J.* **20**, 1863-1874 (2001).
  201. Gerasimenko, O.V. *et al.* The distribution of the endoplasmic reticulum in living pancreatic acinar cells. *Cell Calcium* **32**, 261-268 (2002).
  202. Petersen, O.H., Gerasimenko, O.V., Tepikin, A.V. & Gerasimenko, J.V. Aberrant Ca(2+) signalling through acidic calcium stores in pancreatic acinar cells. *Cell Calcium* **50**, 193-199 (2011).
  203. Petersen, O.H., Gerasimenko, O.V. & Gerasimenko, J.V. Pathobiology of acute pancreatitis: focus on intracellular calcium and calmodulin. *F1000. Med. Rep.* **3**, 15 (2011).
  204. Pinton, P. & Rizzuto, R. Bcl-2 and Ca<sup>2+</sup> homeostasis in the endoplasmic reticulum. *Cell Death. Differ.* **13**, 1409-1418 (2006).
  205. Yang, E. & Korsmeyer, S.J. Molecular thanatopsis: a discourse on the BCL2 family and cell death. *Blood* **88**, 386-401 (1996).

- 
206. Distelhorst,C.W. & Shore,G.C. Bcl-2 and calcium: controversy beneath the surface. *Oncogene* **23**, 2875-2880 (2004).
207. Gerasimenko,J., Ferdek,P., Fischer,L., Gukovskaya,A.S. & Pandol,S.J. Inhibitors of Bcl-2 protein family deplete ER Ca(2+) stores in pancreatic acinar cells. *Pflugers Arch.* (2010).
208. Maruyama,T., Kanaji,T., Nakade,S., Kanno,T. & Mikoshiba,K. 2APB, 2-aminoethoxydiphenyl borate, a membrane-penetrable modulator of Ins(1,4,5)P3-induced Ca2+ release. *J. Biochem.* **122**, 498-505 (1997).
209. Sung,K.F. *et al.* Prosurvival Bcl-2 proteins stabilize pancreatic mitochondria and protect against necrosis in experimental pancreatitis. *Exp. Cell Res.* **315**, 1975-1989 (2009).
210. Xu,X. *et al.* nNOS and Ca2+ influx in rat pancreatic acinar and submandibular salivary gland cells. *Cell Calcium* **22**, 217-228 (1997).
211. Toescu,E.C. & Petersen,O.H. Region-specific activity of the plasma membrane Ca2+ pump and delayed activation of Ca2+ entry characterize the polarized, agonist-evoked Ca2+ signals in exocrine cells. *J. Biol. Chem.* **270**, 8528-8535 (1995).
212. Rong,Y. & Distelhorst,C.W. Bcl-2 protein family members: versatile regulators of calcium signaling in cell survival and apoptosis. *Annu. Rev. Physiol* **70**, 73-91 (2008).
213. Chen,R. *et al.* Bcl-2 functionally interacts with inositol 1,4,5-trisphosphate receptors to regulate calcium release from the ER in response to inositol 1,4,5-trisphosphate. *J. Cell Biol.* **166**, 193-203 (2004).
214. White,C. *et al.* The endoplasmic reticulum gateway to apoptosis by Bcl-X(L) modulation of the InsP3R. *Nat. Cell Biol.* **7**, 1021-1028 (2005).
215. Rong,Y.P. *et al.* The BH4 domain of Bcl-2 inhibits ER calcium release and apoptosis by binding the regulatory and coupling domain of the IP3 receptor. *Proc. Natl. Acad. Sci. U. S. A* **106**, 14397-14402 (2009).
216. Burgoyne,R.D. & Clague,M.J. Calcium and calmodulin in membrane fusion. *Biochim. Biophys. Acta* **1641**, 137-143 (2003).
217. Igarashi,M. & Watanabe,M. Roles of calmodulin and calmodulin-binding proteins in synaptic vesicle recycling during regulated exocytosis at submicromolar Ca2+ concentrations. *Neurosci. Res.* **58**, 226-233 (2007).
218. Jurado,L.A., Chockalingam,P.S. & Jarrett,H.W. Apocalmodulin. *Physiol Rev.* **79**, 661-682 (1999).
219. Chin,D. & Means,A.R. Calmodulin: a prototypical calcium sensor. *Trends Cell Biol.* **10**, 322-328 (2000).

- 
220. Swindells, M.B. & Ikura, M. Pre-formation of the semi-open conformation by the apo-calmodulin C-terminal domain and implications binding IQ-motifs. *Nat. Struct. Biol.* **3**, 501-504 (1996).
221. Tripathy, A., Xu, L., Mann, G. & Meissner, G. Calmodulin activation and inhibition of skeletal muscle Ca<sup>2+</sup> release channel (ryanodine receptor). *Biophys. J.* **69**, 106-119 (1995).
222. Perin, M.S. Mirror image motifs mediate the interaction of the COOH terminus of multiple synaptotagmins with the neurexins and calmodulin. *Biochemistry* **35**, 13808-13816 (1996).
223. Quetglas, S., Leveque, C., Miquelis, R., Sato, K. & Seagar, M. Ca<sup>2+</sup>-dependent regulation of synaptic SNARE complex assembly via a calmodulin- and phospholipid-binding domain of synaptobrevin. *Proc. Natl. Acad. Sci. U. S. A* **97**, 9695-9700 (2000).
224. Campa, M.J., Kuan, C.T., O'Connor-McCourt, M.D., Bigner, D.D. & Patz, E.F., Jr. Design of a novel small peptide targeted against a tumor-specific receptor. *Biochem. Biophys. Res. Commun.* **275**, 631-636 (2000).
225. Gomez, I. *et al.* Hydrophobic complementarity determines interaction of epitope (869)HITDTNNK(876) in *Manduca sexta* Bt-R(1) receptor with loop 2 of domain II of *Bacillus thuringiensis* CryIA toxins. *J. Biol. Chem.* **277**, 30137-30143 (2002).
226. Villain, M. *et al.* De novo design of peptides targeted to the EF hands of calmodulin. *J. Biol. Chem.* **275**, 2676-2685 (2000).
227. Manion, M.K., Su, Z., Villain, M. & Blalock, J.E. A new type of Ca(2+) channel blocker that targets Ca(2+) sensors and prevents Ca(2+)-mediated apoptosis. *FASEB J.* **14**, 1297-1306 (2000).
228. Kitada, S. *et al.* Discovery, characterization, and structure-activity relationships studies of proapoptotic polyphenols targeting B-cell lymphocyte/leukemia-2 proteins. *J. Med. Chem.* **46**, 4259-4264 (2003).
229. Lei, X. *et al.* Gossypol induces Bax/Bak-independent activation of apoptosis and cytochrome c release via a conformational change in Bcl-2. *FASEB J.* **20**, 2147-2149 (2006).
230. Wang, G. *et al.* Structure-based design of potent small-molecule inhibitors of anti-apoptotic Bcl-2 proteins. *J. Med. Chem.* **49**, 6139-6142 (2006).
231. Kang, M.H. & Reynolds, C.P. Bcl-2 inhibitors: targeting mitochondrial apoptotic pathways in cancer therapy. *Clin. Cancer Res.* **15**, 1126-1132 (2009).
232. Apte, M.V., Pirola, R.C. & Wilson, J.S. Individual susceptibility to alcoholic pancreatitis. *J. Gastroenterol. Hepatol.* **23 Suppl 1**, S63-S68 (2008).

- 
233. Han,B. & Logsdon,C.D. CCK stimulates mob-1 expression and NF-kappaB activation via protein kinase C and intracellular Ca(2+). *Am. J. Physiol Cell Physiol* **278**, C344-C351 (2000).
234. Gukovskaya,A.S. *et al.* Pancreatic acinar cells produce, release, and respond to tumor necrosis factor-alpha. Role in regulating cell death and pancreatitis. *J. Clin. Invest* **100**, 1853-1862 (1997).
235. Raraty,M. *et al.* Calcium-dependent enzyme activation and vacuole formation in the apical granular region of pancreatic acinar cells. *Proc. Natl. Acad. Sci. U. S. A* **97**, 13126-13131 (2000).
236. Neoptolemos,J.P., Raraty,M., Finch,M. & Sutton,R. Acute pancreatitis: the substantial human and financial costs. *Gut* **42**, 886-891 (1998).
237. Ward,J.B., Petersen,O.H., Jenkins,S.A. & Sutton,R. Is an elevated concentration of acinar cytosolic free ionised calcium the trigger for acute pancreatitis? *Lancet* **346**, 1016-1019 (1995).
238. Laposata,E.A. & Lange,L.G. Presence of nonoxidative ethanol metabolism in human organs commonly damaged by ethanol abuse. *Science* **231**, 497-499 (1986).
239. Choi,K.J., Kim,K.S., Kim,S.H., Kim,D.K. & Park,H.S. Caffeine and 2-Aminoethoxydiphenyl Borate (2-APB) Have Different Ability to Inhibit Intracellular Calcium Mobilization in Pancreatic Acinar Cell. *Korean J. Physiol Pharmacol.* **14**, 105-111 (2010).
240. Ehrlich,B.E., Kaftan,E., Bezprozvannaya,S. & Bezprozvanny,I. The pharmacology of intracellular Ca(2+)-release channels. *Trends Pharmacol. Sci.* **15**, 145-149 (1994).
241. Toescu,E.C., O'Neill,S.C., Petersen,O.H. & Eisner,D.A. Caffeine inhibits the agonist-evoked cytosolic Ca<sup>2+</sup> signal in mouse pancreatic acinar cells by blocking inositol trisphosphate production. *J. Biol. Chem.* **267**, 23467-23470 (1992).
242. Gerasimenko,J.V. *et al.* Pancreatic protease activation by alcohol metabolite depends on Ca<sup>2+</sup> release via acid store IP<sub>3</sub> receptors. *Proc. Natl. Acad. Sci. U. S. A* **106**, 10758-10763 (2009).
243. Petersen,O.H. *et al.* Fatty acids, alcohol and fatty acid ethyl esters: toxic Ca<sup>2+</sup> signal generation and pancreatitis. *Cell Calcium* **45**, 634-642 (2009).
244. Petersen,O.H. & Tepikin,A.V. Polarized calcium signaling in exocrine gland cells. *Annu. Rev. Physiol* **70**, 273-299 (2008).
245. Jones,A.W. The drunkest drinking driver in Sweden: blood alcohol concentration 0.545% w/v. *J. Stud. Alcohol* **60**, 400-406 (1999).

- 
246. Gerasimenko, J.V. *et al.* Calmodulin protects against alcohol-induced pancreatic trypsinogen activation elicited via Ca<sup>2+</sup> release through IP<sub>3</sub> receptors. *Proc. Natl. Acad. Sci. U. S. A* **108**, 5873-5878 (2011).
247. Craske, M. *et al.* Hormone-induced secretory and nuclear translocation of calmodulin: oscillations of calmodulin concentration with the nucleus as an integrator. *Proc. Natl. Acad. Sci. U. S. A* **96**, 4426-4431 (1999).
248. Gerasimenko, J.V., Tepikin, A.V., Petersen, O.H. & Gerasimenko, O.V. Calcium uptake via endocytosis with rapid release from acidifying endosomes. *Curr. Biol.* **8**, 1335-1338 (1998).
249. Guo, L. *et al.* STAT5-glucocorticoid receptor interaction and MTF-1 regulate the expression of ZnT2 (Slc30a2) in pancreatic acinar cells. *Proc. Natl. Acad. Sci. U. S. A* **107**, 2818-2823 (2010).
250. Gerasimenko, J.V. *et al.* Bile acids induce Ca<sup>2+</sup> release from both the endoplasmic reticulum and acidic intracellular calcium stores through activation of inositol trisphosphate receptors and ryanodine receptors. *J. Biol. Chem.* **281**, 40154-40163 (2006).
251. Kruger, B., Albrecht, E. & Lerch, M.M. The role of intracellular calcium signaling in premature protease activation and the onset of pancreatitis. *Am. J. Pathol.* **157**, 43-50 (2000).
252. Adkins, C.E. *et al.* Ca<sup>2+</sup>-calmodulin inhibits Ca<sup>2+</sup> release mediated by type-1, -2 and -3 inositol trisphosphate receptors. *Biochem. J.* **345 Pt 2**, 357-363 (2000).
253. Kasri, N.N. *et al.* The N-terminal Ca<sup>2+</sup>-independent calmodulin-binding site on the inositol 1,4,5-trisphosphate receptor is responsible for calmodulin inhibition, even though this inhibition requires Ca<sup>2+</sup>. *Mol. Pharmacol.* **66**, 276-284 (2004).
254. Murphy, J.A. *et al.* Direct activation of cytosolic Ca<sup>2+</sup> signaling and enzyme secretion by cholecystokinin in human pancreatic acinar cells. *Gastroenterology* **135**, 632-641 (2008).
255. Sherwood, M.W. *et al.* Activation of trypsinogen in large endocytic vacuoles of pancreatic acinar cells. *Proc. Natl. Acad. Sci. U. S. A* **104**, 5674-5679 (2007).
256. Hofer, A.M., Curci, S., Machen, T.E. & Schulz, I. ATP regulates calcium leak from agonist-sensitive internal calcium stores. *FASEB J.* **10**, 302-308 (1996).
257. Missiaen, L. *et al.* Normal Ca<sup>2+</sup> signalling in glutathione-depleted and dithiothreitol-treated HeLa cells. *Pflugers Arch.* **423**, 480-484 (1993).

- 
258. Wissing,F., Nerou,E.P. & Taylor,C.W. A novel Ca<sup>2+</sup>-induced Ca<sup>2+</sup> release mechanism mediated by neither inositol trisphosphate nor ryanodine receptors. *Biochem. J.* **361**, 605-611 (2002).
259. Mogami,H., Tepikin,A.V. & Petersen,O.H. Termination of cytosolic Ca<sup>2+</sup> signals: Ca<sup>2+</sup> reuptake into intracellular stores is regulated by the free Ca<sup>2+</sup> concentration in the store lumen. *EMBO J.* **17**, 435-442 (1998).
260. Solovyova,N., Veselovsky,N., Toescu,E.C. & Verkhratsky,A. Ca(2+) dynamics in the lumen of the endoplasmic reticulum in sensory neurons: direct visualization of Ca(2+)-induced Ca(2+) release triggered by physiological Ca(2+) entry. *EMBO J.* **21**, 622-630 (2002).
261. Barrero,M.J., Montero,M. & Alvarez,J. Dynamics of [Ca<sup>2+</sup>] in the endoplasmic reticulum and cytoplasm of intact HeLa cells. A comparative study. *J. Biol. Chem.* **272**, 27694-27699 (1997).
262. Simon,S.M. & Blobel,G. A protein-conducting channel in the endoplasmic reticulum. *Cell* **65**, 371-380 (1991).
263. Hamman,B.D., Hendershot,L.M. & Johnson,A.E. BiP maintains the permeability barrier of the ER membrane by sealing the luminal end of the translocon pore before and early in translocation. *Cell* **92**, 747-758 (1998).
264. Bertram,L. *et al.* Genome-wide association analysis reveals putative Alzheimer's disease susceptibility loci in addition to APOE. *Am. J. Hum. Genet.* **83**, 623-632 (2008).
265. Bertram,L. The genetics of Alzheimer's disease. *Handb. Clin. Neurol.* **89**, 223-232 (2008).
266. Supnet,C. & Bezprozvanny,I. Presenilins as endoplasmic reticulum calcium leak channels and Alzheimer's disease pathogenesis. *Sci. China Life Sci.* **54**, 744-751 (2011).
267. Supnet,C. & Bezprozvanny,I. Presenilins function in ER calcium leak and Alzheimer's disease pathogenesis. *Cell Calcium* (2011).
268. Tu,H. *et al.* Presenilins form ER Ca<sup>2+</sup> leak channels, a function disrupted by familial Alzheimer's disease-linked mutations. *Cell* **126**, 981-993 (2006).
269. Nelson,O. *et al.* Familial Alzheimer disease-linked mutations specifically disrupt Ca<sup>2+</sup> leak function of presenilin 1. *J. Clin. Invest* **117**, 1230-1239 (2007).
270. Nelson,O., Supnet,C., Liu,H. & Bezprozvanny,I. Familial Alzheimer's disease mutations in presenilins: effects on endoplasmic reticulum calcium homeostasis and correlation with clinical phenotypes. *J. Alzheimers. Dis.* **21**, 781-793 (2010).

- 
271. Gabow, P.A. Autosomal dominant polycystic kidney disease. *N. Engl. J. Med.* **329**, 332-342 (1993).
272. Nauli, S.M. *et al.* Polycystins 1 and 2 mediate mechanosensation in the primary cilium of kidney cells. *Nat. Genet.* **33**, 129-137 (2003).
273. Mochizuki, T. *et al.* PKD2, a gene for polycystic kidney disease that encodes an integral membrane protein. *Science* **272**, 1339-1342 (1996).
274. Li, Y., Wright, J.M., Qian, F., Germino, G.G. & Guggino, W.B. Polycystin 2 interacts with type I inositol 1,4,5-trisphosphate receptor to modulate intracellular Ca<sup>2+</sup> signaling. *J. Biol. Chem.* **280**, 41298-41306 (2005).
275. Woodward, O.M. *et al.* Identification of a polycystin-1 cleavage product, P100, that regulates store operated Ca entry through interactions with STIM1. *PLoS. One.* **5**, e12305 (2010).
276. Santoso, N.G., Cebotaru, L. & Guggino, W.B. Polycystin-1, 2, and STIM1 interact with IP(3)R to modulate ER Ca release through the PI3K/Akt pathway. *Cell Physiol Biochem.* **27**, 715-726 (2011).
277. Schendel, S.L. *et al.* Channel formation by antiapoptotic protein Bcl-2. *Proc. Natl. Acad. Sci. U. S. A* **94**, 5113-5118 (1997).
278. Minn, A.J. *et al.* Bcl-x(L) forms an ion channel in synthetic lipid membranes. *Nature* **385**, 353-357 (1997).
279. Lam, M. *et al.* Evidence that BCL-2 represses apoptosis by regulating endoplasmic reticulum-associated Ca<sup>2+</sup> fluxes. *Proc. Natl. Acad. Sci. U. S. A* **91**, 6569-6573 (1994).
280. Annis, M.G. *et al.* Bax forms multispinning monomers that oligomerize to permeabilize membranes during apoptosis. *EMBO J.* **24**, 2096-2103 (2005).
281. Petros, A.M., Olejniczak, E.T. & Fesik, S.W. Structural biology of the Bcl-2 family of proteins. *Biochim. Biophys. Acta* **1644**, 83-94 (2004).
282. Schendel, S.L., Montal, M. & Reed, J.C. Bcl-2 family proteins as ion-channels. *Cell Death. Differ.* **5**, 372-380 (1998).
283. Chami, M. *et al.* Bcl-2 and Bax exert opposing effects on Ca<sup>2+</sup> signaling, which do not depend on their putative pore-forming region. *J. Biol. Chem.* **279**, 54581-54589 (2004).
284. Hilgemann, D.W., Nicoll, D.A. & Philipson, K.D. Charge movement during Na<sup>+</sup> translocation by native and cloned cardiac Na<sup>+</sup>/Ca<sup>2+</sup> exchanger. *Nature* **352**, 715-718 (1991).

- 
285. Cervetto,L., Lagnado,L., Perry,R.J., Robinson,D.W. & McNaughton,P.A. Extrusion of calcium from rod outer segments is driven by both sodium and potassium gradients. *Nature* **337**, 740-743 (1989).
286. Li,Z. *et al.* Cloning of the NCX2 isoform of the plasma membrane Na(+)-Ca<sup>2+</sup> exchanger. *J. Biol. Chem.* **269**, 17434-17439 (1994).
287. Nicoll,D.A. *et al.* Cloning of a third mammalian Na<sup>+</sup>-Ca<sup>2+</sup> exchanger, NCX3. *J. Biol. Chem.* **271**, 24914-24921 (1996).
288. Guerini,D., Coletto,L. & Carafoli,E. Exporting calcium from cells. *Cell Calcium* **38**, 281-289 (2005).
289. Niggli,V., Sigel,E. & Carafoli,E. The purified Ca<sup>2+</sup> pump of human erythrocyte membranes catalyzes an electroneutral Ca<sup>2+</sup>-H<sup>+</sup> exchange in reconstituted liposomal systems. *J. Biol. Chem.* **257**, 2350-2356 (1982).
290. Toyoshima,C., Nakasako,M., Nomura,H. & Ogawa,H. Crystal structure of the calcium pump of sarcoplasmic reticulum at 2.6 Å resolution. *Nature* **405**, 647-655 (2000).
291. Brini,M., Bano,D., Manni,S., Rizzuto,R. & Carafoli,E. Effects of PMCA and SERCA pump overexpression on the kinetics of cell Ca(2+) signalling. *EMBO J.* **19**, 4926-4935 (2000).
292. Chicka,M.C. & Strehler,E.E. Alternative splicing of the first intracellular loop of plasma membrane Ca<sup>2+</sup>-ATPase isoform 2 alters its membrane targeting. *J. Biol. Chem.* **278**, 18464-18470 (2003).
293. DeMarco,S.J., Chicka,M.C. & Strehler,E.E. Plasma membrane Ca<sup>2+</sup> ATPase isoform 2b interacts preferentially with Na<sup>+</sup>/H<sup>+</sup> exchanger regulatory factor 2 in apical plasma membranes. *J. Biol. Chem.* **277**, 10506-10511 (2002).
294. Kim,E. *et al.* Plasma membrane Ca<sup>2+</sup> ATPase isoform 4b binds to membrane-associated guanylate kinase (MAGUK) proteins via their PDZ (PSD-95/Dlg/ZO-1) domains. *J. Biol. Chem.* **273**, 1591-1595 (1998).
295. Di Leva,F., Domi,T., Fedrizzi,L., Lim,D. & Carafoli,E. The plasma membrane Ca<sup>2+</sup> ATPase of animal cells: structure, function and regulation. *Arch. Biochem. Biophys.* **476**, 65-74 (2008).
296. Elshorst,B. *et al.* NMR solution structure of a complex of calmodulin with a binding peptide of the Ca<sup>2+</sup> pump. *Biochemistry* **38**, 12320-12332 (1999).
297. Hilfiker,H., Guerini,D. & Carafoli,E. Cloning and expression of isoform 2 of the human plasma membrane Ca<sup>2+</sup> ATPase. Functional properties of the enzyme and its splicing products. *J. Biol. Chem.* **269**, 26178-26183 (1994).

- 
298. James,P.H., Pruschy,M., Vorherr,T.E., Penniston,J.T. & Carafoli,E. Primary structure of the cAMP-dependent phosphorylation site of the plasma membrane calcium pump. *Biochemistry* **28**, 4253-4258 (1989).
299. Dean,W.L., Chen,D., Brandt,P.C. & Vanaman,T.C. Regulation of platelet plasma membrane Ca<sup>2+</sup>-ATPase by cAMP-dependent and tyrosine phosphorylation. *J. Biol. Chem.* **272**, 15113-15119 (1997).
300. Wan,T.C., Zabe,M. & Dean,W.L. Plasma membrane Ca<sup>2+</sup>-ATPase isoform 4b is phosphorylated on tyrosine 1176 in activated human platelets. *Thromb. Haemost.* **89**, 122-131 (2003).
301. Fujimoto,T. Calcium pump of the plasma membrane is localized in caveolae. *J. Cell Biol.* **120**, 1147-1157 (1993).
302. Brodin,P., Falchetto,R., Vorherr,T. & Carafoli,E. Identification of two domains which mediate the binding of activating phospholipids to the plasma-membrane Ca<sup>2+</sup> pump. *Eur. J. Biochem.* **204**, 939-946 (1992).
303. Petersen,O.H. Ca<sup>2+</sup> signalling and Ca<sup>2+</sup>-activated ion channels in exocrine acinar cells. *Cell Calcium* **38**, 171-200 (2005).
304. Voronina,S.G. *et al.* Bile acids induce a cationic current, depolarizing pancreatic acinar cells and increasing the intracellular Na<sup>+</sup> concentration. *J. Biol. Chem.* **280**, 1764-1770 (2005).
305. Porras,O.H., Ruminot,I., Loaiza,A. & Barros,L.F. Na(+)-Ca(2+) cosignaling in the stimulation of the glucose transporter GLUT1 in cultured astrocytes. *Glia* **56**, 59-68 (2008).
306. Szewczyk,M.M., Pande,J. & Grover,A.K. Caloxins: a novel class of selective plasma membrane Ca<sup>2+</sup> pump inhibitors obtained using biotechnology. *Pflugers Arch.* **456**, 255-266 (2008).
307. Rizzuto,R., Bernardi,P. & Pozzan,T. Mitochondria as all-round players of the calcium game. *J. Physiol* **529 Pt 1**, 37-47 (2000).
308. Nagai,T., Sawano,A., Park,E.S. & Miyawaki,A. Circularly permuted green fluorescent proteins engineered to sense Ca<sup>2+</sup>. *Proc. Natl. Acad. Sci. U. S. A* **98**, 3197-3202 (2001).
309. Shimosono,S. *et al.* Confocal imaging of subcellular Ca<sup>2+</sup> concentrations using a dual-excitation ratiometric indicator based on green fluorescent protein. *Sci. STKE.* **2002**, 14 (2002).
310. Carrasco,S. & Meyer,T. STIM Proteins and the Endoplasmic Reticulum-Plasma Membrane Junctions. *Annu. Rev. Biochem.* (2010).

- 
311. Anderie,I., Schulz,I. & Schmid,A. Direct interaction between ER membrane-bound PTP1B and its plasma membrane-anchored targets. *Cell Signal.* **19**, 582-592 (2007).
312. Akao,Y., Otsuki,Y., Kataoka,S., Ito,Y. & Tsujimoto,Y. Multiple subcellular localization of bcl-2: detection in nuclear outer membrane, endoplasmic reticulum membrane, and mitochondrial membranes. *Cancer Res.* **54**, 2468-2471 (1994).
313. Hockenbery,D., Nunez,G., Milliman,C., Schreiber,R.D. & Korsmeyer,S.J. Bcl-2 is an inner mitochondrial membrane protein that blocks programmed cell death. *Nature* **348**, 334-336 (1990).
314. Jouaville,L.S., Pinton,P., Bastianutto,C., Rutter,G.A. & Rizzuto,R. Regulation of mitochondrial ATP synthesis by calcium: evidence for a long-term metabolic priming. *Proc. Natl. Acad. Sci. U. S. A* **96**, 13807-13812 (1999).
315. Szalai,G., Krishnamurthy,R. & Hajnoczky,G. Apoptosis driven by IP(3)-linked mitochondrial calcium signals. *EMBO J.* **18**, 6349-6361 (1999).
316. Vanden Abeele,F. *et al.* Bcl-2-dependent modulation of Ca(2+) homeostasis and store-operated channels in prostate cancer cells. *Cancer Cell* **1**, 169-179 (2002).
317. Pinton,P., Giorgi,C., Siviero,R., Zecchini,E. & Rizzuto,R. Calcium and apoptosis: ER-mitochondria Ca<sup>2+</sup> transfer in the control of apoptosis. *Oncogene* **27**, 6407-6418 (2008).
318. He,H., Lam,M., McCormick,T.S. & Distelhorst,C.W. Maintenance of calcium homeostasis in the endoplasmic reticulum by Bcl-2. *J. Cell Biol.* **138**, 1219-1228 (1997).
319. Zhong,F., Davis,M.C., McColl,K.S. & Distelhorst,C.W. Bcl-2 differentially regulates Ca<sup>2+</sup> signals according to the strength of T cell receptor activation. *J. Cell Biol.* **172**, 127-137 (2006).
320. Cheng,E.H. *et al.* BCL-2, BCL-X(L) sequester BH3 domain-only molecules preventing BAX- and BAK-mediated mitochondrial apoptosis. *Mol. Cell* **8**, 705-711 (2001).
321. Kim,R., Emi,M., Matsuura,K. & Tanabe,K. Antisense and nonantisense effects of antisense Bcl-2 on multiple roles of Bcl-2 as a chemosensitizer in cancer therapy. *Cancer Gene Ther.* **14**, 1-11 (2007).
322. Becattini,B. *et al.* Rational design and real time, in-cell detection of the proapoptotic activity of a novel compound targeting Bcl-X(L). *Chem. Biol.* **11**, 389-395 (2004).

- 
323. Zhang, M. *et al.* Gossypol induces apoptosis in human PC-3 prostate cancer cells by modulating caspase-dependent and caspase-independent cell death pathways. *Life Sci.* **80**, 767-774 (2007).
324. Oliver, C.L. *et al.* In vitro effects of the BH3 mimetic, (-)-gossypol, on head and neck squamous cell carcinoma cells. *Clin. Cancer Res.* **10**, 7757-7763 (2004).
325. Wolter, K.G. *et al.* (-)-gossypol inhibits growth and promotes apoptosis of human head and neck squamous cell carcinoma in vivo. *Neoplasia.* **8**, 163-172 (2006).
326. van Delft, M.F. *et al.* The BH3 mimetic ABT-737 targets selective Bcl-2 proteins and efficiently induces apoptosis via Bak/Bax if Mcl-1 is neutralized. *Cancer Cell* **10**, 389-399 (2006).
327. Halangk, W. *et al.* Role of cathepsin B in intracellular trypsinogen activation and the onset of acute pancreatitis. *J. Clin. Invest* **106**, 773-781 (2000).
328. Hashimoto, D. *et al.* Involvement of autophagy in trypsinogen activation within the pancreatic acinar cells. *J. Cell Biol.* **181**, 1065-1072 (2008).
329. Ohmuraya, M. & Yamamura, K. Autophagy and acute pancreatitis: a novel autophagy theory for trypsinogen activation. *Autophagy.* **4**, 1060-1062 (2008).
330. Chen-Levy, Z., Nourse, J. & Cleary, M.L. The bcl-2 candidate proto-oncogene product is a 24-kilodalton integral-membrane protein highly expressed in lymphoid cell lines and lymphomas carrying the t(14;18) translocation. *Mol. Cell Biol.* **9**, 701-710 (1989).
331. Kelly, P.N. & Strasser, A. The role of Bcl-2 and its pro-survival relatives in tumorigenesis and cancer therapy. *Cell Death. Differ.* **18**, 1414-1424 (2011).
332. Chipuk, J.E., Bouchier-Hayes, L. & Green, D.R. Mitochondrial outer membrane permeabilization during apoptosis: the innocent bystander scenario. *Cell Death. Differ.* **13**, 1396-1402 (2006).
333. Lucken-Ardjomande, S. & Martinou, J.C. Regulation of Bcl-2 proteins and of the permeability of the outer mitochondrial membrane. *C. R. Biol.* **328**, 616-631 (2005).
334. Hanson, C.J., Bootman, M.D., Distelhorst, C.W., Wojcikiewicz, R.J. & Roderick, H.L. Bcl-2 suppresses Ca<sup>2+</sup> release through inositol 1,4,5-trisphosphate receptors and inhibits Ca<sup>2+</sup> uptake by mitochondria without affecting ER calcium store content. *Cell Calcium* **44**, 324-338 (2008).